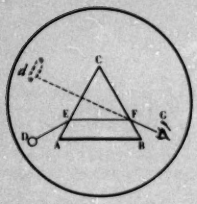

optics and spectroscopy

volume ix
number 5
november 1960

OPTICAL SOCIETY OF AMERICA

USSR ACADEMY OF SCIENCES

RUSSIAN EDITORIAL STAFF FOR
OPTIKA I SPEKTROSKOPIYA sponsored by
USSR ACADEMY OF SCIENCES

Editor: S. E. FRISH

Assistant Editor: P. P. FEOFILOV
Corresponding Secretary: L. S. SAZONOV

Associate Editors:

M. M. GUREVICH M. A. EL'IASHEVICH A. A. LEBEDEV V. P. LINNIK
S. L. MANDEL'SHTAM I. V. OBREIMOV V. K. PROKOF'EV
N. N. SOBOLEV A. N. TERENIN A. I. TUDOROVSKII

Translated from *OPTIKA I SPEKTROSKOPIYA* on the initiative of THE OPTICAL SOCIETY OF AMERICA, INC. with a grant-in-aid from THE NATIONAL SCIENCE FOUNDATION. *Optics and Spectroscopy* is a cover-to-cover translation of *Optika i Spektroskopiya* and no attempt is made to edit the material other than to correct obvious misprints. The views are those of the original authors and do not represent the Optical Society of America.

TRANSLATION EDITORIAL STAFF

Scientific Editors

CYRUS FELDMAN, *Oak Ridge National Laboratory*

CARL W. GARLAND, *Massachusetts Institute of Technology*

MATHEW G. GIBBONS, *Oakland, California*

Administrative Editor: PATRICIA R. WAKELING, *OSA*

Published monthly by the Optical Society of America, Inc. Executive office: 1155 Sixteenth Street, N.W., Washington, D.C. Subscriptions for one year to members of the Society: Associates $13.00; Regular members and Fellows $17.00. Subscriptions for non-members of the Society: One year U. S. and Possessions, $25.00; Foreign $28.00. Back numbers: $3.00 per copy. Subscriptions, changes of address and undeliverable copies should be referred to the Executive offices in Washington, D.C. The office of publication is 2500 South State Street, Ann Arbor, Michigan. Second class postage paid at Ann Arbor, Michigan.

Printed in the U.S.A. by Edwards Brothers, Inc., Ann Arbor, Michigan.

THE INFLUENCE OF DIPOLAR MOLECULES ON THE ABSORPTION OF THE MERCURY RESONANCE LINE AT 2537 A

V. N. Ivanov

Received 15 February 1960

In this study the method and results of an investigation of the absorption spectra of the systems Hg/NO, Hg/CO, and Hg/H_2O are given. An analysis of the diminution of the intensity in the long-wave wing of the line and of its half-width allows one to draw certain conclusions about the influence of the dipole moment of the perturbing molecule on the light absorption by an atom. In the case of broadening due to nitric oxide, the half-width and diminution of the intensity depend substantially on the temperature. This is explained by a change of the dipole moment of the nitric oxide with a change in temperature.

INTRODUCTION

The investigation of the systems Hg/NO, Hg/CO, and Hg/H_2O was undertaken with the goal of revealing the influence of foreign gases on the absorption of the mercury resonance line and of clarifying the role of the dipole moment of the molecule. In addition, the influence of temperature on the broadening of the absorption line was studied. Foreign gases with different values of the dipole moments were chosen ($\mu_{CO} = 0.11$ D, $\mu_{NO} = 0.1$ D, $\mu_{H_2O} = 1.8$ D).

For a clarification of the influence of temperature CO and NO, having similar molecular masses and dipole moments but different thermal properties, were taken. A series of indirect data[1,2] indicate that NO possesses a variable dipole moment, dependent on the temperature.

EXPERIMENTAL

The absorption spectra were obtained by the usual methods of absorption spectroscopy. Into an absorbing, evacuated, and degassed quartz cell with a side-arm a drop of chemically pure mercury and the foreign gas were introduced. The mercury was subjected to multiple vacuum distillations and freezings by liquid nitrogen. The gases were obtained by laboratory means;[3] they were carefully purified and were frozen prior to use. The water was introduced in a glass ampoule, and after the cell was sealed from the vacuum apparatus the ampoule was burst by cooling in liquid nitrogen.

The cell and side-arm were placed in a furnace which determined the concentration of the mercury vapor and the temperature of the absorbing system. The furnace was supplied with a stabilized power supply. The temperature control was produced by means of platinum, platinum-rhodium thermocouples. Before photographing the spectra, the system was equilibrated for several hours to establish the equilibrium concentrations.

The spectra were photographed by an ISP-22 spectrograph on photographic plates "spectral, type 1," using constant operating conditions of the hydrogen lamp and identical exposures. The spectrograms were read by the methods of photographic photometry.

Preliminary experiments with pure mercury enabled a determination of the concentration of mercury atoms (0.83×10^{17} atoms/cm^3), at which concentration the number of Hg_2 molecules forming in the tube on heating is negligibly small and the contour of the absorption line is not perturbed by Hg_2 bands. The concentration of mercury atoms was held constant by a small change of the temperature of the absorption cell.[4] The concentrations of the foreign gases were always identical (1.62×10^{19} molecules/cm^3). The absorption spectra of Hg/NO and Hg/CO were photographed for two temperatures: 220 and 420° C. Absorption curves were constructed from the photometric data.

DISTRIBUTION OF THE INTENSITY IN THE LONG-WAVE WING OF THE LINE

It is known[5] that the distribution of the line intensity for large frequency shifts $\Delta\omega$ is specified by a change of wavelength of the absorbed light as a result of interaction of the absorbing particle with a foreign particle. In this case the distribution of intensity $I(\Delta\omega)$ in the long-wave wing of the line is determined by the statistical theory of line broadening, as a result of which

$$I(\Delta\omega) = B\Delta\omega^{-1-\frac{3}{p}},$$

where B is a constant, p the exponent of the distance r in the interaction law of the particles $E = -c/r^p$.

Taking the logarithm we obtain a linear dependence between $\log I(\Delta\omega)$ and $\log \Delta\omega$, and from the slope of this plot we can estimate the magnitude of p. Such an investigation was first carried out by Kuhn[6] for the case of the broadening of the mercury 2537 A line by argon at high pressures. An analogous method of investigation was applied by Kushnikov[7] to the radiation spectra of Hg in the presence of molecular gases with different dipole moments. In this work it was established that the drop in intensity in the long-wave wing of the line does not depend on the magnitude of the dipole moment of the foreign gas.

This same method was applied also in the current work.

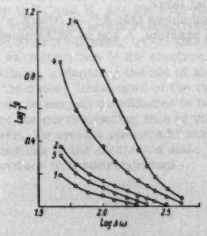

In the Figure are shown graphically the dependences of log (I_0/I) on log $\Delta\omega$. For the systems Hg/CO and Hg/NO straight lines do not occur, as would follow from the formula indicated. Similar deviations also occurred in the other studies[6,7] for large values of $\Delta\omega$.

From the curves 1, 2, and 3 of the Figure, corresponding to the systems Hg/CO, Hg/NO, and Hg/H_2O, for a temperature of 220°, it is seen that the drop of the intensity depends substantially on the nature of the broadening gas. The slope of the curve corresponding to the Hg/H_2O system is particularly pronounced. The water molecule has by far the largest dipole moment, and there are grounds for proposing that the differences in absorption are stipulated only by the properties of the molecule. The slope of the Hg/H_2O curve corresponds to a larger value of p than in the case of Hg/CO and of Hg/NO.

The lack of agreement of this conclusion with the work of Kushnikov can be explained by the particulars of the experimental conditions: a low pressure of foreign gas, the possibility of dissociation of the molecules, and others.

To clarify the influence of temperature on the absorption of Hg/CO and Hg/NO, spectra were photographed at temperatures of 220 and 420°C. There was discovered a rather substantial influence of temperature on the system Hg/NO (curve 4) and an insignificant influence (curve 5) on the Hg/CO system. The masses of the NO and CO molecules differ insignificantly; and, therefore, it is impossible to explain the changes in the absorption by a difference of the kinetic energy of these molecules. Evidently, the fundamental reason for the substantial influence of temperature on the Hg/NO system is a change of the properties of the NO molecule on heating.

Earlier[8] we investigated the influence of temperature on the absorption spectrum of NO and established that an elevation of the temperature leads to the appearance of the bands (o, v) of the γ-system. Since the initial state for these transitions is different, this is evidence of the thermal excitation of the vibrational levels of NO and of changes of the dipole moment of the molecule. This agrees completely with the results of the present work.

THE INFLUENCE OF TEMPERATURE ON THE HALF-WIDTH OF THE ABSORPTION LINE

In this work we use the method of complete absorption for the determination of the half-width of the line.[9] If the central part of the spectral line is completely absorbed, then the total absorption A is determined by the relationship

$$A = 2\pi \int_0^{\infty} (1 - e^{-kl})\, d\omega,$$

where k is the absorption coefficient and l the thickness of the absorbing layer.

Calculation shows that $A \sim \sqrt{\gamma}$ where γ is the line half-width. In practice, A can be determined from the area a, limited by the contour of the absorption line

$$A = 2\pi \frac{a}{I_0},$$

where I_0 is the intensity of the incident radiation.

In the Table are presented values of the ratio of the half-width of the line for 420 and 220°C, found from complete absorption and calculated from the formula of Lorentz.

System	Increase of the half-width in the interval 220-420°C		Deviation from the theoretical calculation (%)
	From the Lorentz formula (%)	From complete absorption (%)	
Hg/CO	120	160	40
Hg/NO	120	420	300

From the Table we see that the broadening of the 2537 A line by CO is greater than the theoretical by 40%, and for NO greater by 300%.

In this instance, as also reported elsewhere,[5,10] there are revealed individual peculiarities in the influence of foreign gases on the line half-width for a change of the temperature. Probably one of the reasons of the significant influence of NO on the half-width is the change of molecular properties of NO with temperature, and above all, of its dipole moment.

In conclusion, the author expresses his gratitude to N. A. Prilezhaevaya for consultations and valuable advice.

REFERENCES

1. M. V. Vol'kenshtein, Stroenie i Fizicheskie Svoistva Molekul (The structure and physical properties of molecules). Akad. Nauk SSSR, Moscow, Leningrad, 1955.
2. N. N. Semenov, O Nekotorykh Problemakh Khimicheskoi Kinetiki i Reaktsionnoi Sposobnosti (On some problems of chemical kinetics and reaction capabilities). Akad. Nauk SSSR, Moscow, 1958.
3. Yu. V. Karyakin and I. I. Angelov, "Chistye Khimicheskie Reaktivy" (Pure Chemical Reagents). Gosudarst. Khim. Inst., 1955.
4. Yu. A. Kushnikov, Dissertation, Tomsk, 1950.
5. Sh. Chen and M. Takeo, Uspekhi Fiz. Nauk 66, 391 (1958).
6. H. Kuhn, Proc. Roy. Soc. A158, 212 (1937).
7. Yu. A. Kushnikov, Izvest. Akad. Nauk SSSR, Ser. Fiz. 12, 366 (1948).
8. V. N. Ivanov, Opt. i Spektr. 7, 813 (1959), Optics and Spectroscopy 7, 476 (1959).
9. A. Mitchell and M. Zemansky, "Rezonansnoe Izluchenie i Vozbuzhdenie Atomy" (Resonance Radiation and Excited Atoms). ONTI (United Scientific and Technical Press), Moscow, 1937.
10. A. A. Misyukas-Misyunas, Fiz. sbornik (L'vovsk. Univ.) 4, 308 (1958).

TOWARD THE THEORY OF ELECTRONIC-VIBRATIONAL TRANSITIONS IN SYSTEMS WITH MANY VIBRATIONAL DEGREES OF FREEDOM

K. K. Rebane

Received 15 February 1960

A simple derivation of a formula for the moments of a spectral band arising as the result of an electronic-vibrational transition in a crystal or in a molecule is given. It is shown that the expressions obtained agree with Lax's formulas,[1] which are valid even when normal coordinates are not introduced to describe the vibrations of the nuclei, the distribution of the systems over the vibration levels is nonequilibrium, and the spectral bands have a partially or entirely linear structure.

The application of the formulas obtained is illustrated by taking as an example the general investigation of the effect of isotropic compression of crystal phosphors on the shape of their spectral bands.

In the theory of electronic-vibrational transitions in complex vibrational systems (crystals or complex molecules), various one-coordinate methods of examination have begun to be widely applied in recent years.[2-9] With all the successes of the application of one-coordinate models to describe complex vibrational systems, and entirely independently of the degree to which in future it may be possible to succeed in demonstrating the validity of these models for the consideration of one or another set of concrete phenomena, one must not forget the known crude nature of one-coordinate models.

Consideration of the vibrational motion of a complex system as a set of quasi-independent normal vibrations is without question substantially the most exact solution of the problem. At the present time there exist a number of works where, on the basis of different variants of this model, the authors have succeeded in systematically carrying out an examination of the electronic-vibrational transitions, allowing for many vibrational degrees of freedom (see refs. 1, 10, 11). However, the legitimacy of introducing quasi-independent normal vibrations is also sometimes subject to doubt. Thus, Stepanov[8] has come to the conclusion that in the case of a complex molecule it is in general not permissible to introduce the idea of quasi-independent normal vibrations.

In the luminescence centers of crystal phosphors (especially in ionic crystals), Stokes losses are very marked. Therefore one may expect that immediately after a transition as a result of which the electronic state of the center has been changed, and also in the first stages of the process of relaxation of excess vibrational energy, the amplitudes of the displacements of the ions closest to the activator are large. Then the effect of the anharmonicity of the vibrations will also be large, in consequence of which the idea of quasi-independent normal vibrations may be very rough.

Starting from this, one is curious to obtain some results which do not depend on whether there are many vibrational degrees of freedom in the system or few, nor on whether the idea of quasi-independent normal vibrations is applicable or not.

It is shown below, taking the effect of pressure on the spectra of crystal phosphors as an example, how some results of this sort may be obtained. Description of the spectral bands with the help of the method of moments proposed by Lax[1] appears to be an expedient approach to a solution of our task.

1. FORMULAS FOR THE MOMENTS OF SPECTRAL BANDS

In this section, we shall give a very simple (as it seems to us) derivation of a formula for the moments of a spectral band arising as the result of an electronic-vibrational transition. The investigation refers equally to both crystals and molecules (complex and diatomic). We note that the results obtained agree with Lax's formulas.[1] In our derivation of these formulas, it can be seen particularly clearly that Lax's formulas are valid even when the vibrational motion of the nuclei is not described by normal coordinates or the distribution of the systems over the vibrational levels is nonequilibrium. Furthermore, the bands may have a partially or entirely linear structure.

The l-th order moment of a spectral curve, S_l, is determined by the expression*

$$S_l = \sum_i n_i \sum_s (E_s - E_i)^l W_{si}. \qquad (1)$$

Here the Franck-Condon factor

$$W_{si} = \left[\int \psi^*_{\mathrm{II}s}(x)\, M(x)\, \psi_{\mathrm{I}i}(x)\, dx\right]^2;$$

n_i is the number of systems on the initial vibrational level denoted by i; E_i and E_s are the energies of the initial and final vibrational levels respectively; M(x) is the electronic matrix element. $\psi_{\mathrm{I}i}(x)$ and $\psi_{\mathrm{II}s}(x)$ are the vibrational wave functions in the electronic states I (initial) and II (final), x denoting the set of all vibrational coordinates of the nuclei (breakdown of the vibrational motion into separate normal coordinates is not assumed), and i and s are the corresponding sets of vibrational quantum numbers. To avoid a plethora of indices, we shall omit the indices of the electronic state wherever this does not produce misunderstandings.

*We write the formulas for discrete vibrational levels, but all the following is also valid in the case of a continuous spectrum. Furthermore, it can be seen from (1) that we are speaking of the intensity distributions which are obtained if the experimental band contours, measured in energy quantities and normalized, are multiplied respectively by ν^{-4} (emission) and ν^{-1} (absorption). Our formulas refer to absorption; their extension to emission is trivial.

Let us consider the quantity

$$(E_s - E_i)^j \psi^*_{11s}(x)\, M(x)\, \psi_{1i}(x)$$

$$= \sum_{k=0}^{j} (-1)^k C_j^k E_s^{j-k} \psi^*_{11s}(x)\, M(x)\, E_i^k \psi_{1i}(x)$$

$$= \sum_{k=0}^{j} (-1)^k C_j^k M(x) \left[\hat{H}_1^k \psi_{1i}(x)\right] \left[\hat{H}_{11}^{*j-k} \psi^*_{11s}(x)\right]. \quad (2)$$

Here $\hat{H}_1$ and $\hat{H}_{11}$ are the Hamiltonian operators describing the vibration of the nuclei in the adiabatic approximation.

Let us integrate with respect to x the equality which we have obtained, and, using the self-conjugate property of the operators $\hat{H}_{11}^{*j-k}$, let us transform the integrals. Then we have

$$(E_s - E_i)^j \int \psi^*_s(x)\, M(x)\, \psi_i(x)\, dx$$

$$= \sum_{k=0}^{j} (-1)^k C_j^k \int \psi^*_s(x)\, \hat{H}_{11}^{j-k} M(x)\, \hat{H}_1^k \psi_i(x)\, dx. \quad (3)$$

Multiplying (3) by the integral

$$\int \psi^*_s(x')\, M^*(x')\, \psi_s(x')\, dx',$$

carrying out the summation of the equations obtained from (3) over all final vibrational states s, and using the completeness condition

$$\sum_s \psi^*_s(x)\, \psi_s(x') = \delta(x - x'),$$

we obtain

$$\sum_s (E_s - E_i)^j W_{si}$$

$$= \sum_{k=0}^{j} (-1)^k C_j^k \int \psi_i^*(x)\, M^*(x)\, \hat{H}_{11}^{j-k} M(x)\, \hat{H}_1^k \psi_i(x)\, dx.$$

To determine the l-th order moment, let us carry out another averaging over the initial vibrational levels, after which we finally have*

*We note that the validity of formula (4) is not limited to the adiabatic approximation: in its derivation, we used only the completeness property of the set of functions ψ_s and we assumed that M(x) is a multiplication operator.

$$S_l = \sum_i n_i \sum_{k=0}^{l} (-1)^k C_l^k \int dx \left\{\psi_i^*(x)\, M^*(x)\, \hat{H}_{11}^{l-k} M(x)\, \hat{H}_1^k \psi_i(x)\right\}. \quad (4)$$

For the zeroth moment we obtain from this

$$S_0 = \sum_i n_i \int |M(x)|^2 |\psi_i(x)|^2\, dx \quad (5a)$$

or, in Condon's approximation (M(x) = const.),

$$S_0 \cong |M|^2 N, \quad (5b)$$

where N is the number of systems in the initial electronic state.

The next three moments are expressed by the formulas

$$S_1 = \sum_i n_i \int dx \left\{\psi_i^*(x) \left[M^*(x)\, \hat{H}_{11} M(x) - |M(x)|^2 \hat{H}_1\right] \psi_i(x)\right\} \quad (5c)$$

$$\cong |M|^2 \sum_i n_i \int dx \left\{\psi_i^*(x) \left[\hat{H}_{11} - \hat{H}_1\right] \psi_i(x)\right\} = |M|^2 \int U(x)\, \rho(x)\, dx,$$

where

$$\rho(x) = \sum_i n_i |\psi_i(x)|^2$$

is the distribution function of the coordinates and U(x) = $U_{11}(x) - U_1(x)$ represents the difference between the values of the adiabatic potentials of the final and initial electronic states;

$$S_2 = \sum_i n_i \int dx \left\{\psi_i^*(x) \left[M^*(\bar{x})\, \hat{H}_{11}^2 M(x) - 2M^*(x)\, \hat{H}_{11} M(x)\, \hat{H}_1 + |M(x)|^2 \hat{H}_1^2\right] \psi_i(x)\right\} \cong |M|^2 \sum_i n_i$$

$$\times \int dx \left\{\psi_i^*(x) \left[\hat{H}_{11}^2 - 2\hat{H}_{11}\hat{H}_1 + \hat{H}_1^2\right] \psi_i(x)\right\} = |M|^2 \int U^2(x)\, \rho(x)\, dx;$$

$$S_3 = \sum_i n_i \int dx \left\{\psi_i^*(x) \left[M^*(x)\, \hat{H}_{11}^3 M(x) - 3M^*(x)\, \hat{H}_{11}^2 M(x)\, \hat{H}_1 + 3M^*(x)\, \hat{H}_{11} M(x)\, \hat{H}_1^2 - |M(x)|^2 \hat{H}_1^3\right] \psi_i(x)\right\} \quad (5d)$$

$$\cong |M|^2 \sum_i n_i \int dx \left\{\psi_i^*(x) \left[\hat{H}_{11}^3 - 3\hat{H}_{11}^2 \hat{H}_1 + 3\hat{H}_{11}\hat{H}_1^2 - \hat{H}_1^3\right] \psi_i(x)\right\}.$$

2. EFFECT OF PRESSURE ON THE SPECTRAL BANDS OF A LUMINESCENCE CENTER IN CRYSTAL PHOSPHORS

We shall have in mind smooth broad spectral bands. It is not difficult to extend the results to bands which have a partially or entirely linear structure. Under the influence of pressure (isotropic compression), the spectral bands of crystal phosphors usually shift somewhat. The shape of the band usually changes insignificantly during this process.[12]

We shall assume at first that the pressure manifests itself only in a displacement of the distribution function $\rho(x)$ toward smaller values for the volume of the system. The adiabatic potentials remain unchanged by this (this approximation was used by Williams and Johnson,[13] but was applied to the one-coordinate model). We shall also consider that the bands under consideration are elementary and that both potential surfaces, in their regions of x which are involved in band formation, are separated from other potential surfaces by significant energy intervals. We shall consider the distribution function function $\rho(x)$ as being the thermal-equilibrium function (with respect to vibrations).

The changes in the first three moments under the influence of pressure are expressed in Condon's approximation by the formulas

$$\Delta S_0^i(p) = \int \delta\rho^i(p, x)\, dx, \quad (6a)$$

$$\Delta S_1^i(p) = \int \delta\rho^i(p, x)\, U(x)\, dx, \quad (6b)$$

$$\Delta S_2^i(p) = \int \delta\rho^i(p, x)\, [U(x)]^2\, dx, \quad (6c)$$

where i is the index of the electronic state and $\delta\rho^i(p,x) \equiv \rho^i(p,x) - \rho^i(0,x)$ is the change in the distribution function under the influence of pressure.

The distribution functions over the vibrations may be normalized to the number of systems in the corresponding electronic state:

$$\int \rho^i(p, x)\, dx = N_i(p). \quad (7)$$

Under our simplifying assumption that the two electronic states of interest to us are separated by significant energy intervals, no redistribution of the systems among the electronic states of one particular luminescence center will take place. However, pressure may

have an effect, through the agency of ionic diffusion, on the number of centers itself.* Inasmuch as ionic processes usually proceed slowly, equilibrium with respect to them will not necessarily be established, and it would be proper to take the dependence on time, t, into account also and write $N_i(p,t)$.

*In particular, the effect of pressure must make itself felt especially perceptibly in regard to the number of defects, the appearance or disappearance of which is associated with significant changes in the volume of the system (for example, ionic vacancies).

We shall confine ourselves to the case where the total number of defects is constant. We shall also consider that the distribution functions $\rho^i(p,x)$ are normalized to unity. In this case we have

$$\Delta S_0^1(p) = \Delta S_0^1(p) = 0, \tag{8}$$

i.e., the areas of the spectral bands do not change under the influence of pressure.

The change in the first moment (displacement of the maximum and of the band as a whole) is different from zero even in Condon's approximation. The corresponding evaluation shows that, to obtain the observed shift of the spectrum, $\Delta\bar{\omega}$, (the ratio $\Delta\bar{\omega}/\bar{\omega} = 0.01$) in the case of the mechanism which we have considered for the action of pressure, pressures of the order of 10^3-10^4 atm are necessary. Just such pressures were used in the experiments.[12]

Let us write down the change in the first moment in the form

$$\Delta S_1(p) = \int_{\mathrm{I}} \delta\rho\,(U_0 + \delta U)\,dx + \int_{\mathrm{II}} \delta\rho\,(U_0 + \delta U)\,dx \tag{9}$$

$$= L_{\mathrm{I}}\delta\rho_{\mathrm{I}}\delta U_{\mathrm{I}} + L\ \delta\rho_{\mathrm{II}}\delta U_{\mathrm{II}},$$

where U_0 = const. is the value of U(x) at the minimum of the initial potential surface. Region of integration I is the region where $\delta\rho(x) > 0$, and II is the region where $\delta\rho(x) < 0$. The positive quantities L_i are the effective extents of the regions of integration (i = I or II). In accordance with the mean value theorem for integrals, the quantities $\delta\rho_i$ and δU_i are the values of the integrand function taken at an appropriate point of the region L_i. A formula in the form (9) is convenient for investigation of the signs of the shift of absorption and emission bands under the influence of pressure: the signs of L_i and $\delta\rho_i$ are known, and the signs of δU_i are determined by the properties of the potential surfaces.

From consideration of the one-configurational-coordinate model according to the theory of Williams and Johnson, the conclusion emerges[12] that the absorption and emission bands resulting from one and the same electronic transition must shift toward the same side under the influence of pressure. Kristofel',[13] using the KCl-Tl crystal as his example, carried out a calculation of the effect of pressure in the one-coordinate approximation; he examined the "static" effect of pressure, shown by means of a diminution of the constant of the lattice surrounding the center, on the potential curves themselves. The fundamental result remained as before: both bands should shift toward the long-wavelength side. For a series of alkali-halide phosphors, in particular for KCl-Tl, experiment[12-14] leads to the opposite result: the emission band shifts toward short waves, the absorption and excitation bands toward long. Kirs was inclined to consider this as a consequence of the nonelementary of the potential curve of the excited state. Certain other experimental facts[15] also speak in favor of this supposition, and it seems to be correct.

However, there is also a certain difficulty which arises on such an interpretation of the phenomenon within the framework of the one-coordinate model. If we carry out a simple numerical estimate on the basis of the parameters given for the potential curves of KCl-Tl by Williams[4] or Kristofel',[8] then it turns out that even on transition of systems under the influence of pressure to the higher potential curve of the excited state, a long-wavelength shift of the emission band is rather to be expected. This is brought about by the fact that the minimum of the upper potential curve (the electronic state $^3P_1$) is located at lower values of the configurational coordinate than the minimum of the lower potential curve (the electronic state $^1S_0$).[4,8]

On the basis of formula (9) it is not difficult to show that, when one takes account of even two vibrations, the changes in the first moment under the influence of pressure are such that the shifts of the two spectral bands need not necessarily have the same signs. We have here an example of how the one-coordinate model leads to incorrect conclusions even in qualitative discussions.*

*A more detailed consideration of the applicability of the one-coordinate model to the description of the effect of pressure, in particular a detailed consideration of the case of a system whose vibrations are described in the harmonic approximation, has been carried out by O. I. Sil'd.

The second moment of a spectral band, $\bar{S}_2$, taken with respect to its center of gravity, characterizes the half-width of the band. The change in this moment, $\Delta\bar{S}_2$, is connected with the changes in the moments relative to E = 0 in the following way:

$$\Delta S_2 = \Delta S_2 - 2S_1\Delta S_1 - (\Delta S_1)^2, \tag{10}$$

where

$$\Delta S_2 = \int \delta\rho U^2 dx, \quad \Delta S_1 = \int \delta\rho U dx.$$

Let us introduce a new function

$$\delta U = U - \left(S_1 + \frac{\Delta S_1}{2}\right). \tag{11}$$

In this case, we have for S_2

$$\Delta S_2 = \int \delta\rho \left\{\left(S_1 + \frac{\Delta S_1}{2}\right)^2 + 2\left(S_1 + \frac{\Delta S_1}{2}\right)\delta U + (\delta U)^2\right\} dx$$

$$= 2\left(S_1 + \frac{\Delta S_1}{2}\right)\Delta S_1 + \int \delta\rho\,(\delta U)^2\,dx,$$

since $\int\delta\rho dx = 0$.

The change in the second moment, $\Delta\bar{S}_2$, is now expressed by the very simple relation

$$\Delta S_2 = \int \delta\rho\,(\delta U)^2\,dx, \tag{12}$$

where δU is determined by formula (11).

In the particular case of a single harmonic oscillator (a luminescence center in the one-coordinate approximation) of unchanging frequency, the quantity $\delta\rho(x)$ is an odd function relative to the point $x_0' = x_0 + (\Delta x/2)$, where Δx is the displacement of the maximum of the distribution $\rho(x)$ under the influence of pressure and x_0 is the coordinate of the maximum of the function $\rho(x)$ at atmospheric pressure. On the other hand, for a harmonic oscillator of unchanging frequency $S_1 + \Delta S_1 = U(x_0 + \Delta x)$. Since U(x) is linear,

$$S_1 + \frac{\Delta S_1}{2} = U\left(x_0 + \frac{\Delta x}{2}\right), \quad \delta U\left(x_0 + \frac{\Delta x}{2}\right) = 0,$$

and $\delta U(x)$ is also an odd function relative to the point

$x_0' = x_0 + (\Delta x/2)$. Consequently, for a harmonic oscillator of unchanging frequency, a change in the halfwidth under the influence of pressure should not take place; i.e., $\Delta\bar{S}_2 = 0$.

In the general case, $\Delta\bar{S}_2$ does not equal zero, and a change in the halfwidth of the band under the influence of pressure may be observed. Since $\int\delta\rho dx = 0$, expression (12) consists of a positive and a negative part, while the sign of the change in half-width may be either positive or negative, depending on the particular case.

If we approximate U(x) by the linear term of an expansion around $U(x_0')$ and $\delta\rho(x)$ is close to an odd function relative to x_0', then $\Delta\bar{S}_2 \approx 0$ approximately. The two assumptions made must hold approximately true in actuality. Therefore, although $\Delta\bar{S}_2$ is indeed different from zero in the general case, it by no means follows that one should expect large changes in half-width under the influence of pressure. One may suppose that the change in half-width will be greater, the more the curvatures of the potential surfaces differ (the curvature of U(x) is greater) and the greater the anharmonicity of the vibrations (the quantities $L_i\delta\rho_i$ will differ more strongly).

From formula (12) it can be seen that the sign of the change in half-width is determined by the sign of the "second differences" of $\delta\rho(x)$ and U(x) analogously to the way in which the sign of the change in the first moment is determined by the signs of the first differences of these functions.

In speaking of the change in half-width under the influence of pressure, one must also not lose sight of a very simple practical circumstance—according to the conditions of the experiment, we encounter the necessity of determining a small change in the half-width of a broad spectral band. It is clear that such an effect will be very inconspicuous. With a change in the first moment, matters are different—we are dealing with a band shift ΔS_1 "in plain sight," while we are totally uninterested in the magnitude of S_1, and the smallness of the ratio $\Delta S_1/S_1$ at a given ΔS_1 does not make the carrying out of the experiment any more difficult.

A change in the higher-order moments also manifests itself experimentally in the form of small relative changes and therefore is inconspicuous. In this is also included the fundamental cause of the fact that the visible influence of pressure comes down, for the most part, to a shift of the spectral band as a whole.

We note in conclusion that pressure may, by means of a change in the boundary conditions of the mechanical part of the problem (calculation of the energy levels), influence the magnitude of the adiabatic potentials themselves. This problem is connected with the calculation of the electronic energy of the system and opens into a whole circle of problems of interest to us, associated with electronic-vibrational transitions. However, from the foregoing information it is not difficult to discern that the relatively small changes in the adiabatic potentials brought about by pressure can hardly change the general qualitative results obtained above.

On the basis of the formulas for the moments of spectral curves, we have considered a further series of questions concerning the shapes of spectral bands. An account of these results will be the subject of a separate article.

The author is sincerely grateful to B. I. Stepanov for his attention to this work and to O. I. Sil'd for his participation in the computations and for discussion of the results.

REFERENCES

1. M. Lax, J. Chem. Phys. **20**, 1752 (1952). (Translation in the collection: "Problemy fiziki poluprovodnikov" (Problems of the Physics of Semiconductors). Izd. Inostrannoi Lit., Moscow, 1957.)
2. F. E. Williams and H. Eyring, J. Chem. Phys. **15**, 289 (1947);
F. E. Williams and M. H. Hebb, Phys. Rev. **84**, 1181 (1951).
3. C. Klick, Phys. Rev. **85**, 154 (1952).
4. F. E. Williams, J. Chem. Phys. **19**, 457 (1951); J. Phys. Chem. **57**, 780 (1953).
5. B. I. Stepanov, "Lyuminestsentsiya slozhnykh molekul" (Luminescence of Complex Molecules), Pt. 1. Izd. Akad. Nauk Belorus.SSR, Minsk, 1955.
6. V. S. Neporent, Trudy Gosudarst. Opt. Inst., Session in memory of S. I. Vavilov, Oboronizdat, 1953.
7. N. E. Lushchik and Ch. B. Lushchik, Trudy Inst. Fiz. i Astron., Akad. Nauk Eston.SSR, No. 6, 5 (1957);
Ch. B. Lushchik, N. E. Lushchik, and K. K. Shvarts, Trudy Inst. Fiz. i Astron., Akad. Nauk Eston.SSR, No. 8, 3 (1958).
8. N. N. Kristofel', Trudy Inst. Fiz. i Astron., Akad. Nauk Eston.SSR, No. 10, 3 (1959); Ibid., No. 7, 85 (1958);
N. L. Potekhina, Opt. i Spektr. **2**, 388 (1957).
9. K. K. Rebane, Trudy Inst. Fiz. i Astron., Akad. Nauk Eston.SSR, No. 7, 62 (1958).
10. S. I. Pekar, Uspekhi Fiz. Nauk **50**, 197 (1953);
S. I. Pekar and M. A. Krivoplaz, Trudy Inst. Fiz., Akad. Nauk Ukr.SSR, No. 4, 37 (1953);
A. F. Lubchenko, Opt. i Spektr. **2**, 388 (1957).
11. Huang Kun and A. Rhys, Proc. Roy. Soc. **A204**, 406 (1950);
R. Kubo and Y. Toyozawa, Progr. Theoret. Phys. (Kyoto) **13**, 160 (1955). (Translation in collection: Problemy fiziki poluprovodnikov (Problems of the Physics of Semiconductors). Izd. Inostrannoi Lit., Moscow, 1957.)
12. Ya. Ya. Kirs, Trudy Inst. Fiz. i Astron., Akad. Nauk Eston.SSR, No. 4, 108 (1956);
Ya. Ya. Kirs and A. I. Laisaar, Dokl. na VII Soveshyh. po Luminests. (Paper given at the VII Conference on Luminescence), Moscow, 1958.
13. P. Johnson and F. Williams, Phys. Rev. **93**, 69 (1954).
14. I. Jacobs, Phys. Rev. **93**, 993 (1954);
R. Eppler and H. Drickamer, J. Phys. Chem. Solids **6**, 180 (1958).
15. N. N. Kristofel', Trudy Inst. Fiz. i Astron., Akad. Nauk Eston.SSR, No. 10, 43 (1959).
16. N. E. Lushchik, Trudy Inst. Fiz. i Astron., Akad. Nauk Eston.SSR, No. 7, 119 (1958); Ibid., No. 10, 68 (1959);
I. K. Plyavin', Opt. i Spektr. **4**, 266 (1958).

EFFECT OF VIBRATIONS ON THE FORBIDDEN TRANSITIONS IN A MOLECULE

A. M. Meleshina

Received 11 January 1960

The oscillator strength of the 2600 A benzene band has been calculated; this band is normally forbidden, but is allowed by an E_g^+ vibration. To determine the wave function used to construct the matrix element, the Schrödinger equation is solved by the small parameter method of Bogoliubov. Satisfactory agreement with experiment is obtained.

In the electronic spectra of molecules some forbidden bands are observed which are made possible by the influence of atomic vibrations on the electronic states. In particular, the 2600 A band in the vapor spectrum of benzene, according to Craig,[1] is to be explained as due to the influence of an E_g^+ vibration. A calculation of the oscillator strength corresponding to this band was first performed by Craig,[1] who used a method of perturbation theory, but Sponer and Herzfeld[2] showed that his results were erroneous. Sponer and Herzfeld calculated the oscillator strength of the forbidden transition made possible by the vibration $\omega = 521$ cm^{-1}; they used a series expansion of the electronic wave function in terms of the normal coordinates of the nuclear displacements, and obtained a value 700 times smaller than the experimental value. Besides, according to their calculations, an oscillator strength of the same order of magnitude as that due to the vibration $\omega = 521$ cm^{-1} results from the vibration $\omega = 1572$ cm^{-1}; the observations of Garforth and Ingold[3] show, however, that either this vibration is inactive or it gives a very weak band.

In this paper another method of calculating the influence of molecular vibrations on the wave functions is proposed. The method is applied to the calculation of the oscillator strength of the forbidden 2600 A band of benzene. It is assumed that the π-electrons are responsible for the transition. The calculation is carried out in the one-electron approximation.

Let $\mathbf{r}$ be the radius vector, Q the normal coordinate of the E_g^+ vibration, and $\Phi(\mathbf{r},Q)$ the wave function of the electron and of the rest atom (of the oscillator). The Schrödinger equation for $\Phi(\mathbf{r},Q)$ is written in the form

$$-\frac{\hbar^2}{2\mu}\nabla^2\Phi - \frac{\hbar^2}{2M}\nabla_Q^2\Phi + U\Phi = E\Phi. \qquad (1)$$

Here μ is the mass of the electron, M the mass of the oscillator, U is the operator of the potential energy equal to the sum $U = U_1(\mathbf{r},Q) + U_2(Q)$ where U_1 is the potential energy of the electron in the field of the rest atom and of the other electrons, and U_2 is the potential energy of the oscillator. The eigenvalue $E = E_{electron} + E_{osc.}$

According to Goeppert-Mayer and Sklar[4] the state of the π-electron (without participation of the vibration) is described by the wave function

$$\Psi_l = (6\sigma_l)^{-\frac{1}{2}} \sum_{k=1}^{6} e^{\frac{2\pi i l}{6}k}\,\psi_2, \qquad (2)$$

where

$$\psi_2 = \left(\frac{\alpha^5}{32\pi}\right)^{\frac{1}{2}} e^{-\frac{\alpha}{2}r_k} z_k.$$

is the solution of the Schrödinger equation

$$-\frac{\hbar^2}{2\mu}\nabla^2\Psi_l + U_1\Psi_l = E_{el.}\Psi_l. \qquad (3)$$

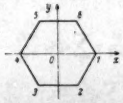

The subscript k in x_k and r_k is used to indicate that the origin of the coordinate system is taken at the center of the k-th carbon atom. Choosing, for instance, the origin of the coordinate system at the center of the benzene ring (see figure), we obtain $x_1 = x - R$, $y_1 = y$, $x_2 = x - R/2$, $y_2 = y - (\sqrt{3}/2)R$, $z_k = x$, etc., where R is the distance between neighboring carbon atoms. In the general case these formulas can be written in the form $x_k = x - a_k$, $y_k = y - b_k$. Transitions are forbidden between states for which $l = -1$ and $l = 2$, or $l = 1$ and $l = -2$

$$z_2 = z - a_2, \quad y_2 = y - b_2.$$

We shall try to find a solution of Eq. (1) in the form

$$\Phi_l = \varphi\Psi_l(1 + F_l), \qquad (4)$$

where φ satisfies the equation

$$-\frac{\hbar^2}{2M}\nabla_Q^2\varphi + U_{el}\varphi = E_{osc.}\varphi. \qquad (5)$$

Substituting Eq. (4) into Eq. (1), and taking into consideration Eqs. (3) and (5), we obtain

$$-\frac{\hbar^2}{2\mu}\varphi\Psi_l\nabla^2 F_l - \frac{\hbar^2}{2\mu}2\nabla\varphi\Psi_l\nabla F_l - \frac{\hbar^2}{2M}\varphi(1+E_l)\nabla_Q^2\Psi_l$$
$$-\frac{\hbar^2}{2M}\varphi\Psi_l\nabla_Q^2 F_l - \frac{\hbar^2}{2M}2\nabla\varphi_Q\Psi_l\nabla_Q F_l - \frac{\hbar^2}{2M}2\Psi_l\nabla_Q\varphi\nabla_Q F_l$$
$$-\frac{\hbar^2}{2M}2(1+F_l)\nabla_Q\varphi\nabla_Q\Psi_l = 0. \qquad (6)$$

According to Craig,[1] we have for the E_g^+ vibration

$$\rho_1 dQ = dx_1; \quad \sigma_1 dQ = dy_1;$$
$$(\rho_2\cos 60° - \sigma_2\cos 30°)\,dQ = dx_2; \quad (\rho_2\cos 30° + \sigma_2\sin 30°)\,dQ = dy_2;$$
$$(-\rho_3\cos 60° - \sigma_3\cos 30°)\,dQ = dx_3; \quad (\rho_3\cos 30° - \sigma_3\sin 30°)\,dQ = dy_3;$$
$$\rho_4 dQ = dx_4; \quad -\sigma_4 dQ = dy_4;$$
$$(-\rho_5\cos 60° + \sigma_5\cos 30°)\,dQ = dx_5; \quad (-\rho_5\cos 30° - \sigma_5\sin 30°)\,dQ = dy_5;$$
$$(\rho_6\cos 60° + \sigma_6\cos 30°)\,dQ = dx_6; \quad (-\rho_6\cos 30° + \sigma_6\sin 30°)\,dQ = dy_6;$$

$$\frac{\rho_k}{\rho} = 0, -1, 1, 0, -1, 1; \quad 2\frac{\sigma_k}{\sigma} = -2, 1, 1, -2, 1, 1;$$

for the vibration $\omega = 521$ cm^{-1} we have $\rho = 0.9$, $\sigma = -0.25$, and for the vibration $\omega = 1572$ cm^{-1}, $\rho = 0.44$, $\sigma = 0.52$.

Let us define

$$z_k \equiv \frac{dx_k}{dQ}, \quad b_k \equiv \frac{dy_k}{dQ}, \quad a_k^{(l)} \equiv (6\sigma_l)^{-\frac{1}{2}} e^{\frac{2\pi i l}{6}k}$$

Then

$$\nabla_0\Psi_i=\sum_k a_k^{(i)}\left(\frac{\partial\psi_k}{\partial x}\varepsilon_k+\frac{\partial\varphi_k}{\partial y}\delta_k\right);$$

$$\nabla_0^2\Psi_i=\sum_k a_k^{(i)}\left(\frac{\partial^2\psi_k}{\partial x^2}\varepsilon_k^2+2\,\frac{\partial\psi_k}{\partial x}\,\frac{\partial\varphi_k}{\partial y}\varepsilon_k\delta_k+\frac{\partial^2\varphi_k}{\partial y^2}\delta_k^2\right).$$

Substituting these expressions into Eq. (6), we have

$$-\frac{\hbar^2}{2\mu}\varphi\sum_k a_k^{(i)}\psi_k\nabla^2 F_i-\frac{\hbar^2}{2M}2\varphi\left(\frac{\partial F_i}{\partial x}\sum_k a_k^{(i)}\frac{\partial\psi_k}{\partial x}+\frac{\partial F_i}{\partial y}\sum_k a_k^{(i)}\frac{\partial\varphi_k}{\partial y}\right.$$

$$\left.+\frac{\partial F_i}{\partial z}\sum_k a_k^{(i)}\frac{\partial\psi_k}{\partial z}\right)-\frac{\hbar^2}{2M}\varphi(1+F_i)\sum_k a_k^{(i)}\left(\frac{\partial^2\psi_k}{\partial x^2}\varepsilon_k^2+2\,\frac{\partial\psi_k}{\partial x}\,\frac{\partial\varphi_k}{\partial y}\varepsilon_k\delta_k\right.$$

$$\left.+\frac{\partial^2\varphi_k}{\partial y^2}\delta_k^2\right)-\frac{\hbar^2}{2M}\varphi\sum_k a_k^{(i)}\psi_k\frac{\partial^2 F_i}{\partial Q^2}-\frac{\hbar^2}{2M}2\varphi\frac{\partial F_i}{\partial Q}$$

$$\times\left(\sum_k a_k^{(i)}\frac{\partial\psi_k}{\partial x}\varepsilon_k+\sum_k a_k^{(i)}\frac{\partial\varphi_k}{\partial y}\delta_k\right)-\frac{\hbar^2}{2M}2\sum_k a_k^{(i)}\psi_k\frac{\partial\varphi}{\partial Q}\frac{\partial F}{\partial Q}$$

$$-\frac{\hbar^2}{2M}2(1+F_i)\frac{d\varphi}{dQ}\left(\sum_k a_k^{(i)}\frac{\partial\psi_k}{\partial x}\varepsilon_k+\sum_k a_k^{(i)}\frac{\partial\varphi_k}{\partial y}\delta_k\right)=0. \quad (7)$$

We shall try to find F_i in the form

$$F_i=\sum_k(\varepsilon_k f_k+\delta_k g_k)+\text{terms containing higher powers of }\varepsilon\text{ and }\delta.$$

Substituting this expression into Eq. (7), and equating the coefficients of the first powers of ε_k and δ_k to zero, we obtain (see, for instance, ref. 5)

$$-\frac{\hbar^2}{2\mu}\varphi\Psi_i\nabla^2 f_k-\frac{\hbar^2}{2M}2\varphi\left[\left(\sum_m a_m^{(i)}\frac{\partial\psi_m}{\partial x}\right)\frac{\partial f_k}{\partial x}+\left(\sum_k a_m^{(i)}\frac{\partial\psi_m}{\partial y}\right)\frac{\partial f_k}{\partial y}\right.$$

$$\left.+\left(\sum_k a_m^{(i)}\frac{\partial\psi_m}{\partial z}\right)\frac{\partial f_k}{\partial z}\right]-\frac{\hbar^2}{2M}\varphi\Psi_i\frac{\partial f_k}{\partial Q^2}-\frac{\hbar^2}{2M}2\Psi_i\frac{d\varphi}{dQ}\frac{\partial f_k}{\partial Q}$$

$$-\frac{\hbar^2}{2M}2\frac{d\varphi}{dQ}a_k^{(i)}\frac{\partial\psi_k}{\partial x}=0; \quad (8a)$$

$$-\frac{\hbar^2}{2M}\varphi\Psi_i\nabla^2 g_k-\frac{\hbar^2}{2M}2\varphi\left[\left(\sum_m a_m^{(i)}\frac{\partial\psi_m}{\partial x}\right)\frac{\partial g_k}{\partial x}+\left(\sum_m a_m^{(i)}\frac{\partial\psi_m}{\partial y}\right)\frac{\partial g_k}{\partial y}\right.$$

$$\left.+\left(\sum_m a_m^{(i)}\frac{\partial\psi_m}{\partial z}\right)\frac{\partial g_k}{\partial z}\right]-\frac{\hbar^2}{2M}\varphi\Psi_i\frac{\partial^2 g_k}{\partial Q^2}-\frac{\hbar^2}{2M}2\Psi_i\frac{d\varphi}{dQ}\frac{\partial g_k}{\partial Q}$$

$$-\frac{\hbar^2}{2M}2\frac{d\varphi}{dQ}a_k^{(i)}\frac{\partial\psi_k}{\partial y}=0. \quad (8b)$$

Equating to zero the coefficients of the higher powers of ε and δ, we obtain equations which enable us to determine the terms in the expressions for F_i containing these higher powers. It is easy to see that these terms are several orders of magnitude smaller than the first order terms in ε and δ, and can thus be left out of consideration in the expressions for F_i.

For different k, the equations (8a) and (8b) differ only in the factors $\alpha_k^{(i)}$. Introducing, therefore,

$$f_k=a_k^{(i)}f_i(x_k),\qquad g_k=a_k^{(i)}g_i(x_k),$$

we obtain altogether two equations for the determination of $f_i(x)$ and $g_i(x)$:

$$\nabla^2 f_i+2\lambda\left(\frac{\partial f_i}{\partial x}\frac{1}{\Psi_i}\frac{\partial\Psi_i}{\partial x}+\frac{\partial f_i}{\partial y}\frac{1}{\Psi_i}\frac{\partial\Psi_i}{\partial y}+\frac{\partial f_i}{\partial z}\frac{1}{\Psi_i}\frac{\partial\Psi_i}{\partial z}\right)$$

$$+\lambda\frac{\partial^2 f_i}{\partial Q^2}+2\lambda\frac{\varphi'}{\varphi}\frac{\partial f_i}{\partial Q}=-2\lambda\frac{\varphi'}{\varphi}\frac{1}{\Psi_i}\frac{\partial\Psi_i}{\partial x}; \quad (9a)$$

$$\nabla^2 g_i+2\lambda\left(\frac{\partial g_i}{\partial x}\frac{1}{\Psi_i}\frac{\partial\Psi_i}{\partial x}+\frac{\partial g_i}{\partial y}\frac{1}{\Psi_i}\frac{\partial\Psi_i}{\partial y}+\frac{\partial g_i}{\partial z}\frac{1}{\Psi_i}\frac{\partial\Psi_i}{\partial z}\right)$$

$$+\lambda\frac{\partial^2 g_i}{\partial Q^2}+2\lambda\frac{\varphi'}{\varphi}\frac{\partial g_i}{\partial Q}=-2\lambda\frac{\varphi'}{\varphi}\frac{1}{\Psi_i}\frac{\partial\Psi_i}{\partial y}. \quad (9b)$$

where $\lambda=\mu/M$.

Let us consider the transition from the first excited state φ_1 into the ground state φ_0. Then

$$\frac{\varphi_1'}{\varphi_1}=\frac{1}{Q}-\frac{Q}{Q_0^2},\qquad \frac{\varphi_0'}{\varphi_0}=-\frac{Q}{Q_0^2},$$

where

$$Q_0=\sqrt{\frac{\hbar}{M\nu_{\text{vibr.}}}}.$$

Using these expressions in Eq. (9a), one obtains, for instance, for the ground state (omitting now the subscripts 1)

$$\nabla^2 f+2\lambda\left(\frac{\partial f}{\partial x}\frac{1}{\Psi}\frac{\partial\Psi}{\partial x}+\frac{\partial f}{\partial y}\frac{1}{\Psi}\frac{\partial\Psi}{\partial y}+\frac{\partial f}{\partial z}\frac{1}{\Psi}\frac{\partial\Psi}{\partial z}\right)$$

$$+\lambda\frac{\partial^2 f}{\partial Q^2}-2\lambda\frac{Q}{Q_0^2}\frac{\partial f}{\partial Q}=2\lambda\frac{Q}{Q_0^2}\frac{1}{\Psi}\frac{\partial\Psi}{\partial x}.$$

We look for a solution of this equation in the form $f=a(x,y,z)Q+b(x,y,z)$. Substituting this expression into the equation, and equating to zero the coefficients of the zeroth and first order in Q, we obtain

$$\nabla^2 a+2\lambda\left(\frac{\partial a}{\partial x}\frac{1}{\Psi}\frac{\partial\Psi}{\partial x}+\frac{\partial a}{\partial y}\frac{1}{\Psi}\frac{\partial\Psi}{\partial y}+\frac{\partial a}{\partial z}\frac{1}{\Psi}\frac{\partial\Psi}{\partial z}\right) \quad (10)$$

$$-\frac{2\lambda}{Q_0^2}a=\frac{2\lambda}{Q_0^2}\frac{1}{\Psi}\frac{\partial\Psi}{\partial x};$$

$$\nabla^2 b+2\lambda\left(\frac{\partial b}{\partial x}\frac{1}{\Psi}\frac{\partial\Psi}{\partial x}+\frac{\partial b}{\partial y}\frac{1}{\Psi}\frac{\partial\Psi}{\partial y}+\frac{\partial b}{\partial z}\frac{1}{\Psi}\frac{\partial\Psi}{\partial z}\right)=0. \quad (11)$$

Equation (11) is fulfilled by the solution b = const. This constant can be determined from the normalization condition for Φ_1. If it is assumed that

$$\int|\varphi\Psi_i|^2\,dQ\,dx\,dy\,dz=1$$

(this can be done, considering that, approximately, φ and Ψ_1 can be taken with the normalization coefficients appearing in the problem where the vibration is ignored), then b can simply be put equal to zero.

The solution of Eq. (10) can be approximately represented in the form

$$a=-\frac{1}{\Psi}\frac{\partial\Psi}{\partial x}.$$

The error committed when this is done amounts to the neglect in Eq. (10) of the term

$$Q_0^2\left[\nabla^2 a+2\lambda\left(\frac{\partial a}{\partial x}\frac{1}{\Psi}\frac{\partial\Psi}{\partial x}+\frac{\partial a}{\partial y}\frac{1}{\Psi}\frac{\partial\Psi}{\partial y}+\frac{\partial a}{\partial z}\frac{1}{\Psi}\frac{\partial\Psi}{\partial z}\right)\right].$$

which has the order of magnitude $Q_0^2\sim 10^{-20}$; this is very much smaller than the term $(\lambda/\Psi)(\delta\Psi/\delta x)$ which has the order of magnitude $\lambda\sim 10^{-3}$.

It is not difficult to see that for $\varphi=\varphi_1$ exactly the same estimates are obtained, and the approximate solution of Eq. (9a) appears in the same form as the solution of Eq. (10).

Thus

$$f=-\frac{1}{\Psi}\frac{\partial\Psi}{\partial x}Q,\qquad g=-\frac{1}{\Psi}\frac{\partial\Psi}{\partial y}Q.$$

and the desired wave function is

$$\Phi_l = \psi\Psi_l - \psi Q\left[\sum_k \varepsilon_k a_k^{(l)}\frac{\partial\psi_k}{\partial x} + \sum_k \mathfrak{d}_k a_k^{(l)}\frac{\partial\psi_k}{\partial y_k}\right].$$

The matrix element of the dipole moment in the direction of the x-axis, which acts on the charge of the electron, can be written in the form

$$\frac{M_x}{e} = \int \Phi_{l_1}^* x \Phi_{l_2}\, dQdxdydz$$

$$= -\int \psi_1^* \Psi_{l_1}^* Q\psi_0 x\left[\sum_k \varepsilon_k a_k^{(l_2)}\frac{\partial\psi_k}{\partial x} + \sum_k \mathfrak{d}_k a_k^{(l_2)}\frac{\partial\psi_k}{\partial y}\right] dQdxdydz$$

$$-\int \psi_1^* Q\psi_0 \Psi_{l_2} x\left[\sum_k \varepsilon_k a_k^{(l_1)*}\frac{\partial\psi_k^*}{\partial x} + \sum_k \mathfrak{d}_k a_k^{(l_1)*}\frac{\partial\psi_k^*}{\partial y}\right] dQdxdydz.$$

In an analogous way one can write the expression for M_y/e:

$$\int \psi_1^* Q\psi_0 dQ = Q_0.$$

Substituting into the expression for the matrix element the wave function Ψ_1 in explicit form, we obtain

$$\frac{M_x}{e} = -Q_0 \cdot 2\left[\sum_k a_k^{(l_2)*} a_k^{(l_1)} \varepsilon_k \int \psi_k^* x \frac{\partial\psi_k}{\partial z}\, dxdydz\right.$$

$$+\sum_k a_k^{(l_2)*} a_k^{(l_1)} \mathfrak{d}_k \int \psi_k^* x \frac{\partial\psi_k}{\partial y}\, dxdydz + \sum_{k\neq m}\sum a_k^{(l_2)*} a_m^{(l_1)} \varepsilon_m \int \psi_k^* x \frac{\partial\psi_m}{\partial x}\, dxdydz$$

$$\left. + \sum_{k\neq m}\sum a_k^{(l_2)*} a_m^{(l_1)} \mathfrak{d}_m \int \psi_k^* x \frac{\partial\psi_m}{\partial y}\, dxdydz\right].$$

Let us now evaluate the required integrals:

$$\int \psi_k^* x \frac{\partial\psi_k}{\partial x}\, dxdydz = \int \psi_k^* x_k \frac{\partial\psi_k}{\partial x}\, dxdydz + a_k \int \psi_k^* \frac{\partial\psi_k}{\partial x}\, dxdydz;$$

$$\int \psi_k^* \frac{\partial\psi_k}{\partial x}\, dxdydz = \frac{z_0^2}{32\pi}\int e^{-\frac{r_k'^2}{2}} z_k e^{-\frac{r_k'^2}{2}}\left(1 - \frac{z_0}{2}\frac{z_k'^2}{r_k'}\right) dxdydz = 0;$$

$$\int \psi_k^* x_k \frac{\partial\psi_k}{\partial x}\, dxdydz = 2.5;$$

$$\int \psi_k^* y_k \frac{\partial\psi_k}{\partial y}\, dxdydz = 0.5;$$

$$\int \psi_k^* y_k \frac{\partial\psi_k}{\partial x}\, dxdydz = \int \psi_k^* x_k \frac{\partial\psi_k}{\partial y}\, dxdydz = \int \psi_k^* z_k \frac{\partial\psi_k}{\partial x}\, dxdydz$$

$$= \int \psi_k^* z_k \frac{\partial\psi_k}{\partial y}\, dxdydz = 0.$$

The integrals in the double sums depend only on the magnitudes of the differences k – m. According to Eq. (7)

$$\begin{aligned} \varepsilon_1 &= \varepsilon_4, \quad \varepsilon_2 = -\varepsilon_5 = \varepsilon_3 = -\varepsilon_6, \\ \mathfrak{d}_1 &= -\mathfrak{d}_4, \quad \mathfrak{d}_2 = -\mathfrak{d}_5 = -\mathfrak{d}_3 = \mathfrak{d}_6. \end{aligned} \tag{12}$$

for $l = \pm 2$

$$a_k^{(\pm 2)*} = (6\sigma_{\pm 2})^{-\frac{1}{2}} e^{\mp\frac{4\pi i}{6}k}, \quad a_1^{(\pm 2)*} = a_4^{(\pm 2)*},$$

$$a_2^{(\pm 2)*} = a_5^{(\pm 2)*}, \quad a_3^{(\pm 2)*} = a_6^{(\pm 2)*};$$

for $l = \mp 1$

$$a_k^{(\mp 1)} = (6\sigma_{\mp 1})^{-\frac{1}{2}} e^{\mp\frac{2\pi i}{6}k}, \quad a_1^{(\mp 1)} = -a_4^{(\mp 1)},$$

$$a_2^{(\mp 1)} = -a_5^{(\mp 1)}, \quad a_3^{(\mp 1)} = -a_6^{(\mp 1)}.$$

Taking into consideration all these relations, one can easily convince oneself that the double sums for $m \neq k$ vanish.

For the transition $l = +2$ to $l = -1$,

$$\frac{M_x}{e} = -2Q_0 \sum_k a_k^{(2)*} a_k^{(-1)} \varepsilon_k \cdot 2.5 = 0.$$

For the transition $l = -2$ to $l = 1$,

$$\frac{M_x}{e} = -2Q_0 \sum_k a_k^{(-2)*} a_k^{(1)} \varepsilon_k \cdot 2.5 = 0.$$

For the vibration $\omega = 521\ \text{cm}^{-1}$, according to Eq. (7),

$$\mathfrak{d}_1 = 0.25, \quad \mathfrak{d}_2 = -0.9\frac{\sqrt{3}}{2} - \frac{1}{4}\cdot 0.25.$$

Then

$$\frac{M_y^{(1)}}{e} = -\frac{2Q_0 \cdot 0.5}{6\,(\sigma_2)^{\frac{1}{2}}\,(\sigma_{-1})^{\frac{1}{2}}}\sum_k e^{-\frac{4\pi i}{6}k} e^{-\frac{2\pi i}{6}k}\mathfrak{d}_k$$

and

$$\frac{M_y^{(2)}}{e} = -\frac{2Q_0 \cdot 0.5}{6\,(\sigma_{-2})^{\frac{1}{2}}\,(\sigma_1)^{\frac{1}{2}}}\sum_k e^{\frac{4\pi i}{6}k} e^{\frac{2\pi i}{6}k}\mathfrak{d}_k.$$

According to ref. 4, $\sigma_1 = 1 + 2s_1\cos(2\pi l/6) + 2s_2\cos(4\pi l/6) + (-1)^l s_3$ where $s_1 = 0.26$, $s_2 = 0.4$, $s_3 = 0.2$. Then $\sigma_2 = \sigma_{-2} = 0.54$, $\sigma_{-1} = \sigma_1 = 0.66$, and

$$\frac{M_y^{(1)}}{e} = -\frac{2Q_0 \cdot 0.5}{6\,(0.54)^{\frac{1}{2}}\,(0.66)^{\frac{1}{2}}}\cdot 3.86, \quad \frac{M_y^{(2)}}{e} = \frac{2Q_0 \cdot 0.5}{6\,(0.54)^{\frac{1}{2}}\,(0.66)^{\frac{1}{2}}}\cdot 3.86.$$

It follows that for the vibration $\omega = 521\ \text{cm}^{-1}$

$$\frac{|M|^2}{e^2} = \frac{Q_0^2 (3.86)^2}{36 \cdot 0.54 \cdot 0.66}.$$

According to ref. 2, the oscillator mass $M = 73.37 \times 10^{-24}$ gm, so that $Q_0 = 2.7 \times 10^{-10}$ cm. Then

$$\frac{|M|^2}{e^2} = 8.6 \cdot 10^{-20}.$$

The oscillator strength

$$f = \frac{8\pi^2 m_\mu}{3e^2 k}\,|M|^2 \nu_{\text{osc}}.$$

Since in our case two transitions are allowed ($l = 2$ to $l = -1$, and $l = -2$ to $l = 1$), and two electrons can participate in each of them, this value of f should still be multiplied by a factor 4.

For the transition made possible by the vibration $\omega = 521\ \text{cm}^{-1}$ we obtain finally

$$f = 4 \cdot 4 \cdot 10^{15} \cdot 8.4 \cdot 10^{-20} = 1.3 \cdot 10^{-3}.$$

The experimental value of the oscillator strength is 1.6×10^{-3}.

Let us calculate the oscillator strength for the vibration $\omega = 1572\ \text{cm}^{-1}$. According to ref. 2, in this case $\delta_1 = -0.52$, $\delta_2 = -0.22\sqrt{3} + (1/4)(0.52)$. Then

$$\frac{M_y^{(1)}}{e} = -\frac{2Q_0 \cdot 0.5}{6\,(\sigma_2)^{\frac{1}{2}}\,(\sigma_{-1})^{\frac{1}{2}}}\cdot 0.04; \quad \frac{M_y^{(2)}}{e} = \frac{2 \cdot Q_0 \cdot 0.5}{6\,(\sigma_{-2})^{\frac{1}{2}}\,(\sigma_1)^{\frac{1}{2}}}\,0.04,$$

$$Q_0 = \frac{2.7}{\sqrt{3}}\,10^{-10}\ \text{cm};$$

$$\frac{|M|^2}{e^2} = 0.0003 \cdot 10^{-20}.$$

With these values one obtains the oscillator strength $f = 0.0048 \times 10^{-5}$; that is, a very small value in agreement with the data of ref. 3.

REFERENCES

1. D. Craig, J. Chem. Soc. p. 59 (1950).
2. H. Sponer and K. Herzfeld, Z. Physik 133, 41 (1952).
3. F. Garforth, C. Ingold, and H. Pooll, J. Chem. Soc. p. 406 (1948).
4. M. Goeppert-Mayer and A. Sklar, J. Chem. Phys. 6, 645 (1938).
5. N. N. Bogoliubov, Lektsii z kvantovoi statistiki (Lectures on Quantum Statistics), Kiev, 1949.

THE FORM OF THE RAMAN TENSOR

L. N. Ovander

Received 8 February 1960

With the aid of group theory, the form of the Raman tensor for all the vibrations of a crystal, belonging to any of the 32 crystal classes, is obtained.

INTRODUCTION

The symmetry of a crystal imposes definite restrictions on different quantities, in particular on the form of the Raman tensor. A method is known[1] for finding the form of the Raman tensor; however, it has the following inadequacies: (a) the tensor is assumed symmetrical; (b) a polarizability theory is used which decreases the generality of the proof; (c) the rule for transformation of the normal coordinates, figuring in the polarizability theory, is not always clear; (d) the procedure is comparatively laborious; (e) the examination does not embrace all vibrational and symmetry types.

In the present work an effort is made to find the form of the Raman tensor, using group theory; such a method is free from the inadequacies stated above.

1. DETERMINATION OF THE RAMAN TENSOR WITH THE ASSISTANCE OF THE METHODS OF GROUP THEORY

The component in the x-direction of the dipole moment, produced in the crystal by the action of the incident light, is written in the form

$$p_x = a_{xy} E_y,$$

where E_γ is a component of the electric vector of the incident light,

$$a_{xy} = \int \Psi_0 \alpha_{xy} \Psi_k d\tau. \qquad (1)$$

is the Raman tensor, Ψ_0 is the wave function of the initial state, α_{xy} is one of the functions, transforming according to the so-called tensor representation (cf. ref. 2, p. 256), Ψ_k is the wave function of the final vibrational state. We will limit ourselves to an examination of sufficiently low temperatures where Ψ_0 can be considered a completely symmetrical function and Ψ_k the first excited vibrational state. The cases of temperatures different from zero, of overtones, of combination tones, and of some other questions will be examined in another part.

In order that (1) be different from zero, it is necessary that the expression under the integral contain a function transforming according to the completely symmetric irreducible representation. This is possible only when the function α_{xy} contains a function transforming according to that same irreducible representation as Ψ_k—one of the functions forming the basis of some irreducible representation.

Here the mistaken idea can arise that the function α_{xy} is symmetric regarding x and y. However, if that were so, then a_{xy} also would be symmetric, and that is not proved. Therefore, α_{xy} must be considered as a component of a nonsymmetric tensor.

Accordingly, a_{xy} will be different from zero in that case when α_{xy} has a projection on the function Ψ_k which is different from zero. The index k essentially contains two indexes: μ, the number of irreducible representations, and j, the number of functions, transforming according to this representation. The projection of the function α_{xy} on the function $\Psi_{j\mu}$ can be obtained using the operator function (ref. 3, p. 384):

$$(\alpha_{xy})_{j\mu} = \frac{l_\mu}{g} \sum_G G^{(\mu)}_{jj} G \alpha_{xy}. \qquad (2)$$

where G is an operation of symmetry, $G^{(\mu)}_{jj}$ are the matrix elements of the μ-th irreducible representation, and g is the order of the group. As a result of the application of the operation (2), we obtain an expression for $(\alpha_{xy})_{j\mu}$ through certain combinations of the α_{xy}.

In this manner $(\alpha_{xy})_{j\mu}$ is found for all values x and y with fixed $j\mu$.

In some cases we find that α_{xy} gives a projection equal to zero, then the corresponding a_{xy} will be zero; sometimes it happens that $(\alpha_{xy})_{j\mu}$ and some other $(\alpha_{uv})_{j\mu}$ are expressed by the same combination of α_{xy}. Then it is clear that the numerical values of a_{xy} and a_{uv} will equal one another.

We must carry out a resolution of α_{xy} into the base functions of the irreducible representations; for this it is necessary to know not just the character, but the total matrix of the irreducible representation. This is not a complicated task once we have chosen functions, for example, such as those indicated in ref. 3. In the case of groups containing threefold and sixfold axes of symmetry, the functions $\xi = x + iy$, $\eta = x - iy$ are used as a basis. Making the resolution indicated above, one can comment on the form of the tensor a_{xy}; some components will be equal to zero, others will be identical.

We also note here that the form of the polarizability tensor can be obtained; for this it is necessary to consider the function Ψ_k as completely symmetric.

The results of the calculations are shown in the Table. For the irreducible representations the symbols

applied in ref. 3 are used. Among the groups only those which do not contain inversions are taken. If it is necessary to take a group G, containing an inversion, which is described in the form of a direct product of the inversion into some group G_1: $G = G_1 \cdot I$, then one must use the results for the group G_1 and as the corresponding irreducible representations take the representations of type g. The group C_1 (no symmetry) is not given in the Table—for it the tensor has an arbitrary form. Only one representative of the totality of isomorphous forms is taken, since the tensors for the respective representations of the isomorphic groups are identical.

C_2

$$a_A = \begin{bmatrix} a_1 & a_2 & 0 \\ a_3 & a_4 & 0 \\ 0 & 0 & a_5 \end{bmatrix} \qquad a_B = \begin{bmatrix} 0 & 0 & a_6 \\ 0 & 0 & a_7 \\ a_8 & a_9 & 0 \end{bmatrix}$$

C_3

$$a_A = \begin{bmatrix} a_1 & a_2 & 0 \\ -a_2 & a_1 & 0 \\ 0 & 0 & a_3 \end{bmatrix} \quad a'_E = \begin{bmatrix} a_4 & ia_4 & a_5 \\ ia_4 & -a_4 & -ia_5 \\ a_6 & ia_6 & 0 \end{bmatrix} \quad a''_E = \begin{bmatrix} a_7 - ia_7 & a_8 \\ -ia_7 & a_7 & ia_8 \\ a_9 & ia_9 & 0 \end{bmatrix}$$

C_{2v}

$$a_{A_1} = \begin{bmatrix} a_1 & 0 & 0 \\ 0 & a_2 & 0 \\ 0 & 0 & a_3 \end{bmatrix} \qquad a_{A_2} = \begin{bmatrix} 0 & a_4 & 0 \\ a_5 & 0 & 0 \\ 0 & 0 & 0 \end{bmatrix}$$

$$a_{B_1} = \begin{bmatrix} 0 & 0 & a_6 \\ 0 & 0 & 0 \\ a_7 & 0 & 0 \end{bmatrix} \qquad a_{B_2} = \begin{bmatrix} 0 & 0 & 0 \\ 0 & 0 & a_8 \\ 0 & a_9 & 0 \end{bmatrix}$$

C_{3v}

$$a_{A_1} = \begin{bmatrix} a_1 & 0 & 0 \\ 0 & a_1 & 0 \\ 0 & 0 & a_2 \end{bmatrix} \qquad a_{A_2} = \begin{bmatrix} 0 & a_3 & 0 \\ -a_3 & 0 & 0 \\ 0 & 0 & 0 \end{bmatrix}$$

$$a'_E = \begin{bmatrix} a_4 - ia_4 & a_5 \\ -ia_4 & a_4 - ia_5 \\ a_6 - ia_6 & 0 \end{bmatrix} \quad a''_E = \begin{bmatrix} a_4 & ia_4 & a_5 \\ ia_4 & a_4 & ia_5 \\ a_6 & ia_6 & 0 \end{bmatrix}$$

C_4

$$a_A = \begin{bmatrix} a_1 & a_2 & 0 \\ -a_2 & a_1 & 0 \\ 0 & 0 & a_3 \end{bmatrix} \qquad a_B = \begin{bmatrix} a_4 & a_5 & 0 \\ a_5 - a_4 & 0 \\ 0 & 0 & 0 \end{bmatrix}$$

$$a'_E = \begin{bmatrix} 0 & 0 & a_6 \\ 0 & 0 - ia_6 \\ a_7 - ia_7 & 0 \end{bmatrix} \qquad a''_E = \begin{bmatrix} 0 & 0 & a_8 \\ 0 & 0 & ia_8 \\ a_9 & ia_9 & 0 \end{bmatrix}$$

C_6

$$a_A = \begin{bmatrix} a_1 & a_2 & 0 \\ -a_2 - a_1 & 0 \\ 0 & 0 & a_3 \end{bmatrix} \qquad a'_{E_1} = \begin{bmatrix} a_4 & a_5 & 0 \\ a_5 & a_4 & 0 \\ 0 & 0 & 0 \end{bmatrix}$$

$$a''_{E_1} = \begin{bmatrix} a_5 - a_5 & 0 \\ -a_5 & a_5 & 0 \\ 0 & 0 & 0 \end{bmatrix} \quad a'_{E_2} = \begin{bmatrix} 0 & 0 & a_6 \\ 0 & 0 - ia_6 \\ a_8 - ia_8 & 0 \end{bmatrix} \quad a''_{E_2} = \begin{bmatrix} 0 & 0 & a_7 \\ 0 & 0 & ia_7 \\ a_8 & ia_8 & 0 \end{bmatrix}$$

C_{4v}

$$a_{A_1} = \begin{bmatrix} a_1 & 0 & 0 \\ 0 & a_1 & 0 \\ 0 & 0 & a_2 \end{bmatrix} \qquad a_{A_2} = \begin{bmatrix} 0 & a_3 & 0 \\ -a_3 & 0 & 0 \\ 0 & 0 & 0 \end{bmatrix} \qquad a_{B_1} = \begin{bmatrix} a_4 & 0 & 0 \\ 0 - a_4 & 0 \\ 0 & 0 & 0 \end{bmatrix}$$

$$a_{B_2} = \begin{bmatrix} 0 & a_5 & 0 \\ a_5 & 0 & 0 \\ 0 & 0 & 0 \end{bmatrix} \qquad a'_E = \begin{bmatrix} 0 & 0 & a_6 \\ 0 & 0 & 0 \\ a_7 & 0 & 0 \end{bmatrix} \qquad a''_E = \begin{bmatrix} 0 & 0 & 0 \\ 0 & 0 & a_8 \\ 0 & a_7 & 0 \end{bmatrix}$$

D_6

$$a_{A_1} = \begin{bmatrix} a_1 & 0 & 0 \\ 0 & a_1 & 0 \\ 0 & 0 & a_2 \end{bmatrix} \qquad a_{A_2} = \begin{bmatrix} 0 & a_3 & 0 \\ -a_3 & 0 & 0 \\ 0 & 0 & 0 \end{bmatrix} \qquad a'_{E_1} = \begin{bmatrix} 0 & 0 & a_4 \\ 0 & 0 & 0 \\ a_5 & 0 & 0 \end{bmatrix}$$

$$a''_{E_1} = \begin{bmatrix} 0 & 0 & 0 \\ 0 & 0 & a_4 \\ 0 & a_5 & 0 \end{bmatrix} \quad a'_{E_2} = \begin{bmatrix} a_6 & a_6 & 0 \\ a_6 & a_6 & 0 \\ 0 & 0 & 0 \end{bmatrix} \quad a''_{E_2} = \begin{bmatrix} a_6 - a_6 & 0 \\ -a_6 & a_6 & 0 \\ 0 & 0 & 0 \end{bmatrix}$$

T

$$a_A = \begin{bmatrix} a_1 & 0 & 0 \\ 0 & a_1 & 0 \\ 0 & 0 & a_1 \end{bmatrix} \qquad a'_E = \begin{bmatrix} a_2 & 0 & 0 \\ 0 & a_2 & 0 \\ 0 & 0 & a_2 \end{bmatrix} \qquad a''_E = \begin{bmatrix} a_3 & 0 & 0 \\ 0 & a_3 & 0 \\ 0 & 0 & a_3 \end{bmatrix}$$

$$a'_{F_1} = \begin{bmatrix} 0 & 0 & 0 \\ 0 & 0 & a_4 \\ 0 & a_4 & 0 \end{bmatrix} \qquad a''_{F_1} = \begin{bmatrix} 0 & 0 & a_5 \\ 0 & 0 & 0 \\ a_5 & 0 & 0 \end{bmatrix} \qquad a'''_F = \begin{bmatrix} 0 & a_5 & 0 \\ a_5 & 0 & 0 \\ 0 & 0 & 0 \end{bmatrix}$$

O

$$a_{A_1} = \begin{bmatrix} a_1 & 0 & 0 \\ 0 & a_1 & 0 \\ 0 & 0 & a_1 \end{bmatrix} \qquad a'_E = \begin{bmatrix} a_2 & 0 & 0 \\ 0 & a_2 & 0 \\ 0 & 0 & a_2 \end{bmatrix} \qquad a''_E = \begin{bmatrix} a_3 & 0 & 0 \\ 0 & a_3 & 0 \\ 0 & 0 & a_3 \end{bmatrix}$$

$$a'_{F_1} = \begin{bmatrix} 0 & 0 & 0 \\ 0 & 0 & a_4 \\ 0 - a_4 & 0 \end{bmatrix} \qquad a''_{F_1} = \begin{bmatrix} 0 & 0 & a_4 \\ 0 & 0 & 0 \\ -a_4 & 0 & 0 \end{bmatrix} \qquad a'''_{F_1} = \begin{bmatrix} 0 & a_4 & 0 \\ -a_4 & 0 & 0 \\ 0 & 0 & 0 \end{bmatrix}$$

$$a'_{F_2} = \begin{bmatrix} 0 & 0 & 0 \\ 0 & 0 & a_5 \\ 0 & a_5 & 0 \end{bmatrix} \qquad a''_{F_2} = \begin{bmatrix} 0 & 0 & a_5 \\ 0 & 0 & 0 \\ a_5 & 0 & 0 \end{bmatrix} \qquad a'''_{F_2} = \begin{bmatrix} 0 & a_5 & 0 \\ a_5 & 0 & 0 \\ 0 & 0 & 0 \end{bmatrix}$$

It is interesting to note that there exists an original "control method" which allows one to determine the number of independent components of a tensor, corresponding to a given vibration. Generalizing the method (ref. 2, p. 148) for the case of a nonunity representation we find that the number of independent components, corresponding to the representation, equals

$$S_\mu = \frac{1}{g} \sum_G \chi^*_\mu \chi_\sigma(G).$$

where χ_μ is the character of the irreducible μ-th representation and χ_σ the character of the tensor representation.

2. SOME POSSIBILITIES OF EXPERIMENTAL VERIFICATION

We will dwell now on the experimental verification of the results obtained. We will examine, as an example, a crystal with symmetry V. Let x, y, z be the coordinate axes of the laboratory system, u, v, w be the axes of the crystal (see Figure). Let an electromagnetic wave fall on the crystal in the direction x and let OM be the direction of polarization of this wave (OM lies in the yz plane). The orientation of the plane of polarization and the axes of the crystal is determined by the angles ψ and Φ. The scattered light is observed in the direction y, the scattering is caused by the vibration B_w. Then the intensity of the scattered light changes according to the law:

$$I \sim |a_{vv}|^2 \cos^2 \Phi \quad \text{for } \psi = 0,$$

$$I \sim |a_{vu}|^2 \cos^2 \Phi \quad \text{for } \psi = \frac{\pi}{2}.$$

For verification of the antisymmetry of the tensor a_{uv}, it is necessary to put $\Phi = 0$, $\psi = \pi/4$. If the intensity of the scattered light is different from zero, then a_{uv} is nonsymmetric, and if it equals zero then it is symmetric.

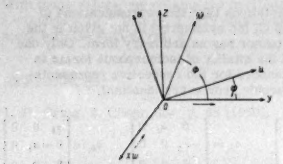

Location of the axes of the laboratory system of coordinates and of the system connected with the crystal.

Having examined the vibration B_u we find that the degree of depolarization is

$$\rho = \frac{I_z^y}{I_z^z} = \infty$$

for $\Phi - \psi \neq 0$. If $\psi = \Phi$, then there will be no scattering in the y-direction.

In a similar manner, one can make an investigation of an arbitrary case, such as may be encountered in practice. The general formula for the intensity of the scattered light for polarized irradiation is written in the form

$$I = \sum_{x=x_2,y_2} \sum_{u=x_1,y_1} \sum_{v=x_1,y_1} \beta_{zx} a_{uv} \gamma_{zu} \beta_{zm} a_{n_1 n_2} \gamma_{n_2 v} I_0,$$

where x_1, y_1, z_1 is a reference system connected with the source, z_1 is the direction of the incident radiation, x_1 the direction of polarization of the incident radiation, y_1 is the third Cartesian axis; u, v, u_1, v_1 are the variables running through a succession of values, x_2, y_2, z_2 the axes of the crystal, x_3, y_3, z_3 the reference system connected with the detector, z_3 the direction of the scattered radiation, γ the transformation coefficients for the transition from x_1, y_1, z_1 to x_2, y_2, z_2, and β the coefficients transforming from x_2, y_2, z_2 to x_3, y_3, z_3. I_0 is the intensity of the incident light.

The degree of depolarization is

$$\rho = \frac{\sum_{uvn_1v_1} \beta_{xu} a_{uv} \gamma_{zv} \beta_{xv_1} a^*_{n_1 v_1} \gamma_{n_2 v_1}}{\sum_{uvn_1v_1} \beta_{yu} a_{uv} \gamma_{zv} \beta_{xv_1} a^*_{n_1 v_1} \gamma_{n_2 v_1}}.$$

For nonpolarized radiation

$$I = \sum_{x=x_2,y_2} \sum_{y=x_2,y_2} \sum_{uv=x_1,y_1} \beta_{xu} a_{uv} \gamma_{zv} \beta_{zm_1} a_{n_1 v_1} \gamma_{n_2 y} \frac{I_0}{2},$$

$$\rho = \frac{\sum_{x=x_2,y_2} \sum_{uvv_1=x_1,y_1} \beta_{xu} a_{uv} \gamma_{zv} \beta_{xv_1} a_{n_1 v_1} \gamma_{n_2 y}}{\sum_{y=x_2,y_2} \sum_{uvv_1=x_1,y_1} \beta_{yu} a_{uv} \gamma_{zv} \beta_{xv_1} a_{n_1 v_1} \gamma_{n_2 y}}. \quad (5)$$

The asymmetry of the Raman tensor can also be studied with the help of the coefficient of rotation.[4] If we take vibration B_u of group V, then in the case of symmetry the components $a_{1,-1}$, $a_{-1,1}$ vanish, and this can be revealed experimentally.

In conclusion, the author expresses his thanks to V. L. Strizhevskii for a series of critical comments.

REFERENCES

1. J. P. Mathieu, "Spectres de vibration et symêtrie des molécules et cristaux." Hermann, Paris, 1945.
2. Ya. G. Lyubarskii, "Teoriya grupp i ee primenenie v fizike" (Group Theory and its Application to Physics). Gosudarst. Izd. Fiz.-Mat. Lit., Moscow, 1958.
3. L. Landau and E. Lifschitz, "Kvantovaya Mekhanika" (Quantum Mechanics). Gosudarst. Izd. Tekh.-Teoret. Lit., Moscow, Leningrad, 1948.
4. G. Placzek, "Releevskoe Rasseyanie i Raman-effekt" (Rayleigh Scattering and the Raman Effect). ONTI (United Scientific and Technical Press), NKTP, 1935.

SECOND-ORDER LINES IN THE RAMAN SPECTRA OF HYDROCARBONS

Yu. I. Naberukhin and M. M. Sushchinskii

Received 12 February 1960

The second-order Raman spectra of cyclohexane and tetramethylethylene are investigated. The intensities and degrees of depolarization of the second-order lines are measured. The intensities of these lines do not exceed 0.5-2 units. An interpretation of the observed lines is given and on its basis the anharmonicity coefficients are calculated. An interpretation agreeing with the selection rules can be given with the assumption that the magnitudes of the anharmonicity coefficients are 0.1-1% of the values of the corresponding frequencies.

In the carrying out of calculations of the vibrations of polyatomic molecules, values of force constants calculated on the basis of the observed values of the frequencies are used. However, due to the anharmonicities of the vibrations, the magnitudes of the observed frequencies do not coincide with the harmonic ones; accordingly, the applied force constants differ from the true ones, i.e., from those constants which would be found on the basis of the harmonic vibrations. In a series of works the anharmonicity is taken account of by the introduction of "spectroscopic masses" for hydrogen. Such a method assumes that the vibrations, in which the hydrogen atoms participate, make far the greatest contribution to the general anharmonicity. However, the latter is doubtful when one compares the anharmonicity coefficients of the CH vibrations in hydrocarbons[1] with the coefficients for heavy molecules, e.g., SO_3,[2] or CCl_4,[3] where these coefficients prove to be of the same order.

The most promising method of accounting for the anharmonicity would be the correction of the observed values of the frequencies of first-order lines using the anharmonicity coefficients obtained experimentally from data on second-order lines. For this extensive experimental information on the overtones is needed; however, this is available only for rather simple molecules (such as CCl_4, $SnBr_4$,[3,4] SO_3,[2] acetylene[5]).

In the present work an attempt is made to investigate second-order lines in the Raman spectra of hydrocarbons. The basic problem appears to be not so much the obtaining of complete data on the anharmonicities, but rather the clarifying of the possibility of measuring the parameters of second-order lines in Raman spectra and the interpretation of the spectra of sufficiently complex molecules. As subjects of the investigation, cyclohexane and tetramethylethylene (2,3-dimethylbutene-2) were chosen since these molecules possess a high symmetry (which simplifies the interpretation) and, in addition, calculations of the vibrations exist for them.

The investigation of second-order lines in the Raman spectra of liquids is extremely poorly represented in the literature. After the first works of Landsberg and Malyshev[4] and of Ananthakrishnan[5] there has appeared only the one work of Welsh, Crawford, and Scott[3] in which are given quantitative data on the frequencies, intensities, and degrees of depolarization of second-order lines for the molecules CCl_4, $SnCl_4$, and $SnBr_4$. Finally, quite limited data on overtones in the Molecules $TiCl_4$,[7] $CHCl_3$, $C_2H_2Cl_2$, $C_2H_4Cl_2$, CH_3OH, C_6H_5Cl, and CS_2[8] have been recently published.

The insignificant number of studies devoted to examination of second-order Raman lines is explained on the basis of the difficulties of the investigation, stipulated by the low intensity of these lines and by the necessity of separating them from the continuous background. However, with the increase in the use of low-pressure mercury lamps as sources the last difficulty can be considered to be eliminated to a considerable degree. Indeed, in work with high-pressure lamps, the level of the background is such that the minimum intensity of reliably recorded lines is of the order of 5 units[9] on a scale where the maximum intensity of the 802 cm^{-1} line of cyclohexane is taken as 250 (we will use this scale throughout the present work). Using low-pressure lamps of the Sosinskii type, we reliably measured for a series of cases line intensities of the order of 0.5. It should be noted that even this intensity does not appear to be the limiting one, since the background still disturbed the measurements only slightly. Thus, using low-pressure lamps, one can investigate lines with an intensity of the order of 0.1* with the aid of conventional methods.

*In working with high-pressure lamps it is possible to decrease significantly the level of the background by the application of interference filters. However, the exposure is then greatly increased. We applied this method for the control plates (the exclusion of weak mercury lines).

By far the greatest difficulty in our investigations concerned the separation of close, sometimes partially overlapping, lines. In particular, due to the presence of a large number of first-order lines in the 900-1460 cm^{-1} interval, this region proved difficultly accessible for investigation.

For the measurements of the intensities and depolarization ratios we used a two-prism Hilger spectrograph (relative aperture 1:1.5, dispersion 64 A/mm). With the use of a standard elliptical light source, one lamp and Agfa Raman-ortho plates, the exposure times necessary for the measurement of the intensities of second-order lines were 2-4 hr without filters and 6-10 hr with filters. The determination of the intensities was carried out by the conventional method of photographic photometry.[9] In this method in order to find the relative intensity of lines of the first and second order, photographs of the spectrum were made for a determined exposure time with a neutral filter, chosen in such a manner that the first and second-order lines being compared differed little in density, and the exposure times of the two pictures differed no more than a factor of two.

Table 1. Cyclohexane

$\Delta\nu$ (cm^{-1})	I_0	ρ	Interpretation and vibrational type	κ_{ik} (cm^{-1})
482	0.8	0.39	$2 \cdot 245 = 490$ $(A_{1g} + E_g)$	−4
527	0.3	0.47	γ A_{2u} aasup.	—
771	0.1 *	p	$2 \cdot 384 = 768$ (A_{1g})	1.5
785	2*	d ?	δ E_g	—
852	0.5 *	p	$2 \cdot 427 = 854$ $(A_{1g} + E_g)$	−1
905	0.5 *	p	β A_{2u} aasup.	—
1469	1*	—	$427 + 1029 = 1456$ $(A_{1g} + (A_{2g}) + E_g)$	6.5
1489	1*	—	$245 + 1259 = 1504$ $(A_{1g} + (A_{2g}) + E_g)$	−7.5
1540	0.8 ± 0.25	0.2 ± 0.04	$384 + 1158 = 1542$ (A_{1g})	−2
1574	1.2 ± 0.23	0.65 ± 0.12	$2 \cdot 785 = 1570$ $(A_{1g} + E_g)$	2
~1604	0.7	p	$2 \cdot 802 = 1604$ (A_{1g})	~0
~1642 ?	0.1 *	d	$384 + 1267 = 1651$ (E_g)	−4.5
1691	2.0 ± 0.26	0.67 ± 0.16	$427 + 1267 = 1694$ $(A_{1g} + (A_{2g}) + E_g)$ $245 + 1452 = 1697$ (E_g) $245 + 1452$ $E_u = 1697$ $(A_{1g} + (A_{2g}) + E_g)$	−6
~1722	1.2	0.47 ± 0.13	$2 \cdot 862 = 1724$ $(A_{1g} + E_g)$	−1
~1777	0.4 ± 0.15	0.28	$427 + 1348 = 1775$ $(A_{1g} + (A_{2g}) + E_g)$	−2
~1810	0.5 ± 0.13	0.42	$2 \cdot 905 = 1810$ (A_{1g})	~0
1870	1.0 ± 0.25	0.63 ± 0.15	$427 + 1445$ $(E_g) = 1872$ $(A_{1g} + (A_{2g}) + E_g)$	−2
1952	1.5 ± 0.4	0.67 ± 0.12	$525 + 1452$ $(A_{2u}) = 1977$ (A_{1g})	−25
1978	1.9 ± 0.4		$525 + 1452$ $(E_g) = 1977$ (E_g)	1
2056	1.4 ± 0.3	0.54 ± 0.11	$2 \cdot 1029 = 2058$ $(A_{1g} + E_g)$ $785 + 1267 = 2052$ $(A_{1g} + (A_{2g}) + E_g)$	−1 4
2119	1.0 ± 0.22	0.53 ± 0.09	$2 \cdot 1040 = 2080$ $(A_{1g} + E_g)$ $862 + 1259 = 2121$ $(A_{1g} + (A_{2g}) + E_g)$	19.5 −3
2162	1.5 ± 0.23	0.62 ± 0.11	$785 + 1348 = 2133$ $(A_{1g} + (A_{2g}) + E_g)$	29
2227 2254	2.7 ± 0.5	0.78 ± 0.16	$802 + 1445$ $(A_{1g}) = 2247$ (A_{1g}) $802 + 1445$ $(E_g) = 2247$ (E_g)	−20 7
2351 2374	3.4 ± 0.6 0.7 *	0.78 ± 0.12	$905 + 1452$ $(E_u) = 2357$ (E_g) $905 + 1452$ $(A_{2u}) = 2357$ (A_{1g})	−6 17
2458	3.5 ± 0.7	0.82 ± 0.16	$1029 + 1445$ $(A_{1g}) = 2474$ (E_g)	−16
2529	1.3 ± 0.33	0.58 ± 0.11	$2 \cdot 1259 = 2518$ $(A_{1g} + E_g)$	5.5
2581	1*	—	$2 \cdot 1287 = 2534$ $(A_{1g} + E_g)$	23.5
2635	6*	0.05		—
2667	32 ± 5	0.17 ± 0.08	$2 \cdot 1348 = 2496$ $(A_{1g} + E_g)$	—
2689	2*	—	$2 \cdot 1350 = 2700$ $(A_{1g} + E_g)$	—
2700	16 ± 5	0.33 ± 0.06		—

*The intensity was evaluated visually.

For the measurement of the degrees of depolarization we used the most luminous method of tubular polaroids, in which the aperture of the exciting light was not limited. The photographing in this case was carried out without filters, and the exposure time for each component was about 12 hr. Calibration of the arrangement was made with the CCl_4 spectrum.

A B-P spectrograph (relative aperture 1:4.7, dispersion 18 A/mm) was applied for the measurement of the frequencies. For the photographing, a light source with two lamps was used (with a $NaNO_2$ filter the exposures lasted 25-30 hr).

The characteristics of the Raman lines (frequency $\Delta\nu$, intensity at the maximum I_0, the degree of depolarization ρ) obtained are given in Tables 1 and 2. The error in the frequency measurements is ± 2 cm^{-1} (except for frequencies preceded by the symbol ~, the values of which were roughly determined from the microphotograms). The error for ρ consists of the mean-square error of the measurement and of the error introduced by the graphical calibration. The values of the intensities indicated by asterisks were determined by visual evaluation, obtained by means of a comparison with neighboring lines. In the case of tetramethylethylene, the error in the magnitudes of the intensities is about 50%.

In all of the measurements we paid particular attention to the exclusion of mercury lines and of first order Raman lines (from different exciting lines). In some cases this was not a simple problem.

Since the spectrum of tetramethylethylene has been studied only slightly, we present in Table 2 all of the frequencies which we observed. It should be noted that many of the lines observed by Goubeau,[10] and which should appear stronger than the overtones investigated in the present work, were not discovered by us (the frequencies 319,

Table 2. Tetramethylethylene†

$\Delta\nu$ (cm^{-1})	I_s	ρ	Interpretation and vibrational type	$\varkappa_{ik}$ (cm^{-1})
407	1	0.19 ± 0.04	A_{1g}	—
500	1	(0.7)	B_{3g}	—
685	1	(0.15)	A_g	—
795	—	0.24 ± 0.04	?	—
945	1	0.41 ± 0.08	A_g	—
1019	1	(0.77)	B_{1g}, B_{2g}	—
1064	1	(0.7)	B_{3g}	—
1262	1	(0.8)	B_{1g}	—
1366	1	—	B_{1g}	—
1390	1	(0.37)	A_g	—
1442	1	(0.78)	A_g, B_{1g}, B_{2g}, B_{3g}	—
1614	—	—		
1642	—	—	190 + 1447 = 1637 408 + 1265 = 1673	—
1668	1	(0.24)	A_g	—
1710	2*	—	688 + 1023 = 1711 (B_{1g}, B_{3g})	—1
1781	1.3	0.19 ± 0.14	315 + 1447 = 1762 (A_g, B_{2g}, B_{3g})	—1
~1890	0.24	p	2 · 946 = 1892 (A_g)	—1
~1973	0.26	p	2 · 979 = 1958 (A_g)	7.5
~2048	0.42	0.7 ± 0.27	2 · 1023 = 2046 (A_g) 1023 (B_{1g}) + 1023 (B_{3g}) = 2046 (B_{2g})	1 2
~2120	0.15	0.61 ± 0.34	971 + 1156 = 2127 (A_g)	—7
~2210	0.1*	0.58 ± 0.20	502 + 1672 = 2174 (A_g) 893 + 1370 = 2263 (A_g, B_{1g})	36 —53
2301	1.5	0.38 ± 0.14	2 · 1156 = 2312 (A_g)	—5.5
2358	2.2	0.48 ± 0.14	688 + 1672 = 2360 (A_g)	—7
2426	1.3	0.88 ± 0.25	1066 + 1366 = 2432 (B_{3g})	—6
2521	1.0	0.5 ± 0.38	1156 + 1370 = 2526 (A_g, B_{1g})	—5
2624	0.3*	0.83	1167 + 1447 = 2614 (A_g, B_{1g}, B_{3g}) 946 + 1672 = 2618 (A_g)	10 6
2657	0.3*	0.16	1265 + 1366 = 2631 (A_g)	26
2718	15*	0.15	2 · 1366 = 2732 (A_g) 2 · 1370 = 2740 (A_g)	— —
2858	1	—	—	—
2910	1	—	—	—
2986	1	—	—	—
3299	0.5*	—	2 · 1672 = 3344 (A_g)	—27.5

†First-order lines are denoted by the symbol 1.
*The intensity was evaluated visually.

597, 745, 821, 1148, 1309, and 2779 cm^{-1}).

An interpretation of the second-order spectra can be realized, starting from an interpretation of the fundamental frequencies. Such an interpretation is carried out for cyclohexane on the basis of the vibrational calculations of Beckett and co-workers,[11] of Sushchinskii,[12] and of Aleksandrov.[13] In general it agrees with experiment and needs further refinements at only two points. The calculation requires the presence of lines at about 800 cm^{-1} (E_g) and 200 cm^{-1} (E_u). In the 800 cm^{-1} region there has been observed till now only one line with the frequency 802 cm^{-1}, which is assigned to type A_{1g}. Therefore, the E_g line either coincides with the 802 cm^{-1} line or generally it is not observed. In the current work a line of frequency 785 cm^{-1}, which evidently is depolarized, was discovered close to the 802 cm^{-1} line. One may consider this line as the combination tone 384 + 427 = 811 (E_g) or 245 + 525 = 770 (E_g). However, taking into consideration that it is much more intense than neighboring second-order lines, we assumed that it is the fundamental line of type E_g.

The line at about 200 cm^{-1} is active only in the infrared spectrum, and has evidently not been observed directly. Larnaudie[14] gives the value of 238 cm^{-1} but without indication of the source; hence, his data require confirmation. Beckett, Pitzer, and Spitzer[11] are led to the value of 231 cm^{-1} on the basis of a thermodynamic calculation. It should be noted, however, that their calculation is based partially on factually inaccurate data, partially on unsubstantiated assumptions about the anharmonicity coefficients of the low frequencies. We carried out an analogous calculation, starting from our own data on the magnitudes of the anharmonicity coefficients. Then a value of 245 ± 4 cm^{-1} was obtained.*

*The inaccuracy in the frequency determination arises from the inaccuracy in the experimental determination of the heat capacity. Together with Beckett and coworkers we took account of the contribution of the chair-tub tautomerism to the heat capacity. If this is not done, then a value of the frequency of 250 cm^{-1} is obtained.

Table 3. Interpretation of the Fundamental Lines of Tetramethylethylene (frequencies in cm^{-1})

Experimental (Raman)	Calculated[12]	Experimental (infrared from ref. 17)	Calculated[12]
408	307 (A_g)	—	190 (B_{3u})
502	445 (B_{2g})	315	273 (B_{2u})
—	509 (B_{1g})	420	405 (B_{3u})
688	674 (A_g)	863	858 (B_{2u})
946	1007 (A_g)	971	976 (B_{2u})
1023	915 (B_{1g}) 959 (B_{3g})	1068	1035 (B_{1u}) 1179 (B_{3u})
1066	1038 (B_{2g})	1167	1193 (B_{2u})
1265	1301 (B_{1g})	1370	1379 (B_{3u})
1366	1379 (B_{1g})		1383 (B_{2u})
1393	1381 (A_g)	1447	1470 (B_{2u})
1442	1454 (A_g) 1471 (B_{1g}) 1473 (B_{3g}) 1485 (B_{2g})		1475 (B_{1u}) 1472 (B_{3u})
1672	1707 (A_g)		

The interpretation of the second-order lines for cyclohexane and the values of the anharmonicity coefficients calculated on its basis are shown in Table 1. This interpretation cannot be considered to be single-valued since almost always there can be several combinations of the fundamental frequencies, allowed by the selection rules and sufficiently close to the frequency of the given line. In all such cases we used that combination which gives the smallest anharmonicity coefficient. Of course it is not possible to verify this principle, but if it is ignored there remains no guide line for the interpretation. The selection rules for the polarization are of essential assistance. For example, the interpretation given for the 2162 cm^{-1} line is single-valued. It is possible to compose a series of combinations closer in frequency to 2162 than the chosen one of 2133. However, all such combinations should belong to type E_g and, accordingly, should be depolarized; and this is in contradiction with the observed polarization.

The lines 527 and 905 cm^{-1} merit particular attention. They can only be explained as fundamental lines of type A_{2u}, forbidden in the Raman effect.*

*In the interpretation combinations with component vibrations of types A_{1u} and A_{2g}, forbidden in the Raman and infrared spectra, were not considered. It is not possible to say anything about the values of their combinations. Difference combinations also were not considered, since in the 1400-2700 cm^{-1} region their intensity is one thousand times less than the corresponding sum combinations.

In the interpretation of the fundamental lines of tetramethylethylene we used Sverdlov's calculation[15] of its vibrations. However, it was necessary to make several changes in Sverdlov's interpretation because it does not agree with the experimental polarization data (cf. Table 2, where the values of the polarizations, enclosed in brackets, are taken from ref. 16). Our interpretation is given in Table 3. The assignment of the second-order lines was based on the same principle as in the cyclohexane case, and is given in Table 2.

As is easily seen from the data shown in Tables 1 and 2, the anharmonicity coefficients are 0.1-1% of the values of the respective frequencies. We failed to dis-

cover a definite dependence of the magnitude of the anharmonicity coefficients on the type and form of the vibration.

REFERENCES

1. V. D. Bogdanov and M. M. Sushchinskii, Izvest. Akad. Nauk SSSR, Ser. Fiz. 22, 1067 (1958).
2. W. H. Stockmayer, G. M. Kavanagh, and H S. Mickely, J. Chem. Phys. 12, 408 (1944).
3. H. L. Welsh, M. F. Crawford, and G. D. Scott, J. Chem. Phys. 16, 97 (1948).
4. G. S. Landsberg and V. I. Malyshev, Doklady Akad. Nauk. SSSR 3, 365 (1936).
5. T. Y. Wu and others, J. Chem. Phys. 7, 178 (1939); Ibid. 8, 489 (1940).
6. R. Ananthakrishnan, Proc. Indian Acad. Sci. 2, 452 (1935).
7. B. Moszynska, Bull. acad. polon. sci. 7, 455 (1959).
8. K. Venkateswarlu and G. Thyagarajan, Z. Physik 156, 569 (1959).
9. G. S. Landsberg, P. A. Bazhulin, and M. M. Sushchinskii, Osnovye Parametry Spektrov Combinatsionnogo Rasseyaniya Uglevodorodov (Fundamental parameters of the Raman spectra of hydrocarbons), Moscow, 1956.
10. J. Goubeau, Z. angew. Chem., Beihefte No. 56, 1948.
11. C. M. Beckett, K. S. Pitzer, and R. Spitzer, J. Am. Chem. Soc. 69, 2488 (1947).
12. M. M. Sushchinskii, Dokt. diss., Fiz. Inst. Akad. Nauk SSSR, 1957.
13. G. A. Aleksandrov, Opt. i Spektr. 3, 202 (1957).
14. M. Larnaudie, J. phys. radium 15, 365 (1954).
15. L. M. Sverdlov, Opt. i Spektr. 1, 752 (1956).
16. W. G. Braun, D. F. Spooner, and M. R. Fenske, Analyt. Chem. 22, 1074 (1950).
17. Am. Petrol. Inst., Res. Project No. 44.

THE TEMPERATURE DEPENDENCE OF THE INTENSITY OF RAMAN LINES IN THE VAPOR AND LIQUID PHASES

A. I. Sokolovskaya

Received 20 February 1960

The temperature dependence of the intensity of Raman lines of carbon tetrachloride, chloroform, benzene, acetone, and acetonitrile in the vapor and liquid phases is investigated. The results obtained are compared with the conclusions of the theory.

In works published earlier[1-4] it was established experimentally that the temperature dependence of the Stokes and anti-Stokes Raman lines differs from that predicted by theory.[5] This raises the question—does the observed anomaly appear as a result of intermolecular interactions in the liquid or is it connected with the internal dynamics of the molecule? An investigation of the temperature dependence of the intensity of Raman lines in vapors or gases, where the role of intermolecular interactions is not large, may aid in the resolution of this question. It is expedient to compare the dependence of the intensity on temperature for Raman lines of the same compound in the liquid and vapor states. Regrettably, such data are absent from the literature. Pivovarov and Bobovitch[6] gave measurements of Raman line intensities of gaseous N_2 and CO_2 for changes of temperature. However, the small temperature effect and also the absence of data on the temperature dependence of the lines of N_2 and CO_2 in the liquid state do not permit a complete comparison with theory. From this viewpoint it is of interest to investigate, in the liquid and vapor phases, substances whose spectra have sufficiently intense lines in the low frequency region. Carbon tetrachloride, chloroform, acetone, acetonitrile, and benzene were chosen as such compounds.

The investigations were carried out photographically as well as photoelectrically. In the photographic method we used a three-prism French "Heuet" spectrograph with a dispersion of 8 A/mm in the blue region, and in the photoelectric method a DFS-4 diffraction spectrophotometer with a dispersion of 6.4 A/mm in the first order. In this the photoelectric part of the DFS-4 was modernized in several ways. The constant-current amplifier, fitted with a single-lamp bridge scheme, was replaced with a constant-current EMU-3 amplifier, very stable in operation and having a wide range of amplification. The signal was registered on a recorder of Type EPP-09. The time constant of the recording apparatus could be changed from 5 to 40 sec with the aid of suitable RC circuits.

A low-pressure mercury lamp[7] was used as a light source, with a lamp about one meter long[8] being used for the investigation of the vapors. The scattering volume was focused on the entrance slit in such a manner that the image of the walls of the cell did not enter the apparatus.[9] The spectral slit width of the spectrograph in the focal plane varied from 1 to 3 cm^{-1}, depending on the width of the line being investigated. The widths of the entrance and exit slits of the DFS-4 equalled 1 cm^{-1}, the height of the entrance slit 18 mm. For the investigation of the temperature dependence in the vapor a sample tube 800 mm in length and 30 mm in diameter was used. The simple construction of the cell excluded the possible errors introduced by multiple reflection cells.

In our investigations measures were taken to exclude the influence of pressure[10,11] on the Raman line intensities of the vapor with changes of the temperature. For this purpose the cell was equipped with a side-arm, in which some of the investigated liquid was kept at constant temperature, fixing the vapor pressure in the cell. The working part of the cell was enclosed in a heater, in which the temperature distribution was controlled with the aid of a differential thermocouple. The temperature of the illuminated part of the cell was always considerably higher than the temperature of the side-arm and was changed from 100 to 200°C. The vapor pressure in the cell was 2 atm. Both for the vapors and for the liquids the intensity was measured by planimetering the contour of the line and calculating it for one molecule of the substance. For the determination of the pure Raman line in-

Table 1

Substance	$\Delta\nu$ (cm^{-1})	t (°C)	$I_{St.}$ experimental	$I_{St.}$ theoretical
			Liquid	
Acetone	786	−40	100	100
		±60	70	102
	2922	−40	100	100
		+60	75	100
			Vapor	
	786	+120	100	100
		+200	106	104
	2922	+120	100	100
		+200	109	100
			Liquid	
Benzene	992	+20	100	100
		+80	71	101
	3062	+20	100	100
		+80	80	100
			Vapor	
	992	+100	100	100
		+190	110	103
	3062	+110	100	100
		+190	104	100
			Liquid	
Acetonitrile	2942	−30	100	100
		+70	83	100
			Vapor	
	2942	+120	100	100
		+290	98	100

Table 2

Substance	$\Delta\nu$ (cm^{-1})	t (°C)	$I_{St.}$ experimental	$I_{St.}$ theoretical	$I_{anti-St.}$ experimental	$I_{anti-St.}$ theoretical	$I_{St.}/I_{anti-St.}$ experimental	$I_{St.}/I_{anti-St.}$ theoretical
					Vapor			
Chloroform	366	120	88	88	34	27	2.6	3.3
		200	123	97	58	46	2.1	2.0
	665	120	100	100	—	—	—	—
		200	101	105	—	—	—	—
	3018	120	82	82	—	—	—	—
		200	90	82	—	—	—	—
					Liquid			
	366	−40	98	98	12	11	8.3	8.6
		+60	75	111	19	26	4.0	4.3
	665	−40	100	100	—	—	—	—
		+60	86	104	—	—	—	—
	3018	−40	50	50	—	—	—	—
		+60	39	50	—	—	—	—
					Vapor			
Carbon tetrachloride	314	112	87	87	26	25	3.3	3.2
		190	103	97	38	40	2.7	2.4
	459	112	100	100	20	21	4.9	4.8
		190	117	108	30	30	3.9	3.6
					Liquid			
	314	−20	100	100	18	19	5.5	5.3
		+70	79	114	23	34	3.2	3.3
	459	−20	100	100	9	9	11.6	11.6
		+70	82	103	14	19	6.8	5.9

tensity in the liquid, corrections for the change of density and of refractive index on increase of the temperature[12] were introduced. The change of the number of molecules in the scattering volume in the vapor state of the compound on an increase of temperature was calculated from the Clapeyron equation. As a check of the reproducibility of the experimental results, the measurements were made for both increasing and decreasing temperatures. The final result was obtained from the averaging of 4 or 5 spectrograms. The relative intensity from measurements by the photographic method was determined with an accuracy of 7-8%, and from measurements by the photoelectric method with an accuracy of 2-3%.

The experimental results are given in Tables 1 and 2. In columns 4, 6, and 8 of Table 2 are shown the relatively measured values of the intensities of the Stokes, of the anti-Stokes, and of the magnitude of their ratio; in columns 5, 7, and 9 are the calculated values of these same quantities. In Table 1 are given data only for the Stokes lines.

From the data shown it is evident that in all of the substances investigated in the vapor state the intensity of the Stokes line grows or remains constant with an increase of the temperature. These changes, as a rule, are close to the theoretical. In the liquids the intensities of the same lines decrease with an increase of the temperature. Thus, for example, in liquid acetone, on increasing the temperature by 100° C the intensities of the 786 and 2922 cm^{-1} lines decrease nearly 30%; in the vapor these remain constant within the limits of error. Similarly, for CCl_4 the intensity of the 314 and 459 cm^{-1} lines in the liquid phase decrease by 20% on changing the temperature by 90° C, while in the vapor the intensities of the same lines grow by approximately 10%.

For the close frequencies of chloroform (366 cm^{-1}) and of carbon tetrachloride (314 and 459 cm^{-1}) we measured the temperature dependence in the liquid and in the vapor, both for the Stokes and for the anti-Stokes lines. These results permitted us also to follow the ratio of the intensities of these components for changes in temperature. As seen from Table 2, in the liquids and in the gases the sign of the change of intensity of the anti-Stokes line coincides with theoretical. However, the experimental data of the current work and of others[4] show that in liquids the intensity of the anti-Stokes lines always changes more slowly than theory suggests. For the vapor state (columns 7 and 8) the intensities of the anti-Stokes lines of CCl_4 and of $CHCl_3$, as a rule, change with temperature in accordance with theory. It should be noted that the data on the temperature dependence of the Raman line intensities of vapors and gases, obtained in the present work, agree with the results of similar investigations of infrared absorption spectra.[10, 13, 14]

In spite of the apparent strong difference between the temperature dependence of the Raman line intensities for liquids and vapors, the ratio of the magnitudes of the intensities of the Stokes and anti-Stokes component in both phases remains close to theoretical (Table 2, columns 8 and 9). The results of the present work lead to the conclusion that a statistical treatment of the temperature dependence is adequate for gases, where the intermolecular interactions are not large. In the liquid phase (as seen from the data of the present work and of ref. 4) the law of the dependence of the intensity on the distribution of the molecules over the levels derived for the isolated molecule is also valid; however, it is disturbed by intermolecular interactions.

In spite of the large number of publications connected with studies of the temperature dependence of vibrational spectra, it is not possible at the present time to consider the indicated problem to be solved. The interpretations and data in the literature[15-18] evidently cannot explain the observed phenomenon.[2] It has not been excluded that the temperature changes of Raman intensities are connected with the temperature changes of the electronic absorption spectra of the molecules.[19,20] The latter proposal does not solve the question of the temperature anomaly of Raman spectra in liquids, but makes it more universal, extending it also to the region of electronic absorption spectra. Due to the manifold forms of the intermolecular interaction in liquids for the explanation of the observed phenomenon, it is obviously impossible to limit oneself to any one mechanism. However, the constant sign of the temperature anomaly of the Raman line intensities forces

one to assume that the interaction responsible for this is common to all of the liquids without exception.

From this viewpoint one may assume that the change of the intensity with temperature is dependent on the influence of the liquid as an external dielectric medium on the magnitude of the effective internal field of the light wave.[21-23] However, an evaluation of the influence of the internal field on the temperature dependence of infrared vibrational absorption spectra[11] gives an effect small in comparison with the observed effect. For clarification of the dependence of Raman line intensities on temperature, a further development of the theory is required.

In conclusion I express deep thanks to P. A. Bazhulin for his constant interest in the work and for valuable comments.

REFERENCES

1. A. I. Sokolovskaya and P. A. Bazhulin, Mater. VIII Vsesoyuz. Sovesh. po Spektr. (Proceedings of the VIII All-Union Conference on Spectroscopy) 1, 225 (1957).
2. A. I. Sokolovskaya and P. A. Bazhulin, Izvest. Akad. Nauk SSSR, Ser. Fiz. 22, 1068 (1958).
3. A. I. Sokolovskaya and Z. Kercki, Bull. Acad. Polon. Sci., Ser. Chim., Geol., et Geogr. 4, 2, 133 (1958).
4. A. I. Sokolovskaya and P. A. Bazhulin, Opt. i Spektr. 8, 394 (1960), Optics and Spectroscopy 8, 203 (1960).
5. G. S. Landsberg and L. I. Mandel'shtam, Z. Physik 60, 364 (1930).
6. V. M. Pivovarov and Ya. S. Bobovich, Opt. i Spektr. 6, 249 (1959), Optics and Spectroscopy 6, 160 (1959).
7. N. I. Rezaev, Vestnik Moskov. Gosudarst. Univ. No. 2, 145 (1957).
8. B. P. Stoicheff, Can. J. Phys. 32, 330; Ibid., 32, 339 630 (1954).
9. S. G. Rautian, Zhur. Eksptl. Teor. Fiz. 27, 11 (1954).
10. V. N. Smirnov and P. A. Bazhulin, Opt. i Spektr. 7, 193 (1959).
11. W. B. Person, J. Chem. Phys. 28, 319 (1958).
12. A. I. Sokolovskaya and S. G. Rautian, Opt. i Spektr. 6, 51 (1959), Optics and Spectroscopy 6, 29 (1959).
13. P. A. Bazhulin and V. N. Smirnov, Opt. i Spektr. 6, 745 (1959), Optics and Spectroscopy 6, 485 (1959).
14. M. P. Lisitsa, V. N. Malinko, and I. N. Khalimonova, Opt. i Spektr. 4, 638 (1959).
15. F. G. Rosler, Acta Phys. Austriaca 5, 477 (1952).
16. P. P. Venkateswarlu, Nature 159, 96 (1947); Current Sci. (India) 16 15 (1947).
17. Ya. S. Bobovich, Doklady Akad. Nauk SSSR, 98, 39 (1954).
18. E. J. Slowinsky and G. C. Claver, J. Opt. Soc. Am. 45, 396 (1955).
19. T. M. Tarasova, Zhur. Eksptl. Teor. Fiz., 21, 83 (1951).
20. Ya. S. Bobovich and V. M. Pivovarov, Opt. i Spektr. 3, 227 (1957).
21. L. Onsager, J. Am. Chem. Soc. 58, 1486 (1936).
22. D. G. Rea, J. Opt. Soc. Am. 49, 90 (1959).
23. V. M. Pivovarov, Opt. i Spektr. 4, 101 (1959).

INFRARED REFLECTION SPECTRUM OF BORIC ANHYDRIDE AND FUSED QUARTZ AT HIGH TEMPERATURES*

*Preliminary results of the investigation of infrared reflection spectra of boric anhydride at high temperatures were presented at the Eleventh All-State Spectroscopy Conference in December 1957.

E. P. Markin and N. N. Sobolev

Received 25 February 1960

We investigated the infrared reflection spectrum of boric anhydride and of fused quartz in the temperature interval 21-1000°C and −190-2000°C, respectively. It was determined that the infrared reflection spectrum of B_2O_3 remains unchanged on transition from the glasslike to the liquid state. The most intense band of SiO_2 ($\lambda = 8.9\mu$ at −190°C) also remains unchanged within the range of temperatures investigated. The bands shift to lower frequencies with increase in temperature.

The constancy of the infrared spectrum of B_2O_3 up to 1000°C and of the fundamental frequency of SiO_2 up to 2000°C indicates that the basic structural unit in the fused B_2O_3 and SiO_2 remains unchanged in the molten state.

Notwithstanding the large number of investigations of the fused state, there does not exist at present a widely accepted theory of its structure. Because of this, every new experimental fact obtained by physical or chemical methods is invaluable in the study of the fused state.

The present paper is dedicated to the investigation of infrared spectra of fused boric anhydride and quartz and belongs to the large research program on the infrared spectra of glass-forming oxides being carried out at the Physics Institute.[1-8]

In the preceding investigations in our laboratory, we performed a detailed study of the vibrational spectrum of boric anhydride.[1,4,8] The interpretation of the experimental results obtained by us then was based on the assumption, formulated by Fajans and Barber,[9] that boric anhydride possesses a molecular structure. Calculation and study of the Raman and infrared absorption spectra have shown that a satisfactory explanation of the B_2O_3 vibrational spectrum can be provided if it is assumed that its fundamental structural unit in the fused state is the molecule B_4O_6 belonging to the point symmetry group T_d. The same conclusion follows from the study of isotopic shift in the infrared spectrum of boric anhydride enriched with B^{10} and from the fact that the frequencies in the Raman spectrum remain unchanged during the transition from the fused to the liquid state.[1] No infrared spectra of liquid B_2O_3 were obtained.

The vibrational spectra of fused and crystalline quartz have been investigated many times.[8,10-18] Up to the present time there were no data in the literature on the vibrational spectrum of molten quartz, even though

this information (just as in the case of the boron oxide) would be very valuable.

The investigation of the infrared absorption spectra of molten boric anhydride and quartz presents an almost insurmountable problem. A thin layer of boron oxide when liquefied coagulates into a drop. In the case of quartz, because of its high melting point, it is impossible to find a suitable material for plates on which to deposit the quartz (the plates must be transparent in the infrared region of the spectrum and not melt). Because of this, we were forced to use the method of reflection to obtain the infrared spectra of the two substances. It must be kept in mind that the method of reflection possesses a number of shortcomings relative to the absorption method. Firstly, the method of reflection is less sensitive: only the most intense infrared bands can be investigated. Secondly, the surface layer of the sample investigated by the reflection method must be very clean. Finally, it must be remembered that the maxima of the infrared reflection bands are always slightly shifted relative to the maxima of the corresponding absorption bands.

APPARATUS

A special attachment to a single-beam spectrophotometer IKS-11 was developed and built for measuring the infrared reflection spectra of substances at high temperatures (Fig. 1).

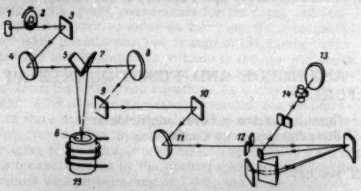

Fig. 1. Optical schematic diagram of instrument used in the investigation of infrared reflection spectra of substances at high temperatures.

The method of modulation was used to eliminate the continuous spectrum emitted by the substance investigated and the oven at high temperatures. A chopper 2 rotating at 9 cycles, was placed in front of the radiation source (Silit resistor 1). The modulated beam of infrared light was focused by the system of mirrors 3, 4, and 5 at the surface of the sample 6. The beam of emitted infrared radiation was focused by the system of mirrors 7-11 at the entrance slit 12 of the monochromator IKS-11 (the mirrors 10 and 11 are placed inside the monochromator). From the monochromator, the radiation beam was reflected by the mirror 13 at the bolometer 14 which fed the signal into an alternating current amplifier 17. Thus, only the modulated radiation from the globar reflected by the sample was amplified. The chopper was covered with dull black paper in order to prevent the entrance of modulated radiation emitted by the sample at high temperatures along the path 6-5-4-3-2-3-4-5-6.

The block-schematic diagram of the amplifying system is shown in Fig. 2. The low frequency signal of 9 cycles was amplified using a generated carrier frequency of 4000 cycles. The main amplification (amplification factor of about 10^6) was performed at 4000 cycles, and then at 9 cycles using a narrow band amplifier (amplification factor about 2×10^3). In subsequent stages the signal was amplified by another factor of 10^2, as a result of which the total amplification factor was about 10^{10}. The method described above was developed for a double-beam spectrophotometer.[17] Since our spectrophotometer was a single-beam instrument, we fed the signal directly from the phase-sensitive detector into a fact response pen recorder EPP-09.

EXPERIMENTAL MEASUREMENT OF INFRARED REFLECTION SPECTRA OF MOLTEN BORIC ANHYDRIDE AND QUARTZ

Fused boric anhydride was melted in a corundum crucible placed inside a shaft furnace kept at 1200°C for five to six hours until all the bubbles escaped from the melt. The infrared reflection spectrum of B_2O_3 was measured in the temperature interval of 21-1000°C.* No measurements were performed higher than 1000°C because of enhanced formation of bubbles in the molten sample and at places of contact with the crucible walls. The temperature of the molten B_2O_3 was measured by means of a chromel-alumel thermocouple. The latter was protected by a quartz cap. A flat aluminized mirror was used as a standard in determining the absolute magnitude of the reflection coefficient.

*A NaCl prism was used in investigating the infrared spectra of B_2O_3 and SiO_2. A spectral slit-width of 5.5 cm^{-1} was used in the case of B_2O_3 and one of 3 cm^{-1} in that of SiO_2.

A 30 kw high-frequency oven of the type LGPZ-30 was used to melt the quartz. The molten quartz (as a cylinder 25 mm in diameter and 30 mm high) was placed in a cylindrical graphite crucible 50-60 mm in diameter (15 in Fig. 1). The crucible was made of the purest graphite available in order to insure its thermal stability. The inside of the crucible was covered with powdered

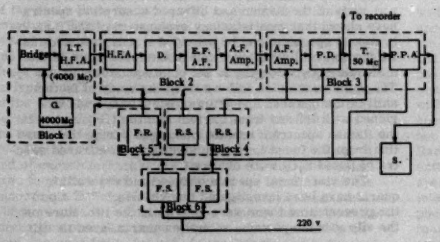

Fig. 2. Block-schematic diagram of the amplifying system of the infrared spectrophotometer. I.T.—inlet transformer; D—detector; E.F.—electrical filter; P.D.—phase-sensitive detector, direct current filter; T.—transformer; P.P.A.—phase-sensitive power amplifier; F.R.—filament rectifier; R.S.—rectifier and stabilizer; S.—servomotor; F.S.—ferroresonance stabilizer; G—generator.

H.F.A. = High Frequency Amphere
A.F. = Audio Frequency
A.F. Amp. = Audio Frequency Amplifier

SiC and baked (the silicon carbide excluded the possibility of any reaction between SiO_2 and carbon) prior to the introduction of quartz. The crucible could be heated in place by high-frequency current to 2500°C. Measurements were performed to 2000°C only, because at higher temperatures silicon dioxide has a high vapor pressure which could affect the measurements (137 mm of Hg at 2000°C and 400 mm of Hg at 2141°C[18-19]). During each experiment, a stream of heated pure argon was directed at the crucible and the surface of the quartz. The temperature was measured by means of an optical pyrometer calibrated against a standard temperature lamp. We could extend the use of our pyrometer to 2300°C by using Schott filters NG65 and NG68. The temperature of the crucible walls and of the quartz surface were measured. Usually the temperature of the quartz surface was 50-100°C lower than that of the crucible walls. This fact could be due to either weaker radiative emission of quartz relative to graphite or to a real difference in temperature between the two.

The use of an argon stream helped temperature measurements, since it prevented condensation of silicon dioxide vapors in the upper part of the crucible.

EXPERIMENTAL RESULTS

Boric anhydride. Figure 3 shows the results of our investigation of the infrared reflection spectra of boric anhydride in the temperature interval 20-1000°C. As can be seen from the figure, the bands at 3241, 1542 and 1184 cm^{-1}, observed at room temperature and belonging to the boric acid formed at the surface of boric anhydride, disappear at 170°C. The two bands at 1316 and 720 cm^{-1} persist till 1000°C. The 1316 cm^{-1} band shifts its position

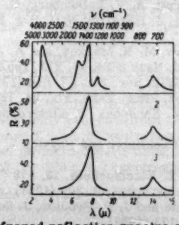

Fig. 3. Infrared reflection spectra of boric anhydride at various temperatures. Temperatures (in °C): 1—20; 2—170; 3—1000.

with increase in temperature towards the low frequency side and at 1000°C this shift reaches 40 cm^{-1}. No shift was detected in the position of the 720 cm^{-1} band (more precisely, if there was a shift it was of the same magnitude as the experimental error ± 5 cm^{-1}). The two reflection bands correspond to the infrared absorption bands at 1260 and 718 cm^{-1} of fused boric anhydride[4] (Fig. 4). Thus, the fundamental infrared frequencies of boric anhydride found in the fused state occur also in the liquid state to 1000°C at which temperature, the viscosity of the boric anhydride is equal to 74 poises.[20]

The conservation of the infrared reflection spectrum of boric anhydride on transition from the fused to the liquid state (and the conservation of the Raman spectrum[1]) indicates that the fundamental structural unit of boric anhydride in both states is the same. Since analysis of the physico-chemical properties of boric anhydride[3] and of

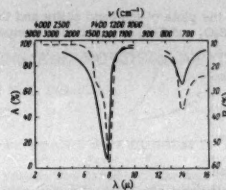

Fig. 4. Infrared reflection spectrum (R) of liquid boric anhydride at 1000°C (full line) and the infrared absorption spectrum (A) of fused boric anhydride (dotted line).

its vibrational spectrum[1,4,6] in the fused state shows that it consists of molecules of B_3O_6 of symmetry T_d, then the same structure must occur in the liquid state.

Let us note that Harrand's paper[21] published after ours,[1] substantiates our assumptions concerning the molecular structure of boric anhydride. It was shown that the degree of depolarization of the most intense line at 808 cm^{-1} in the Raman spectrum of boric anhydride was equal to 0.85.[1] This contradicted the assignment of this line to the completely symmetric vibration of the B_3O_6 molecule. It was supposed that such a large degree of depolarization is due to the presence of tensions in the given sample of boric anhydride. When the latter was baked, the depolarization fell to 0.63. The depolarization of the 808 cm^{-1} line of liquid boric anhydride (T = 700°C) was found by Harrand to be equal to 0.2, indicating that this line belongs to the fully symmetric vibration. Thus the results of Harrand, as well as ours, substantiate the conclusion concerning the molecular structure of boric anhydride in the liquid and the fused states.

Molten quartz. The infrared reflection spectra of molten quartz are shown in Fig. 5. At −190 and 21°C there are two bands at 1120 and 788 cm^{-1} and a shoulder on the former at 1216 cm^{-1}.[22] With increase in temperature, the 1216 cm^{-1} (8.22μ) band disappears while the 1120 cm^{-1} (8.9μ) band becomes more symmetrical, decreasing in intensity at the peak maximum (by a factor of two at 2000°C) and shifts slowly to lower frequencies. At 2000°C the shift reaches 66 cm^{-1}, i.e., at this temperature, the band maximum occurs at 1054 cm^{-1} (9.5μ).

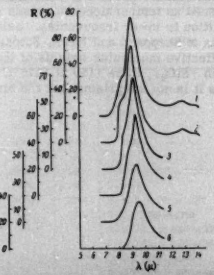

Fig. 5. Infrared reflection spectra of molten quartz at different temperatures. Temperature (in °C): Curve 1— −190; curve 2—21; curve 3—500; curve 4—1000; curve 5—1500; curve 6—2000.

Figure 6 shows the plots of the band shifts and the viscosities[23,24] of B_2O_3 and SiO_2 as function of temperature.

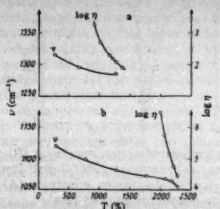

Fig. 6. Band position (ν) and viscosities (η) of B_2O_3 (a) and SiO_2 (b) as functions of temperature.

We did not investigate the 788 cm^{-1} band at high temperatures since this would have necessitated working with wide slit-widths and the excessive amount of background radiation could damage the bolometer.

Thus the fundamental infrared band of fused quartz at 1120 cm^{-1} is conserved on transition from the fused to the liquid state. At first glance, this result can be interpreted in the same way as for boric anhydride. Conservation of one of the fundamental frequencies of the infrared spectrum on transition from one to another state of aggregation seems to indicate the same molecular structure. However such a conclusion would be too hasty. Firstly, a coordination structure was found for crystalline quartz by means of x-ray diffraction. Secondly, we have determined the conservation not of the whole spectrum but of only the strongest band, on transition from the fused to the liquid state. The 1216 cm^{-1} band disappears, i.e., the spectrum is not conserved completely. Thirdly, molten quartz is not really a liquid but a very viscous melt. Indeed according to Solomin[24] the viscosity of quartz at 2000°C is 2.8×10^4 poises.

All these facts lead us to agreement with the assumption of Solomin[24] that molten quartz consists of associates $|SiO_2|_n$. These associates possess the same internal structure in the solid and liquid quartz which explains the conservation of the fundamental frequency of quartz. In other words, the short range order is conservation of the fundamental frequency of quartz. The bond is weakened as temperature increases and the band shifts its position to lower frequencies. Using the viscosity formula of Sheppard and Hawk, Solomin has calculated the effective molecular weights of the associates and found n in $|SiO_2|_n$ to be 1150 at 1275°C and 590 at 2000°C. Thus it is not surprising that the fundamental frequency of the fused quartz remains unchainged in the liquid state.

In conclusion, we would like to express our deep gratitude to A. F. Volodin of the Baikov Institute of Metallurgy of the Academy of Sciences of USSR for his help in the experimental work and to A. N. Danil'chenko for his constant interest in our investigation.

REFERENCES

1. E. N. Lotkova, V. V. Obukhov-Denisov, N. N. Sobolev, and V. P. Cheremisinov, Opt. i Spektr. **1**, 722 (1956).
2. T. A. Sidorov and N. N. Sobolev, Opt. i Spektr. **2**, 711 (1957).
3. T. A. Sidorov and N. N. Sobolev, Opt. i Spektr. **2**, 713 (1957).
4. T. A. Sidorov and N. N. Sobolev, Opt. i Spektr. **3**, 560 (1957).
5. E. P. Markin and N. N. Sobolev, Izvest. Akad. Nauk SSSR, Ser. Fiz. **22**, 1097 (1958).
6. T. A. Sidorov and N. N. Sovolev, Opt. i Spektr. **4**, 9 (1958).
7. V. P. Cheremesinov, Opt. i Spektr. **7**, 454 (1959), Optics and Spectroscopy **7**, 293 (1959).
8. T. A. Sidorov, Opt. i Spektr. **4**, 800 (1958).
9. K. Fajans and S. W. Barber, J. Am. Chem. Soc. **74**, 2761 (1952).
10. B. D. Saksena, Proc. Indian Acad. Sci. **A12**, 93 (1940).
11. R. S. Krishnan, Proc. Indian Acad. Sci. **22**, 329 (1945).
12. F. Matossi, J. Chem. Phys. **17**, 679 (1949).
13. J. Simon and McMahon, J. Chem. Phys. **21**, 23 (1953).
14. N. A. Sevchenko and V. A. Florinskaya, Doklady Akad. Nauk SSSR **109**, 1115 (1958).
15. M. Haccuria, Bull. soc. chim. Belges **62**, 428 (1958).
16. E. R. Lippincott, A. V. Valkenburg, C. E. Weiz, and E. N. Bunting, J. Research Natl. Bur. Standards **61** 61 (1958).
17. V. I. Malyshev, M. N. Markov, and A. A. Shubin, Doklady Akad. Nauk SSSR **86**, 273 (1952); Izvest. Akad. Nauk SSSR, Ser. Fiz. **17**, 654 (1953); M. N. Markov, Zhur. Tekh. Fiz. **24**, 1867 (1954).
18. O. Ruff and M. Konschak, Z. Elektrochem. **32**, 515 (1926).
19. Handbook of Chemistry and Physics **7**, 2163 (1955-1956).
20. K. Z. Arndt, Z. Electrochem. **13**, 578 (1907).
21. M. Harrand, Ann. phys. **2**, 309 (1957).
22. P. E. Jellyman and J. P. Proctor, J. Soc. Glass Technol. **29**, 173 (1953).
23. M. P. Volarovich and R. S. Friedman, Zhur. Tekh. Fiz. **9**, 177 (1937).
24. N. N. Solomin, Papers presented at Symposium on Viscosity of Liquids and Colloidal Solutions, I.

THE LUMINESCENCE OF CHRYSENE SOLUTIONS AND POWDERS AT 77° K

P. N. Nurmukhametov, E. G. Popova, and N. S. Dokunikhin

Received 18 February 1960

Emission and absorption spectra of chrysene solutions and powders were studied at 77° K by the method of Shpol'skii.

A vibrational analysis of the spectra was made and the results compared with the data of other authors. On the basis of both spectral and x-ray data obtained from powders, conclusions were drawn concerning the influence of mechanical-physical inhomogeneities on the spectral characteristics of powdered chrysene.

As stated in papers by Shpol'skii and his collaborators,[1] many aromatic hydrocarbons have emission and absorption spectra in n-hydrocarbon solution at 77° K which are quasi-linear and show structure. Chrysene is one of the aromatic hydrocarbons which was not investigated by this method.

It is known that chrysene has a deep blue fluorescence in neutral solutions.[2] In EPA solution at −190° C, chrysene has a distinctive structure band fluorescence spectrum with its first band at $\nu_{00F} = 27000\ cm^{-1}$, and also a phosphorescence spectrum ($\nu_{00P} = 20000\ cm^{-1}$) containing 9 bands (Table 1).[3,4] The investigation of the phosphorescence of a series of aromatic compounds studied in ref. 3 was repeated in ref. 5. Vibrational differences of 1436 and 1597 cm^{-1} were isolated in the chrysene spectrum. In a study of the luminescence of crystalline layers of chrysene obtained by evaporation onto a quartz support, a spectrum of broad bands with a difference of 1370 cm^{-1} was obtained at room temperature.[6] It was noticed that specimens of varying degrees of uniformity, and spectra of varying degrees of diffuseness were obtained, depending on the solvent from which the evaporation was made.

We had at our disposition two specimens of chrysene with a melting point of 253° (±0.5°), which had been chromatographically purified on aluminum oxide. Specimen I was subsequently recrystallized from chlorobenzene and specimen II from butanol. The luminescence was investigated photographically using ISP-51 (f = 270 mm) and ISP-67 (f = 500 mm.) spectrographs. Excitation was accomplished with 313 and 365 mμ radiation from a PRK-2 lamp.

At 77° K, solutions of both specimens in n-hydrocar-

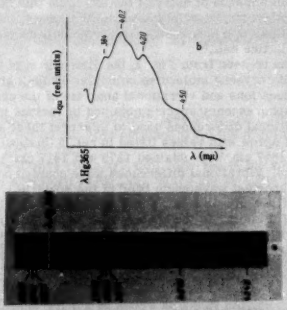

Fig. 1. Fluorescence spectra of chrysene solution (a) and vapor (b). a—in octane at 77° K; $\lambda_{exc.} = 313$ mμ; the spectrum was obtained with a Qu-24 spectrograph. b—spectrum obtained with excitation by light from an SVDSh lamp = 250, filtered to isolate λ = 365 mμ.

Table 1. Fluorescence Spectrum of Chrysene in Octane at 77° K Excited with 313 mμ* Radiation

λ′ (A)	ν′ (cm^{-1})	I***	Δν (cm^{-1})	λ″ (A)	ν″ (cm^{-1})	Δν (cm^{-1})	λ‴ (A)	ν‴ (cm^{-1})	Δν (cm^{-1})	Interpretation
3606.4	27721	s.	0	3612.6	27673	0	3622.9	27594	0	0—0
3646.1	27419	m.	302	—	—	—	—	—	—	0—295
3724.6	26839	w.	882	3732	26787	886	3742.5	26712	882	0—875
3766.5	26542	w.	1179	3773.2	26492	1181	3786	26406	1188	0—1180
3796.7	26331	v.w.	1390	3804.5	26280	1393	3815	26204	1390	0—1395
3822	—	—	—	—	—	—	—	—	—	—
3839.6	26037	m.	1684	3847	25986	1687	3858	25912	1682	0—1395 + 295 = 1690
3881.9	25753	w.	1968	3888.5	25709	1964	3899.5	25636	1958	0—1965
3927	25457	w.	2264	3935	25405	2268	3947	25328	2266	0—1395 + 875 = 2270
4010 **	24931	s.	2790	—	—	—	—	—	—	0—2 × 1395 = 2790
4060	24624	m.	3097	—	—	—	—	—	—	0—295 + 2 × 1395 = 3085
4154	24066	w.	3655	—	—	—	—	—	—	0—875 + 2 × 1395 = 3665
4248	23533	m.	4188	—	—	—	—	—	—	0—3 × 1395 = 4185
4300	23249	w.	4472	—	—	—	—	—	—	0—3 × 1395 + 295 = 4480
4410	22669	w.	5052	—	—	—	—	—	—	0—3 × 1395 + 875 = 5060
4514	22147	w.	5574	—	—	—	—	—	—	0—4 × 1395 = 5580

*One, two, and three primes correspond to the different splitting components.

**Beginning at 4010 A, the bands on the spectrogram cannot be resolved into triplets due to the decrease in dispersion, and also, apparently, due to an increase in the diffuseness of the components.

***I – qualitative estimate of intensity (s. – strong, v.s. – very strong, m. – medium, w. – weak, v.w. – very weak band).

bons have a light blue luminescence and a bright yellow-green phosphorescence. The phosphorescence spectrum proved to be composed of comparatively narrow bands (width $\Delta\nu \sim 20$ cm^{-1}), which are singlets in hexane and heptane and doublets in octane, with a splitting of ~40 cm^{-1}. The fluorescence bands in octane have the appearance of triplets with differences of 50-75 cm^{-1} between the components (Table 1). The first triplet is fairly intense, which indicates that this is an allowed transition (ν_{00} for the first component is 27,720 cm^{-1}). The fluorescence spectrum coincides in position with the spectrum of chrysene vapor (Fig. 1). This confirms the concept of such solutions being "frozen gases," the crystallinity of the solvent causing the peculiar "splitting" effect.

The appearance of molecular spectrum structure in solutions is caused by a successful penetration of the luminescent molecule into the lattice of the solvent, combined with a minimum perturbation of electron shells; the multiplicity is associated with the existence of several possible means of entry of the molecule into the lattice.[7] When the molecules are commensurate, the luminescent particle apparently replaces a solvent molecule in a lattice cell.[8]

As can be seen from Fig. 2, the dimensions of the octane and chrysene molecules coincide. Table 2 gives the band locations and vibrational analysis of the chrysene phosphorescence spectra obtained in various media. The vibrational differences used to interpret these spectra do not agree with values listed in ref. 5 (instead of 1436 and 1597 cm^{-1} we obtained 1375 and 1617 cm^{-1} respectively). Vibrational differences were counted not from the shortest wavelength band of the spectrum, but from the first intense band. Some weak bands existing in front of it appear in the spectrum when a wide slit and a long exposure are used; thus their location is less exactly determined than the location of the other spectral bands. The first intense band appears apparently as a result of the removal of forbiddenness by the quantum of one of the vibrations, with which the remaining frequencies subsequently combine.

Powdered chrysene has a green fluorescence. Since it is easily crystallized from n-hydrocarbons, the luminescence of precipitated crystallites (more diffuse) is superposed upon the luminescence of the solution and it

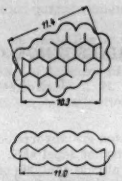

Fig. 2. Models and dimensions of chrysene (1) and octane (2) molecules.

is consequently necessary to work with concentrations $C \approx 10^{-6}$-10^{-7} mole/liter. It was found while studying chrysene powders at 77° K that the spectrum of specimen I has a fairly pronounced structure and contains more than 20 bands, while the spectrum of specimen II consists of four broad bands (Fig. 3 a,b). After additional recrystallization of specimen II from chlorobenzene and sublimation, the spectrum of the new specimen III acquired an intermediate character (Fig. 3 c). The observed changes in the appearance of the emission spectrum of powdered chrysene are similar to broadening and displacement effects in single crystal spectra due to deformations and tensions in the crystals, and to their thickness.[9]

Because of the overlapping of bands, caused by various vibrational sublevels, in diffuse spectra the differences between band maxima only very approximately reflect the vibrational frequencies in the spectrum of a single molecule. Tables 3 and 4 show band locations and a vibrational analysis of fluorescence and absorption spectra of specimen I which has the clearest and best resolved spectrum, consisting of narrow bands.

An x-ray investigation was made of powders of the two specimens to find whether the observed changes in the structure of the luminescence spectra were caused by different conditions of crystallization or by some other structural changes. It was shown by this method in ref. 10 that single crystals of chrysene belong to the monoclinic system (space group $C_{2h}^5 = I2/c$). The unit cell, (a = 8.34, b = 6.18, c = 25.0 A, and $\beta = 115.8°$) con-

Table 2. Phosphorescence Spectra of Chrysene Solutions in Various Solvents at 77° K

Polyisobutylene	Heptane	EPA [7]	Octane*						
λ (A)	λ (A)	ν (cm^{-1})	λ' (A)	ν' (cm^{-1})	λ' (A)	ν' (cm^{-1})	I	Δν (cm^{-1})	Interpretation
—	—	—	4786	20885	—	—	v.w.	—	—
—	—	—	4805	20799	—	—	v.w.	—	—
—	—	—	4918	20323	—	—	v.w.	—	—
4992	4986	20030	4990	20034	5000	19994	s.	0	—
5065	5062	19700	5065	19737	5074	19702	m.	297	300
—	—	—	5103	19590	—	—	v.s.	544	645
5143	5144	19500	5145	19430	5157	19385	w.	604	2 × 300 = 600
—	—	—	5317	18802	5328	18783	v.w.	1232	1230
5352	5360	18800	5358	18658	5372	18609	s.	1376	1375
5434	5448	18400	5428	18417	5442	18370	v.w.	1617	1617
5517	5516	18200	5517	18120	—	—	s.	1914	300 + 1617 = 1917
—	5634	—	5614	17807	—	—	w.	2227	2 × 300 + 1617 = 2217
5778	—	—	5786	17278	5800	17236	m.	2756	2 × 1375 = 2750
5906	5868	17050	5868	17042	5880	17002	v.s.	2992	1375 + 1617 = 2992
5946	5970	16700	5970	16745	5984	16706	v.s.	3289	200 + 1375 + 1617 = 3292
6069	—	—	6065	16483	6082	16437	m.	3551	—
—	—	—	6148	16260	—	—	v.s.	3774	—
—	6301	—	6295	15906	—	—	w.	4128	3 × 1375 = 4125
6384	6390	15500	6390	15645	6405	15608	s.	4389	2 × 1375 + 1617 = 4367
6487	6492	—	6490	15404	6505	15368	s.	4630	2 × 1375 + 300 = 4667

*The symbols are the same as in Table I.

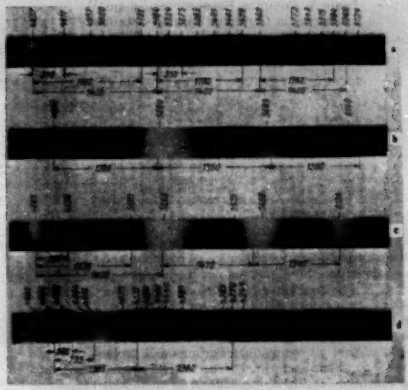

Fig. 3. Fluorescence (a-c) and absorption (d) spectra of various specimens of powdered chrysene at 77°K. a,d—specimen I; b—specimen II; c—specimen III.

tains 4 molecules. It was found that the chrysene molecule is flat, the benzene nuclei forming regular hexagons.

Powdered chrysene placed in collodion capillaries was investigated in an RKV-86 type camera, using CuK_α radiation. An analysis of the Debye pictures obtained indicates that no structural differences can be observed among specimens obtained under different crystallization conditions. There is nevertheless a certain difference in the diffraction pictures obtained from the specimens investigated, to wit:

The Debye rings are well resolved in the x-ray picture of specimen I (Fig. 4a), which shows signs of texture. It can be ascertained from the intensity distribution of the Debye rings that the powder is homogeneous and contains crystallites of the order of 10^{-3} to 10^{-4} cm in size. The resolution of Debye lines is much worse in the x-ray picture of specimen II (Fig. 4b). A number of lines are diffuse. This indicates a higher degree of dispersion in the powder in specimen II compared to the powder in specimen I. Figure 4c shows an x-ray picture obtained from specimen III. As can be seen in the illustration, this Debye picture corresponds to an apparently intermediate case between the pictures obtained from specimens I and II. In this picture single points appear along with continuous diffusion rings, indicating the presence of large crystalline particles in the chrysene powder. The

Table 3. Fluorescence Spectrum of Powdered Chrysene (Specimen I) at 77°K

No. of band	λ (A)	ν (cm⁻¹)	I*	Δν (cm⁻¹)	Interpretation
1	4837.7	20665	v.s.	0	—
2	4911.4	20355	s.	310	310
3	4987	20046	w.	619	2×310
4	5019.8	19915	m.	750	750
5	5069	19644	v.w.	1021	1020
6	5131.1	19483	s.	1182	1180
7	5184.3	19283	v.s.	1382	1400
8	5224	19134	s.	1531	1530
9	5238.4	19084	s.	1581	1580
10	5275.6	18949	m.	1716	1400 + 310 = 1710
11	5339.5	18783	w.	1942	1940
12	5400.8	18510	m.	2155	1400 + 750 = 2150
13	5461	18306	m.	2359	2360
14	5528	18084	s.	2581	1400 + 1180 = 2580
15	5589.41	17884	v.s.	2781	2×1400 = 2800
16	5638	17732	s.	2933	1400 + 1530 = 2930
17	5654	17681	s.	2984	1400 + 1580 = 2980
18	5772.2	17319	v.w.	3346	1400 + 1940 = 3340
19	5843	17109	v.w.	3556	2×1400 + 750 = 3550
20	5915.6	16899	p.	3766	1400 + 2360 = 3760
21	5984.2	16706	s.	3960	2×1400 + 1180 = 3980
22	6065	16483	s.	4182	3×1400 = 4200
23	6124	16324	s.	4341	2×1400 + 1530 = 4330
24	6141.9	16277	w.	4388	2×1400 + 1580 = 4380

*For symbols, see footnote to Table 1.

Table 4. Absorption Spectrum of Powdered Chrysene at 77°K (Specimen I)

λ (A)	ν (cm⁻¹)	Δν (cm⁻¹)	Interpretation
4832	20680	0	—
4762.5	20991	302	304
4694	21297	608	2×304 = 608
4666.5	21423	734	735
4575	21851	1162	1160
4563	21909	1220	1220
4533	22054	1365	1365
4503	22206	1517	1517
4463	22400	1711	1710
4440	22516	1827	1827
4395	22786	2100	1365 + 735 = 2100
4303	23239	2550	1365 + 1160 = 2525
4240	23584	3447	2×1365 + 735 = 3465

Fig. 4. Debye pictures of various specimens of powdered chrysene. a—specimen I; b—specimen II; c—specimen III.

Table 5. Common Frequencies (in cm^{-1}) Appearing in Chrysene Spectra Obtained under Different Conditions at 77° K

Dyed solution		Crystalline powder	
Phosphorescence	Fluorescence	Fluorescence	Absorption
300	295	310	304
—	1185	1180	1160
1375 *	1395	1400	1365

*It was first observed in an analysis of quasi-linear spectra exhibiting structure[4] that the frequency value of a given vibration can vary, depending on the quantum vibrational number and the electronic transition coupled to this transition. Excited electronic states and other vibrations introduce irregular changes in the value of the most intensive vibrations appearing in chrysene emission spectra ($\nu \sim 1400$ cm^{-1}), are connected with such a perturbation.

x-ray results obtained indicate a complete correlation between the diffraction pictures of powders and the spectrographic data for the same specimen given in Fig. 3.

It can be concluded on the basis of the spectral and x-ray data obtained that the larger and the more homogeneous the crystallites, the greater the degree of structure shown by its spectrum.

The part played by deformations and surface stresses, which lead to perturbation and displacement of the electrical levels of molecules, is much more important in a fine powder. Mechanical-physical inhomogeneities perturb not only the outer levels (diffuse spectra) but the inner levels as well (broadening of interference rings in Debye pictures). These factors also have a smaller influence on the properties of vibrational levels and the probability distributions of transitions between electronic-vibrational levels. Thus, on changing from a solution to powder, the levels responsible for fluorescence are displaced by the interval $\Delta\nu = \nu_{0,0\ F\ solution} = \nu_{0,0\ F\ powder} = 27{,}720\text{-}20{,}665 = 7055$ cm^{-1}. At the same time, the common frequencies appearing in luminescence spectra of solutions and powders show little change (Table 5). The appearance of additional vibrational frequencies (as compared to solutions) is also possible in the crystalline state, because of the removal of forbiddenness as a result of strong intermolecular interactions.

In conclusion, the authors express their gratitude to A. I. Kitaigorodskii for a discussion of results and to V. Tolkachev for his kind measurement of fluorescence spectra of chrysene vapors.

REFERENCES

1. E. V. Shpol'skii, Uspekhi Fiz. Nauk **68**, 51 (1959).
2. P. Pringsheim and M. Vogel, "Luminestsentsiya zhidkikh i tverdykh tel" (Luminescence of Liquids and Solids). Izd. Inostrannoi Lit., Moscow, 1948.
3. G. Lewis and M. Kasha, J. Am. Chem. Soc. **66**, 2100 (1944).
4. M. Kasha, Chem. Revs. **41**, 401 (1947).
5. A. Rousset, R. Lochet, and I. L. Dubarry, Compt. Rend. **248**, 54 (1959).
6. I. B. Birks and A. I. W. Cameron, Proc. Roy. Soc. **A249**, 297 (1959).
7. E. V. Shpol'skii and E. A. Girdzhiyauskaite, Opt. i Spektr. **4**, 620 (1958);
   D. N. Shigorin, N. A. Shcheglova, R. N. Nurmykhametov, and N. S. Dokunikhin, Doklady Akad. Nauk SSSR **120**, 1242 (1959);
   L. Pesteil and A. Cials, Compt. Rend. **249**, 528 (1959).
8. T. N. Bolotnikova, Izvest. Akad. Nauk SSSR, Ser. Fiz. **23**, 29 (1959).
9. V. L. Broude, A. F. Prikhot'ko, and E. I. Rashba, Uspekhi Fiz. Nauk **67**, 99 (1959).
10. I. J. Ball, Proc. Roy. Soc. **A146**, 140 (1934).
11. O. E. Waigang and W. W. Robertson, J. Chem. Phys. **30**, 1413 (1959);
    L. Pesteil, Compt. Rend. **250**, 497 (1960).

Opening of Subscriptions

to the journals of the Academy of Sciences, USSR

for the Year 1961

Subscriptions are received generally at subscription points of the "Union Press," Post Offices, communication offices and departments, scientific research institutes, educational institutes and organizations, by public representatives in plants and factories, and by departments and stores of "Academy Books" and the "Academy Books" office at the address: Moscow, K-12, B. Cherkasskii Lane, 2/10.

The journal "Optics and Spectroscopy" appears monthly, 2 volumes per year (6 issues per volume). Subscription rate: Yearly, 162 rubles. Half-yearly, 81 rubles.

THE CONCENTRATION QUENCHING OF LUMINESCENCE IN ORGANOLUMINORS

G. A. Mokeeva and B. Ya. Sveshnikov

Received 27 February 1960

We have investigated the influence of activator concentration on the duration, spectrum, and yield of fluorescence and phosphorescence of sugar luminors activated with trypaflavine and of boro-glycerine luminors activated with fluorescein, at 20° and −183°C. We have shown that in the former case the variation of the luminescence characteristics with concentration is due to molecular association. No indications of molecular association have been found for the second luminor in the concentration range investigated.

We have shown that the molecules that go into the phosphorescent state are quenched at the fluorescence level. The presence of concentration quenching of molecules in the metastable state is demonstrated. However, the nature of the variation of the relative yield and duration of the phosphorescence is unusual, since the yield decreases more slowly than the duration.

It has been shown[1] that short wavelength phosphorescence (α-phosphorescence, in the terminology of Lewis) should be quenched much more rapidly than the fluorescence or the total radiation, even in the absence of quenching at the metastable level. This conclusion follows from a theoretical analysis of the kinetics of luminescence for the three-level scheme, proposed by Jabloński, subject to the additional assumptions that transitions to the metastable state take place during the entire time that the molecules are in the fluorescent state, and that the probability of quenching in the fluorescent state is proportional to the time that the molecule stays in this state. On the other hand, the yield of the long wavelength phosphorescence (β-phosphorescence, in Lewis' terminology) should vary in the same way as the fluorescence yield if there is no additional quenching in the metastable state.

An analogous phenomenon should be observed for the concentration polarization of both types of phosphorescence in organoluminors. Actually, as the activator concentration increases, the degree of polarization of α-phosphorescence decreases more rapidly than that of fluorescence.[2] Surprisingly, however, the degree of polarization of β-phosphorescence varies much less with increasing activator concentration than the degree of fluorescence polarization. Thus, complete agreement between the experimental results and theory has not been obtained.

In view of the situation, we deemed it important to ascertain whether the theory is applicable to the concentration quenching of α- and β-phosphorescence.

The experiments had to be performed with organoluminors showing both types of phosphorescence. The number of luminors with this property is small. These include, primarily, boric and boro-glycerine[3] phosphors activated with fluorescein, and sugar candy activated with acridine orange, trypaflavine, benzoflavine, eosine, and erythroeosine. According to Zanker[4] and Sveshnikova and Kuznetsova,[5] a large number of associated pairs is produced in the case of acridine orange, even in alcoholic solution at concentrations from 4×10^{-5} to 1×10^{-3} moles/liter at liquid-air temperature. These complexes have different fluorescence and absorption spectra, with a fluorescence duration longer than that of the monomers. At room temperature, according to Kuznetsova et. al and Molchanov,[6] the changes in the fluorescence and absorption spectra in the same solutions and in the same concentration interval are small, while the changes (reduction) in the yield and duration of the glow are in the same direction. In sugar candy activated by acridine orange, radical changes in the fluorescence and absorption spectra take place at high dye concentrations, both at room temperature and at low temperatures.

Similar phenomena are observed in luminors activated with trypaflavine. At room temperature, the form of the long wavelength absorption band of alcoholic solutions of trypaflavine changes relatively little as the concentration increases from 1×10^{-5} to 1×10^{-2} mole/liter —there is merely a slight increase in the absorption in the short wavelength absorption band (Fig. 1). As the dye concentration is increased, the fluorescence spectra in thick layers shift noticeably toward the red, but this shift, as was demonstrated by experiments with thin layers, is induced to a considerable extent by reabsorption of the luminescence. At high dye concentrations (2×10^{-3} to 1×10^{-2} mole/liter) the long wavelength part of the fluorescence spectrum is deformed somewhat.

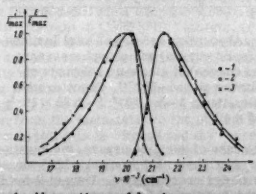

Fig. 1. Absorption and luminescence spectra of alcoholic solutions of trypaflavine at 20°C. Concentration (in mole/liter): 1—5×10^{-4}; 2—1×10^{-3}; 3—1×10^{-2}.

As in the case of alcohol solutions of acridine orange, the yield and duration of the fluorescence of alcohol solutions of trypaflavine have a parallel course at room temperature (Fig. 2a) and can apparently be reconciled with modern theories of concentration quenching.[7] At liquid-air temperature, the changes in the total luminescence spectra occur much earlier and are quite substantial. As can be seen from Fig. 3, the maximum of the total-luminescence spectrum of trypaflavine shifts 2000 cm^{-1} on going from a concentration of 1×10^{-5} mole/liter to 1×10^{-2} mole/liter, and the appearance of the spectrum changes considerably. The β-phosphorescence spectrum, as in the case of frozen alcoholic solutions of acridine orange, depends very little on the dye concentration and shifts only slightly toward the red with

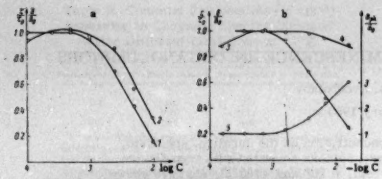

Fig. 2. Concentration quenching of the luminescence of alcoholic solutions of trypaflavine at 20°C (a) and −183°C (b) (C in mole/liter). Curve 1—fluorescence yield; curve 2—duration of fluorescence; curve 3—total luminescence yield; curve 4—duration of phosphorescence; curve 5—relative yield of phosphorescence. (The values of these quantities are arbitrarily taken as unity at low concentrations.)

increasing concentration. If, by analogy with concentrated solutions of acridine orange, we attribute the foregoing phenomena to molecular association, we can say that in alcoholic solutions of both dyes, molecular association influences the fluorescence spectra much more than the phosphorescence spectrum.

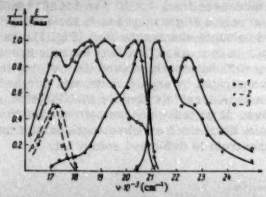

Fig. 3. Absorption spectra of total luminescence (solid curves) and phosphorescence (dashed curves) of alcoholic solutions of trypaflavine at t = −183°C. Concentration (in mole/liter): 1—5×10^{-5}; 2—1.25×10^{-3}; 3—1.25×10^{-2}.

As in the case of acridine orange, the duration of fluorescence of alcoholic solutions at −183° increases with increasing dye concentration. Thus at 2.5×10^{-5} mole/liter, the duration of fluorescence of an alcoholic solution of trypaflavine is 5.3×10^{-9} sec, increasing to 13.3×10^{-9} sec at 5×10^{-3} mole/liter. The duration of the phosphorescence changes hardly at all in this range of concentrations (Fig. 2b). The same figure shows that between 1×10^{-3} and 1.25×10^{-2} mole/liter, the total-emission yield decreases fourfold, and the relative fluorescence yield triples (from 3 to 9 percent).

Within the framework of the generally accepted theory of phosphorescence of organoluminors, the increase in the relative phosphorescence yield can be attributed to a considerable extent to the increase in the duration of fluorescence. As regards the frequency of transition from the fluorescent to the metastable state, it apparently changes little in association.

Of all the substances investigated, the boro-glycerine luminors activated with fluorescein were the only ones in which the absorption spectra at room temperature remained unchanged as the concentration was varied from 1×10^{-4} to 1×10^{-2} gm/gm, and the total-luminescence spectra and the α- and β-phosphorescences shifted to the red without noticeable distortion in the form of the spectrum (Figs. 5 and 6).

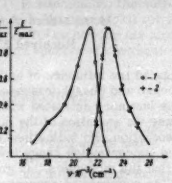

Fig. 4

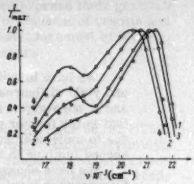

Fig. 5

Fig. 4. Absorption and luminescence spectra of boro-glycerine phosphors activated with fluorescein, at 20°C. Concentration (in gm/gm): 1—1×10^{-4}; 2—1×10^{-2}.

Fig. 5. Spectra of total luminescence and α-phosphorescence of boro-glycerine phosphors activated with fluorescein, at 20°C. Concentration (in gm/gm): Curves 1, 3—5×10^{-4}; curves 2,4—1×10^{-2}.

Since the fluorescence and absorption spectra of boro-glycerine luminors overlap (Fig. 4) and the absolute luminescence yield is fairly high, the effect of reabsorption of radiation must be taken into account in investigating the variation of the yield and duration of fluorescence with dye concentration.

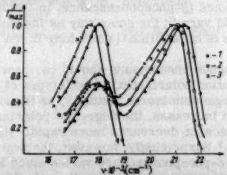

Fig. 6. Spectra of total luminescence and β-phosphorescence of boro-glycerine phosphors activated with fluorescein, at −183°C. Concentration (in gm/gm): 1—5×10^{-4}; 2—1×10^{-3}; 3—1×10^{-2}.

For this purpose, we measured the duration of fluorescence of boro-glycerine luminors activated with fluorescein, with a dye concentration of 5×10^{-4} gm/gm and a layer thickness ranging from 0.05 to 2 mm. The exciting light was the 436 mμ mercury line, and all observations were carried out from the excitation side. The data obtained by us are listed in the Table.

Using these data as a guide, we measured the duration of fluorescence for activator concentrations of 2 ×

Variation of Duration of Fluorescence of Boro-Glycerine Phosphors at 20°C ($\tau \times 10^9$ sec)

C (gm/gm) \ Layer thickness, mm	0.05	0.1	0.5	1	2
$1 \cdot 10^{-4}$		3.8			
$5 \cdot 10^{-4}$	3.8	3.85	3.9	4.15	4.4

10^{-3} to 1×10^{-2} gm/gm in luminor layers thinner than 0.01 mm, and for concentrations of 5×10^{-4} to 2×10^{-2} gm/gm in layers not thicker than 0.05 mm, at 20° and −183°. It was assumed that the data obtained in this manner were free from the effects of reabsorption of fluorescence. These data are shown in Fig. 7. The data on the variation of the total luminescence yield* are less independent of the influence of reabsorption and are less accurate. We made these measurements in layers which were thick enough to guarantee total absorption of the exciting light. It is obvious that in this case, the effect of reabsorption decreases with increasing quenching (naturally, reabsorption plays a greater role at room temperature than at liquid-air temperature). The data on the variation of the total emission yield with activator concentration are also shown in Fig. 7. The same diagrams show the variations of the relative yields and the mean duration of the phosphorescence.* The decay law of the afterglow was investigated with a phosphoroscope setup similar to that used by Pilipovich and Sveshnikov.[3]

*In this case, total emission is the sum of α-phosphorescence and fluorescence.

*Inasmuch as the decay of the phosphorescence is not exponential, the mean duration of phosphorescence was determined from the ration $\int f(t)t\,dt/\int f(t)\,dt$ (where f(t) represents the decay law) by graphical integration.

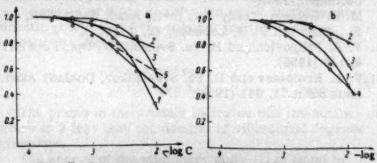

Fig. 7. Concentration quenching of luminescence of boro-glycerine phosphors activated with fluorescein at 20°C (a) and −183°C (b) (C in gm/gm) curve 1—total-luminescence yield; curve 2—duration of fluorescence; curve 3—relative phosphorescence yield; curve 4—duration of phosphorescence; curve 5—duration of phosphorescence with correction for secondary transitions. (The values of the quantities indicated are arbitrarily taken as unity at low concentrations.)

It should be noted that even if the decay is exponential, the reciprocal of the decrement (λ_s^{-1}) is not equal to the true duration of phosphorescence (τ_2), owing to the effect of repeated transitions between the fluorescent and metastable levels, which play an important role in the case of boro-glycerine phosphors activated with fluorescein; this is a consequence of the high relative phosphorescence yield. The change in the total luminescence yield is therefore not proportional to the change in the mean duration of fluorescence.

Sveshnikov[1] derived the following equation for an exponential decay law:

$$\lambda_s \tau_2 = 1 - \frac{I_\alpha}{I_s}. \qquad (1)$$

where I_α and I_s are the intensities of the α-fluorescence and the total emission, respectively, for a constant level of excitation.

In our case the decay of phosphorescence, and probably also of fluorescence, is not exponential, and the change in the yields of these types of emission is not proportional to the change in duration. Nevertheless, we attempted to use Eq. (1) in order to obtain some idea of the magnitude of the possible corrections that must be applied to the duration of the afterglow to take account of repeated transitions between the fluorescent and metastable levels. The curve obtained in this manner for τ_2 is shown dashed in Fig. 7a.

According to the theory developed at the beginning of this article, the fluorescence yield depends on the quenching both at the fluorescence and at the phosphorescence levels. It would be most desirable to separate the two types of quenching. This is readily done by investigating the variation of the initial phosphorescence intensity of the luminors for periods of excitation and observation which are much shorter than the duration of phosphorescence, i.e., under conditions such that the time-dependent quenching at the metastable level has no time to develop. Naturally, in this case the phosphor must be thick enough to ensure total absorption of the exciting light for all activator concentrations.

The experimental procedure was very simple. The specimen was placed between the two disks of a Becquerel phosphoroscope, each with a 10° notch, shifted 10° relative to each other (the disks were rotated at 10 rps). A photographic shutter was placed in front of the light source and was opened prior to the passage of the disk notches, after which it was closed to ensure complete deexcitation of the phosphor. The observations were carried out from the excitation side, and the initial phosphorescence intensity was determined from a photomultiplier signal on a long-persistence oscilloscope screen. The initial intensities of α- and β-phosphorescence were investigated for luminors with concentrations of 5×10^{-4}, 2×10^{-3}, and 1×10^{-2} gm/gm. The ratios obtained were 1/1.3/0.95 and 1/1.18/0.75 for α- and β-phosphorescence, respectively.

Let us first consider the case of β-phosphorescence. Since the fluorescence yield drops to 0.88 on going from $C = 5 \times 10^{-4}$ gm/gm to $C = 2 \times 10^{-3}$ gm/gm, (Fig. 7b), theory would lead us to expect the initial phosphorescence intensity to decrease to 0.88. Instead, it increases to 1.18. This may be due either to an increase in the frequency of transition from the fluorescent to the metastable state (r), or to an increase in the frequency of transition from the metastable to the normal state (r'). If the first hypothesis is adopted and the decrease in phosphorescence duration is regarded as a characteristic of quenching at the metastable level, then, as can be seen from elementary calculations,[1] to obtain an increase of initial phosphorescence intensity of 1.18 simultaneously with a decrease of fluorescence yield to 0.88, it is necessary to increase the frequency of transition r by 1.4 fold* over the value corresponding to $C = 5 \times 10^{-4}$ gm/gm (r_0). The relative phosphorescence yield will in this case be 1.04 times the afterglow yield at $C = 5 \times 10^{-4}$ gm/gm. If $C = 1 \times 10^{-2}$ gm/gm, satisfactory agreement with experimental data can be obtained if one assumes that r is increased by a factor of 1.5 compared with its value at $C = 5 \times 10^{-4}$ gm/gm.

*It follows from the data on the relative phosphorescence yield and fluorescence duration that $r \approx 1 \times 10^9$ sec^{-1} when $C = 5 \times 10^{-4}$ gm/gm.

According to the second hypothesis, the initial intensity of β-phosphorescence should be $0.88/0.79 \approx 1.11$ at $C = 2 \times 10^{-3}$ gm/gm and $0.52/0.49 \approx 1.06$ at $C = 1 \times 10^{-2}$ gm/gm. It is readily seen that the last figure does not agree at all with the experimental data. Nor can this hypothesis explain the considerable drop in the relative

yield of β-phosphorescence when the activator concentration is 1×10^{-2} gm/gm.

According to the theory given at the beginning of the article, the relative yield of α-phosphorescence should decrease with quenching more rapidly than the fluorescence yield, since the molecules responsible for the α-phosphorescence should be quenched a second time at the fluorescence level on returning from the metastable state to the fluorescence state, and, furthermore, the relative phosphorescence yield should decrease, owing to quenching at the metastable level. As seen from Fig. 7a, this does not occur.

The most likely explanation of this phenomenon apparently lies in the fact that the molecules of a highly concentrated activator produce different groupings, which have different luminescence characteristics. These cannot yet be regarded as associated, for there are no clear indications that the absorption spectra change at these activator concentrations, but these groupings differ considerably from monomers of the given activator as regards the values of the fluorescence and phosphorescence yields and durations. The existence of such fluctuating formations of activator molecules at high activator concentration in the luminor is confirmed all the more by the fact that the decay curves of the phosphorescence of boro-glycerine organoluminors disclose an ever increasing deviation from exponential form with increasing activator concentration (Fig. 8).

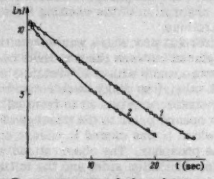

Fig. 8. Decay curves of phosphorescence of boro-glycerine phosphors activated with fluorescein, at t = −183°C. Concentration (in gm/gm): Curve 1—5×10^{-4}; curve 2—1×10^{-2}.

REFERENCES

1. B. Ya. Sveshnikov, Zhur. Eksptl. i Teoret. Fiz. 18, 878 (1948).
2. B. Ya. Sveshnikov, Doklady Akad. Nauk SSSR 58, 49 (1947);
P. I. Kudryashov and B. Ya. Sveshnikov, Opt. i Spektr. 8, 651 (1960), Optics and Spectroscopy 8, 344 (1960).
3. P. I. Kudryashov, B. Ya. Sveshnikov, G. A. Tishenko, and A. S. Cherkasov, Inzh.-Fiz. Zhur. 2, 62 (1959).
4. W. Zanker, Z. phys. Chem. 200, 250 (1952).
5. L. A. Kuznetsova and B. Ya. Sveshnikov, Izvest. Akad. Nauk SSSR, Ser. Fiz. 20, 433 (1956).
6. L. A. Kuznetsova, B. Ya. Sveshnikov, and V. A. Molchanov, Doklady Akad. Nauk SSSR, 109, 746 (1956).
7. S. I. Vavilov, Collected Works, Vol. II, Izd. Akad. Nauk SSSR, 1952;
Th. Förster, Fluoreszenz organischer Verbindungen, Göttingen, 1951;
M. D. Galanin, Trudy Fiz. Inst., Akad. Nauk SSSR, Fiz. Inst. im. P. N. Lebedev, 12, 3 (1960).
8. V. A. Pilipovich and B. Ya. Sveshnikov, Opt. i Spektr. 4, 146 (1956).
9. V. L. Ermolaev and B. Ya. Sveshnikov, Doklady Akad. Nauk SSSR 71, 647 (1950).

THE THEORY OF PHOTOIONIZATION OF F-CENTERS

Yu. E. Perlin and M. E. Palistrant

Received 26 February 1960

The states of the continuous spectrum of an F-center are interpreted to be polarons moving in the screened Coulomb field of an anion vacancy. The probability is calculated for a phototransition from the ground state of an F-center into such ionized states. It is shown that since phonons take part in the phototransition, the dependence of the probability of ionization on the frequency of the absorbed light has the form of an asymmetrical curve with a maximum. On the long wavelength side of the maximum, this curve coincides with Pekar's curve for phototransitions in the discrete spectrum. On the short wavelength side, it decreases more smoothly. As the temperature rises, the height of the photoionization maximum decreases, while the half-width of the curve increases.

The appearance of photoconductivity as a result of the absorption of light in the F-band is connected primarily with a thermo-optical ionization of the color centers, i.e., with a two-step process which includes excitation of the center after absorption of a photon, with subsequent thermal ionization. At low temperatures, however, the second (thermal) stage of the process has a very low probability. The photoconductivity observed[1] under these conditions must be ascribed to direct photoionization of the F-centers.

The internal photoeffect in F-centers was investigated by Deigen[2] and Dykman.[3] The quantum mechanical calculation of the phototransition from the fundamental state of the color center to the continuous spectrum was carried out in ref. 2 using the Frank-Condon approximation, i.e., on the assumption that the polarization potential well of the F-center remains "frozen" during the phototransition. The spectral light absorption curve computed in ref. 2 increases monotonically, starting from the red edge. Reference[3] took into account the appearance of phonons, which is connected with a change in the equilibrium configuration of the lattice when the electronic states change in the process of phototransition. However, the photons whose absorption was considered[3] had relatively higher energies (of the order of 4 ev) and created fast electrons, for which the polaron effect may be neglected.

In the present paper, we consider the ionization of

the F-center by photons whose energy does not differ appreciably from the ionization energy (of the order of 2 ev). The dissociated state of the F-center must therefore be identified with a polaron, and not with a free (zone) electron.

In an article devoted to the thermal ionization of an F-center,[4] one of the present authors proposed a method for describing both the ground state and the excited states of an F-center by means of the variables of Pekar's polaron theory.[5] According to ref. 4, the wave function of the ground state of an F-center may be represented by

$$\Psi_{n_1 \dots n_s^0 \dots} = \psi_g(r)\,\varphi_g(\xi)\prod_s{}' \Phi_{n_s^0}(q_s' - r_s), \tag{1}$$

where $\psi_s(r)$ is the electronic wave function of the ground state, which we shall express in the form[5]

$$\psi_g(r) = \frac{(a_0\gamma)^{3/2}}{\sqrt{\pi}}(1 + a_0\gamma r)\exp(-a_0\gamma r), \tag{2}$$

$$a_0 = \frac{\mu e^2 c}{2\hbar^2}; \quad \gamma = 1 + \frac{3}{\varepsilon c}$$

ξ is the translation vector of the polaron

$$\varphi_g(\xi) = \frac{(a_0\lambda)^{3/2}}{\sqrt{\pi}}\exp(-a_0\lambda\xi) \tag{3}$$

(λ is a variational parameter determined by numerical methods); $\Phi_{n_s}^0$ are the wave functions of normal oscillators of longitudinal optical vibrations of the lattice; q_χ are the corresponding normal coordinates; $q_{\chi\xi}$ and $q_{\chi F}$ are the values of these coordinates which minimize the adiabatic potentials of the polaron and the F-center, respectively. Here

$$\left.\begin{aligned} q_s' &= q_s - q_{sq}; \\ r_s &= q_{sF} - q_{sq}|_{\xi=0}. \end{aligned}\right\} \tag{4}$$

The prime in the product indicates that the number of factors is 3 less than the number of vibrational degrees of freedom.

The energy of the stationary state (1) is equal to

$$H_{n_1 \dots n_s^0 \dots} = I_F + \hbar\omega\sum_s\left(n_s^0 + \frac{1}{2}\right) + \frac{3}{2}\hbar\omega, \tag{5}$$

where I_F is the minimum value of the adiabatic potential of the F-center and ω is the limiting frequency of the longitudinal polarization vibrations of the crystal. The wave function of the dissociated state of the F-center is

$$\Psi_{k, \dots n_s \dots}' = \psi_0(|r - \xi|)\,\varphi_k(\xi)\prod_s{}' \Phi_{n_s}(q_s'), \tag{6}$$

where $\psi_0(r)$ is the wave function of the electron and polaron, written as[5]

$$\psi_0(r) = \frac{a_0^{3/2}}{\sqrt{\pi}}(1 + a_0 r)\exp(-a_0 r); \tag{7}$$

$\varphi_k(\xi)$ is determined from Schrödinger's equation

$$\left[-\frac{\hbar^2}{2M}\Delta_\xi + W(\xi)\right]\varphi_k(\xi) = E_k\varphi_k(\xi), \tag{8}$$

in which M refers to the effective mass of the polaron

$$E_k = \frac{\hbar^2 k^2}{2M}$$

and

$$W(\xi) = -\frac{e^2}{\varepsilon}\int\frac{\psi_0^2(|r - \xi|)}{r}\,d\tau \tag{9}$$

represents the effective field in which the polaron moves.

The energy of the stationary state (6) is

$$H_{k, \dots n_s \dots} = I_0 + E_k + \hbar\omega\sum_s\left(n_s + \frac{1}{2}\right), \tag{10}$$

where I_0 is the minimum value of the adiabatic potential of the polaron.

Assuming that the wavelength of the absorbed light is long as compared with the radii of the electronic states of the polaron and the F-center, we can carry out the calculation for the phototransition in a semiclassical approximation, choosing our perturbation operator in the form

$$H' = -e\mathcal{E}z, \tag{11}$$

Here $\mathcal{E}$ is the strength of the effective electric field of the light wave. This field is periodic in time (with frequency Ω) and is polarized along the z-axis.

The electronic matrix element

$$Z(\xi) = \int\psi_0(|r - \xi|)\,z\psi_g(r)\,d\tau, \tag{12}$$

computed by means of the wave functions (2) and (7) is found to be equal to

$$Z(\xi) = \frac{\cos\vartheta}{a_0}K(\xi);$$

$$K(\xi) = \frac{32\gamma^{3/2}}{7(\gamma^2 - 1)^3 a_0^{3/2}}\{[480\gamma^3 + 480\gamma^2 a_0\xi - 96\gamma^3(\gamma^2 - 1)a_0^2\xi^2 + 6\gamma^3(\gamma^2 - 1)^2 a_0^3\xi^3]\exp(-a_0\xi) - [480\gamma^3 + 480\gamma^2 a_0\xi + 144\gamma^3(\gamma^2 - 1)a_0^2\xi^2 + (\gamma^2 - 1)^2(19\gamma^2 - 1)a_0^3\xi^3 + \gamma(\gamma^2 - 1)^3 a_0^4\xi^4]\exp(-a_0\gamma\xi)\}, \tag{13}$$

where

$$\cos\vartheta = \frac{(\delta, \xi)}{\delta\xi}.$$

The wave function $\varphi_k(\xi)$ is spherically symmetrical. Therefore the only transitions allowed are in the p-state of Eq. (8). We shall choose wave functions for them in the form

$$\varphi_k(\xi) = \frac{\chi_{k1}(\xi)}{\xi}\sqrt{\frac{3}{4\pi}}\cos\vartheta, \tag{14}$$

where $\chi_{k1}(\xi)$ is determined from the equation

$$\chi_{k1}'' + \left[\frac{2M}{\hbar^2}|W(\xi)| + k^2\right]\chi_{k1} - \frac{2}{\xi^2}\chi_{k1} = 0. \tag{15}$$

It has been shown[4] that the potential energy $W(\xi)$ satisfies the criterion for being quasi-classical for $E_k \ll \hbar\omega$. In the case of p-states, however, this criterion is violated for the centrifugal term in Eq. (15) for small values of ξ. Let us choose the point ξ_0 so that $W(\xi)$ can be considered constant and equal to $W(0)$ in the region $\xi \ll \xi_0$, while the centrifugal energy can be neglected in the region $\xi > \xi_0$. In the first of these regions, Eq. (15) takes the form

$$\left.\begin{aligned} &\chi_{k1}'' + k_0^2\chi_{k1} - \frac{2}{\xi^2}\chi_{k1} = 0; \\ &k_0^2 = k^2 + \frac{2M}{\hbar^2}|W(0)|. \end{aligned}\right\} \tag{16}$$

We know that the solution of Eq. (16) which satisfies the requirement $\chi(0) = 0$ is

$$\chi_{k1}^{(I)} = A_k\left[\cos k_0\xi - \frac{\sin k_0\xi}{k_0\xi}\right]. \tag{17}$$

The quasi-classical wave function in the region $\xi > \xi_0$ is

$$\chi_{k1}^{(II)} = \frac{C_k}{\sqrt{p(\xi)}}\sin\left[\frac{1}{\hbar}\int_{\xi_0}^{\xi}p(\xi)\,d\xi + \vartheta\right], \tag{18}$$

where

$$p(\xi)\cong\sqrt{2M\left[E_k-W(\xi)\right]}.$$

The constants A_k and δ are easily determined by "joining" the functions (17) and (18) and their first derivatives at the point ξ_0. For A_k we find

$$A_k^2\left(1+\frac{1-2\sin^2 x}{x^2}-\frac{2\sin x\cos x}{x^3}+\frac{\sin^2 x}{x^2}\right)=\frac{C_k^2}{\hbar k_0},$$

where

$$x=k_0\xi_0.$$

A study of the potential $W(\xi)$ shows that $\xi_0\sim\alpha_0^{-1}$ satisfies the conditions formulated above. But in that case $\chi\gg 1$ and we may set

$$A_k\cong\frac{C_k}{\sqrt{\hbar k_0}}. \tag{19}$$

The constant C_k is determined as in ref. 4 by normalizing over a sphere of radius $L\to\infty$, i.e.,

$$C_k=\sqrt{\frac{2\hbar k}{L}}. \tag{20}$$

We will not introduce the expression for the phase δ. Due to the presence of the rapidly decreasing function $\varphi_s(\xi)$, we may, in computing the matrix element, replace $\varphi_k(\xi)$ by its asymptotic expression at small values of ξ, a high degree of accuracy being preserved. This means that we may set

$$\psi_k(\xi)\cong\sqrt{\frac{3kk_0}{2\pi L}}\left[\frac{\cos k_0\xi}{k_0\xi}-\frac{\sin k_0\xi}{k_0^2\xi^2}\right]\cos\theta. \tag{21}$$

Furthermore, let us introduce the notations

$$\zeta(k)=\int\psi_k(\xi)\,Z(\xi)\,\psi_s(\xi)\,d\tau_\xi; \tag{22}$$

$$S_{n_s,n_s^0}=\int\Phi_{n_s}(q_s')\,\Phi_{n_s^0}(q_s'-r_s)\,dq_s'. \tag{23}$$

Using them, the probability of a transition to one of the states of the continuous spectrum may be written in the form

$$w_{i0}=\frac{2\pi e^2\mathcal{E}_0^2}{\hbar}|\zeta(k)|^2\sum_{n_1^0=0}^{\infty}\cdots\sum_{n_s^0=0}^{\infty}\left\{\prod_s' S_{n_s,n_s^0}^2\,2\,\mathrm{Sh}\,\frac{\beta}{2}\exp\left[-\beta\left(n_s^0+\frac{1}{2}\right)\right]\right\}$$
$$\times\delta(H_k-H_i-\hbar\Omega), \tag{24}$$

where $\mathcal{E}_0$ is the amplitude of the electric vector and

$$\beta=\frac{\hbar\omega}{kT}.$$

As usual in a study of multiphonon processes, formula (24) contains a statistical averaging over the initial values n_γ^0 and a summation over the final values n_γ of the population numbers of the phonon field. The operation indicated may be carried out by means of the integral representation of the δ-function and Slater's formula for the matrix of the oscillator density. The corresponding computations are quite analogous to those of ref. 4 so that we shall omit the details and merely give the result

$$w_{i0}=\frac{2\pi e^2\mathcal{E}_0^2|\zeta(k)|^2}{\hbar^2\omega}\exp\left(-\frac{a}{2}\,\mathrm{cth}\,\frac{\beta}{2}-\frac{n\beta}{2}\right)$$
$$\times I_l\left(\frac{a}{2\,\mathrm{Sh}\,\frac{\beta}{2}}\right)\sum_{n=0}^{\infty}\delta(l-n), \tag{25}$$

where

$$a=\sum_s r_{s,s}^2; \tag{26}$$

$$l=\frac{\Delta I^2}{2M\omega}+\frac{\Delta I-\hbar\Omega}{\hbar\omega}, \tag{27}$$

In these formulas $\Delta I=I_0-I_F-3\hbar\omega/2$ is the ionization energy of the F-center and I_l is the Bessel function of imaginary argument.

The ionization probability is obtained from Eq. (25) by integrating over all p-states of the continuous spectrum

$$w_{i\infty}=\frac{L}{\pi}\int_0^\infty w_{i0}dk=\frac{LM\omega}{\pi\hbar}\int_{l_0}^\infty\frac{w_{i0}}{k}\,dl, \tag{28}$$

where

$$l_0=\frac{\Delta I-\hbar\Omega}{\hbar\omega}. \tag{29}$$

Substitution of Eq. (25) in Eq. (28) gives

$$w_{i\infty}=\frac{2LM\mathcal{E}_0^2\delta_0^2}{\hbar^3}\exp\left(-\frac{a}{2}\,\mathrm{cth}\,\frac{\beta}{2}\right)$$
$$\times\sum_{n\ge l_0}^{\infty}\frac{|\zeta(k)|^2}{k}\exp\left(-\frac{n\beta}{2}\right)I_n\left(\frac{a}{2\,\mathrm{Sh}\,\frac{\beta}{2}}\right), \tag{30}$$

where k and n are connected by the relationship

$$k=\sqrt{\frac{2M\omega}{\hbar}(n-l_0)}. \tag{31}$$

Formula (30) expresses (through l_0) the dependence of the probability of photoionization on the frequency Ω of the incident light. The matrix element $\zeta(k)$ which appears in Eq. (30) can readily be calculated by using Eqs. (21) and (22). It turns out to be

$$\zeta(k)=\frac{2^7(\lambda\gamma)^{3/2}}{21\left(\gamma^2-1\right)^2\alpha_0^2}\sqrt{\frac{3k}{2\pi_0 L}}\,F(\varkappa_0), \tag{32}$$

where

$$F(\varkappa_0)=\frac{480\gamma^3}{\varkappa_0}\left[\lambda\cdot\arctan\frac{\varkappa_0(\gamma-1)}{(\lambda+1)(\lambda+\gamma)+\varkappa_0^2}\right.$$
$$\left.-\frac{\gamma(\lambda+\gamma)\varkappa_0}{\varkappa_0^2+(\lambda+\gamma)^2}+\frac{(\lambda+1)\varkappa_0}{\varkappa_0^2+(\lambda+1)^2}\right]$$
$$+96\gamma^3(\gamma^2-1)\varkappa_0^3\left\{\frac{2}{\left[\varkappa_0^2+(\lambda+1)^2\right]^3}+\frac{3}{\left[\varkappa_0^2+(\lambda+\gamma)^2\right]^3}\right\}$$
$$-8\varkappa_0^3(\gamma^2-1)^3\times\left\{\frac{6\gamma^3(\lambda+1)}{\left[\varkappa_0^2+(\lambda+1)^2\right]^3}-\frac{(\lambda+\gamma)(19\gamma^2-1)}{\left[\varkappa_0^2+(\lambda+\gamma)^2\right]^3}\right\}$$
$$-\frac{8\varkappa_0^3\left[\varkappa_0^2-5(\lambda+\gamma)^2\right]\gamma(\gamma^2-1)^3}{\left[\varkappa_0^2+(\lambda+\gamma)^2\right]^3}. \tag{32a}$$

Here $\chi_0=k_0/\alpha_0$ is connected through k with the summation index n. (See formulas (16) and (31).) Substituting Eq. (31) into Eq. (29), we obtain

$$\frac{w_{i\infty}}{\omega}=\frac{3\cdot 2^{14}(\lambda\gamma)^3}{21^2(\gamma^2-1)^{13}}\left(\frac{e\mathcal{E}_0}{\hbar\omega\alpha_0}\right)^2\frac{M\omega}{\hbar\alpha_0^2}$$
$$\times\exp\left(-\frac{a}{2}\,\mathrm{cth}\,\frac{\beta}{2}\right)\sum_{n\ge l_0}^{\infty}\frac{F^2(\varkappa_0)}{\varkappa_0}\exp\left(-\frac{n\beta}{2}\right)I_n\left(\frac{a}{2\,\mathrm{Sh}\,\frac{\beta}{2}}\right). \tag{33}$$

The expression for the parameter a is given in ref. 4.

The frequency dependence expressed by Eq. (32) is complicated and must be evaluated by numerical methods for each crystal. On the basis of the considerations given below, however, we may qualitatively determine the shape of the spectral photoionization curve. As shown by Eq. (32a), the expression $[F(\chi_0)/\sqrt{\chi_0}]^2$ is a monotonically (and relatively smoothly) decreasing function of n. On the other hand, the expression

$$R_n = \exp\left(-\frac{n\beta}{2}\right) I_n\left(\frac{a}{2\,\mathrm{Sh}\frac{\beta}{2}}\right). \tag{34}$$

which represents the curve for the absorption of light by an impurity in the discrete spectrum obtained by Pekar,[5] has a maximum at $n = -(a/2)$. Therefore, in the frequency region

$$\hbar\Omega \leqslant \Delta I + \frac{a}{2}\hbar\omega \tag{35}$$

the series terms in (33) decrease starting with $n = l_0$, so that to a rough approximation the series may be approximated by the leading term. For $n = l_0$, χ_0 is independent of the frequency Ω of the absorbed light. Consequently, the absorption curve in the frequency region (35) exhibits approximately the same features as in the case of excitation to a discrete level, i.e.,

$$w_{i\text{-}m} \sim \exp\left(-\frac{l_0\beta}{2}\right) I_{l_0}\left(\frac{a}{2\,\mathrm{Sh}\frac{\beta}{2}}\right). \tag{36}$$

We should emphasize that Eq. (36) is particularly approximate, since the evaluation of the sum of the series in Eq. (33) usually requires that several of the leading terms be taken into account.

In the frequency range

$$\hbar\Omega > \Delta I + \frac{a}{2}\hbar\omega \tag{37}$$

the terms of the series in Eq. (33) start by increasing, and decrease only after passing through a maximum. Taking advantage of the relatively smooth variation of the multiplying factor $[F(\chi_0)/\sqrt{\chi_0}]^2$ with respect to Eq. (34), we can place it outside the summation sign for $n = -(a/2)$. It can easily be shown that

$$\exp\left(-\frac{a}{2}\,\mathrm{cth}\frac{\beta}{2}\right) \sum_{n>l_0} R_n \cong 1,$$

so that for the frequency range (37) the spectral dependence has the form

$$w_{i\text{-}m} \sim \frac{F^2(\varkappa_0)}{\varkappa_0}, \tag{38}$$

where

$$\varkappa_0^2 = \frac{2M}{\hbar^2 a^2}\left[\hbar\Omega + |W(0)| - \Delta I - \frac{a}{2}\hbar\omega\right]. \tag{39}$$

Equation (38) represents a monotonic curve, which is smoother than the one given by Eq. (34) and which decreases toward shorter wavelengths.

Thus both the photoionization curve of the impurity center and the photoexcitation curve have maxima near the frequency

$$\hbar\Omega_m = \Delta I + \frac{a}{2}\hbar\omega. \tag{40}$$

The photoionization curve differs from the photoexcitation curve primarily by its smoother decrease on the short wavelength side.

The qualitative conclusions stated above were checked by a direct tabulation of values for the KCl crystal using Eq. (33). (The values of the parameters are: $a = 43$, $\gamma = 3.5$, $\lambda = 2.1$, $|W(0)| = 32\hbar\omega$.) The temperatures chosen were 76 and 294°K. The curves obtained are shown in the Figure (the ordinate scale is arbitrary). The shape of the low temperature curve agrees very well with the experimental curve of ref. 1 in the corresponding frequency range. However, we must keep in mind that the identification of our curve with the experimental curve for the internal photoeffect in F-centers is legitimate only at temperatures which exclude the possibility of thermo-optical ionization. It has not yet been definitely settled whether thermo-optical ionization is possible at the temperature of liquid hydrogen, which was used in ref. 1. We plan to return to this question in later publications.

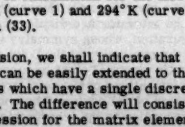

Results of calculations for the KCl crystal at 76°K (curve 1) and 294°K (curve 2), using formula (33).

In conclusion, we shall indicate that the theory developed here can be easily extended to the case of impurity centers which have a single discrete level (the ground state). The difference will consist only in the explicit expression for the matrix element $\zeta(k)$. In this connection we should point out that the well-known asymmetrical character of F′-band absorption in alkali halide crystals is fully explained by formula (33).

REFERENCES

1. N. Inchauspe, Phys. Rev. 108, 5 (1957).
2. M. F. Deigen, Zhur. Eksptl. i Teoret. Fiz. 18, 818 (1948).
3. I. M. Dykman, Zhur. Eksptl. i Teoret. Fiz. 25, 6 (1955).
4. Yu. E. Perlin, Fiz. Tverd. Tel. 2, 242 (1960).
5. S. I. Pekar, "Issledovaniya po elektronnoi teorii kristallov" (Investigations in the Electron Theory of Crystals). Gosudarst. Tekh.-Teoret. Izd., Leningrad, 1951.

THE INTERACTION BETWEEN ACTIVATOR AND NON-TOTALLY SYMMETRIC LOCAL VIBRATIONS

N. N. Kristofel'

Received 3 March 1960

The interaction between activator and non-totally symmetric local vibrations (the Jahn-Teller effect) is considered as exemplified by the $^3P_1$ state of the luminescence center in the KCl:Tl phosphor. Certain problems connected with it are discussed.

The luminescence center in an alkali halide phosphor may be considered as a certain quasi-molecule in a crystal.[1] The ion of the activator, whose electrons interact with local vibrations, is the optically active "nucleus" of the center. The quasi-molecule includes ions which take part in these vibrations. In this sense, the "dimensions" of the center are vibrational in nature, since the effective electronic radius of the activator is less than the depth of penetration of the local vibration into the lattice.

The symmetry of the normal coordinates y_μ of the local vibrations is easily determined by means of group theory. We use the point group of the matrix as the symmetry group of the center. The angular parts of the electronic wave functions consist of the corresponding lattice harmonics.[2]

Since the interaction of the activator with the surrounding lattice differs from the interaction of the lattice with the cation being replaced, the adiabatic potential of the center contains a term linear with respect to y_μ. The ions surrounding the activator are displaced into a new equilibrium configuration, whose symmetry in general can be lower than the symmetry of the point group of the matrix. The adiabatic potential must be invariant with regard to all transformations of the point group of the equilibrium symmetry of the center. The coordinates y_μ are transformed according to the irreducible representations Γ_μ of the symmetry group of the center, while the one-electron wave functions of the activator ψ_{1n} (n takes account of possible orbital degeneracy) are transformed according to the irreducible representations Γ_{a1} of the same group. The product $\psi_{1n}\psi_{1n}$ is transformed according to the symmetric product of Γ_{a1} by itself $[\Gamma^2_{a1}]_s$.

The integrand in the coefficient preceding y_μ in the term linear with respect to y_μ is transformed according to the representation

$$[\Gamma_{a1}]_s \times \Gamma_\mu. \tag{1}$$

The integral of this function with respect to the electronic coordinates fails to vanish only when (1) contains the identity representation Γ_1.

For a nondegenerate state, $[\Gamma^2_{a1}]_s \equiv \Gamma_1$, and the linear term contains only the normal coordinate y_0 of the totally symmetrical vibration. This means that the displacements of the equilibrium positions of the ions occur due only to the interaction of the activator with the totally symmetrical vibration. If the state is degenerate, then only those y_μ will appear in the linear term whose Γ_μ are contained in the resolution of $[\Gamma^2_{a1}]_s$ into irreducible parts. The representation Γ_1 must appear in this resolution, but not all other irreducible representations with dimensions greater than 1. In this case, therefore, the effect of activator interaction with certain non-totally symmetric vibrations is added onto the totally symmetrical variation in the equilibrium positions of the ions. The corresponding non-totally symmetric displacements of the equilibrium positions of the ions result in a lowering of the symmetry and a removal of the degeneracy. This is analogous to the so-called Jahn-Teller effect (JTE), known for polyatomic molecules.[3] The non-totally symmetric displacements of the ions will correspond to the totally symmetric vibration of the new group of the equilibrium symmetry of the center.

The one-oscillator approximation, in which the activator interacts only with the totally symmetric vibration, was considered in ref. 1. Let us consider the interaction of the activator with the non-totally symmetric vibrations by perturbation methods. We shall take as the perturbation operator the term in the expansion of the electronic energy operator in the adiabatic approximation which is linear with respect to y_μ ($\mu \neq 0$). If we neglect exchange interactions and corrections for the nonorthogonality of wave functions of different ions, and integrate over the coordinates of the electrons of the matrix ions, we obtain this operator in the form

$$H_1 = \sum_{\mu,\mu\neq 0} H_{1\mu} y_\mu, \tag{2}$$

$$H_{1\mu} = -e^2 \sum_\alpha \varepsilon_\alpha \Phi_\alpha(r) \frac{(r - R^0_\alpha)}{|r - R^0_\alpha|^3} B(\alpha|\mu). \tag{3}$$

The quantity R^0_α describes the positions of the points of the ideal lattice of the matrix, ε_α is the valency of ion number α, r is the radius vector of the optical electron of the activator, $B_1(\alpha|\mu)$ is the matrix for transformation to normal coordinates. (See ref. 1.) The function

$$\Phi_\alpha(r) = 1 + (2\varepsilon_\alpha R^0_\alpha r)^{-1} \int_{|R^0_\alpha - r|}^{|R^0_\alpha + r|} \xi\, d\xi \int_\xi^\infty u_\alpha(r')\, dr', \tag{4}$$

takes into account the "departure from point form" of the activator's neighbors; the expression $u_\alpha(r)$ represents the radial charge density. Averaging over polar angles has been carried out in expression (4). The expression $(r - R^0_\alpha)/|r - R^0_\alpha|^{-3}$ was expanded as a power series in r for $r > R^0_\alpha$, and in R^0_α for $r > R^0_\alpha$ (up to the terms $\sim r^4/R^5$ and $\sim R^3/r^5$, respectively).

Let us consider $^3P_1$, the state of the luminescence center in the KCl:Tl phosphor. The point symmetry group of the center in this case is O_h. Assuming that only the six Cl^- ions nearest to the Tl^+ ion take part in the local vibrations, we obtain 15 normal vibrations of the following symmetry types: A_{1g}, E_g, F_{2g}, $2F_{1u}$, F_{2u}. Nine vibrations of the last two types are odd and do not take part in the JTE. The wave function of the $^3P_1$ state belongs to $F_{1u} \cdot [\Gamma^2_{1u}]_s = A_{1g} + E_g + F_{2g}$. The following may be active in the JTE: the doubly degenerate vibration of the E_g type (y_1 and y_2) and the triply degenerate vibration of the F_{2g} type (y_3, y_4, y_5). (They are indicated in Fig. 1.)

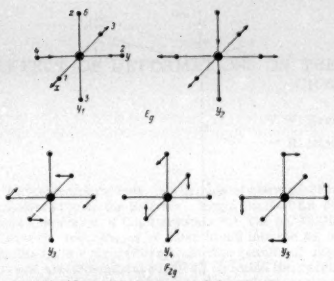

Fig. 1. Normal vibrations of the quasi-molecule (types E_g and F_{2g}).

The JTE for octahedral complexes has already been considered in part.[4,5]

The perturbation matrix has the form

$$H_1^{\mathrm{III}'} = \begin{pmatrix} -C(\eta_1+\eta_2) & C'y_6 & C'y_5 \\ C'y_6 & C\eta_1 & C'y_3 \\ C'y_5 & C'y_3 & C\eta_2 \end{pmatrix}, \tag{5}$$

$$\left.\begin{aligned} C &= \frac{6}{5}\frac{e^2}{a^4}\left[\int_0^a \Phi(r) f_{\varepsilon_g}^2(r) r^3 dr - \frac{2a^5}{5}\int_a^\infty \Phi(r) f_{\varepsilon_g}^2(r)\frac{dr}{r^3}\right], \\ C' &= \frac{6}{5}\frac{e^2}{a^4}\left[\int_0^a \Phi(r) f_{\varepsilon_g}^2(r) r^3 dr + a^5\int_a^\infty \Phi(r) f_{\varepsilon_g}^2(r)\frac{dr}{r^3}\right]. \end{aligned}\right\} \tag{6}$$

where

$$\left.\begin{aligned} \eta_1 &= -\frac{3}{2}\left(y_1 + \frac{y_2}{\sqrt{3}}\right), \\ \eta_2 &= \frac{3}{2}\left(y_1 - \frac{y_2}{\sqrt{3}}\right). \end{aligned}\right\} \tag{7}$$

The portion of the adiabatic potential which corresponds to the vibrations in question is

$$I = \Delta E(y_\mu) + V = \Delta E(y_\mu) + \frac{1}{2}k\left[(\eta_1^2+\eta_2^2)+(\eta_1+\eta_2)^2\right] + \frac{1}{2}k'(y_3^2+y_4^2+y_5^2), \tag{8}$$

$$\left.\begin{aligned} k &= \frac{2}{9}M_-\omega_{1'}^2 \\ k' &= M_-\omega_{2'}^2 \end{aligned}\right\} \tag{9}$$

where M_- is the mass of Cl^- and ω_1 and ω_2 are the vibration frequencies of E_g and F_{2g} types, respectively. The energy correction $\Delta E(y_\mu)$ is determined by the usual perturbation methods.

The required local vibration frequencies (and the quantities C, C') may be computed on the basis of results given in ref. 1. They are listed in Table 1. The frequency ω_2 of "transverse" vibrations increases in the excited state as opposed to the "longitudinal" frequencies ω_0 and ω_1. In the latter case the totally symmetrical vibration frequency ω_0 is no longer the highest of the local frequencies. We obtained the following values: $9k/2 = 3.57$, $k' = 6.89$ (ev/A²); $C = 0.394$, $C' = 0.464$ (ev/A).

The equilibrium ion configuration and the corresponding splitting of the adiabatic potential may be found by the methods used in ref. 5. Using the criterion

$$\frac{kC'}{k'C} < \frac{1}{2}, \tag{10}$$

Table 1

Frequency, sec^{-1}	ω_0	ω_1
$\omega_0 \cdot 10^{-13}$	4.51	3.79
$\omega_1 \cdot 10^{-13}$	3.93	3.09
$\omega_2 \cdot 10^{-13}$	4.21	4.30

which holds true in our case, we conclude that the adiabatic potential has a minimum for configurations with tetragonal symmetry.* These are listed in Table 2. The

*It is easy to see that $(\eta_1+\eta_2)$, η_1, η_2 correspond to D_{4h} symmetry.

coefficients a_n determine the correct linear combination of the degenerate electronic functions. The three variant forms of the solutions in Table 2 correspond to the three possible orientations of the fourfold axis along which the "dumbbell" of the Tl^+ 6p function is directed.

Table 2

a_n	$\begin{pmatrix}0\\0\\1\end{pmatrix}$	$\begin{pmatrix}0\\1\\0\end{pmatrix}$	$\begin{pmatrix}1\\0\\0\end{pmatrix}$
$\gamma_{1\eta}$	$\frac{C}{3k}$	$-\frac{2C}{3k}$	$\frac{C}{3k}$
$\gamma_{2\eta}$	$-\frac{2C}{3k}$	$\frac{C}{3k}$	$\frac{C}{3k}$
$\gamma_{i\alpha}$ (i = 3, 4, 5) . .	0	0	0
ΔE_{min}	$-\frac{2C^2}{3k}$		

Thus the interaction of Tl^+ with non-totally symmetric vibrations reduces the equilibrium symmetry of the center in the $^3P_1$ state to D_{4h}. For D_{4h} symmetry, the F_{1u} term of the O_h group is split into A_{2u} and E_u. For the first, $\Delta E_{min} = -(2C^2/3k)$ while for the doubly degenerate E_u level, $\Delta E = -(C^2/3k)$. Thus, for an equilibrium configuration we obtain from (8)

$$I_\varphi = \begin{cases} -\dfrac{3C^2}{2M_-\omega_1^2} = -0.065, \text{ ev} \\ \dfrac{3C^2}{M_-\omega_1^2} = 0.13 \text{ ev}. \end{cases} \tag{11}$$

The splitting obtained is smaller than the multiplet splitting.

Since only the vibrations of E_g symmetry matter, we may investigate the JTE by setting $y_3 = y_4 = y_5 = 0$ in Eq. (5). The condition of solubility of the secular equations gives three "sheets" for the adiabatic potential

$$\left.\begin{aligned} I_1 &= -C(\eta_1+\eta_2)+V, \\ I_2 &= C\eta_1+V, \\ I_3 &= C\eta_2+V, \end{aligned}\right\} \tag{12}$$

each of which has the minimum value $-(C^2/3k)$ for one of the configurations in Table 2. For a given equilibrium configuration, the two remaining "sheets" intersect for the value $2C^2/3k$. In the case of the first configuration (Table 2), for which the C_4-axis coincides with the y-axis, the following configuration is superimposed on the change in equilibrium positions caused by the interaction with the totally symmetric vibration (in which the Cl^- ions move 0.065 A closer to the Tl^+ ions[1]): $q_x(1) = q_z(6) = -0.055$, $q_x(3) = q_z(5) = 0.055$, $q_y(2) = 0.110$, $q_y(4) = -0.110$ (A).

It is natural that the Cl^- ions move away from Tl^+ in the direction of the y-axis since the electron density of Tl^+ is higher there, while conversely, in the directions of the x- and z-axes the Cl^- ions move closer to Tl^+.

The magnitude of the JTE depends on the dimensions of the electron cloud of the activator (6). As the radius increases, the JTE at first increases, but then begins to

decrease. When the radius of the center is large enough to interact with lattice vibrations, the JTE is apparently absent.

A comparison with experimental data indicates that the value obtained for the JTE is obviously somewhat too high. No splitting has been observed in KCl:Tl for $^1S_0 \leftrightarrow {}^3P_1$ bands, though there are indications[6,7] that the corresponding emission band is not fundamental. We could indicate reasons, however, for the absence of splitting in the spectrum for the given magnitude of the effect. The factors affected most by the JTE are apparently the displacements of the equilibrium positions of the ions and, of course, the polarization characteristics.

Polarization of the $^3P_1 \leftrightarrow {}^1S_0$ radiation in KCl:Tl has been observed[8] which corresponds to the orientation of dipoles along the fourfold axes (D_{4h} symmetry), and which disappears when the temperature is raised to the boiling point of liquid nitrogen. This result is confirmed by the present calculation. Actually, at sufficiently low temperatures, the quasi-molecule in an excited state may be in one of the three equilibrium configurations of D_{4h} symmetry which differ in the direction of the fourfold axis. In the presence of sufficient activation energy, any one of these configurations may be transformed into another. This results in a loss of anisotropy. (The η_0 sums in Table 2 vanish.) If these transitions occur through the point $\eta_1 = \eta_3 = 0$, then the height of the potential barrier is 0.065 ev, and an estimate gives just $T \sim 70°K$ as the temperature for the disappearance of polarization. Thus the observed polarization dependence[8] is not necessarily connected with the presence of a defect in the vicinity of a "normal" center. It may also be vibrational in nature.

The three "sheets" of the adiabatic potential have a common value of zero at $\eta_1 = \eta_2 = 0$. If the absorption corresponds to a transition near this configuration, then the Stokes losses in the $^3P_1$ state which correspond to vibrations of the E_u type amount to 0.065 ev. In the total Stokes losses of the $^1S_0 \leftrightarrow {}^3P_1$ transitions about 0.15 ev corresponds to these vibrations. This constitutes only 15-20% of the total Stokes losses. The remaining part belongs to the totally symmetrical vibration. Thus the activator interacts most strongly with the totally symmetrical vibration, and the fundamental effects may be explained in the one-oscillator approximation. In studying more refined problems, it is necessary to take account of the non-totally symmetric vibrations. They have already[10] been used for this purpose.

After we obtained the above results, we came across ref. 11, which considers the JTE for the $^3P_0$, $^3P_1$, $^3P_2$, and $^1P_1$ states of the luminescence center in KCl:Tl. That paper uses a semiempirical method: quantities analogous to ω_1, C, etc. are determined from experimental data. It assumes that only the γ_3 vibration takes place while all other $\gamma_\beta = 0$. The picture of the splitting of the adiabatic potential of the $^3P_1$ state obtained in ref. 11 corresponds to the intersection of our potential surfaces by the $\eta_1 = \eta_2 = \eta$ plane.* Our results are given in Fig. 2, which shows also the potential curve of the $^1S_0$ state. The solid and dotted curves correspond to the equilibrium configuration of the totally symmetrical vibration in the $^3P_1$ state ($q_0 = -0.065$ A) and the $^1S_0$ state ($q_0 = 0.093$ A), respectively. The authors[11] connect the emission bands near 3050 and 4750 A in the KCl:Tl spectra with transitions from the two minima of the $^3P_1$ curve. Such an explanation cannot be considered correct: the minimum in the E_u curve in Fig. 2 is not absolute but corresponds only to a particular intersection $\eta_1 = \eta_2$. Furthermore, even if two such emission bands did arise, their maxima would have been separated by approximately 0.08 ev, while the experimental value for this difference is near 1.5 ev.

*A certain difference occurs due to the "contamination" of the $^3P_1$ state by other states in ref. 11.

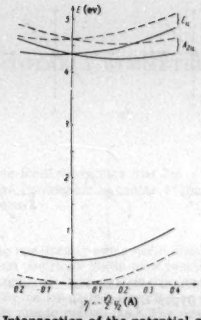

Fig. 2. Intersection of the potential surfaces of the $^3P_1$ and $^1S_0$ states by the $\eta_1 = \eta_2$ plane. Solid lines—$^3P_1$ state; dashed lines—$^1S_0$ state.

A more detailed communication will be published in Trudy Inst. Fiz. i Astron., Akad. Nauk Eston.SSR.

The author is grateful to M. I. Petrashen' and K. K. Rebane for their extremely valuable comments.

REFERENCES

1. N. N. Kristofel', Trudy Inst. Fiz. i Astron., Akad. Nauk Eston.SSR, No. 7, 85 (1958); Ibid. No. 10, 3 (1959); Ibid. No. 11, 180 (1960).
2. D. Bell, Revs. Modern Phys. **26**, 311 (1954).
3. H. Jahn and E. Teller, Proc. Roy Soc. **A161**, 220 (1937);
H. Jahn, Proc. Roy. Soc. **A164**, 117 (1938).
4. J. H. Van Vleck, J. Chem. Phys. **7**, 72 (1939).
5. U. Öpik and M. Pryce, Proc. Roy. Soc. **A238**, 425 (1957).
6. I. K. Piyavin', Candidate's Dissertation. Fiz. Inst. Akad. Nauk SSSR, 1958.
7. Ya. Ya. Kirs and A. I. Laisaar, Trudy Inst. Fiz. i Astron., Akad. Nauk Eston.SSR, No. 10, 51 (1959).
8. C. Klick and W. Compton, J. Phys. Chem. Solids **7**, 170 (1958).
9. P. P. Feofilof, "Polyarizovannaya lyuminestsentsiya atomov, molekul i kristallov" (Polarized Luminescence of Atoms, Molecules, and Crystals). Gosudarst. Izd. Fiz.-Mat. Lit., 1959.
10. N. E. Lushchik and Ch. B. Lushchik, Trudy Inst. Fiz. i Astron., Akad. Nauk Eston.SSR, No. 6, 5 (1957).
11. H. Kamimura and S. Sugano, J. Phys. Soc. Japan **14**, 1612 (1959).

EFFECT OF DEFORMATIONS ON THE ABSORPTION SPECTRUM OF CUPROUS OXIDE CRYSTALS AT 20° K

V. V. Eremenko and L. I. Chuiko

Received 23 February 1960

At low temperatures, two groups of convergent bands are observed near the long-wavelength limit of the continuous absorption of Cu_2O crystals.[1-4] The possibility of fitting the frequencies of these bands into the series formulas for a hydrogenlike atom, the results of magneto- and electro-optical studies,[5] and also the recently-discovered lack of dependence of the band intensities on the concentration of excess oxygen in the Cu_2O[6] all testify to the exciton character of the narrow-banded structure of the long-wavelength absorption edge of these crystals.

However, the causes of the appearance of two series (and, according to the communications of some authors,[3] even three) have been obscure up to now. According to one point of view,[3] the bands of the shorter-wavelength "green" series are produced by optical transitions from the same bonding zone as the bands of the "yellow" series, but in combination with lattice vibrations. It appears no less probable to assume that the two series are produced by optical transitions from different bonding zones.[7,8]

It seemed to us that comparison of the effect of external influences (for example, of an electric field or deformations of the crystal) on the bands of these series would help to some extent to reveal which of the points of view just cited deserves preference.

EXPERIMENTAL PROCEDURE

To investigate the effect of uniaxial compression of Cu_2O crystals on their absorption spectrum at T = 20° K, we used a press with transparent pistons, the construction of which has been described in ref. 9, and a metal liquid-hydrogen cryostat with quartz windows,[10] in which the optical path is free from the refrigerating liquid. The latter circumstance enables us, with the help of a microprojector,[11] to investigate the absorption spectra of different portions of a crystal, which is particularly important in the case of nonuniform deformation of the sample.

During the investigation of the effect of a uniform electric field on the absorption spectrum of Cu_2O, samples were immersed directly in liquid hydrogen. For this purpose, a cryostat was used in which the distance between the internal windows was reduced to 4 mm, in order to diminish the scattering of light by the boiling hydrogen.[10]

The absorption spectra were photographed on a Stein-heil type spectrograph whose linear dispersion in the neighborhood of λ = 5000 A was about 12 A/mm.

EXPERIMENTAL RESULTS

1. At 20° K, one may observe, in the absorption spectrum of relatively thin (d = 20-30μ) polycrystalline discs of Cu_2O, four bands of the "yellow" series (17320, 17425, 17459, 17470 cm^{-1}) and three broader and more intense bands of the "green" series (18270, 18440, and 18498 cm^{-1}). In addition, a narrow absorption line at 16390 cm^{-1} is observed in thick samples (d ~ 1 mm).

In agreement with the literature data,[1-4] the frequencies of these bands can be fitted into the formula

$$\nu_n = \nu_\infty - \frac{R'}{n^2},$$

where ν_∞ = 17509 cm^{-1}, R' = 778 cm^{-1}, and n = 2, 3, 4, 5 for the yellow series, and ν_∞ = 18570 cm^{-1}, R' = 1202 cm^{-1}, and n = 2, 3, 4 for the green series.

2. The band frequencies given above are observed only in the spectra of free crystals (fastened to a paper diaphragm). The frequencies of the absorption bands in the spectra of Cu_2O crystals rigidly attached to some support (glass, quartz) vary somewhat.

A certain discrepancy among the data published in the literature on the frequencies of the absorption bands of cuprous oxide is apparently connected with this circumstance. It is interesting to note that the shift on the frequency scale is the same for all bands of the yellow series. At 20° K, for example, the bands of the yellow series in the spectrum of a sample of Cu_2O cemented to a fused-quartz support (Fig. 1, spectrogram 2) are shifted by approximately 25 cm^{-1} toward the long-wavelength end relative to the position of these same bands in the spectrum of a free crystal (spectrogram 1).

Fig. 1. Effect of deformations on the absorption bands of the "yellow" series in Cu_2O crystals. T = 20° K. 1—free sample; 2—sample cemented to a quartz support; 3-5—absorption spectra under progressively increasing compression in a press.

The variation in the frequencies of the absorption bands of Cu_2O as a function of the conditions of attachment of the samples, as also in the case of other crystals (naphthalene and anthracene,[9] CdS,[9,12] Ge[13]), is apparently governed by the variation in the stresses which

arise on cooling on account of the difference in the coefficients of thermal contraction of the sample and the support.

A sample cemented to a fused-quartz support (the coefficient of thermal contraction of which is very small) and cooled to 20° K must be somewhat stretched in comparison with a free sample. Thus planar stretching of a Cu_2O disc leads to a shift of the bands of the yellow series toward the long-wavelength end of the spectrum. Here only one parameter of the series—ν_∞—is changing, but R′ does not change, inasmuch as the intervals between the bands do not change.

3. An analogous phenomenon is observed on uniaxial compression (in the direction perpendicular to the plane of the disc) of a Cu_2O crystal in a press: the whole yellow series of absorption bands shifts, as a whole and without change in the intervals between the bands, toward the long-wavelength end of the spectrum (Fig. 1, spectrograms 3 and 4). At the same time, the bands are strongly broadened. This is very similar to the changes in the spectrum which take place on heating the crystal; even the values of the ratio of band broadening (in cm^{-1}) to band shift on the frequency scale, as measured on compression and on elevation of the temperature from 20 to 77° K, are very close together.* At the present time, we

*We note that in some experiments we observed, on compression of the samples in the press, a shift of the bands toward the short-wavelength end of the spectrum. In this case also all the bands of the yellow series shifted equally, and the ratio of band broadening to band shift was the same as in the case of a displacement toward the long-wavelength end. It is not yet clear whether such a direction of shift—toward the short-wavelength end—is associated with peculiarities of the samples or with peculiarities of their deformation in these experiments, which constituted a rare exception.

cannot give a quantitative dependence of the magnitude of the shift on the pressure, since the latter could not be directly measured on account of the nonuniformity of the sample. But if we consider that the magnitude of the shift of the absorption edge of CdS crystals at 20° K is the same as at room temperature (0.02 A/atm),[14] then the results of our previous work[2] show that pressures reaching 5000 atm are developed in isolated portions of the sample. Along with this, the shift of the bands of the yellow series of Cu_2O reaches 200-250 cm^{-1}.

4. Using thin crystals of Cu_2O (d = 20μ), we could simultaneously observe the bands of the yellow and of the green series. This enabled us to compare the behavior of the bands of the two different series under progressively increasing pressure.

For a detailed comparison of the effect of pressure on the bands of the yellow and of the green series, curves were constructed showing the dependence of the magnitude of the shift of the bands 18250 cm^{-1} (n = 2) and 18420 cm^{-1} (n = 3) of the green series on the shift of the bands of the yellow series (Fig. 2). At low pressures, the n = 3 band of the green series is displaced considerably more than the n = 2 band and the whole yellow series, which are displaced practically equally. However, on further compression the yellow series continues to shift toward the long-wavelength end of the spectrum more strongly than the two bands of the green series (n = 2 and n = 3).

The variation of the constant R′ of the green series may be estimated from measurements of the frequencies of two bands, if we suppose that, during such a variation, its hydrogen-likeness is preserved. We did not succeed in investigating the behavior of the third band of this series (n = 4) in detail: at a sample thickness ~20μ, it is poorly resolved in the spectrum of the free crystal and is completely merged with the continuous absorption at small deformations of the crystal. It turns out that R′ changes from the value 1200 cm^{-1} for the free sample to 900 cm^{-1} under a deformation corresponding to a shift of the yellow series by 60 cm^{-1}, and on further increase of the pressure R′ remains practically unchanged.

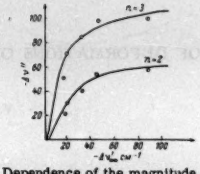

Fig. 2. Dependence of the magnitude of the shift of bands of the "green" series on the displacement of the "yellow" series ($-\Delta\nu'_\infty$) on compression in a press.

5. We also studied the effect of a constant, uniform electric field on the structure of both the yellow and the green series of absorption bands of cuprous oxide crystals at T = 20° K.

In agreement with the literature data,[3] we observed the appearance of satellites of the fundamental bands of the yellow series, while on further increase of the electric field voltage there was a merging of the bands, starting from the higher terms of the series, with the continuous absorption advancing from the short-wavelength region of the spectrum (Fig. 3, a). The effect of an electric field on the structure of the green series, which has been investigated by us for the first time, consists only in a small broadening of the bands and a progressive merging of them with the continuous absorption, which takes place at lower electric field voltages than for the bands of the yellow series with the same values of the principal quantum number n (Fig. 3, b).

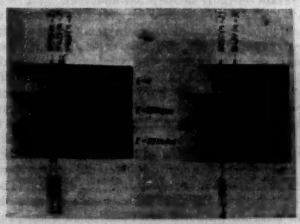

Fig. 3. Effect of an electric field on the "yellow" (a) and "green" (b) series. T = 20° K.

DISCUSSION OF THE RESULTS

The explanation of the existence of several hydrogen-like series of absorption bands of Cu_2O by assuming the combination of exciton transitions with lattice vibrations[3] encounters a number of objections.[7]

It seems to us that the different behavior found for the bands of the two series under uniaxial compression of the Cu_2O crystals also contradicts this hypothesis.

Actually, the shift of the yellow series as a whole denotes only a change in the energy gap between the corresponding bonding and free zones. The behavior of the bands of the green series, on the other hand, indicates that the Rydberg constant of this series changes on compression: i.e., the effective mass of electrons or holes changes. Hence it follows that only one of the zones—either the bonding zone or the free one—can be common to both series.

Accepting the more widespread hypothesis that the conduction zone is the one in common and that the presence of two series is brought about by optical transitions to exciton levels from different bonding zones, between the upper limits of which there is a gap equal to the frequency interval between the convergence limits of the yellow and the green series ($\delta\nu = 1100\ cm^{-1}$), we may estimate the value of the effective masses for the respective zones.

As the results of magneto-optical studies show,[8] the electron and hole effective masses for the yellow series are equal to one another ($m_e^* = m_p^*$). Knowing the value of R′ for the yellow ($R' = 780\ cm^{-1}$) and the green series ($R' = 1200\ cm^{-1}$) in the free sample, we may determine the effective mass of the holes in that bonding zone from which optical transitions bring about the appearance of the bands of the green series: $m_{p_2}^* = 3.34\ m_e^*$. On compression of the crystal, R'_{green} diminishes to $900\ cm^{-1}$, which corresponds to a diminution of the effective mass of the holes to $m_{p_2}^* = 1.37\ m_e^*$.

In conclusion, we take the opportunity to express our gratitude to A. F. Prikhot'ko and V. L. Broude for their constant attention to and interest in the work.

REFERENCES

1. M. Hayashi and K. Katsuki, J. Phys. Soc. Japan 7, 599 (1952).
2. E. F. Gross and N. A. Karryev, Doklady Akad. Nauk SSSR 84, 261, 471 (1952);
E. F. Gross and B. P. Zakharchenya, Doklady Akad. Nauk SSSR 90, 745 (1953);
E. F. Gross, B. P. Zakharchenya, and N. M. Reinov, Doklady Akad. Nauk SSSR 92, 265 (1953); Ibid. 99, 231, 527 (1954).
3. S. Nikitine, I. Perny, L. Couture, R. Reiss, and M. Sieskind, Compt. Rend. 238, 67, 1781, 1981 (1954); Ibid. 240, 505, 1415 (1955).
4. T. H. Apfel and L. N. Hadley, Phys. Rev. 100, 1689 (1955).
5. A. A. Kalinyak and L. G. Fedorovich, Doklady Akad. Nauk SSSR 96, 1137 (1954);
E. F. Gross, B. P. Zakharchenya, and N. M. Reinov, Doklady Akad. Nauk SSSR 97, 57, 221 (1954);
E. F. Gross and B. P. Zakharchenya, Doklady Akad. Nauk SSSR 111, 564 (1956);
E. F. Gross and B. P. Zakharchenya, Zhur. Tekh. Fiz. 27, 1940 (1957);
E. F. Gross, B. P. Zakharchenya, and P. P. Tsavinskii, Zhur. Tekh. Fiz. 27, 2197 (1957).
6. I. S. Gorban', Communication at the Meeting of the Commission of the Academy of Sciences, Ukrain.SSR, on Semiconductors, Odessa, 1959.
7. S. A. Moskalenko, Opt. i Spektr. 9, 369 (1960); Optics and Spectroscopy 9, 192 (1960).
8. R. I. Elliott, Phys. Rev. 108, 6, 1384 (1957).
9. V. L. Broude, V. V. Eremenko, V. S. Medvedev, O. S. Pakhomova, and A. F. Prikhot'ko, Ukrain. Fiz. Zhur. 3, 231 (1958).
10. V. P. Babenko, V. L. Broude, V. S. Medvedev, and A. F. Prikhot'ko, Pribory i Tekh. Ekspt. 1 (1958).
11. V. L. Broude, O. S. Pakhomova, and A. F. Prikhot'ko, Opt. i Spektr. 2, 327 (1957).
12. E. F. Gross and B. S. Rizbirin, Zhur. Tekh. Fiz. 27, 2173 (1957).
13. J. J. Macfarlane, T. P. McLean, J. E. Quarington, and V. Roberts, Phys. Rev. (Letter) 2, No. 6, 282 (1959).
14. I. Höhler, Ann. Physik (6) 4, No. 6, 1949.

EXPERIMENTAL STUDY OF LIGHT AMPLIFICATION IN A "PHOTOCONDUCTOR-FERROELECTRIC-ELECTROLUMINOR" ELEMENT

I. N. Orlov and N. I. Taborko

Received 20 February 1960

A circuit is described for an electroluminescent image amplifier element in which a photoconductor and a ferroelectric material are used. A qualitative basis is given for choosing the parameters of this circuit. Experimental characteristics are listed for a single-element light amplifier. It is shown that using a zinc sulfide electroluminor with green luminescence, a photoconductive cadmium sulfide powder and a single crystal of Triglycin Sulfate, it is possible to obtain a light flux amplification coefficient of about 50,000 at low input illumination (of the order of 0.01 lux).

The element of an electroluminescent image amplifier described in the literature[1-3] is a series combination of a photoconductor (active resistance) and an electroluminor (capacitance), energized by an ac voltage. The change in resistance of the photoconductor, when illuminated, changes the value of the voltage applied to the electroluminescent capacitor, i.e., the light flux value at the amplifier output. Because of the high sensitivity of the photoconductor and the nonlinearity of the brightness-ac voltage curve of the electroluminor, a small light flux at the input can control a much larger light flux at the output of the light amplifier.

A study of the indicated light amplifier circuit shows that the use of a resistance-capacitance voltage divider does not lead to the maximum light amplification which could be expected from the properties of the materials used.

There are a number of reasons for this. First, the sensitivity of the photoconductor on alternating voltage is 3 to 4 times lower than on direct voltage; it is known[4] that this is a consequence of the nonlinearity of the volt-ampere characteristic of photosensitive cadmium sulfide powder layers. In a layer with a nonlinear characteristic, the time for the passage of a noticeable photocurrent

corresponds to only a small fraction of the half-cycle, coinciding with the maximum of the line voltage. As a result, the average photocurrent in such a layer is substantially smaller than in a layer with linear dependence of current on voltage. Secondly, in a resistance-capacitance divider it is impossible to exploit the dependence of the luminescence brightness of the electroluminor on frequency to the fullest extent in order to obtain additional gain in amplification. We indirectly determine the optimum frequency of the effective voltage when we select the dark resistance of the photoconductor and the amplitude of the alternating voltage so as to give no light emission from the electroluminor when the photoconductor is not illuminated. An increase in frequency beyond some definite value leads to a drop in the effective voltage due to an increase in capacitive conductance of the electroluminor; this decreases the luminescence brightness to a greater extent than the brightness is increased due to increasing frequency. The optimum frequency for a light amplifier of the indicated type is below 1000 cps.

Due to the indicated limitations, the light flux amplification coefficient does not exceed 1000 in a "photoconductor-electroluminor" element. In multielement image amplifiers based on the resistance-capacitance divider circuit, there are a number of constructional difficulties which further decrease the amplification coefficient (to 100-150).

The application of ferroelectric materials in electroluminescent light amplifiers overcomes the above-mentioned difficulties and considerably increases the amplification coefficient. (This possibly was briefly mentioned for the first time in ref. 10 without experimental confirmation.) The schematic circuit of a light amplifier using a ferroelectric (Fig. 1a) corresponds to a scheme of a dielectric power amplifier with a sinusoidal voltage supply in series,[11] having an electroluminescent capacitor as a load, the controlling (amplified) signals being formed in a direct current circuit by means of a photoconductor included in this circuit. As long as there is no noticeable constant bias on the ferroelectric material (the photoconductor is not illuminated), the capacitance of the ferroelectric capacitor is at a maximum and practically the full voltage of the power supply is applied to the electroluminor. When the photoconductor is illuminated, a large constant bias is applied to the ferroelectric, the capacitance of the ferroelectric is decreased, decreasing the voltage on the load, and the luminescence brightness of the electroluminor drops. Such a "negative" connection between input and output light fluxes is not an answer to an image amplifier problem. Therefore an additional resistance R_s is added to the dc circuit in the actual amplifier cell (Fig. 1b). In this case, the potential at point A is lower, the greater the illumination on the photoconductor. Correspondingly, the brightness of the electroluminor is greater, the more intense the illumination on the photoconductor. The value R_s is obtained from the condition that in a change from darkness to the full given illumination of the photoconductor, the voltage drop at point A $\Delta V_A = V_{A\,max} - V_{A\,min}$ must be a maximum. It follows from Fig. 1b that

$$\Delta V_A = \frac{V R_{pcd}}{R_s + R_{pcd}} - \frac{V R'_{pc}}{R_s + R'_{pc}},$$

where V is the full voltage in the dc circuit, R_{pcd} is the dark resistance of the photoconductor and R'_{pc} the photoconductor resistance in light. Introducing the designations $\beta = R_{pcd}/R'_{pc}$ and $\alpha = R_s/R'_{pc}$ we obtain

$$\Delta V_A = \frac{\alpha(\beta - 1)V}{(\alpha + \beta)(1 + \alpha)}.$$

The maximum value of ΔV_A is obtained from the condition $d(\Delta V_A)/d\alpha = 0$ or

$$V\frac{(\alpha+\beta)(\alpha+1) - \alpha(\alpha+\beta-\alpha+1)}{(\alpha+\beta)^2(\alpha+1)^2} = 0,$$

from which $\beta = \alpha^2$. Consequently $R_s = \sqrt{R_{pcd} R'_{pc}}$. A check of the influence of R_s on the voltage drop at point A at various illumination levels indicated that it is advantageous to select R_s close to R_{pcd}.

It is also necessary to introduce an additional linear capacitance C_d (Fig. 1b) into the circuit of a light amplifier in order to eliminate the influence of the alternating voltage on the controlling signal. The value of the additional capacitance is determined by two factors. On one hand, this capacitance must be large compared to the capacitances of the ferroelectric and the electroluminor so that the voltage of the ac generator will be negligible at point A. On the other hand, the product $C_d R_{pc}$ determines the rise time of the required charge in point A for a given value of the controlling signal. In order to shorten this time, the smallest possible value of C_d should be selected. It was found experimentally that C_d can be chosen about equal to the maximum capacitance of the ferroelectric as a compromise between these contradictory requirements.

All other conditions being equal, the possible voltage drop at the electroluminor (i.e., the possible range of luminescence brightness at the output of the device) is greater, the greater the capacitance drop achieved at the ferroelectric capacitor. Single crystal Triglycine-Sulfate was therefore selected for experiments, as its capacitance can vary 40 fold or more. We obtained the capacitors, prepared from a single crystal of Triglycine-Sulfate, from the laboratory of I. S. Rez.

The elements of an experimental light amplifier, constructed as indicated in the circuit shown in Fig. 1b, had the following parameters: The capacitance of the electroluminescent capacitor was 700 $\mu\mu$f for a layer thickness of about 70μ and an area of 800 mm^2. The maximum capacitance of the ferroelectric capacitor was 800$\mu\mu$f. The dark resistance of the photoconductor (a thick layer of cadmium sulfide powder cemented with polystyrene to a glass base bearing silver electrodes separated by a gap 0.6 mm wide and 20 mm long) was 500 megohms at 550 volts dc. With the same voltage and 0.6 lux, the resistance of the photoconductor was 600 times less. The optimum amplitude of the ac voltage in this circuit lies between 450 and 500 volts, and the best frequency is in the range of 2-5 kc. The upper frequency limit is determined by the decrease of the capacitance drop of the ferroelectric with increasing frequency. The maximum brightness of luminescence of a zinc sulfide electroluminor with green emission was 100-150 nit (1 nit = 1 candle/meter^2) under the given conditions.

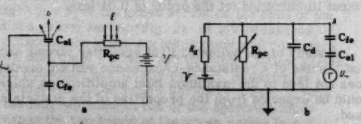

Fig. 1. Schematic circuit of a light amplifier element using a ferroelectric (a) and a working circuit of a single element amplifier (b). C_{fe}—ferroelectric capacitor; C_{el}—electroluminescent capacitor; R_{pc}—photoconductor; R_s—ohmic resistor; C_d—additional linear capacitor.

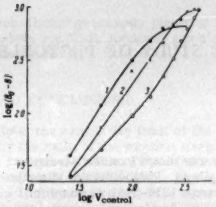

Fig. 2. Dependence of the brightness change of electroluminor emission on the value of the constant bias on the ferroelectric. B_0—brightness at zero bias; B—brightness for a given bias. Alternating voltage (volts): curve 1—400; curve 2—500; curve 3—600.

high illumination levels on the photoconductor, but the brightness change interval is small. On the other hand, at large values of R_a the range of controlling illumination levels is small, but the slope of the control curve

The curve relating the brightness of the electroluminor luminescence to the dc voltage at A (Fig. 2) is well described over most of its length by a power function with an exponent of 2.5-1.5. The higher the alternating voltage, the broader the region of "controlled" luminescence brightness. The dependence of the luminescence brightness of the electroluminor on the illumination on the photoconductor is shown in Fig. 3 for different values of R_a. At small R_a values, the output brightness can be controlled over a wide range of medium and is much greater than at small values of R_a. The maximum brightness of electroluminor luminescence increases with increasing R_a, and the light amplification coefficient increases accordingly. Thus, large amplification coefficients can be achieved with large R_a when the input illumination is low. It can be seen from Fig. 4 that the light flux amplification coefficient can attain a value of 50,000 at a photoconductor illumination of about 0.01 lux (circuit parameters—$U_\sim$ = 450 volts, f = 2 kc, V = 600 volts, R_a = 68 megohms).

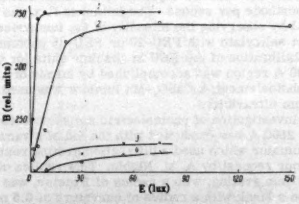

Fig. 3. The dependence of electroluminor emission brightness on the illumination of the photoconductor for various values of R_a ($U_\sim$ = 500 volts, V = 750 volts, f = 2 kc). Values of R_a (megohms): curve 1—68; curve 2—6.5; curve 3—1.5; curve 4—0.7.

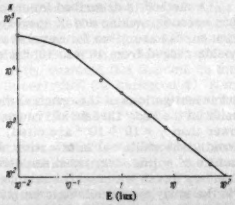

Fig. 4. Dependence of the amplification coefficient of the light flux K on the illumination on the photoconductor E.

The practical realization of multielement amplifiers using ferroelectrics is hampered mainly by the lack of low inertia powder-type photoconductors and of ferroelectrics combining the electrical properties of Triglycine-Sulfate with the technological and operational properties of ceramic barium titanate.

REFERENCES

1. B. Kazan and F. H. Nicoll, Proc. I.R.E. 43, 1888 (1955).
2. J. E. Rosenthal, Proc. I.R.E. 43, 1882 (1955).
3. G. Diemer, H. A. Klasens, and J. G. van Santen, Philips Res. Repts. 10, 401 (1955).
4. B. Kazan and F. H. Nicoll, J. Opt. Soc. Am. 47, 887 (1957).
5. B. Kazan, Proc. I.R.E. 45, 1358 (1957).
6. G. Diemer, H. A. Klasens, and P. Zalm, Philips Tech. Rev. 19, 1 (1957).
7. B. Kazan, RCA Rev. 19 (1958).
8. G. F. J. Garlick, J. Sci. Instr. 34, 473 (1957).
9. B. Kazan, Proc. I.R.E. 47, 12 (1959).
10. E. A. Sack, I.R.E. Natl. Convention Record, Pt. 3, p. 31, 1958.
11. A. R. Von Hippel (Editor), "Dielektriki i ikh primenenie," p. 267. Gosenergizdat, 1959. Translation of "Dielectric Materials and Applications." Wiley, New York, 1954.

MEASUREMENT OF SMALL PHOTOCURRENTS IN THE STUDY OF PHOTOELECTRIC EMISSION

A. M. Tyutikov and Yu. A. Shuba

Received 8 February 1960

A method is described for measuring low photoelectric currents (down to a few electrons per second), making use of open-type, secondary-electron multipliers. Photoemission distribution curves are given for several substances over the spectral range 1216-5461 A; quantum yields ranged from 10^{-2} to 10^{-14} electrons per quantum.

In current investigations of the spectral distribution of photoemission in the red "threshold" range, no quantum yields lower than $\gamma = 10^{-7}$-10^{-8} are cited. Increased sensitivity would yield additional information about the electron structure of solids. Increased sensitivity is also necessary when one works with small luminous fluxes, as for example in the study of photoelectric emission in the far ultraviolet.

To solve this problem we used the open-type,[1] secondary-electron multiplier (SEM), which makes it possible to detect currents down to 10^{-15} amp. The amplification coefficient of this SEM is high, and shows good stability on prolonged exposure to air.[2]

EXPERIMENTAL TECHNIQUE

In order to measure the photoelectric emission, monochromatic radiation was directed upon an interchangeable SEM photocathode made of the material under investigation. The block diagram of the setup is shown in Fig. 1. Every photoelectron was converted into a voltage pulse at the output of the multiplier and was registered by a SU (PS-10,000, "Tyul'pan") counter.

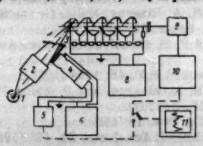

Fig. 1. Block diagram of the setup. 1—Source of radiation; 2—monochromator; 3—rotating reflector directing the light beam to the PM tube (photomultiplier); 4—PM tube recording light flux; 5—current measuring device of the PM tube (galvanometer or dc amplifier); 6—stabilized rectified power supply for the PM tube; 7—secondary-electron multiplier; 8—rectifier-power supply for the SEM, 0-5000 volts; 9—cathode follower; 10—counter ("Tyul'pan" or PS-10,000 with count-rate meter); 11—EPP-09.

Although the pulses from the SEM had a wide spread of amplitudes (Fig. 2) as a result of the high amplification factor (starting with a certain voltage applied to the potentiometer of the multiplier), practically all of the pulses considerably exceeded the operational threshold value of the SU(0.5-1 mv), and registered perfectly well. In this case, the count rate vs. voltage curve of the SEM (for a source of constant intensity) had a plateau within which the variation in count rate did not exceed ±3% for a voltage variation of ±10%. Thus the number of photoelectrons could be measured with satisfactory accuracy.

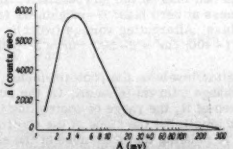

Fig. 2. Distribution of pulse amplitudes (A) at the output of the secondary-electron multiplier. The voltage applied to the potentiometer of the photomultiplier F was 3800 volts.

The quantum yield of the photoeffect was computed as the ratio of the count rate (counts per second registered by the SU) to the number of quanta of radiation striking the photocathode per second. The luminous flux was measured by observing the intensity of the luminescence of sodium salicylate with FEU-20 or FEU-25 photomultipliers. Calibration of the FEU in absolute units for the 2150-5500 A region was accomplished by means of a magnesium photoelement; a $CaSO_4$-Mn luminor was used for the vacuum ultraviolet.

The investigation of photoelectric emission between 1100 and 2600 A was conducted with the aid of a vacuum monochromator which used a diffraction grating replica[3] made at our request by A. M. Nizhin. This replica of a 600 lines/mm grating, with a radius of 1 meter, was deposited on a blank with a radius of curvature of 0.5 meter. The source of radiation was a hydrogen tube, working on direct current, with a LiF window 1 mm thick. To reduce interferences due to short-wavelength radiation, we used fluoride, strontium fluoride, white-sapphire, and fused quartz filters in series. The SEM was located in a chamber with a separate vacuum pump which maintained a 10^{-5} mm vacuum. The spectral distribution of the intensity of the source and of the photoelectric emission were recorded automatically by an EPP-09 recorder. The spectrum was scanned at the rate of 100 A/min by rotating the grating. Depending upon the material under investigation, the slit-widths of the monochromator ranged from 10 to 200μ. The minimum light fluxes measured were 10^{-11}-10^{-10} w.

Investigations between 2150 and 5500 A were made using a Hilger quartz monochromator, having an aperture of f/6.5. The source of radiation was a SVD-120 A mercury lamp. The SEM was placed in an evacuated glass vessel having a window of LiF or CaF_2. The vacuum was maintained at 1.10^{-5} mm. To decrease the effect of the scattered short-wavelength background, we used a set

of interference filters[4] graciously placed at our disposal by P. C. Sokolova and T. H. Krylova, and a standard set of colored glass filters.

RESULTS AND CONCLUSIONS

In principle, the sensitivity limit of the method is determined by the ratio of the weakest useful signal to the intrinsic background of the SEM. The background of sealed-off samples of the SEM with a photocathode made of Ni (vacuum 10^{-7} mm mercury) was several counts per minute for an operational threshold of the Cu of ~1 mv. For this operation the SEM was kept in total darkness, thoroughly screened, while all steps were taken to reduce the background caused by "breakdown" pulses caused by the presence of high voltages on the divider (up to 5000 volts).

In our case the potentiometers of the SEM were located in an evacuated space, which reduced the magnitude of the "breakdown" pulses to a level lower than the operational threshold of the SU. Nevertheless, because of the insufficiently high vacuum in the systems (10^{-5}-10^{-6} mm of mercury) and the imperfect screening and protection from light, the intrinsic background of the SEM increased (by comparison with the sealed off sample) to 1-2 pulses per second in the case of metallic photocathodes and even further in the case of photocathodes with higher photoemission in the long wavelengths. The presence of the indicated background and the relatively low intensity of the sources of radiation did limit the smallest measurable values of the quantum yield of the photoeffect (at a signal-to-noise ratio of 2:1) to ~10^{-14} electrons per quantum (Fig. 3).

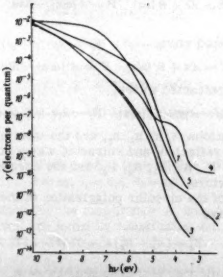

Fig. 3. Spectral distribution of the quantum yield of the photoemission of several substances. Curve 1—Platinum; curve 2—beryllium bronze oxidized by the method described in ref. 2; curve 3—same as 2, after a second oxidation; curve 4—layer of strontium fluoride; curve 5—copper, treated with iodine (CuI).

The scatter in the values of the quantum yield of the photoemission from one measurement to another did not exceed ±30%, even near the edge of the plateau of the SEM characteristic. We estimated the calibration accuracy of the measurements of light flux to be ±15% between 2150 and 5500 A and ±50% between 1100 and 2600 A. Thus, the error in determining the absolute values of the quantum yield of the photoeffect, apparently did not exceed ±45% and 80%, respectively (the reflection of radiation from the sample was not taken into account). Values of the quantum yield for the same samples, determined independently in each of the instruments, in the overlapping spectral range (2150-2600 A), differed by no more than ±50%. The "joining" of the curves was done in terms of the γ values obtained between 2150 and 5500 A.

The use of the filters did not completely eliminate the background of scattered short wavelength radiation. This factor had a particularly strong effect on the accuracy of measurement at $\gamma < 10^{-9}$. For this reason low values of quantum yield were measured only in the neighborhood of strong emission lines of the source; measurements were made in terms of the ratio of the count rate of the SEM to the quantum flux incident on the photocathode (both corrected for background). Some results of the measurements of the quantum yield of the photoeffect between 1215 and 5461 A (10-2-2.265 ev) are shown in Fig. 3.

To check the method a measurement was made of the photoeffect of Pt heated in air to white heat. The results are represented by curve 1 in Fig. 3 and agree satisfactorily with published data[5] (for $h\nu = 10/2$ ev the values of the quantum yield are respectively 1.4×10^{-2} and 1.7×10^{-2}).

The applicability and potential of the method for the investigation of photoemission in the red "threshold" range of the photoeffect are illustrated by the curves 2, 3, and 4 in Fig. 3. Curve 2 refers to photocathodes made of oxidized (at 840°C and oxygen pressure of 10^{-2} mm mercury with an additional oxidation at 650°C[2]) beryllium bronze, on the surface of which there was a film of BeO. Curve 3 refers to similar photocathodes but which, after exposure to air, were subjected to a second oxidation at 650°C. From curves 2 and 3 one can see that the effect of special features of the photocathode preparation technique was most pronounced in the long wavelength region, where $\gamma = 10^{-14}$-10^{-9}. Curve 4 or Fig. 3 characterizes the photoemission of a layer of SrF_2 5000 A thick, obtained by vacuum evaporation of a pure monocrystal on a Ni base. The curve has a plateau at $h\nu = 3.8$-4.7 ev, and indicates the existence of appreciable photoemission up to 2.25 ev, with $\gamma = 10^{-7}$-10^{-10}. The quantum yield at $h\nu = 2.5$-5.75 ev increases rapidly after measurement in the vacuum ultraviolet (to values corresponding to curve 4). This indicates that the long wavelength radiation emitted by these SrF_2 samples, as well as by alkali halides (for example, CsI),[6] is a result of the creation of color centers.

Curve 5 of Fig. 3 characterizes the photoemission from CuI, samples of which were obtained by treating the surface of copper with iodine and subsequently removing the excess. The spectral curve of the quantum yield of such samples has a plateau for $h\nu > 7.3$ ev at $\gamma \approx 10^{-2}$, which is connected, apparently, with emission from a filled band (apparently the 6p band of iodine). This curve is also characterized by very small γ values for the visible range of the spectrum. This type of behavior, which is characteristic of other iodides as well, suggests that the open-type SEM, with a photocathode made from stable metallic iodides, can serve as a highly sensitive radiation detector for the vacuum ultraviolet, possessing constant sensitivity over a broad range and low sensitivity in the visible.

The above results also show that near the red "threshold" of the photoeffect, the proposed method permits the recording of photoemission from centers of very low concentration. In many cases this will enable us to broaden our concepts of the energy structure of solids.

In conclusion we wish to express our appreciation to Academician A. A. Lebedev for his interest and supervision.

REFERENCES

1. A. M. Tyutikov and A. I. Efremov, Doklady Akad. Nauk SSSR, Ser. Fiz. 118, 286 (1958).
2. A. M. Tyutikov, Radiotekh. i Electron. 4, 1884 (1959).
3. A. M. Nizhin and F. Z. Pedos, Izvest. Akad. Nauk SSSR, Ser. Fiz. 19, 35 (1955).
4. P. C. Sokolova and T. P. Krylova, Opt. i Spektr. 6, 788 (1959), Optics and Spectroscopy 6, 513 (1959).
5. W. C. Walker, N. Wainfan, and G. L. Weissler, J. Appl. Phys. 26, 1366 (1955).
6. H. R. Phillip and E. A. Taft, J. Phys. Chem. Solids, 1, 159 (1956).

REFLECTION AND REFRACTION OF LIGHT IN OPTICALLY ISOTROPIC ACTIVE MEDIA

B. V. Bokut and F. I. Fedorov

Received 4 January 1960

Exact formulas are derived for the reflection of polarized light from an optically active isotropic medium or from a crystal of cubic symmetry. It is shown that, for any angle of incidence, the polarization of the reflected wave shows maximum ellipticity of polarization when the incident wave is polarized either parallel or perpendicular to the plane of incidence. At a certain intermediate azimuth angle of the oscillations of the incident wave with respect to the plane of incidence the reflected wave becomes linearly polarized. It is shown that when this azimuth angle is zero the polarization of the reflected wave changes very sharply from circular to linear and back to circular of opposite rotational direction for a change in the angle of incidence of a few seconds of arc in the neighborhood of a specific angle (which is close to Brewster's angle).

In the present paper the problem of reflection and refraction of electromagnetic plane waves at the surface of optically active transparent isotropic media or of crystals of the cubic system is analyzed. The medium of the incident wave is assumed to be transparent, isotropic and nonactive.

It is shown in ref. 1 that the refractivity vectors $\mathbf{m}_3$ of the reflected and $\mathbf{m}_1$ and $\mathbf{m}_2$ of the refracted waves, respectively, can always be written in the form

$$\mathbf{m}_s = \mathbf{b} + \eta_s \mathbf{q}, \tag{1}$$

where $\mathbf{b} = [\mathbf{q}[\mathbf{mq}]]$, $\mathbf{m} = n\mathbf{n}$ is the refractivity vector of the incident wave, n is the index of refraction of the nonactive medium, $\mathbf{n}$ is the wave normal (i.e., a unit vector in the direction of the wave normal) of the incident wave, $\mathbf{q}$ is the unit vector normal to the boundary surface and directed into the optically active medium, and $\eta_s = \mathbf{m}_s\mathbf{q}$ are parameters which are determined by the equation of normals for the given medium. Assuming that the parameter $\eta = \mathbf{mq}$ for the incident wave is known and setting $\mathbf{m}_3 = \mathbf{m}'$, we find[1] from the equation $\mathbf{m}'^2 = \varepsilon_0$ the refractivity vector of the reflected wave, namely, $\mathbf{m}' = \mathbf{b} - \eta\mathbf{q}$.

The refractivity vectors of the refracted waves must satisfy the equation of normals which, for our special case, can be written in the form[2]

$$(\mathbf{m}_s^2)^2 - (2\varepsilon + p^2)\,\mathbf{m}_s^2 + \varepsilon^2 = 0, \tag{2}$$

where $p = k\alpha$, α is the electrical coefficient of optical activity, $k = 2\pi/\lambda_0$ is the wave number for vacuum, and ε is the dielectric permeability of the active medium. The magnetic activity of the medium is not taken into consideration here.

Substituting Eq. (1) into Eq. (2) and setting $\mathbf{a} = [\mathbf{mq}]$ we obtain

$$\eta_s^4 - (2\varepsilon - 2a^2 + p^2)\,\eta_s^2 + [\varepsilon^2 - (2\varepsilon + p^2)\,a^2 + a^4] = 0, \tag{3}$$

whence

$$\left.\begin{aligned} \eta_{s1}^2 &= \varepsilon - a^2 + \frac{p^2}{2} + \frac{p}{2}\sqrt{4\varepsilon + p^2}, \\ \eta_{s2}^2 &= \varepsilon - a^2 + \frac{p^2}{2} - \frac{p}{2}\sqrt{4\varepsilon + p^2}. \end{aligned}\right\} \tag{4}$$

It is seen that η_1 and η_2 differ only by the sign of p, which corresponds to left-hand and right-hand circularly polarized waves.[3-5]

We will now decompose the incident, reflected, and refracted waves in the directions perpendicular and parallel to the plane of incidence. We obtain, for the incident wave,[1]

$$\mathbf{E} = A\mathbf{a} + B[\mathbf{na}], \quad \mathbf{H} = A[\mathbf{ma}] - B\mathbf{na}, \tag{5}$$

for the reflected wave,

$$\mathbf{E}' = A'\mathbf{a} + B'[\mathbf{n}'\mathbf{a}], \quad \mathbf{H}' = A'[\mathbf{m}'\mathbf{a}] - B'\mathbf{n}'\mathbf{a} \tag{6}$$

and, for the refracted waves,

$$\mathbf{E}_1 = A_1\mathbf{a} + B_1[\mathbf{n}_1\mathbf{a}], \quad \mathbf{E}_2 = A_2\mathbf{a} + B_2[\mathbf{n}_2\mathbf{a}]. \tag{7}$$

In these equations $\mathbf{n}$, $\mathbf{n}'$, $\mathbf{n}_1$, $\mathbf{n}_2$, are the wave normals of the incident, reflected, and refracted waves, respectively, and A, B, A', B', A_1, B_1, A_2, B_2, are the corresponding amplitude factors.

In view of the circular polarization of the vectors $\mathbf{E}_1$ and $\mathbf{E}_2$ we have

$$\mathbf{E}_k^2 = (A_k^2 + B_k^2)\,\mathbf{a}^2 = 0 \quad (k = 1, 2),$$

that is,

$$B_k = \pm iA_k. \tag{8}$$

Furthermore, since $\mathbf{E}_1$ is right-hand circularly polarized ($\mathbf{E}_1 = +i[\mathbf{n}_1\mathbf{E}_1]$) and $\mathbf{E}_2$ is left-hand circularly polarized ($\mathbf{E}_2 = -i[\mathbf{n}_2\mathbf{E}_2]$),[1] we obtain from Eqs. (7) and (8)

$$\mathbf{E}_1 = A_1(\mathbf{a} + i[\mathbf{n}_1\mathbf{a}]), \quad \mathbf{H}_1 = A_1([\mathbf{n}_1\mathbf{a}] - i\mathbf{n}_1\mathbf{a}), \tag{9}$$

$$\mathbf{E}_2 = A_2(\mathbf{a} - i[\mathbf{n}_2\mathbf{a}]), \quad \mathbf{H}_2 = A_2([\mathbf{n}_2\mathbf{a}] + i\mathbf{n}_2\mathbf{a}). \tag{10}$$

Here $n_1 = \sqrt{\eta_1^2 + \mathbf{a}^2}$ and $n_2 = \sqrt{\eta_2^2 + \mathbf{a}^2}$ are the refractive indices of the refracted waves.

We will now use the boundary conditions in vector form[1]

$$\mathbf{H} + \mathbf{H}' - \mathbf{H}_1 - \mathbf{H}_2 = 0, \tag{11}$$

$$[\mathbf{q}, \mathbf{E} + \mathbf{E}' - \mathbf{E}_1 - \mathbf{E}_2] = 0. \tag{12}$$

Substituting Eqs. (5), (6), (9), and (10) into Eqs. (11) and (12), we find that

$$[Am + A'm' - A_1m_1 - A_2m_2,\ a]$$

$$-(Bn + B'n - iA_1n_1 + iA_2n_2)\,a = 0, \tag{13}$$

$$(A + A' - A_1 - A_2)\,b - (Bnq + B'n'q - iA_1n_1q + iA_2n_2q)\,a = 0. \tag{14}$$

Since the two members in each of Eqs. (13) and (14) are mutually orthogonal, i.e., linearly independent vectors, we obtain

$$Bn + B'n - iA_1n_1 + iA_2n_2 = 0, \tag{15}$$

$$Am + A'm' - A_1m_1 - A_2m_2 = 0, \tag{16}$$

$$A + A' - A_1 - A_2 = 0, \tag{17}$$

$$Bnq + B'n'q - iA_1n_1q + iA_2n_2q = 0. \tag{18}$$

Substituting Eq. (1) into Eq. (16) and taking the linear independence of the vectors b and q into consideration, we obtain, in addition to Eq. (17), the relation

$$(A - A')\,\eta - A_1\eta_1 - A_2\eta_2 = 0. \tag{19}$$

From Eqs. (17) and (19) we find that

$$A_1 = \frac{1}{\eta_2 - \eta_1}\,(A(\eta_2 - \eta) + A'(\eta_2 + \eta)), \tag{20}$$

$$A_2 = -\frac{1}{\eta_2 - \eta_1}\,(A(\eta_1 - \eta) + A'(\eta_1 + \eta)). \tag{21}$$

Substituting Eqs. (20) and (21) into Eqs. (15) and (18), we obtain two simultaneous equations for the amplitude factors A′ and B′ of the reflected wave. The solution of these equations gives

$$A' = -\frac{1}{\Delta}\,(2iB\eta(\eta_2 - \eta_1)$$

$$+ A[(\eta_2 - \eta)(n\theta_1 + n_1\theta) + (\eta_1 - \eta)(n\theta_2 + n_2\theta)]), \tag{22}$$

$$B' = \frac{1}{\Delta}\,(2iA\eta(n_1\theta_2 - n_2\theta_1)$$

$$+ B[(\eta_2 + \eta)(n_1\theta - n\theta_1) + (\eta_1 + \eta)(n_2\theta - n\theta_2)]), \tag{23}$$

where

$$\left.\begin{aligned}\Delta &= (\eta_2 + \eta)(n\theta_1 + n_1\theta) + (\eta_1 + \eta)(n\theta_2 + n_2\theta),\\ \theta &= nq.\quad \theta_1 = n_1q.\quad \theta_2 = n_2q.\end{aligned}\right\} \tag{24}$$

Expressions for the amplitudes A_1 and A_2 of the refracted waves are found by substituting Eq. (22) into Eqs. (20) and (21). Thus,

$$\left.\begin{aligned}A_1 &= \frac{2\eta}{\Delta}\,[A(n\theta_2 + n_2\theta) - iB(\eta_2 + \eta)],\\ A_1 &= \frac{2\eta}{\Delta}\,[A(n\theta_1 + n_1\theta) + iB(\eta_1 + \eta)].\end{aligned}\right\} \tag{25}$$

From Eqs. (22) and (23) it follows that, contrary to the case of nonactive media, the reflected wave is generally elliptically polarized.

Let χ be the azimuth angle of the oscillations of the incident, linearly polarized wave, and let

$$\varkappa' = \frac{A'}{B'} = \tag{26}$$

$$\frac{2\eta(\eta_2 - \eta_1) - i\tan\chi\,[(\eta_2 - \eta)(n\theta_1 + n_1\theta) + (\eta_1 - \eta)(n\theta_2 + n_2\theta)]}{2\tan\chi\cdot\eta(n_2\theta_1 - n_1\theta_2) - i[(\eta_2 + \eta)(n\theta_1 - n_1\theta) + (\eta_1 + \eta)(n\theta_2 - n_2\theta)]}.$$

The degree of elliptical polarization, or "ellipticity," of a wave is determined by[1]

$$\left(\frac{b}{a}\right)^2 = \frac{1 - \sqrt{1 + \left(\frac{\varkappa' - \varkappa'^*}{1 + |\varkappa'|^2}\right)^2}}{1 + \sqrt{1 + \left(\frac{\varkappa' - \varkappa'^*}{1 + |\varkappa'|^2}\right)^2}}, \tag{27}$$

where b/a is the ratio of the semiminor axis to the semimajor axis of the polarization ellipse of the reflected wave. Using Eq. (26) we find a general expression for the "ellipticity" of the reflected wave. Thus,

$$\left(\frac{b}{a}\right)^2 = \frac{c_1 + \varkappa^2 d_1 - \sqrt{(c_1 + \varkappa^2 d_1)^2 - (a_1 - \varkappa^2 b_1)^2}}{c_1 + \varkappa^2 d_1 + \sqrt{(c_1 + \varkappa^2 d_1)^2 - (a_1 - \varkappa^2 b_1)^2}}, \tag{28}$$

where

$$\left.\begin{aligned}a_1 &= 4\eta(\eta_2 - \eta_1)[(\eta_2 + \eta)(n\theta_1 - n_1\theta) + (\eta_1 + \eta)(n\theta_2 - n_2\theta)],\\ b_1 &= 4\eta(n_2\theta_1 - n_1\theta_2)[(\eta_2 - \eta)(n\theta_1 + n_1\theta) + (\eta_1 - \eta)(n\theta_2 + n_2\theta)],\\ c_1 &= 4\eta^2(\eta_2 - \eta_1)^2 + [(\eta_2 + \eta)(n\theta_1 - n_1\theta) + (\eta_1 + \eta)(n\theta_2 - n_2\theta)]^2,\\ d_1 &= 4\eta^2(n_2\theta_1 - n_1\theta_2)^2 + [(\eta_2 - \eta)(n\theta_1 + n_1\theta) + (\eta_1 - \eta)(n\theta_2 + n_2\theta)]^2,\\ \varkappa &= \tan\chi = \frac{A}{B}.\end{aligned}\right\} \tag{29}$$

We will now determine the extreme values of the ellipticity of the reflected wave as a function of the azimuth angle of the oscillations of the incident wave. Setting equal to zero the derivative with respect to $\varkappa$ of Eq. (28) and solving for $\varkappa$ we obtain

$$\varkappa_1 = 0,\quad \varkappa_2 = \infty, \tag{30}$$

$$\varkappa_3 = +\sqrt{\frac{a_1}{b_1}},\quad \varkappa_4 = -\sqrt{\frac{a_1}{b_1}}. \tag{31}$$

According to Eq. (28), the values of $\varkappa_3$ and $\varkappa_4$ correspond to the minimum value, namely zero, of the ratio b/a, i.e., to linear polarization of the reflected wave. From Eqs. (26) and (29) it is seen that the azimuth angle of the oscillations of the reflected wave is in this case determined by

$$\tan\chi' = \varkappa' = \frac{A'}{B'} = \pm\sqrt{\frac{b_1}{a_1}}\cdot\frac{\eta_1 - \eta_2}{n_1\theta_2 - n_2\theta_1}. \tag{32}$$

We can thus draw the following conclusion: when linearly polarized light is reflected from an optically isotropic active medium, there are two azimuth angles of the oscillations of the incident wave symmetrically located with respect to the plane of incidence for which the reflected waves are also linearly polarized and have symmetrical azimuth angles of oscillation determined by Eq. (32).

It is obvious that the values $\varkappa_1$ and $\varkappa_2$ correspond to maximum ellipticity. We have

$$\left(\frac{b}{a}\right)_1 = \frac{c_1 - \sqrt{c_1^2 - a_1^2}}{c_1 + \sqrt{c_1^2 - a_1^2}}, \tag{33}$$

$$\left(\frac{b}{a}\right)_2 = \frac{d_1 - \sqrt{d_1^2 - b_1^2}}{d_1 + \sqrt{d_1^2 - b_1^2}} \tag{34}$$

or, in view of Eqs. (29) and (24),

$$\left(\frac{b}{a}\right)_1 = \frac{2\eta(\eta_2 - \eta_1)}{(\eta_2 + \eta)(nn_1q - n_1nq) + (\eta_1 + \eta)(n\cdot n_2q - n_2nq)}, \tag{35}$$

$$\left(\frac{b}{a}\right)_2 = \frac{2\eta(n_2n_1q - n_1n_2q)}{(\eta_2 - \eta)(nn_1q + n_1nq) + (\eta_1 - \eta)(n\cdot n_2q + n_2nq)}. \tag{36}$$

Maximum ellipticity of the reflected wave is thus obtained when the incident wave is linearly polarized perpendicular ($\varkappa = \chi = 0$) or parallel ($\varkappa = \infty$, $\chi = \pi/2$) to the plane of incidence.

It is well known that elliptical polarization is also obtained when linearly polarized light is reflected from an absorbing medium. However, there is a difference in the properties of the light reflected from an isotropic absorbing medium and that reflected from an isotropic transparent active medium. In the first case linear polarization of the reflected wave is obtained when the incident wave is polarized either perpendicular or parallel to the plane of incidence. Maximum ellipticity of polarization is reached at some intermediate azimuth angles of the oscillations of the incident wave, which are symmetrically located with respect to the plane of incidence. On the contrary, when light is reflected from isotropic active media maximum ellipticity of polarization is obtained in the general case $\chi = 0$ or $\chi = \pi/2$ and linear polarization at intermediate angles.

According to Eqs. (6), (22), (23), and (30) the electric vectors of the reflected wave for the cases $\chi = 0$ and $\chi = \pi/2$ are given by

$$\mathbf{E}'_{\parallel} = \frac{B}{\Delta}\{[(\varkappa_2 + \varkappa_1)(n_1\vartheta - n\vartheta_1) + (\varkappa_{11} + \varkappa_1)(n_2\vartheta - n\vartheta_2)] \cdot [\mathbf{n}'\mathbf{a}] + 2i\eta(\varkappa_{11} - \varkappa_{12})\mathbf{a}\}, \quad (37)$$

$$\mathbf{E}'_{\perp} = \frac{B}{\Delta}\{[(\varkappa_2 - \varkappa_1)(n_1\vartheta + n\vartheta_1) + (\varkappa_{11} - \varkappa_1)(n_2\vartheta + n\vartheta_2)]\mathbf{a} - 2i\eta(n_1\vartheta_2 - n_2\vartheta_1)[\mathbf{n}'\mathbf{a}]\}. \quad (38)$$

In view of Eqs. (4) and (24) it follows from Eqs. (37) and (38) that when $\chi = 0$ the semimajor axis of the ellipse lies in the plane of incidence and the semiminor axis is perpendicular to it, whereas the opposite is true when $\chi = \pi/2$. Substituting Eq. (37) into the expression $(\mathbf{in}'[\mathbf{E}'_{\parallel}\mathbf{E}'^{*}_{\parallel}])$ which determines the direction of rotation of the polarization ellipse,[1] we find for the case $\chi = 0$ that the reflected light is right-hand polarized if

$$(\varkappa_2 + \varkappa_1)(n\vartheta_1 - n_1\vartheta) + (\varkappa_{11} + \varkappa_1)(n\vartheta_2 - n_2\vartheta) > 0, \quad (39)$$

and left-hand polarized if

$$(\varkappa_2 + \varkappa_1)(n\vartheta_1 - n_1\vartheta) + (\varkappa_{11} + \varkappa_1)(n\vartheta_2 - n_2\vartheta) < 0. \quad (40)$$

It is thus obvious that at an incident angle ψ_0 which satisfies the relation

$$(\varkappa_2 + \varkappa_1)(n\vartheta_1 - n_1\vartheta) + (\varkappa_{11} + \varkappa_1)(n\vartheta_2 - n_2\vartheta) = 0, \quad (41)$$

the reflected light is linearly polarized with its plane of oscillation normal to the plane of incidence. Equation (41) is a full cubic equation with respect to $\sin^2\psi$, where ψ is the incident angle. The angle ψ_0 which is a solution of this equation is very close to the Brewster angle of the medium and differs from it only by a quantity of the order of magnitude of the square of the parameter of optical activity. It is interesting to note that for the case in question ($\chi = 0$) as the incident angle is increased from zero the ellipticity of the reflected wave increases at first only slightly, but as the angle closely approaches ψ_0 the ellipticity starts to increase very sharply, goes through circular polarization and then falls off sharply until the wave becomes linearly polarized at the angle ψ_0. As the incident angle is further increased slightly the ellipticity again increases sharply, then goes through circular polarization of opposite rotational direction and the wave becomes linearly polarized at grazing incidence ($\psi = \pi/2$).

It is obvious that it would be very desirable to test experimentally this extraordinary change in the polarization of the reflected wave as a function of the incident angle. Unfortunately, the experimental verification of this very interesting phenomenon presents almost unsurmountable difficulties. Indeed, numerical calculations made for a relatively strongly active cubic crystal, such as sodium chlorate ($NaClO_3$), show that all changes in the polarization of the reflected wave—from circular through linear, at $\psi = \psi_0$, and back to circular polarization of opposite direction—take place for a change in the angle of incidence of the order of three seconds of arc. In order that the described polarization picture be not blurred as a result of averaging, it is therefore necessary that the collimation of the incident beam be held within one second of arc.

When $\chi = \pi/2$ the rotational direction of the polarization does not change with the incident angle and the ellipticity remains small and changes only within a negligible range of values.

REFERENCES

1. F. I. Fedorov, "Optika anisotropnykh sred" (Optics of Anisotropic Media). Izd. Akad. Nauk Belorus.SSR, Minsk, 1958.
2. B. V. Bokut and F. I. Fedorov, Opt. i Spektr. 6, 537 (1959), Optics and Spectroscopy 6, 342 (1959).
3. F. I. Fedorov, Opt. i Spektr. 6, 85 (1959), Optics and Spectroscopy 6, 49 (1959).
4. F. I. Fedorov, Opt. i Spektr. 6, 377 (1959), Optics and Spectroscopy 6, 237 (1959).
5. B. V. Bokut and F. I. Fedorov, Opt. i Spektr. 7, 558 (1959), Optics and Spectroscopy 7, 344 (1960).

THE MAGNITUDE AND SIGN OF THE PHASE DIFFERENCE $\Delta = \delta_p - \delta_s$

I. N. Shklyarevskii, N. A. Vlasenko, V. K. Miloslavskii, and N. A. Noculenko

Received 17 March 1960

By using polarization and interferometric measurements the magnitude and sign of the phase difference $\Delta = \delta_p - \delta_s$ occurring on reflection of light from metal surfaces have been measured.

In the great majority of polarization methods of determining the optical constants of metals, the phase difference $\Delta = \delta_p - \delta_s$ is used in the calculation; here δ_p and δ_s are the phase shifts of the p and s components of the electric vector, respectively, for a given angle of incidence φ of light on the metal surface. In textbooks and in monographs on this topic the variation of Δ with φ is illustrated by graphs calculated from relations derived from Fresnel's equations for the amplitude coefficients of reflection r_p and r_s.

Since the Fresnel equations are written with different signs, it is usually considered that with normal incidence of light on the metal surface a phase difference of 180° occurs between the p and s components,[1-5] falling to 90° for the principal angle of incidence (φ_0) and to 0° for grazing incidence. However, this introduces several contradictions in connection with the fact that at normal incidence of the light the p and s components become indistinguishable.

These contradictions can be removed in two ways: firstly, by writing the Fresnel equations with identical signs,[6-8] that is,

$$\left.\begin{aligned} r_p &= -\frac{\tan(\varphi-\chi)}{\tan(\varphi+\chi)} \cdot a_p = |r_p| e^{i\delta_p}, \\ r_s &= -\frac{\sin(\varphi-\chi)}{\sin(\varphi+\chi)} \cdot a_s = |r_s| e^{i\delta_s}, \end{aligned}\right\} \quad (1)$$

where a_p and a_s are the amplitudes in the incident light and χ is the angle of refraction (identical signs can be obtained in the Fresnel equations by using a different sign convention in their derivation[9]); and secondly, by retaining the different signs in the Fresnel equations and keeping in mind that when light is reflected from the surface of a metal (or dielectric) the electric vector of the p component changes direction, that is, a phase shift again occurs, essentially.[9-11] In both these cases the phase difference occurring on reflection of the light from the metal surface varies from 0 to −180° as the angle of incidence changes from 0 to 90°.*

*In ref. 10 Δ varies from 0 to 180°.

Despite the different approaches of different authors to the question of the magnitude and sign of the phase difference $\Delta = \delta_p - \delta_s$ and the consequent uncertainty, we have not found any papers in the literature devoted to the direct measurement of this phase difference and its variation with the angle of incidence of light on a metal surface. Polarization and interferometric methods can be used to measure the magnitude and sign of the phase difference Δ.

MEASUREMENT OF Δ WITH A BEREK COMPENSATOR

The phase difference occurring on reflection of light from a metal surface can be compensated (and, consequently, measured) by using a Babinet compensator, a Berek compensator, etc.

Figure 1 is a diagram of the arrangement for these measurements. A parallel beam of white light, linearly polarized at an angle of 45° to the plane of incidence by means of a Nicol prism P, falls on the metallized glass plates (1,2) fixed parallel to each other in special carriages on a goniometer table. The light reflected from the metal surface enters the horizontally disposed tube of an MP-5 polarization microscope. Here A is the analyzer crossed with the polarizer P; S is a slit; L, L_1, and L_2 are lenses, and K is a Berek compensator, the axial direction N_z of which can coincide with the directions of the p or s components of the electric vector. By shifting the plate (from position 2 to 2′) it is possible, without changing the angle of incidence, to pass from a single to an m-fold reflection of the light and to measure the corresponding quantities Δ and $\Delta' = m\Delta$ (the latter measurement serves as a check). A slight modification of the arrangement permits the investigation of light that has undergone an even number of reflections from the metallized plates. It must be borne in mind that while the Nicols P and A are crossed for incident light, they are crossed for the reflected light with an even number of reflections from the metal surface and are parallel for an odd number (including one). With this apparatus measurements are most conveniently made on metals in which r_p/r_s is close to unity. In other cases the interference bands seen in the compensator are very much diluted by white light (especially with multiple reflections), which makes measurement difficult.

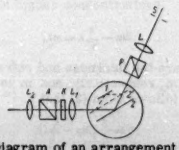

Fig. 1. Diagram of an arrangement for measuring the sign and magnitude of the phase difference Δ as a function of the angle of incidence of light on a metal surface.

Our experiments showed that the phase difference occurring on reflection of light from a metal surface can be compensated only if the axis N_z is oriented parallel to the s component. This means that the s component leads the p component. It was subsequently established that with normal incidence of light on the metal surface the phase difference $\Delta = 0$. Going from single to multiple reflection does not upset the compensation at all in this case, that is, a faint dark cross remains in the field of view when the Nicols are crossed.

Figure 2 gives the results of the measurements with aluminum. The solid curve was constructed from the

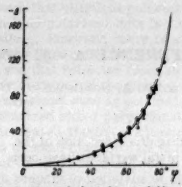

Fig. 2. Variation of the phase difference Δ with the angle of incidence φ for aluminum.

values of the optical constants measured earlier at $\lambda = 550$ mμ.[8] The solid circles and triangles show values of Δ obtained with single and triple reflection respectively, using crossed Nicols, and the open circles and triangles show values obtained with parallel Nicols. In the last case the measurement was made in the first colored band, and the phase difference was calculated using the obvious relation:

$$\Delta = \frac{\Delta' - 180^\circ}{m}.$$

Therefore the phase difference $\Delta = 0$, that is, $\delta_p - \delta_s$ when the light falls normally on the metal surface. Since for oblique incidence of light the s component leads the p component and $|\delta_s| > |\delta_p|$, the phase difference $\Delta = \delta_p - \delta_s$ is negative and the phase shifts δ_p and δ_s are positive.

MEASUREMENT OF Δ BY USING LINES OF EQUAL CHROMATIC ORDER

In ref. 12 experiments are described in which measurements were made of the magnitude and sign of the phase shift occurring when light is reflected at a dielectric/metal interface. It was there assumed that for $\varphi = 0$, $\delta_p = \delta_s = \delta$. In the paper mentioned it was shown that for a dielectric film bounded by metal surfaces, for each transmission interference band the following equation is valid:

$$2t\mu - \frac{\delta}{\pi}\lambda = m\lambda, \qquad (2)$$

where t and μ are the thickness and refractive index of the dielectric film, respectively, and m is the order of interference. It follows from (2) that

$$\delta = \frac{\pi}{\lambda}(2t\mu - m\lambda) \qquad (3)$$

is positive,[12] in complete agreement with the results of the present work. For an air/silver interface at $\lambda = 589$ mμ, $\delta \approx 150^\circ$.*

*In refs. 12, 13 the phase shift δ is designated by ψ.

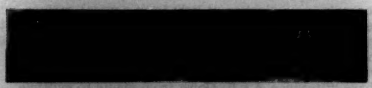

Fig. 3. Photographs of the p and s components (below) of lines of equal chromatic order. Obtained with aluminized plates by the use of an ISP-67 spectrograph (1500 mm focal length camera).

The magnitude and sign of the differences in the phase shift Δ can be determined by using interference lines. For oblique incidence of the light on the interferometer plates the interference lines split up as a result of the difference in the phase shifts for the p and s components. The magnitude of the splitting increases with increasing angle of incidence. The following equations apply to the components of the split line.

$$\left.\begin{aligned} 2t\cos\varphi - \frac{\delta_p}{\pi}\lambda_p &= m\lambda_p \\ 2t\cos\varphi - \frac{\delta_s}{\pi}\lambda_s &= m\lambda_s \end{aligned}\right| \qquad (4)$$

Here we see that $\lambda_p > \lambda_s$, from which it follows that for positive δ_p and δ_s,[13] $\delta_s > \delta_p$ and $\Delta = \delta_p - \delta_s$ is negative. If we measure the wavelength of several split lines of equal chromatic order and plot curves of $m\lambda = f(\lambda)$ for the p and s components, the difference in ordinates between these two curves for any given wavelength λ determines the quantity $\Delta\lambda/\pi$.[14]

Figure 3 shows photographs of the p and s components of lines of equal chromatic order, obtained by using a polaroid oriented in the appropriate manner. The interference plates were aluminized and the angle of incidence of the light on the aluminum surface was $\varphi = 52^\circ$. The crosses in Fig. 2 show the values of Δ obtained by means of the interferogram of Fig. 3 and two other similar ones.

We note that the absence of splitting in the interference lines in the Lloyd's mirror experiment is very frequently cited as an argument against Δ being -180° for grazing incidence. We see that this argument is untenable if we consider the special position of the electric vector of the p component of reflected light at $\varphi \approx 90^\circ$ (Fig. 4).

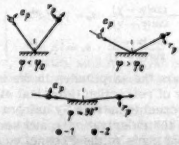

Fig. 4. Orientation of the electric vectors of the p and s components for different angles of incidence of the light. 1—Out of the paper; 2—into the paper.

The measurements of the magnitude and sign of Δ were undertaken as a result of discussions between the authors and N. Ya. Gorban and I. A. Shaikevich, colleagues at Kiev University.

REFERENCES

1. M. Born, "Optika" (Optics), Ob'edinenie Nauch.-Tekh. Izd. Gosudarst. Nauch.-Tekh. Izd. Ukrain., Kharkov-Kiev, 1937.
2. K. Shefer, "Teoreticheskaya Fizika" (Theoretical Physics), Vol. 3, Chap. 2, Gosudarst. Ob'edinenie Nauch.-Tekh. Izd., Moscow, 1938.
3. S. E. Frish and A. V. Timoreva, "Kurs Obshchei Fiziki" (General Physics Course), Vol. 3 Gosudarst. Izd. Tekh.-Teoret. Lit., Moscow-Leningrad, 1951.
4. V. L. Ginzburg and G. P. Motulevich, Uspekhi Fiz. Nauk 55, 469 (1955).
5. "Osnovnye Formuly Fiziki" (Basic Formulas of Physics). Izd. Inostrannoi Lit., Moscow, 1957.

6. J. R. Beattie and G. K. T. Conn, Phil. Mag. **46**, 222 (1955).
7. G. V. Rozenberg, "Optika tonkosloinykh pokrytii" (The Optics of Thin Films). Gosudarst. Izd. Fiz.-Mat. Lit., Moscow, 1958.
8. I. N. Shklyarevskii and V. K. Miloslavskii, Opt. i Spektr. **3**, 361 (1957).
9. P. Drude, "Optika" (Optics), Ob'edinie Nauch.-Tekh. Izd., Moscow-Leningrad, 1935.
10. G. S. Landsberg, "Optika" (Optics). Gosudarst. Izd. Tekh.-Teoret. Lit., Moscow, 1952.
11. R. V. Pol', "Vvedenie v optiku" (Introduction to Optics). Gosudarst. Izd. Tekh.-Teoret. Lit., Moscow, 1947.
12. I. N. Shklyarevskii, Zhur. Tekh. Fiz. **26**, 333 (1956).
13. I. N. Shklyarevskii and A. N. Ryazanov, Zhur. Tekh. Fiz. **26**, 659 (1956).
14. I. N. Shklyarevskii, Opt. i Spektr. **3**, 638 (1957).

STUDY OF THE OPTICAL PROPERTIES AND STRUCTURE OF TITANIUM DIOXIDE FILMS

T. N. Krylova and G. O. Bagdyk'yants

Received 27 February 1960

Thin films of titanium dioxide are now widely used in optics and other branches of physics. This compound is found in nature in two crystalline modifications: anatase and rutile. Anatase has a rhombic structure, and is stable below 850°. Rutile has a denser structure, and is stable above 1000°. The transition of pure anatase to rutile takes place at temperatures of about 900°; however, in the presence of small amounts of modifying impurities, the transition temperature may be lowered to 400°. Titanium dioxide has a high refractive index. For instance, the refractive indices of a prism made of a synthetic single crystal of rutile, in the wavelength range 4350 to 15,300 A are, for the ordinary ray, 2.853 to 2.451, and for the extraordinary ray, 3.216 to 2.709, according to deVore.[1]

Titanium dioxide obtained by hydrolysis of titanium tetrachloride, as well as of various organic compounds of titanium, is amorphous.[2] Upon heating, in addition to the formation of polymers, peroxide hydrates are found which, in a free state, are yellowish-brownish sediments.[3] X-ray diffraction analysis of titanium dioxide catalysts which were obtained by hydrolysis of pure components of the type $Ti(OC_2H_5)_4$, has shown the presence of crystal formation of both anatase and rutile with a phase transition which can be observed already at temperatures of 300 to 400°.[4]

Because of the high refractive indices, titanium dioxide film is extensively used for increasing and decreasing the reflectance from the surfaces of the optical parts. On the other hand, the nature of these films is not established in many cases. At the present time, different techniques have been made available for obtaining films of titanium dioxide. The transition from the solid state to a film is usually accompanied by a change of structure that goes together with a decrease of the refractive index (deviation from a stoichiometric composition, formation of pores,[5] etc.). The highest values for the refractive indices of titanium dioxide films were obtained by Hass[6] by oxidation at temperatures of 400 to 450° of thin layers of metallic titanium, deposited in high vacuum. The film has the rutile structure, and increases the reflectance from the glass surface from 4 to 44%, which corresponds to a refractive index of about 2.7. Conjeaud has demonstrated that the evaporation of a single crystal of rutile or of anatase in vacuum and deposition on any substrate results in a formation of an amorphous film which obtains the anatase structure mostly mixed with rutile, only after heating to 550°.

As our own investigations have shown,[7] the refractive indices of titanium dioxide films which were obtained from alcohol solutions of ethyl ether of orthotitanic acid, are determined essentially by the drying temperature of the films, and depend also on the concentration of the solution. Systematic observations of the change in thickness, and of the refractive indices permitted the detection of a number of transitions in the temperature range from 120 to 900°, which indicated structural changes in the films.

The present paper is dedicated to further study of the optical properties and the structure of titanium dioxide films obtained from solutions of $Ti(OC_2H_5)_4$.

The method of investigation consisted of measurements of the spectral dependence of the reflectance of films of various optical thickness (0.15 to 1 μ) in the visible part of spectrum. Figure 1 gives an example of the spectral curves for the reflectance of titanium dioxide films deposited on the surface of fused quartz. The curves 1 and 2 correspond to films with an optical thickness of about 4300 and 3500 A, respectively, after drying at 120° and 400°. One can obtain layers, which are optically more dense, from solutions of low concentrations by using several ones for deposition. The curve 3 represents such a layer with an optical thickness of 4300 A. The maximum reflectance is considerably greater here than in the case of curve 2 obtained from solutions of higher concentrations.

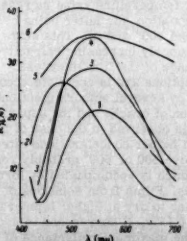

Fig. 1. Spectral dependence of the reflection coefficient of titanium dioxide films obtained by various means.

The results of the investigation are represented in Figs. 2 and 3. In Fig. 2 the dependence of the refractive index of films is given, obtained from solutions of higher (curves 1 and 2) and lower (curve 3) concentrations. For comparison, the data by de Vore[1] and Hess[6] for single

crystals of rutile and anatase are also given (curves 4 and 5, respectively), as well as for $TiCl_4$ films dried at 300° (curve 6). The results of observations of the change of the refractive indices in the range of 500 to 550 mμ for films obtained from solutions of ethyl ethers of orthotitanic acid, as a function of heating temperature, are given in Fig. 3. The character of these changes and the parallel observations of the light transmittance of the films make it possible to distinguish, in a preliminary way, three stages in the above mentioned temperature range of 120 to 900°:

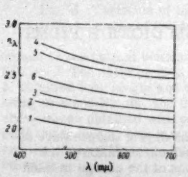

Fig. 2

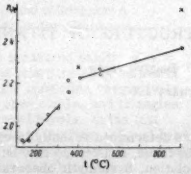

Fig. 3

Fig. 2. Spectral dependence of the refractive index of titanium dioxide films.
Fig. 3. Temperature dependence of the refractive index of titanium dioxide films.

1. In the temperature range of 120 to 300°, as a result of removing traces of water and alcohol, there is an increase of film density, accompanied by a continuous increase of the refractive indices. In the vicinity of 200 to 250° a yellowish-brownish coloration appears, due to formation of intermediate titanium compounds (of the type of peroxide hydrates), which causes an increase of absorption in the short wavelength part of the spectrum (400 to 500 mμ).

2. In the comparatively narrow temperature range of 300 to 350°, there is a sudden change of the film thickness that goes together with an increase of the refractive indices. This range is characteristic of the beginning of the crystallization process of titanium dioxide. The disappearance of coloration is observed, and the light transmittance is completely restored.

3. A further temperature raise increases the degree of phase transformation, the latter being completed at temperatures from 400° and up. This stage is characterized by continuously increasing refractive indices, upon a small change of the film thickness.

These conceptions are in complete accord with the results obtained by several authors mentioned above.

The formation of cracks and the separation from the substrate which is observed in the case of films obtained from solutions of higher concentrations after drying at temperatures above 500 or 600° probably results from crystallization which is accompanied by formation of larger aggregates. Films from solutions of low concentrations are easier to dry at higher temperatures. The curves 4, 5, and 6 (Fig. 1) correspond to such films dried at 900°. The maximum reflectance of these films is 35 to 40 percent, and even higher, corresponding to refractive indices of about 2.37 to 2.55 in the region of 500 to 550 mμ. The results of measurements of films obtained from solutions of low concentrations are marked in Figs. 2 and 3 with crosses.

Electron diffraction studies, the results of which are given in Fig. 4, furnish an additional lucid confirmation of the above-mentioned conceptions concerning the nature of films obtained from solutions of ethyl ether of orthotitanic acid, at various stages of film formation. The films were deposited on small samples of fused quartz, and were thermally treated at various temperatures. The electron diffraction patterns of Fig. 4 show that the films are amorphous in the range of 120 to 250° (pictures 1 and 2). The first traces of rings indicating the appearance of crystalline structure correspond to the temperature of 350° (picture 3). Raising the temperature up to 400°, 500° and higher causes a further formation of the crystalline phase (pictures 4, 5, and 6). The interpretation of the electron diffraction patterns has demonstrated that the crystalline phase corresponded in all cases (even by heating up to 900°) to the anatase structure. Data concerning the space distribution of atoms in the resulting crystalline formations, which confirm the presence of an anatase structure in the latter, are given in the Table.

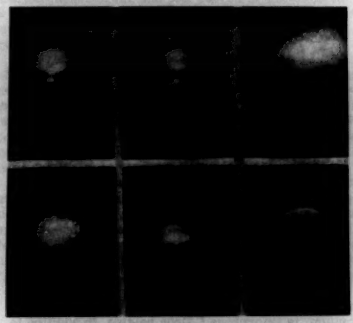

Fig. 4. Electron diffraction patterns illustrating structural changes in titanium dioxide films during thermal treatment. Temperature (in °C): 1—120; 2—350; 3—350; 4—400-500; 5—800; 6—900.

A prolonged heating at 900° of the films obtained from solutions of low concentrations causes an increase of the refractive indices which, probably, is the result of a transformation to the rutile structure.

Results of the Study of the Space Distribution of Atoms in the Crystalline Formation

d (A)	
Experimental values	Anatase (table values)
3.63	3.52
2.34	2.37
1.92	1.88
1.71	1.70
1.49	1.48
1.36	1.362
1.27	1.262
1.16	1.164
1.04	1.045

REFERENCES

1. J. R. de Vore, J. Opt. Soc. Am. 41, 416 (1951).
2. Z. N. Berestneva and V. A. Kargin, Uspekhi Khim. 24, 249 (1955).

3. A. N. Nesmeyanov, E. M. Brainina, and R. Ch. Freidlina, Doklady Akad. Nauk SSSR 85, 571 (1952).
4. A. M. Rubinstein and S. G. Kulikov, Izvest. Akad. Nauk SSSR, Ser. Khim. 14, 84 (1950).
5. D. P. Dobychin and Yu. N. Andreev, Zhur. Fiz. Khim. 28, 1465 (1954).
6. G. Hass, Vacuum 2, 331 (1952).
7. P. Conjeaud Compt. Rend. 238, 2075 (1954).
8. T. N. Krylova, Trudy Gosudarst. Opt. Inst., Leningrad 145, 146 (1956).

INTERFERENCE FILTERS WITH A TRANSMISSION BAND OF 1.5 A HALF-WIDTH

F. A. Korolev, A. Yu. Klement'eva and T. F. Meshcheryakova

Received 2 February 1960

Multilayer all-dielectric interference filters were prepared using the method of evaporation in a vacuum and having transmission bands of narrow half-widths which in some cases approached 1.5 A. The transmission coefficient of the interference filters at the maximum of the transmission band was of the order of 15%. Investigations leading to a further improvement of the properties of multilayer filters are described.

INTRODUCTION

All-dielectric interference filters which isolate a narrow spectral band have important practical applications. The problem of obtaining highly monochromatic radiations using interference filters is very important in optics, astrophysics, the physics of cosmic space, spectral analysis, automation, and a multitude of other branches of science and technology.

The properties of all-dielectric interference filters and the methods of manufacture and inspection have been previously described by the authors.[1,2] Here we shall only point out that the basic requirements for obtaining an interference filter with a transmission peak at some desired wavelength λ_0 are a high uniformity of the thicknesses of the layers and accurate monitoring of the optical thicknesses of the films during the manufacture. Uniformity of the thicknesses of the layers is obtained through the use of a suitable rotation of the specimen during the manufacture. In our experiments the optical thicknesses of the films are monitored by measuring the intensity of a transmitted light beam whose magnitude depends on the interference within the layers. The monitoring sensitivity increases with an increase in the number of layers and because of this the precision of measurement of the thickness of each layer is high and hence a high reproducibility of location of λ_{max} of the filter, approaching ±10 A (that is, approximately 0.005 λ_0), is achieved.

By using different substances for the layers the authors were able to construct filters for the 2500-2000 A region of the spectrum with transmission bands with half-widths $2\delta\lambda$ = 20-30 A and high transmission coefficient T = 50-75% (the background far from the maximum of the transmission band was less than 0.5%). Measurements have shown that the experimental determinations of the properties of interference filters are in good agreement with the calculated values. Experimental sets of such interference filters were successfully applied to the solution of problems in connection with the automation of spectral analysis and to the solution of other important scientific and technical problems. In our further studies the half-width of the transmission band of interference filters was reduced to 8-10 A in the central part of the visible region of the spectrum.

In many scientific studies even smaller half-widths (of the order of 1-3 A) of transmission bands are required. The subject of this paper is the preparation of interference filters with such half-widths, based on the application of previously developed methods of evaporation in vacuum, and the use of new methods of optical monitoring with increased precision.

METHODS FOR OBTAINING INTERFERENCE FILTERS WITH HIGH MONOCHROMATICITY

The formula for the half-widths of the transmission bands of an all-dielectric interference filter taking into account the dispersion of the phase change on reflection from the multilayer reflecting stacks is of the following form

$$2\delta\lambda = \frac{\lambda}{k - \frac{\lambda}{\pi}\cdot\frac{\partial\delta}{\partial\lambda}} \cdot \frac{1-R}{\pi\sqrt{R}}, \qquad (1)$$

where λ is the wavelength of the maximum of the transmission band, k is the order of the interference filter, R is the reflection coefficient of the reflecting stacks, and δ is the phase change on reflection from the reflecting stacks and is linearly dependent on the order of interference in the layer. From the above it follows that there are three ways of reducing the half-width of the transmission band: (1) by increasing the reflection coefficient R, (2) by increasing the order k of the interference filter, and (3) by increasing the absolute value of the phase dispersion $\partial\delta/\partial\lambda$.

A direct calculation according to formula (1) shows that the maximum narrowing of the transmission band is obtained by increasing the reflection coefficient. Thus, if two layers are added to each of the reflecting layer stacks consisting of quarter wavelength layers of ZnS and Na_3AlF_6, the half-width of the transmission band of of the interference filter should be reduced by two-thirds.

Thus, with an interference filter consisting of 14-layer reflecting stacks and a $\lambda/2$ thick ZnS spacer layer one should obtain a transmission band of half-width $2\delta\lambda$ = 1.4 A. Specimens of interference filters of this type prepared by the authors had wider transmission bands of 2.6 A. The reason for the widening is that actual dielectric layers have porous structures and inhomogeneities on the microscopic scale. Such defects at the boundaries and within the central layer give rise to changes $\Delta(nh)$ in the optical thickness of the layer and consequently result in displacements $\Delta\lambda_{max}$ of the transmission peaks of the interference filter. Thus, when the whole filter is used its transmission band broadens together with a simultaneous decrease in transmission at the maximum.

We note that during the process of evaporation of the layers one also obtains a regular change in the thickness of the layer over the extent of the useful area of the specimen, which also widens the transmission band values of $\Delta h/h_0 = 0{,}02\%$ and $\lambda = 5000$ A cause a displacement of $\Delta\lambda_{max} = 1$ A). However, this variation can be made sufficiently small by choosing a suitable geometrical arrangement of the apparatus (see ref. 2). In our case $\Delta\lambda$ was equal to 1 A over an area of 30 mm diameter (the specimens were measured with a parallel beam of light of 20 mm diameter). The effect of the (irregular) inhomogeneities of the central layer could be substantially reduced by increasing the order k of the interference filter. This follows from the fundamental equation for an interference filter:

$$2nh = k\lambda.$$

If we differentiate the above, treating nh and λ as variables, we obtain

$$\Delta\lambda = \frac{2\Delta(nh)}{k}. \qquad (2)$$

From this it follows that the shift in the transmission band $\Delta\lambda$ is smaller the larger the value of k. According to formula (1), by increasing the order k one obtains a significant narrowing of the transmission band $2\delta\lambda$. This was fully achieved experimentally with a central ZnS layer for which $nh = 10\lambda/2$. Such an interference filter has adequate stability and a good transmission coefficient.

EXPERIMENTAL RESULTS

The experimental results are shown in Table 1 in which are given the properties of interference filters of different types constructed by the authors and also their comparison with calculated values. The maxima of the transmission bands of the interference filters were in the region of 5600 to 5900 A.

When computing the quantity $2\delta\lambda$ the authors employed the methods for the calculation of the values of the reflection coefficient R of the reflecting layer stacks and of the dispersion of the phase change $\partial\delta/\partial\lambda$ described in refs. 3-5. The properties of the interference filters were measured photographically on a KS-55 spectrograph and on a DFS-4 diffraction spectrograph with automatic recording of the spectrum. When calculating the half-width $2\delta\lambda$ of the transmission bands the absorption in the films was not taken into account; it has a fundamental effect on the transmission of the interference filter but not on the half-width of the transmission bands.

Table 1

No.	Type of interference filter	$2\delta\lambda_{exp.}$ (A)	$2\delta\lambda_{theor.}$ (A)	$T_{exp.}$ (%)
1	$\underbrace{HL\ldots HL}_{8} - 3H \cdot 2 - \underbrace{LH\ldots LH}_{8}$	15.0	13.8	55
2	$\underbrace{HL\ldots HL}_{8} - 10H \cdot 2 - \underbrace{LH\ldots LH}_{8}$	8.0	6.6	45
3	$\underbrace{HL\ldots HL}_{10} - H \cdot 2 - \underbrace{LH\ldots LH}_{10}$	11.0	10.0	55
4	$\underbrace{HL\ldots HL}_{10} - 5H \cdot 2 - \underbrace{LH\ldots LH}_{10}$	6.2	3.8	40
5	$\underbrace{HL\ldots HL}_{10} - 10H \cdot 2 - \underbrace{LH\ldots LH}_{10}$	4.0	2.3	35
6	$\underbrace{HL\ldots HL}_{12} - H \cdot 2 - \underbrace{LH\ldots LH}_{12}$	4.2	3.5	50
7	$\underbrace{HL\ldots HL}_{12} - 5H \cdot 2 - \underbrace{LH\ldots LH}_{12}$	1.57	1.3	15
8	$\underbrace{HL\ldots HL}_{14} - H \cdot 2 - \underbrace{LH\ldots LH}_{14}$	2.6	1.4	15

In Table 1 the letter H represents a quarter wavelength layer with a high refractive index (ZnS) and the letter L represents a quarter wavelength layer made out of a substance with a low refractive index (cryolite). The experimental and theoretical values of the half-widths of the transmission bands are given in columns $2\delta\lambda_{exp.}$ and $2\delta\lambda_{theor.}$; the experimental values of the transmission coefficients at the maxima are given in column $T_{exp.}$.

Figure 1 shows the transmission of a first order interference filter with 12-layer reflecting stacks ($\lambda_{max} = 5930$ A, $2\delta\lambda = 4.5$ A, T = 50%). The record was made on a spectrograph with a 15 μ wide slit and a linear dispersion of 0.112 A/mm. Under these conditions the linear dimension of the width of the transmission band on the photographic plate was 40 mm. It can be seen that the transmission in the wings of the transmission band is significant for distances closer than 15 A from the maximum. At this distance it is reduced to about 1% and farther out it continues to fall rapidly. Figure 2 represents the corresponding curve for a first order interference filter with 14-layer reflecting stacks ($\lambda_{max} = 5710$ A, $2\delta\lambda = 2.6$ A, T = 15%). The wings have a significant value

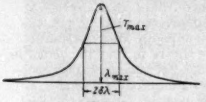

Fig. 1

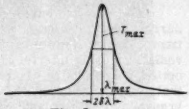

Fig. 2

(approximately 1%) for distances of up to 10 A away from the maximum. Figure 3a represents the trace of the transmission band of a fifth order interference filter with 12-layer reflecting stacks with $\lambda_{max} = 5800$ A, $2\delta\lambda = 1.57$ A, and $T_{max} = 15\%$; Fig. 3b is a trace of the contours of two mercury lines. In this case the transmission in the wings is significant for distances of up to 10 A from the maximum.

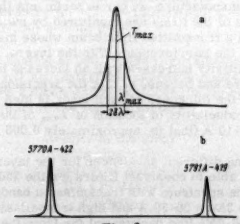

Fig. 3

It can be seen from the above data that the most efficient layer combination consists of 12-layer reflecting stacks with a $5\lambda/2$ thick ZnS spacer layer. This type of interference filter has a transmission band of half-width $2\delta\lambda = 1.57$ A and a transmission coefficient of 15%. A k-th order interference filter has k-1 additional transmission peaks which must be eliminated. This is achieved by depositing a wide band interference filter (with $2\delta\lambda = 50$-70 A and T = 80-90%) onto the narrow band filter.

According to formula (1), the third method of reducing the half-width of the transmission band is based on obtaining larger phase dispersions $\partial\delta/\partial\lambda$ at the reflecting stacks. The so-called "narrow band" reflecting

stacks which consist of films of thicknesses $k\lambda/4$, where k is an odd number, or of layers of more complex composition, have a larger phase dispersion. A reflecting layer stack the width of whose reflection maximum is k times narrower than that of the "classical" reflecting layer stack has a phase dispersion that is k times larger. However, this method proves to be very cumbersome in practice as it requires the deposition of a large number of layers (about 50-100 layers of $\lambda/4$ thickness). We prepared interference filters with reflecting stacks having reflecting regions of the order of 1000 and 600 A in the central part of the spectrum, that is, reflecting stacks with 1.5 and 2 times narrower reflecting regions than the usual stacks. The composition and properties of interference filters with such reflecting layer stacks are given in Table 2.

Table 2

No.	Type of interference filter	$2\delta\lambda$ (A)	T (%)
1	$\underbrace{3H, L \ldots 3H, L}_{13} - 2H - L, \underbrace{3H \ldots L, 3H}_{13} \ldots\ldots$	4.4	60
2	$\underbrace{5H, L \ldots 5H, L}_{13} - 2H - L, \underbrace{5H \ldots L, 5H}_{13} \ldots\ldots$	3.6	30

It can be seen from this table that interference filters constructed according to the above method possess some advantage with respect to the transmission when compared with the interference filters described in Table 1.

Further improvement of the properties of interference filters can be brought about by refining the process of deposition of layers in a vacuum, by the use of purer materials, etc. In connection with the above, the reduction of the transmission in the wings of the transmission bands appears to be especially important.

The authors hope to reduce the magnitude of the transmission coefficient in the wings to 1% at a distance from the maximum equal to twice the half-width of the transmission band. The attained results make it possible to extend the field of application of interference filters to a very broad class of spectroscopic investigations, and in a large number of cases to replace prismatic and diffraction instruments with interference filters.

REFERENCES

1. F. A. Korolev, Vestnik Moskov. Gosudarst. Univ. No. 3, 97 (1958).
2. F. A. Korolev, A. Yu. Klement'eva, and T. F. Meshcheryakova, Inzh.-Fiz. Zhur. No. 1, 55 (1960).
3. G. V. Rozenberg, "Optika tonkosloinyhk pokrytii" (Optics of Thin Layer Coatings). Gosudarst. Izd. Tekh.-Teoret. Lit., Moscow, 1958.
4. C. Dufour and A. Herpin. Rev. opt. **32**, 321 (1956).
5. M. P. Lisitsa, Zhur. Tekh. Fiz. **24**, 1837 (1954).

MEASUREMENT OF THE PHOTOELECTRIC YIELD OF THE EXTERNAL PHOTOEFFECT UNDER THE ACTION OF X-RAYS IN THE WAVELENGTH RANGE 1.54-13.3 A

A. P. Lukirskii, M. A. Rumsh, and I. A. Karpovich

Received 26 January 1960

The use of an Allen-type photomultiplier for the measurement of photoemission produced by x-radiation with wavelengths from 1.54 to 13.3 A is described. The measured photoelectric yields for a series of photocathodes are presented.

INTRODUCTION

In ref. 1 the experimental difficulties met in the measurement of photoelectric yields in the ultrasoft x-ray region were discussed, and a method of measurement was proposed in which the x-ray intensity is determined using a Geiger counter and the number of photoelectrons is found using an Allen-type photomultiplier.[2] In this paper the application of this method for another range of x-ray wavelengths is described, and the measured photoelectric yields are presented for certain metallic and nonmetallic photocathodes. The work was carried out with the vacuum x-ray monochromator (using Bragg reflection) which was described in ref. 3. The method of counting the number of quanta with the Geiger counter was also considered in detail in ref. 3.

USE OF THE ALLEN-TYPE PHOTOMULTIPLIER FOR RECORDING PHOTOEMISSION

The supply and recording circuits used in this investigation were analogous to those described earlier[1] with the exception that the first dynode of the photomultiplier was grounded and the photocathode was at a negative potential. A parallel plate capacitor was placed before the photocathode to prevent the penetration of ions into the photomultiplier. The placement of the photomultiplier relative to the parts of the monochromator is shown in Fig. 1.

Preliminary tests with the photomultiplier showed that separation of the characteristic lines was greatly hampered by a high intensity background. It was established that this background was due to ultraviolet radiation which was also generated in the x-ray tube. Since ultraviolet radiation reflects from the crystal according to the laws of optics and in the Bragg spectrometer the angle of reflection always equals the angle of incidence, this radiation falls on the photocathode under any conditions. In order to filter the ultraviolet light the window of the x-ray rube was covered by a celluloid sheet Φ (Fig. 1) of about 1μ thickness. Such a filter absorbs the ultraviolet radiation and makes it possible to observe "contrasty" characteristic lines. When working in the region of small Bragg angles reflection of ultrasoft x-rays from the crystal also took place as a result of "total external reflection." This radiation was almost completely absorbed by placing one of the absorbers O (aluminum foil of thickness about 5μ) in the beam. This absorber is only introduced for small Bragg angles,

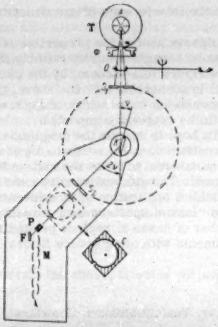

Fig. 1. Diagram of vacuum x-ray monochromator. T—x-ray tube; A—anode of x-ray tube; Φ—filter; O—absorber; S_1—entrance slit of monochromator; K—crystal; S_2—exit slit of monochromator; P—parallel-plate capacitor (to decrease background); F—photocathode; M—electron multiplier; O—Geiger counter.

i.e., when using comparatively hard radiation. After the described filtration the characteristic lines registered by the photomultiplier have good "contrast."

A detailed discussion of the operation of the photomultiplier is presented below because the characteristics differed from those of a photomultiplier operating in the region of ultrasoft radiation. The curves of Fig. 2 show the dependence of the counting rate on the gain of the electronic circuit G (in nominal units given by the ratio 1000/P, where P is the "operating threshold" of the recording apparatus). All curves presented in Fig. 2 were obtained with a tungsten photocathode and constant intensity Cu-K_α radiation (λ = 1.54 A). Curve 1 gives the dependence of the counting rate on G for a potential difference of U_F = 400 volts between the photocathode and the first dynode. This dependence differs from that for ultrasoft radiation[1] in that there is no horizontal part in the region of high G. It was noted that with no potential difference between the photocathode and the first dynode an appreciable counting rate of the photomultiplier is observed for sufficiently high values of the gain (curve 3 of Fig. 2). The count of the photomultiplier for U_F = 0 can be caused either by fast electrons falling on the first dynode or by quanta which remove photoelectrons from the first dynode. High-speed electrons arise during illumination of the photocathode by x-rays[4] but their relative abundance is completely unknown. From an analysis of the curves of the collected photoelectrons (i.e., the dependence of the count on U_F) and a series of additional experiments, which will be mentioned below, it follows that the fraction of fast electrons is negligibly small. Quanta, resulting from fluorescence of the photocathode under the action of x-radiation, can strike the first dynode. For each event of quantum absorption in the photocathode there will arise an excited state whose most probable level will be one close to the energy of the absorbed quantum. This excited state can be deactivated by the emission of a cascade of quanta of various frequencies. Among these quanta will be found some (very soft quanta) for which the photoelectric yield from the first dynode will be large. Since the magnitude of the photo-

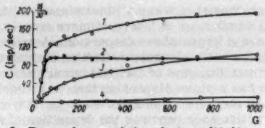

Fig. 2. Dependence of the photomultiplier counting rate on the gain of the electronic circuit. Curve 1—U_F = −400 volts; curve 2—obtained by subtracting curve 3 from curve 1; curve 3—U_F = 0; curve 4—U_T = 0 (first and second dynodes connected to photocathode).

electric yield of metallic photocathodes for x-rays is small (see results of measurement at end of article), the fraction of impulses arising because of fluorescence of the photocathode and the subsequent photoeffect at the first dynode can be relatively large.

Curve 3 (Fig. 2) starts up at higher values of the gain than does curve 1. This is easily explained by the fact that impulses originating in the photomultiplier are smaller by a factor of σ (σ is the coefficient of secondary electron emission from the dynodes.).

Curve 4 in Fig. 2 was obtained under the condition that the photocathode and the first and second dynodes were at the same potential. The count of the photomultiplier in this case is explained by fluorescence of the first dynode activated by fluorescence of the photocathode and can also be explained by the photoeffect at the second dynode. Curve 4 begins to rise for even higher values of the gain since the amplification factor of the photomultiplier for this process if σ^2 times smaller.

From the above it is seen that curve 3 represents the total count of the photomultiplier caused by fluorescence of the photocathode with photoemission at the first dynode, by the subsequent fluorescence of the first dynode with photoemission at the second dynode, etc. This can explain the fact that curve 3 does not have a horizontal region.

The recording of the photoelectrons which originate at the photocathode is of primary interest. The fraction of impulses referring only to these electrons can be found by subtracting curve 3 from curve 1 (curve 2 is the result of this subtraction). This curve has a long horizontal region and agrees in form with curves obtained for ultrasoft radiation, for which with zero potential difference between photocathode and first dynode no count of the photomultiplier was observed because of low fluorescence yields and relatively high photoelectric yields. In chosing the operating conditions of the photomultiplier which would insure counting of all photoelectrons a value of the gain was taken corresponding to the horizontal part of curve 2, for which the photomultiplier records only photoelectrons from the photocathode. This value of the gain was used in the investigation of other characteristics of the photomultiplier.

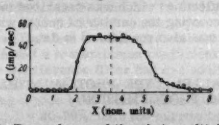

Fig. 3. Dependence of the photomultiplier counting rate on the point of incidence of the beam on the photocathode (1 division = 0.4 mm).

Let us consider some of these other characteristics. In Fig. 3 the dependence of the photomultiplier counting rate on the point of incidence of the monochromatic beam on the photocathode is presented. This curve was obtained for a tungsten photocathode using copper radiation (one nominal unit of translation of the beam along the photocathode is equal to 0.4 mm). The horizontal portion of the curve is considerably wider than the monochromatic beam.

The dependence of the counting rate of the photomultiplier on the voltage between the photocathode and the first dynode is presented in Fig. 4. Curve 1 was obtained for a tungsten photocathode using Cu-K_α radiation (1.54 A) and curve 2 for a tantalum photocathode using B-K_α radiation (67 A).* If we subtract the fluorescence contribution from curve 1, it agrees in form with curve 2. In both curves we observe a broad horizontal portion and a slight drop in counting rate in the high-voltage region. This drop is associated with a decrease in the coefficient of secondary electron emission from the first dynode for high velocity electrons, and this is accompanied by a drop in the amplification factor of the photomultiplier which, because of the slope of curve 1 of Fig. 2, leads to a decrease in the counting rate of the photomultiplier even for high gain of the electronics. A second consequence of the decrease in the coefficient of secondary electron emission is the decrease in the probability that, under the action of a photoelectron from the first dynode, not a single secondary electron will be released (i.e., this photoelectron will not be recorded). This also will lead to a drop in the count of the photomultiplier in the region of high potential difference between the photocathode and the first dynode.

*This curve was obtained while the vacuum monochromator was being used for ultrasoft x-radiation.[5]

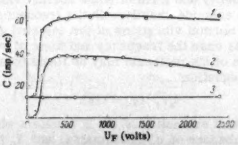

Fig. 4. Dependence of the photomultiplier counting rate on the voltage between photocathode and first dynode. Curve 1—Cu-K_α radiation (1.54 A); curve 2—B-K_α radiation (67 A); curve 3—count of the photomultiplier due to fluorescence produced in the photocathode by Cu-K_α radiation.

The presence of the horizontal portion of curve 1 (Fig. 4) indicates the practical absence of fast electrons. In order to test this assertion an experiment was performed with the photomultiplier by placing a grid (30-μ mesh) between the first dynode and the photocathode. The grid was at the potential of the first dynode, and the photocathode was given a positive potential (retarding the electrons). There were practically no counts detected in the interval of photocathode potentials from 0 to +3000 volts. This result indicates a relatively small number of fast electrons.

After correcting the photomultiplier characteristics for the fluorescence part of the count they agreed completely with the corresponding characteristics for the ultrasoft region. Operating on the horizontal parts of these characteristic curves insured conditions for almost complete count of all photoelectrons.

MEASUREMENT OF THE PHOTOELECTRIC YIELD

The technique of measuring the photoelectric yield consisted of successive measurements of radiation intensity with the Geiger counter and of the number of electrons with the photomultiplier. A selection of graduated absorbers made it possible to measure considerable intensities with the Geiger counter. The measurements were performed using the characteristic lines. The background of the lines (continuous spectrum in various orders and scattered radiation) and the natural background of the detectors were excluded by subtracting the appropriate values from the results obtained.

Photoelectric yields were determined for a series of photocathodes consisting of metals and of ionic crystals. The metallic surfaces were cleaned with emery cloth, and the photocathodes of ionic crystals were prepared by vacuum evaporation on a nickel substrate. The angle of incidence of the radiation on the photocathode amounted to approximately 60°. The values obtained for the photoelectric yields are presented in the Table. In view of the fact that the surfaces were not specially cleaned and the yields were not measured for various thicknesses of the sputtered photocathodes, the data presented in the Table should be considered as tentative, although the precision of measurement can be set at about 10%.

Values of the Photoelectric Yields of Various Photocathodes (%)

No.	Photocathode \ Radiation (A)	$Cu K_\alpha$	$Cr K_\alpha$	$Ti K_\alpha$	$Cu K_\alpha$	$Cl K_\alpha$	$Al K_\alpha$	$Na K_\alpha$	$Cu L_\alpha$
		1.537	2.278	2.74	3.35	4.72	8.32	11.9	13.3
1	Ti (sample No. 1)	0.26	0.41	0.09	0.10	0.27	0.66	1.60	—
2	Ti (sample No. 1, second measurement)	0.25	0.39	0.11	0.12	0.24	0.67	1.73	2.8
3	W	0.36	0.82	0.60	0.80	1.50	0.94	1.70	2.3
4	Pt	0.44	0.80	1.1	1.6	2.0	1.18	2.5	3.3
5	NaBr (sample No. 1)	0.76	1.5	2.1	2.8	5.9	5.1	6.8	9.6
6	NaBr (sample No. 2)	1.3	4.6	3.5	3.6	6.1	3.3	5.6	17.8
7	CsJ	5.7	10.8	4.9	31.5	14.1	35.8	76.0	94.5
8	SrF_2	1.4	5.8	3.6	6.64	11.6	21.6	12.3	15.5

The following conclusions can be drawn from the tabulated data. The fact that the photoelectric yield has a tendency to rise with increasing wavelength probably is associated with the decreased depth of penetration of the radiation into the photocathode. Departure from this regularity, as is observed, for example, in the case of Ti for Ti-K_α radiation and in the majority of other cases, is explained by the presence of absorption jumps in the corresponding spectral region. Attention is also drawn to the fact that the photocathodes of ionic crystals have photoelectric yields which considerably exceed those of the metallic photocathodes. It is interesting to note that approximately the same relationship is found for the coefficients of secondary electron emission for ionic crystals and metals.

In conclusion it should be noted that the use of an electron multiplier operating in a system for counting separate impulses permits the determination not of the total number of photoelectrons originating during irradiation of the photocathode but of the number of quantum absorption events accompanied by the emission of photoelectrons. If the magnitude of the photoelectric yield is small, as it is for metallic photocathodes, then the probability of the simultaneous release of several photoelectrons by one quantum is very small, and the value of the photoelectric yield determined by the described method represents the true yield. For photocathodes with large yields (e.g., for CsI) the values we have measured are somewhat less than the true yields.

The authors express their gratitude to Academician A. A. Lebedev for discussions and his interest in this investigation and also to A. I. Efremov and A. M. Tyutikov for the photomultiplier and the samples.

REFERENCES

1. A. P. Lukirskii, M. A. Rumsh, and L. A. Smirnov, Opt. i Spektr. 9, 511 (1960), Optics and Spectroscopy 9, 265 (1960).
2. N. O. Chechik, S. M. Fainshtein, and T. M. Lifshits, "Elektronnye umnozhiteli" (Electron Multipliers). Gosudarst. Izd. Tekh.-Teoret. Lit., Moscow, 1957.
3. M. A. Rumsh, A. P. Lukirskii, I. A. Karpovich, and V. N. Shchemelev, Prib. i Tekh. Ekspt. 5, 67 (1960).
4. M. A. Blokhin, "Fizika rentgenovskikh luchei" (The Physics of X-Rays). Gosudarst. Izd. Tekh.-Teoret. Lit., Leningrad, 1953.
5. A. P. Lukirskii, M. A. Rumsh, and L. A. Smirnov, Opt. i Spektr. 9, 505 (1960), Optics and Spectroscopy 9, 262 (1960).

INTENSITIES AND POLARIZATIONS OF SPECIFIC VIBRATIONS IN THE INFRARED ABSORPTION SPECTRA OF POLYATOMIC MOLECULES

L. A. Gribov

Received 30 March 1960

The question of the intensities and polarizations of fully specific vibrations is considered. Methods are indicated which simplify the corresponding computations. The concept of vibrations which are fully specific with respect to polarization and intensity is introduced, and an attempt is made to indicate the conditions necessary for this.

Study of the vibrational absorption spectra of polyatomic molecules has shown that to definite chemical groups there correspond definite, so-called characteristic or specific vibration frequencies and form, which change relatively little on transfer of such groups from one molecule to another. This property of the vibrations of polyatomic molecules has, to a considerable extent, been responsible for the very wide penetration of spectral methods of investigation into science and industry.

The intensities and polarizations of the absorption bands, the measurement of which may give extremely valuable information on the internal structure of a molecule and on the types of chemical bonds, are no less important characteristics of the vibrational spectrum of polyatomic molecules. However, by reason of the complexity of the question, extensive investigations in this field have begun only in very recent years. In particular, the problem of computing the intensities and polarizations of specific vibrations and an attempt to clarify the conditions necessary for the appearance of specificity of infrared absorption bands with respect to polarization and intensity are extremely timely. This question presents enormous interest both from the point of view of the practical possibility of calculating the electro-optical parameters of a molecule in terms of data from infrared spectral measurements, and also from the point of view of obtaining an additional criterion for the assignment of the absorption bands observed in the spectrum to the corresponding normal vibrations of the molecule. The investigation of specificity with respect to polarization, furthermore, is significant in principle for measurements whose purpose is the establishment of the arrangement of bonds and groups of atoms within a molecule with respect to the direction of the vector for the change in dipole moment in a given normal vibration.

A theory of the specific vibration frequencies of polyatomic molecules has been worked out by Mayants,[1] in which a well-grounded definition of the specificity of vibrations was introduced and approximate methods were proposed for the calculation of the frequencies and forms of the specific vibrations; these methods significantly simplified the practical solution of the mechanical problem. It is therefore entirely natural to pose the question of the calculation of the intensities and polarizations of specific absorption bands in vibrational spectra, basing one's work on the definition of specificity given by Mayants.

Let us select in the molecule a chemically characteristic group of atoms, the vibrations of which are described by n' internal coordinates from the set of all n internal coordinates of the molecule. Let us consider the limiting case of a vibration which is fully specific for the given group of n' coordinates. By definition this means that the frequency and form of some normal vibration of the molecule coincide exactly with the frequency and form of one of the normal vibrations of the selected group of atoms. In this case the frequency and form of such a normal vibration of the molecule may be found from the solution of the equation

$$\theta_0 Y_0^{-1} \| q \| = \lambda \| q \|,$$

where θ_0 is that submatrix of the T^{-1} matrix which refers to the subspace of n' coordinates, and Y_0 is the analogous submatrix of the U^{-1} matrix. θ_0 and Y_0 are known to be uniquely determined by the choice of n' and do not depend on the remaining $n - n'$ coordinates. The normalizing factor in this case will equal

$$\frac{\sqrt{h\nu}}{\sqrt{(q)\, Y_0^{-1} \| q \|}},$$

and will likewise not depend on $n - n'$ of the coordinates.

Let us turn now to the analysis of the intensities and polarizations of such a fully specific vibration.

From the theory of the absorption of light by molecules, it is known that the probability of the corresponding transition between vibrational levels is proportional to the square of the modulus of the vector for the change in dipole moment of the molecule, $|\Delta\mu_m|^2$, during a vibration of the given form, and that the polarization is determined by the direction of $\Delta\mu_m$. In the zero-order approximation of the valence-optical scheme, the dipole moment of the molecule is represented in the form

$$\mu = \sum_i \mu_i^0 e_i,$$

where μ_i^0 is the dipole moment of an isolated bond and e_i is its direction vector. In the next approximation one

must take into account the fact that, by virtue of the interaction of the given bond with other bonds in the molecule, μ_k, generally speaking, will not coincide with the direction of the bond; i.e., $\mu_k = \mu_k^0 + \mu_k'$, where μ_k' is a vector correction depending on the presence of the other bonds.

Let us represent μ_k' in the form

$$\mu_k' = \sum_{l \neq k} \mu_{kl} \cdot e_l.$$

Then

$$\mu = \sum_k \mu_k = \sum_k \mu_k^0 e_k + \sum_k \sum_{l \neq k} \mu_{kl} e_l = \sum_k \left(\mu_k^0 + \sum_{l \neq k} \mu_{lk}\right) e_k = \sum_k \left(\mu_k^0 + \mu_k'\right) e_k = \sum_k \mu_k e_k. \quad (1)$$

Thus a formula is obtained which is entirely analogous to the case of the zero-order approximation except for the additional term μ_k', which includes all the corrections introduced into the value of the dipole moment of the given bond by its surroundings. It is μ_k^0 which presents the greatest practical interest, since this is the quantity which is characteristic for the given bond. The introduction of the correction for nonadditivity is to a considerable degree arbitrary, provided only that the vector sum of all the bond dipole moments be equal to the dipole moment of the molecule. As will be clear from what follows, investigation of the specific intensities and polarizations opens paths for the most exact determination of the actual values of μ_k^0.

When these remarks are taken into account, formula (5) of ref. 2, which expresses $\Delta\mu_m$ explicitly in terms of the electro-optical and mechanical parameters of the molecule and the form of the vibration, may be used for the calculation of $\Delta\mu_m$. Here the quantities $\mu_1 = \mu_1^0 + \mu_1'$ will figure and the elements of the row matrix $\{\mu_1\}$, and the matrix

$$\left| \begin{matrix} \left(\frac{\partial\mu_1}{\partial q_1}\right)_0 \left(\frac{\partial\mu_1}{\partial q_2}\right)_0 \cdots \left(\frac{\partial\mu_1}{\partial \tau_{11}}\right)_0 \cdots \\ \cdots\cdots\cdots\cdots\cdots \\ \left(\frac{\partial\mu_{N-1}}{\partial q_1}\right)_0 \left(\frac{\partial\mu_{N-1}}{\partial \tau_{11}}\right)_0 \cdots \left(\frac{\partial\mu_{N-1}}{\partial \tau_{11}}\right)_0 \end{matrix} \right| =$$

$$\left| \begin{matrix} \left(\frac{\partial\mu_1^0}{\partial q_1}\right)_0 \left(\frac{\partial\mu_1^0}{\partial q_2}\right)_0 \cdots \left(\frac{\partial\mu_1'}{\partial \tau_{11}}\right)_0 \cdots \\ \cdots\cdots\cdots\cdots\cdots \\ \left(\frac{\partial\mu_{N-1}}{\partial q_1}\right)_0 \left(\frac{\partial\mu_{N-1}}{\partial q_2}\right)_0 \cdots \left(\frac{\partial\mu_{N-1}}{\partial \tau_{11}}\right)_0 \cdots \end{matrix} \right|,$$

inasmuch as μ_i^0 is a function only of "its own" coordinate of type q and μ_i' is determined entirely by the surroundings of the bond.

In the zero-order approximation, all the μ_i''s and their derivatives are equal to zero. Then, retaining the symbols adopted in refs. 2 and 3, we may write the expression for $\Delta\mu_m$, taking account of the nonadditivity corrections, in the following form, which is appropriate for the case of a fully specific vibration considered here:

$$\Delta\mu_m = \left[(e_1, e_2) \left| \begin{matrix} \frac{\partial\mu_1}{\partial q_1} & \frac{\partial\mu_1}{\partial q_2} \\ \frac{\partial\mu_2}{\partial q_1} & \frac{\partial\mu_2}{\partial q_2} \end{matrix} \right| + (\mu_1, \mu_2) \left| \begin{matrix} a_1 & 0 \\ 0 & a_2 \end{matrix} \right| \left(\left| \begin{matrix} \Delta s_1 \\ \Delta s_2 \end{matrix} \right| \cdot \left| \tilde{B}_1, \tilde{B}_2 \right| \right. \right.$$

$$\left. \left. \times \left| \begin{matrix} \tau_{11} & \tau_{12} \\ \tau_{21} & \tau_{22} \end{matrix} \right| - \left| \begin{matrix} E_1 & 0 \\ 0 & E_2 \end{matrix} \right| \right) \right] \left\| \begin{matrix} q_1^0 \\ 0 \end{matrix} \right\|.$$

Here the indexes 1 and 2 designate those sets of quantities which refer respectively to the selected group of atoms and to the remaining part of the molecule. In other words, e_1 and e_2, μ_1 and μ_2 ($\mu_k = \mu_k^0 + \mu_k'$) are submatrices of the row matrices $\{e_k\}$ and $\{\mu_k\}$; $\partial\mu_i/\partial q_j$ are rectangular submatrices of the matrix of the derivatives of the bond dipole moments of the first and second groups with respect to the vibrational coordinates; $\tilde{B}_1$ and $\tilde{B}_2$ are rectangular submatrices of the matrix $\tilde{B}$ with N (the number of atoms in the molecule) rows and n′ and n − n′ columns respectively, etc.; $\| q^0 \|$ is a column of the zero-order amplitudes of the internal vibrational coordinates of any type. By virtue of the condition of full specificity of the vibration under consideration, the zero-order amplitudes of the coordinates of group 2 are equal to zero.

The matrix T is the inverse of the matrix

$$T^{-1} = \left| \begin{matrix} \theta_{11} & \theta_{12} \\ \theta_{21} & \theta_{22} \end{matrix} \right|,$$

while $\tau_{11} = \theta_{11}^{-1} + \tau_{11}'$, where $\tau_{11}' = \theta_{11}^{-1}\theta_{12}(\theta_{22} - \theta_{21}\theta_{11}^{-1}\theta_{12})^{-1}\theta_{21}\theta_{11}^{-1}$ (see ref. 4).

Taking this note into account and carrying out the multiplication in formula (1), we obtain

$$\Delta\mu_m = \underline{\{e_1\} \left| \frac{\partial\mu_1}{\partial q_1} \right| \| q_1^0 \|_m + \{\mu_1\} a_1 \left(\Delta s_1 \tilde{B}_1 \theta_{11}^{-1} - E_1\right) \| q_1^0 \|_m}$$

$$\underline{+ \{e_2\} \left| \frac{\partial\mu_2}{\partial q_1} \right| \| q_1^0 \|_m + \{\mu_1\} a_1 \left(\Delta s_1 \tilde{B}_1 \tau_{11}'\right) \| q_1^0 \|_m + \{\mu_1\} a_1 \left(\Delta s_1 \tilde{B}_2 \tau_{21}\right) \| q_1^0 \|_m}$$

$$\underline{+ \{\mu_2\} a_2 \Delta s_2 \left(\tilde{B}_1 \tau_{11}' + \tilde{B}_2 \tau_{21}\right) \| q_1^0 \|_m} = \Delta\mu_{11} + \Delta\mu_{12};$$

$$\tau_{21} = -\left(\theta_{22} - \theta_{21}\theta_{11}^{-1}\theta_{12}\right)^{-1}\theta_{21}\theta_{11}^{-1}. \quad (2)$$

Thus the expression for $\Delta\mu_m$ has been divided into the two components $\Delta\mu_{11}$ and $\Delta\mu_{12}$ (singly and doubly underlined), one of which depends only on the elements of the selected group of atoms and characterizes the magnitude of the vector $\Delta\mu$ during vibrations of the atom group 1 as a free molecule (with the same values for the bond dipole moments), while the second determines the electrical and mechanical interactions with the remaining part of the molecule. The physical sense of the components of $\Delta\mu_{12}$ consists in the following. The first term characterizes the magnitude of the changes in the bond dipole moments of group 2 during changes in the equilibrium configuration of group 1. Its contribution depends on the degree of overlap of the electron clouds of the two groups. The second term appears by virtue of the fact that the elements of the submatrix τ_{11} are not invariant with respect to the coordinate system and will change with changes in group 2, even if all the elements of group 1 are retained. The closer the T^{-1} matrix is to being quasi-diagonal, the smaller the magnitude of this term will be. The third and fourth terms represent respectively corrections to the deflections of the bonds of the first group of atoms and those deflections in space of the bonds of the second group, which may arise from the necessity of conserving the center of mass and the angular momentum of the whole molecule during a vibration such that the equilibrium distances and angles within the selected group of atoms change (which is generally implied under the term "form" of the vibration).

Formula (2), regardless of its apparent complexity, enables us to simplify significantly the calculation of the vector $\Delta\mu_m$ for fully specific vibrations, since in practice basing one's work on the physical sense of the interaction terms and on their form, one can in many cases easily estimate their numerical value and draw conclusions concerning their influence. Furthermore, one should note a number of circumstances which simplify the calculations. First, the matrix τ_{11}' is symmetric, and to evaluate it one need only deal with submatrices of de-

gree n′ and n − n′. Secondly, by virtue of their motion as a whole, the deflection vectors for the bonds of group 2, $\| \Delta e_2 \| = \sigma_2 \Delta c_2 (\tilde{B}_1 \tau_{11} + \cdots)$, will be equal with respect to their moduli, and their directions can easily be determined from consideration of the character of the motion of this group. The vectors

$$\| \Delta e_1' \| = \sigma_1 (\lambda_1 \tilde{B}_2 \tau_{21}) \| q_1^0 \|.$$

must also possess the same property. In some cases, when group 2 is sufficiently complex and it is evident that vibrations in group 1 may lead to deflections of the bonds of group 2, it is sensible to replace group 2 by a single effective "bond" in such a way that its kinetic energy in the given vibration is equal to the kinetic energy of the whole group. The dipole moment of such a "bond" will equal the sum of the projections of all the dipole moments of group 2 onto the direction of the "bond," and the mass of the terminal atom will be the sum of the masses of the atoms of group 2. With such a description of the motion of group 2, the degree of the T matrix is also correspondingly lowered.

The representation of the vector $\Delta\mu_m$ in the form of two components enables us to pose the question of the specificity of vibrations with respect to polarization and intensity, and of the stability of such specificity on transfer of the selected group of atoms from one molecule to another. It is just those vibrations whose specificity is stable which present the greatest physical interest. It is altogether evident that such a phenomenon can exist only in the case when the influence of the surroundings of the given chemical group is small.

Let us call a vibration of a molecule fully specific in polarization and intensity for a given group of atoms if $\Delta\mu_{12} = 0$. In the general case, as one can easily convince oneself, this can be so only on complete breakaway of the atom group under consideration from the remaining part of the molecule. Consequently, in reality, one may speak only of the approximate specificity of $\Delta\mu_m$. The less the magnitude of $\Delta\mu_{12}$ in comparison with $\Delta\mu_{11}$, the more specific will be the given vibration with respect to intensity and polarization. In this sense $\Delta\mu_{12}$ may serve in its own way as a measure of nonspecificity.

By virtue of this, it is in all probability impossible to set down general necessary and sufficient conditions for full specificity of a vibration with respect to intensity and polarization. All the terms of $\Delta\mu_{12}$ represent a series of factors (matrix factors) whose product may be equal to zero even if no one of the factors is equal to zero. Nevertheless, one can designate a number of criteria, physically quite real, in the presence of which the quantity $\Delta\mu_{12}$ may be neglected. The following will be such necessary conditions for specificity of a vibration for a given group of atoms with respect to intensity and polarization:

(1) The presence of full specificity in frequency and form; (2) weak interaction of the electron clouds of groups 1 and 2; i.e., the elements of the submatrix $|\partial\mu_2/\partial q_1|$ must be negligibly small in comparison with the elements $|\partial\mu_1/\partial q_1|$; (3) the groups 1 and 2 must have the least possible number of atoms in common and $T' \approx 0$; (4) the absence of deflections of the bonds of group 2 during vibrations of a given form.

In order to retain specificity of a vibration with respect to intensity and polarization on transfer of the characteristic atom group unchanged into another molecule (aside from retention of full specificity in frequency and form and the other conditions enumerated above), it is necessary to have constancy of the values of the bond dipole moments in the group under consideration, and this means that we must have $|\partial\mu_2/\partial q_2| = 0$. In other words, we arrive at the requirement that the electro-optical parameters of the selected group of atoms be additive. The experimental discovery in infrared absorption spectra of bands specific in polarization and intensity, and the stability of the specificity, may serve as one weighty indication of the closed character of the electron clouds of the corresponding groups of atoms (see also ref. 5).

Stability of specificity in frequency and form is usually associated with specific chemical forces which manifest themselves in the smallness of the nondiagonal elements in the U matrix. Since the force field and the electric field in the molecule, generally speaking, must be connected with each other, then in all probability the smallness of the corresponding nondiagonal elements in the matrix of the derivatives of the bond dipole moments with respect to the vibrational coordinates will be a consequence of the smallness of the analogous elements in the matrix of the force constants.

The supposition may be expressed that vibrations which are specific in intensity will necessarily be specific in frequency and form, and that vibrations which are specific in polarization will be accompanied by specificity in form. If such a supposition proves to be true, it will be natural to divide the absorption bands in the vibrational spectrum of a polyatomic molecule into those specific in intensity and polarization, those specific in polarization, and those specific in frequency. In this connection, specificity of any type may be experimentally investigated. The highest form of specificity—specificity in intensity and polarization—which requires a whole series of conditions for its existence, must be encountered relatively rarely. We note that, for specificity of $\Delta\mu_m$ in direction, the requirement of specificity in frequency is not necessary. However, in reality stable specific frequencies in the spectrum will most frequently correspond to vibrations which are specific in both frequency and form. Therefore, special prescriptions relative to the conditions for specificity in polarization do not present any substantial interest.

Let us now adduce examples illustrating the positions developed.

1. Vibration of a single bond. We assume that the given normal vibration of the molecule is fully specific for one of the bonds (No. 1). We assume further that the bond does not enter into the make-up of a ring structure and that its vibrations do not lead to deflections of the remaining bonds in the molecule. This may be so if either a straight line drawn along the bond passes through the center of mass of the surrounding groups, or if the mass of one of the atoms of the given bond is significantly less than the masses of the remaining atoms in the molecule.

Then, evidently,

$$\Delta\mu = e_1 \left(\frac{\partial\mu_1}{\partial q_1}\right)_0 q_1^0 + \sum_{n \neq 1} e_n \left(\frac{\partial\mu_n}{\partial q_1}\right)_0 q_1^0 .$$

If $(\partial\mu_1/\partial q_1)_0 \gg (\partial\mu_n/\partial q_1)_0$, then the term $\sum e_n (\partial\mu_n/\partial q_1)_0 q_1^0$ may be neglected, and the vibration will be fully specific in polarization and intensity. Such, in all probability, is the state of affairs in the vibrations of OH, NH, and other bonds which possess a large intrinsic dipole moment.

In the case of symmetrical bonds of the type C=C, C≡C, N=N, etc., the vibration of which is often fully specific in frequency and form, the intrinsic dipole moment and the derivative $(\partial\mu_1/\partial q_1)_0$ are equal to zero. Consequently, the vector $\Delta\mu$ will be entirely determined by the surroundings of the given bond and will not be specific. Experimental study of the intensities and polarizations of the corresponding absorption bands might shed

light on the magnitude of the nondiagonal elements in the matrix of the derivatives of the bond dipole moments with respect to the vibrational coordinates and, consequently, might clarify the influence of the correction on the nonadditivity.

2. Vibrations of groups of the type XY_2 and XY_3. Let there be, in the make-up of the molecule, nonlinear symmetric groups of atoms, XY_2 and XY_3, the normal vibrations being fully specific in frequency and form for these groups. Let us suppose further that these groups are joined to the remaining part of the molecule only through the atom X, and that the overlap of the electron clouds of the groups under consideration and of the rest of the molecule is small. The groups CH_2 and CH_3 in particular should possess such properties. From the general conditions for specificity it is clear that the symmetric vibrations of these groups have the greatest probability of being specific in intensity and polarization (especially if the symmetry axis of the group passes through the center of mass of the molecule).

Antisymmetric and degenerate vibrations are accompanied by such displacements of the atom X and deflections of the group themselves as may lead to deflection of other parts of the molecule. For this reason the degree of specificity of such vibrations will probably be less.

As an example, we may adduce the expressions for $\Delta\mu$ corresponding to the symmetric and antisymmetric vibrations of the group XY_2 (CH_2), free and entering into the ethylene molecule, which we obtained in refs. 2 and 6.

REFERENCES

1. L. S. Mayants, Doct. diss., Trudy Fiz. Inst. Akad. Nauk SSSR, 5 (1950).
2. L. A. Gribov, Opt. i spektr. 8, 769 (1960), Optics and Spectroscopy 8, 404 (1960).
3. L. A. Gribov, Doklady Akad. Nauk SSSR 127, 788 (1959).
4. R. Fraser, V. Duncan, and A. Kollar, "Teoriya matrits i ee prilozheniya" (Matrix Theory and Its Applications). Izd. Inostrannoi Lit., Moscow, 1950.
5. M. V. Vol'kenshtein, M. A. El'yashevich, and B. I. Stepanov, "Kolebaniya molekul" (Molecular Vibrations), Vol. 2. Gosudarst. Izd. Tekh.-Teor. Lit., Moscow-Leningrad, 1949.
6. L. A. Gribov, Opt. i Spektr. 9, 176 (1960), Optics and Spectroscopy 9, 93 (1960).

SHORT COMMUNICATIONS

A METHOD FOR DETERMINATION OF THE RADIATION PROBABILITY OF GASES AND VAPORS

Ya. I. Gerlovin

Received 21 March 1960

The radiation probability which corresponds to the rotational-vibrational absorption bands of gases and vapors has not been measured yet by a direct method, but was calculated from the value of the Kravets[1] integral. The value of this integral is found now by methods described in a number of papers.[2-6] The application of these methods requires the measurement of spectral transmittance at various effective thicknesses of the layer of absorbing gas and at various total pressures.*

*With the exception of the method by Veingerov-Slobodskaya.

In the present communication, a method is described which permits the determination of the spontaneous radiation by means of one or two measurements. The method consists essentially in a comparison of the intensities of the radiation of a gas and of a black body of the same temperature which is higher than that of the receiver used for the comparison.

When the effective thickness of the gas layer is very small, the signal S′ caused by the gas radiation is given by

$$S' = RAh\nu N' l F_1 F_2,$$

where R is the proportionality coefficient which is determined by the measuring apparatus, A is the probability of spontaneous radiation, h is the Planck constant, N′ is the number of excited molecules in 1 cm³, corresponding to frequency ν, l is the cell length, F_1 is the area of the cell window, and F_2 is the effective surface of the receiver.

If instead of the gas cell, a black body is placed at the same distance from the receiver having a radiating surface equal to that of the cell window, then the expression for the signal S (taking into consideration that the temperature of the receiver is much lower than that of the black body) will be

$$S = R\sigma T^4 a F_1 F_2,$$

where σ is the Stefan-Boltzman constant, T is the absolute temperature of the black body and

$$a = \frac{\int_0^\infty f_1(\nu) f_2(\nu) f_3(\nu)\, d\nu}{\int_0^\infty f_1(\nu)\, d\nu}.$$

Here $f_1(\nu)$ is the spectral intensity distribution of the black body radiation, $f_2(\nu)$ is the spectral sensitivity of the receiver, and $f_3(\nu)$ is the transmittance of the filter used.

It follows from these relationships, that

$$A = \frac{S'\sigma T^4 a}{Sh\nu N' l}.$$

Inasmuch as the probability of the transition of the excitation energy of the molecules into heat by collisions is considerably greater, for the infrared bands, than the probability of spontaneous emission, the number of the excited molecules (for not too high a temperature of the gas in question) will differ little from $N_0 \exp(-h\nu/kT)$, where N_0 is the total number of molecules in 1 cm³. Therefore

$$A = \frac{S'\sigma T^4 a}{Sh\nu e^{-\frac{h\nu}{kT}} l N_0}.$$

It follows from this expression that the error of the method depends additively on the errors of measure-

ments of α, T, S, S', and 1 (it should not exceed 10 per cent).

The applicability of the described method was demonstrated on an absorption band of carbon dioxide in the region 4.3μ with an apparatus of which the scheme is shown in the Figure. An interference filter, 2, was

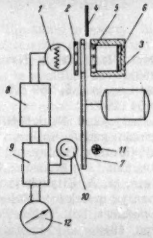

placed before a lead telluride photoconductor, 1, cooled by liquid air. Behind the filter, either the cell, 3, with carbon dioxide was placed, or a plate covered with lampblack, substituting a black body; its emissivity was assumed to be that of a black body. The gas cell and the lamp-black plate were at room temperature. The coefficient determined by graphic integration, was found to be 8.5×10^{-3}. The cell length was 1 cm, the diameter 3 cm, so that the radiation from the cell walls, for all practical purposes, did not reach the receiver. The effective surface of the receiver was 4 mm². A fluorite window, 5, was glued on to the front end of the cell, and a flat surface mirror to the back end. A reflecting modulating disc, 7, with holes rotated before the window. The photoconductor was connected to an amplifier, 8, equiped with a synchronous detector, 9, for which the supporting electromotive force was generated by the photoelement, 10, illuminated by a little lamp, 11. The frequency of modulation was 400 Mc.

Because it was difficult to obtain the equality of the reflection coefficients of the modulating disc and of the mirror, the cell was first flushed with dry nitrogen or oxygen, the corresponding signal was measured with the output instrument, 12, and then the cell was flushed with a 1 percent mixture of carbon dioxide with nitrogen or oxygen, and the signal recorded again. The difference, which was the signal caused by the radiation from carbon dioxide, was found to be ten times smaller than the signal caused by the radiation of the black surface.

Calculation by means of the relationships derived above gives for the probability of radiation of the corresponding absorption band CO_2 in the region 4.3μ, a value of approximately 350 sec^{-1}.

It should be mentioned in conclusion that the measurements were made not with the purpose of establishing the exact value of the radiation probability, but for the evaluation of the method. The values of S and S' were therefore determined only approximately, and the value of A should for the time being be considered as a preliminary one.

REFERENCES

1. T. N. Kravets, Izvest. Moskov. Inzh. Uchil. 2, No. 6 (1912); "Trudy po fizike" (Papers on Physics) p. 33 Izd. Akad. Nauk SSSR, Leningrad-Moscow, 1959.
2. A. J. Wells and E. B. Wilson, J. Chem. Phys. 14, 578 (1946).
3. S. S. Penner and D. Weber, J. Chem. Phys. 19, 807 (1951).
4. L. D. Kaplan and D. F. Eggers, J. Chem. Phys. 25, 876 (1956).
5. J. Overend, M. J. Joungquist, E. C. Curtis, and B. Crawford, J. Chem. Phys. 30, 532 (1959).
6. M. L. Veingerov and P. V Slobodskaya, Izvest. Akad. Nauk SSSR, Ser. Fiz. 11, 420 (1947).

INFRARED ABSORPTION BAND INTENSITIES OF THE HYDROPEROXIDE GROUP

L. A. Gribov and A. V. Karyakin

Received 7 April 1960

The investigation of the structure of hydroperoxides is of great importance in view of the varied and very valuable applications of these compounds. In this respect, infrared spectroscopy possesses substantial advantages over chemical methods, since the weak perturbation caused by the absorption of a quantum of infrared radiation allows the detection of any change in the structure of the molecule undergoing oxidation, and of the formation and decomposition of products in situ, without affecting the natural course of the reaction. However, this type of investigation becomes possible only after carrying out a sufficiently detailed assignment of the absorption bands to the normal vibrational modes of the molecule or functional group.

A number of frequencies appearing in the infrared spectra of hydroperoxides have been assigned experimentally to the COOH group. Lately, Kovner, Karyakin, and Efimov[1] have calculated theoretically the vibrational modes of the free COOH (COOD) group, assuming the geometrical configuration shown in the Figure (see ref.

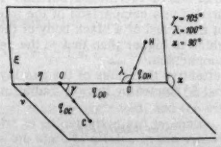

2). In the calculation, the force constants of the angles and the bonds between nonadjacent atoms, the force constants of interaction between two adjacent bonds, and the force constants of interaction between the coordinate κ and the other coordinates were all assumed to be zero. The other force constants were assumed to be equal to the corresponding ones in alcohols. The variation method was used to determine the elements of the matrix U.

Good agreement was obtained between the calculated and the observed frequencies, but the configuration of the

vibrational modes was not calculated.

However, the spectral manifestation of the vibrations of a polyatomic molecule is characterized not only by a series of frequencies but also by the intensities of the corresponding absorption bands. A theoretical investigation of absorption band intensities yields additional information on the structure and spectral manifestation of the molecule or group of atoms under investigation; moreover, the strong dependence of the vibrational intensities on the configuration of the vibrational modes can be used to check and refine the assignment of calculated modes to the experimental frequencies.

As a concrete case, the sharp difference in the intensities of the 835 and 883 cm^{-1} bands of the COOH group is of great interest, the more so since the 883 cm^{-1} vibration cannot be assigned entirely, (as done in ref. 1) to the variation in the length of the —O—O— bond (see Table 1). Besides, it is important to find out how characteristic of the COOH group are the various absorption bands assigned to its vibrations.

Table 1. Frequencies and Normalized Configurations of the COOH Group Vibrations

Band assignment	Frequency (cm^{-1})	Amplitudes of the variations in the vibrational coordinates					
		q_{CO}	τ	q_{OO}	λ	q_{OH}	$\varkappa$
q_{OH}	3450	0	0	—0.01	+0.01	1.03	0.01
λ	1322	0.03	—0.01	0.03	—1.14	0.05	—0.06
q_{CO}, τ . . .	1155	0.39	—0.12	—0.09	0.09	0	0.02
τ, q_{OO}, $\varkappa$ . . .	883	0.03	—0.30	0.30	—0.03	0	—0.46
$\varkappa$	835	0.02	—0.01	0.15	—0.05	0	1.08
τ, $\varkappa$	588	0.03	0.30	0.10	—0.04	0	0.18

We calculated the frequencies of the COOH and COOD groups, on the basis of initial results kindly put at our disposal by M. A. Kovner, the configurations of the vibrational modes, and the shifts in the positions of all the atoms during the vibration. The results were used in an approximate evaluation of intensities based on the general method proposed by Gribov.[3,4] Because we were interested in an approximate, semiquantitative evaluation of the intensities, we felt justified in using the zeroth approximation of the valence-optical method, particularly if we included the geometric structure of the COOH group. We took into consideration the fact that the dipole moment of the —O—O— bond can be assumed, with sufficient accuracy, to be zero, while the other dipole moments and the products of their derivatives with respect to "their" coordinates and the corresponding zero amplitudes, are equal to each other in magnitude. Thus, the contribution of the electro-optical parameters in the expression for $\Delta\mu$ will be determined mainly by the absolute magnitudes of the zero natural coordinates q_{OH}, q_{OC} and by the rotation vectors of the bonds in the given normal vibration. In performing the calculations, we neglected all values that were smaller than the principal value by more than one order of magnitude. Moreover, since $|\Delta\mu|^2 = |\Delta\mu_\xi|^2 + |\Delta\mu_\eta|^2 + |\Delta\mu_\nu|^2$, we could neglect the contribution to $|\Delta\mu|^2$ of those projections of the vector $\Delta\mu$ which were five to six times smaller than the principal value.

As a result of the calculations, we obtained expressions for $|\Delta\mu|^2$ in the various normal vibrations of the COOH group, as shown in Table 2 (on a relative scale of magnitudes, common to all the vibrations).

Thus the intensities of the first two bands are mainly determined by the derivatives $(\partial\mu_{OC}/\partial q_{OC})_0$ and $(\partial\mu_{OH}/\partial q_{OH})_0$, which, as is well known, are quite large, while the intensities of all the other bands are mainly determined by the dipole moments of the OH and OC bonds (to a larger extent by the dipole moment of the OH bond). This is not a surprising conclusion if it is remembered that the OH bond, because of the small size and weight of the hydrogen atom, is the most mobile, thus exerting a great influence on the intensities of those vibrations where the largest variations occur in the interbond angles and in the interplanar angle κ. The magnitudes of the corresponding intensities will therefore be substantially dependent on the magnitude of Δe_{OH} in the vibration of a given configuration. It is interesting to note that this rationalization holds true even for the 588 cm^{-1} vibration, where the main variation occurs in the coordinate γ.

Table 2

Frequency (cm^{-1})	Expression for $\lvert\Delta\mu\rvert^2$	Usual evaluation of the intensity
1. 1155	$\left(\frac{\partial\mu_{OC}}{\partial q_{OC}}\right)_0^2$	Very strong
2. 3450	$4\left(\frac{\partial\mu_{OH}}{\partial q_{OH}}\right)_0^2$	Very strong
3. 1322	$9\cdot p_{OH}^2$	Strong
4. 883	$p_{OH}^2 + 0.36p_{OC}^2$	Weak
5. 588	$4p_{OH}^2 + 0.49p_{OC}^2$	Average
6. 835	$9\cdot p_{OH}^2$	Strong

Assuming the dipole moments of the OH and OC bonds to be 1.58 and 1.12 D respectively, we shall obtain the following ratios of intensities: $\nu_3 : \nu_4 : \nu_5 : \nu_6 = 9 : 1.2 : 4.3 : 9$. The experimentally obtained ratios of the same vibrations in the case of isopropylbenzene hydroperoxide are, 9.5 : 1.2 : 11 : 9.5.

Thus it is possible to provide an adequate explanation of the intensity distribution in the spectrum of the hydroperoxide group, nonwithstanding the rather extensive approximations made in our calculations. It is quite likely that this is not a coincidence, but is a consequence of the preservation of the COOH group structure in various compounds and of the isolation of its potential and electric fields and of the applicability of the additive method to the COOH group.

It can be seen from Table 2 that the intensity of the 883 cm^{-1} band, which is assigned by the authors of ref. 1 to the vibration of the —O—O— bond, is determined by the dipole moments of the OH and OC bonds and possesses an observable magnitude only because in this vibration, a substantial role is also played by the coordinates γ and κ (see Table 1) leading to corresponding rotation of the two bonds. In the 835 cm^{-1} vibration the variation in the interplanar angle is much larger causing a greater absorption band intensity.

After the foregoing analysis of the absorption band intensities corresponding to the normal vibrations of the COOH group it is possible to approach the problem of finding out whether the absorption band intensities will be characteristic of the COOH group.

According to the general theory of the intensities of characteristic vibrations,[5] the necessary conditions for the intensity and polarization of a vibration to be characteristic, are: (1) the frequency and configuration of the vibration have to be completely characteristic; (2) the given group of atoms must be "electrically" independent; (3) the submatrix of the matrix T related to the given group of atoms must depend very little on the coordinates of the surrounding groups of atoms; (4) the characteristic vibration of the given group of atoms must not cause any rotation in space, of bonds in other parts of the molecule as a consequence of the principle of conservation of momentum.

In the case of the COOH group, the two vibrations having the frequencies 1322 cm^{-1} (variation in OOH angle)

and the valence vibration of the OH bond with frequency 3450 cm^{-1} are the two vibrations which best fulfill the requirements enumerated above:

These vibrations, to a very good degree of approximation, can be considered to depend only on the variations in the coordinates λ and q_{OH} respectively. The corresponding force constants will depend very little on the surroundings of the COOH group. During these vibrations, the shifts in the positions of the C, O_1, and O_2 atoms will be small and the variation in the rotation of the OH bond and in its length will be very characteristic, while the submatrices T_λ and T_{OH}, obtained from the inversion of the whole matrix T^{-1} for the COOH group and from the inversion of the corresponding diagonal elements of the matrix T^{-1}, will have almost the same magnitude (0.939 and 0.936 for q_{OH} and 0.765 and 0.793 for λ).

The intensities of the other vibrations of the COOH group will be much less characteristic and will be influenced by the environment. The 835 cm^{-1} vibration will be somewhat characteristic, while the intensity of the 588 cm^{-1} vibration will be the most sensitive to environment. The latter is explained by the fact that during the vibration the variation in the COO angle is very marked. This leads to a strong dependence of bond rotation in the vibration of this configuration, from the remainder of the molecule, both as a result of influence on the CO bond force constant and the COO angle and as a result of the great kinematic dependence of the motion of the COO atoms on the neighboring atoms. Apart from this, the submatrix T_γ is strongly dependent on the other coordinates. It is very likely that this is the explanation for the considerable divergence between the calculated and the experimental intensity of this vibration.

It must be noted that the method of evaluating intensity described above does not require extensive calculation, provided the shifts in the positions of the atoms are known, and, it seems to us, can be successfully applied to many molecules particularly if a collection of electro-optical parameters of different bonds will be worked out. Results obtained by our method can be of substantial help in the identification of absorption bands of polyatomic molecules.

In conclusion, the authors would like to express their appreciation to M. A. Kovner for kindly putting at their disposal the material necessary for the solution of the mechanical problem.

REFERENCES

1. M. A. Kovner, A. B. Karyakin, and A. P. Efimov, Opt. i Spektr. **8**, 128 (1960), Optics and Spectroscopy **8**, 64 (1960).
2. P. A. Giguere and A. Weingartshoffer, Can. J. Chem. **30**, 821 (1952).
3. L. A. Gribov, Doklady Akad. Nauk SSSR **127**, 788 (1959).
4. L. A. Gribov, Opt. i Spektr. **8**, 769 (1960), Optics and Spectroscopy **8**, 404 (1960).
5. L. A. Gribov, Opt. i Spektr. **9**, 176 (1960), Optics and Spectroscopy **9**, 93 (1960).

THE INFLUENCE OF THE REFRACTIVE INDEX ON THE TEMPERATURE SHIFT OF RAMAN BAND INTENSITIES

T. P. Tulub and Ya. S. Bobovich

Received 2 July 1960

If the temperature anomalies of the intensities of Raman bands in liquids (similar to the concentration effects[1,2]) are indeed due to the universal interaction of molecules (which manifests itself in the behavior of the internal field of the medium, characterized in particular by the derivative $\partial n/\partial t$ where n is the refractive index and t the temperature of the medium[3,4]), then the temperature shift of the band intensities obviously should depend on the state of aggregation of the substance, since the derivative $\partial n/\partial t$ in each case has a substantially different order of magnitude. For liquids and liquid solutions, on the other hand, a dependence of the effect on the magnitude of the derivative $\partial n/\partial t$ of the solvent should be revealed.

The above considerations have been verified by us experimentally. We measured the intensity of bands as a function of temperature in the spectra of solid and liquid (molten) sodium nitrate and stilbene. The first substance in the solid state was investigated in the form of a single crystal, formed into a cylinder. The heating of this sample was carried out in the same manner as described previously.[4] Since we had at our disposal only small crystals of stilbene, we used a special conical cell with a cylindrical, upright side-arm. The substance filled up the conical part of the cell and a saturated aqueous solution of NaCl was poured in. The latter served as an immersing and heat-conducting medium, at the same time blocking the sublimation of the crystals on the internal surface of the cone. The substance was heated by a helical electric coil wound on the cylindrical part of the cell. The temperature was measured with a thermocouple. The melting was also achieved by heating with the electric coil.

The results of the experiments performed are given in Table 1. As is seen from the Table, the intensity of the 180 cm^{-1} band in the spectrum of the crystalline nitrate increases with temperature, while the intensity of the 725 and 1070 cm^{-1} bands remains constant, which is in qualitative correspondence with the conclusions of the theory.

Table 1. Temperature Shift of Band Intensities in the Spectra of Solid and Molten Sodium Nitrate and Stilbene

Substance	State of aggregation	Temperature (°K) T_1	Temperature (°K) T_2	Band frequency (cm^{-1})	Ratio of the band intensities $\left(\frac{I_{T_2}}{I_{T_1}}\right)_{exp.}$	Ratio of the band intensities $\left(\frac{I_{T_2}}{I_{T_1}}\right)_{theor.}$
Sodium nitrate	Crystal	290	420	180	1.46	1.27
				725	1.00	1.05
				1070	1.00	1.02
				1385	0.84	~1.00
	Melt	640	825	700	0.87	1.05
				1050	0.80	1.02
				1350	1.25	~1.00
Stilbene	Crystals	290	375	1200	0.97	
				1325	0.96	
				1580	1.03	
				1630	1.07	
	Melt	415	525	1010	0.74	~1.00
				1200	0.77	
				1325	0.79	
				1580	0.84	
				1630	0.87	

At the same time the analogies of the last two bands in the spectrum of the melt sharply decrease in intensity with an increase in temperature. Only the 1350-1385 cm^{-1} band is unique; it behaves anomalously in the spectra of both the solid and liquid substances. The band intensities of crystalline stilbene, as follows from the theory, within the limits of experimental error do not change in the working temperature range. On the other hand, for the melt there is a characteristic distinct fall in all of the band intensities with temperature.

Water proved suitable as a solvent with a very low temperature coefficient of refractive index. For water, this quantity is approximately 9×10^{-5}, while for the majority of other liquids it is 5 to 10 times larger.[5,6] Table 2 gives data on the temperature shift of the band intensities in the spectra of solutions of zinc chloride and trichloracetic acid in water, dioxane, and acetic acid. It is easy to see that the spectra of the aqueous solutions are characterized by almost exact agreement with the theoretical ratios. To the best of our knowledge, a normal temperature shift of band intensities for substances in the liquid state has not been observed before. At the same time in the case of solutions of the same substance in dioxane and acetic acid (i.e., in solvents, differing by substantially larger coefficients $\partial n/\partial t$ from water), there appears an anomaly, completely analogous to that which has been repeatedly observed in a large number of liquids.

Thus, all of the results described above confirm the view expressed earlier by us[4] that for the temperature anomalies of Raman band intensities in liquids the temperature shift of the refractive index of the medium is mainly responsible.

Table 2. Temperature Shift of the Band Intensities in the Spectra of Solutions of Zinc Chloride and Trichloracetic Acid

Substance	Solvent	$\frac{dn}{dt} \cdot 10^{-4}$ of the solvent	Temperature (°K) T_1	Temperature (°K) T_2	Band frequency (cm^{-1})	Ratio of the band intensities $\left(\frac{I_{T_2}}{I_{T_1}}\right)_{exp.}$	Ratio of the band intensities $\left(\frac{I_{T_2}}{I_{T_1}}\right)_{theor.}$
Zinc chloride	Water . .	9 [5]	290	370	280	1.11	1.14
Trichloracetic acid	Water . .	9 [5]	290	365	180	1.24	1.18
					270	1.16	1.12
					430	1.09	1.07
	Dioxane .	~40 [6]	290	365	180	0.73	1.18
					270	0.89	1.12
					430	0.79	1.07
	Acetic acid	~40 [6]	290	370	180	0.94	1.18
					270	0.97	1.12
					430	0.96	1.07

REFERENCES

1. Ya. S. Bobovich and T. P. Tulub, Zhur. Eksptl. i Teoret. Fiz. **30**, 189 (1955).
2. V. M. Pivovarov and Ya. S. Bobovich, Opt. i Spektr. **3**, 134 (1957).
3. V. M. Pivovarov, Opt. i Spektr. **6**, 101 (1959), Optics and Spectroscopy **6**, 60 (1959).
4. Ya. S. Bobovich and T. P. Tulub, Opt. i Spektr. **6**, 566 (1959), Optics and Spectroscopy **6**, 362 (1959).
5. "Handbook of Experimental Physics," Vol. 19, p. 149. Leipzig, 1928.
6. A. Weissberger, E. Proskauer, J. Riddick, and E. Toops, "Organicheskie Rastvoriteli" (Organic Solvents). Izd. Inostrannoi Lit., Moscow, 1958.

CONDITIONS FOR SPECIFICITY OF THE POLARIZATION OF THE INFRARED BANDS OF POLYATOMIC MOLECULES

L. M. Sverdlov

Received 21 June 1960

In the previous work,[1] we introduced a quantitative criterion for specificity of the intensity of a molecular vibration for a group of coordinates, and we formulated four conditions for specificity of the intensity of infrared bands. We shall show* that the same conditions are also sufficient for specificity of the polarization of infrared bands.

*The symbols are the same as in the previous work.[1]

Let us select, within a molecule having n vibrational degrees of freedom, a group of n′ internal coordinates, S'_k, associated with the given structural element (the remaining coordinates are S''_k).

Let us denote by $\mathbf{p}$, $\mathbf{p}'$, and $\mathbf{p}''$, respectively, the dipole moments of the molecule of the given structural element and of the remaining part of the molecule:

$$\mathbf{p} = \mathbf{p}' + \mathbf{p}''. \qquad (1)$$

The polarization of the l-th normal vibration of the molecule is determined by the direction of the derivative of the dipole moment vector of the molecule with respect to the normal coordinate Q_l, i.e.:

$$\frac{\partial \mathbf{p}}{\partial Q_l} = \sum_{k=1}^{n} \frac{\partial p}{\partial S_k} L_{kl} = \sum_{k=1}^{n'} \frac{\partial \mathbf{p}'}{\partial S'_k} L'_{kl} + \sum_{k=n'+1}^{n} \frac{\partial \mathbf{p}'}{\partial S''_k} L''_{kl} + \sum_{k=1}^{n} \frac{\partial \mathbf{p}''}{\partial S_k} L_{kl}. \qquad (2)$$

The polarization of the l′-th normal vibration of the indicated group of coordinates, considered in isolation, is determined by the direction of the derivative of the dipole moment vector of the given structural element with respect to the normal coordinate $Q_{l'}$:

$$\frac{\partial \mathbf{p}'}{\partial Q_{l'}} = \sum_{k=1}^{n'} \frac{\partial \mathbf{p}'}{\partial S'_k} L_{kl'}. \qquad (3)$$

If the polarization of the l-th normal vibration of the molecule is close to the polarization of the l′-th normal vibration of the selected group of coordinates, we designate this normal vibration as specific with respect to polarization for the given group of coordinates. In the case of exact coincidence of the polarization of the l-th normal vibration of the molecule and the l′-th normal vibration

of the given group of coordinates, we designate such a normal vibration of the molecule as fully specific with respect to polarization for the given group of coordinates.

As a quantitative criterion for specificity of the polarization of a molecular vibration for a given group of coordinates, we may introduce some function of the angle between the vector $\partial p/\partial Q_1$ ($\equiv p_1$) and the vector $\partial p'/\partial Q_{1'}$ ($\equiv p'_{1'}$), for example, the tangent or the sine of the corresponding angle, i.e.,

$$\operatorname{tg}\left(\widehat{\frac{\partial p}{\partial Q_1}\frac{\partial p'}{\partial Q_{1'}}}\right)=\sqrt{\frac{(p_1)^2(p_{1'})^2-(p_1p_{1'})^2}{(p_1p_{1'})^2}}$$

$$=\sqrt{\frac{(p_1)^2(p_{1'})^2}{(p_1p_{1'})^2}-1} \qquad (4)$$

(Mayants[2] introduced a quantitative criterion for specificity of the form of a vibration in an entirely analogous way) or

$$\sin\left(\widehat{\frac{\partial p}{\partial Q_1}\frac{\partial p'}{\partial Q_{1'}}}\right)=\sqrt{\frac{(p_1)^2(p_{1'})^2-(p_1p_{1'})^2}{(p_1)^2(p_{1'})^2}}$$

$$=\sqrt{1-\frac{(p_1p_{1'})^2}{(p_1)^2(p_{1'})^2}}. \qquad (5)$$

We shall designate the quantities (4) and (5) respectively as the coefficients of nonspecificity of the polarization of a vibration for the given group of coordinates, δ_t and δ_s. The ambiguity associated with the presence of n' different δ_t's (δ_s's), if the group consists of n' coordinates, may be eliminated by choosing that δ_t (δ_s) which is smallest in absolute value. In the case of full specificity of the polarization, $\delta_t = \delta_s = 0$.

To clarify the conditions for specificity of the polarization of the infrared band corresponding to the l-th normal vibration of the molecule, let us for example write down formula (5) for δ_s in expanded form. Thus we obtain

$$\delta_s=\sqrt{1-\frac{\left[\left(\sum_{k=1}^{n'}\frac{\partial p'}{\partial S'_k}L'_{kl}+\sum_{k=1}^{n'}\frac{\partial p''}{\partial S'_k}L'_{kl}+\sum_{k=n'+1}^{n}\frac{\partial p}{\partial S''_k}L''_{kl}\right)\sum_{k=1}^{n}\frac{\partial p'}{\partial S'_k}L_{kl'}\right]^2}{\left(\sum_{k=1}^{n'}\frac{\partial p'}{\partial S'_k}L'_{kl}+\sum_{k=1}^{n'}\frac{\partial p''}{\partial S'_k}L'_{kl}+\sum_{k=n'+1}^{n}\frac{\partial p}{\partial S''_k}L''_{kl}\right)^2\left(\sum_{k=1}^{n}\frac{\partial p'}{\partial S'_k}L_{kl'}\right)^2}}. \qquad (6)$$

From the expression obtained it can be seen that, in order for δ_s to have a minimum value, we need fulfillment of the same four conditions as were necessary for specificity of the intensity.[1] Let us recall briefly what these conditions consist of.

1. The l-th normal vibration of the molecule must be specific in frequency and form for the given group of coordinates, i.e.,

$$L'_{kl}\simeq L_{kl'}\ (k=1, 2, \ldots n');\ L''_{kl}\simeq 0\ \ (k=n'+1, \ldots n). \qquad (7)$$

2.
$$\left|\frac{\partial p''}{\partial S''_k}\right| \ll \left|\frac{\partial p'}{\partial S'_k}\right|. \qquad (8)$$

3.
$$\left|\frac{\partial p}{\partial S''_k}L''_{kl}\right|\approx 0. \qquad (9)$$

4. The quantities $\partial p'/\partial S'_k$ must not change significantly on going from one molecule to another.

Thus, if some normal vibration is specific with respect to intensity, it will necessarily also be specific with respect to its polarization. The converse, however, is not always true; namely, the normal vibrations of certain classes of symmetrical molecules will possess full specificity of polarization merely in consequence of their symmetry. For example, for all the totally symmetric vibrations of molecules of the methyl halide type CH_3Z, the vectors $\partial p/\partial S_k^{A_1}$ and $\partial p/\partial S_k^{A_1}$ will be directed parallel to the third-order symmetry axis, and for all the degenerate vibrations the vectors $\partial p/\partial S_k^E$ and $\partial p/\partial Q_i^E$ are perpendicular to the third-order symmetry axis. In particular, this holds for the C—H valence vibrations $\nu_1^{A_1}$ and ν_4^E of the methyl halides CH_3Cl, CH_3Br, and CH_3I. On the other hand, in the series just cited, specificity of the intensities of the infrared bands ν_1 and ν_4 is lacking.[1,3]

Analogously, the nonplanar vibrations of planar molecules of the type of ethylene, benzene, and others are always polarized in such a way that the vectors $\partial p/\partial Q_l$ are perpendicular to the plane of the molecule. For all the planar vibrations, the vectors $\partial p/\partial Q_l$ will be parallel to the plane of the molecule.

As an example,[1,4,5] let us consider the antisymmetric valence vibration of ethylene $\nu_9^{B_{2u}}$ (C—H) = 3105 cm^{-1}. This vibration is specific in frequency and form for the group of coordinates which includes changes in the lengths of all four C—H bonds. The coefficient of nonspecificity of frequency,[2] α, and the coefficient of nonspecificity of form of the vibration in the narrow sense,[2] β_γ, are equal to zero. The vector $\partial p/\partial Q_9^{B_{2u}}$ is directed perpendicular to the C=C axis, $I_9 = 112.4$ cm^{-1}/cm-atm.

On going over to the group of coordinates consisting of changes in the lengths of three C—H bonds (q_2, q_3, and q_4), specificity of the frequency is not lost ($\nu = 3103$ cm^{-1}, $\alpha \doteq 0$), but specificity of the form is disrupted ($\beta_\gamma = 0.66$), in consequence of which the first condition for specificity of the intensity and the polarization is not fulfilled. Therefore the intensity is markedly lowered ($I_9 = 82.2$ cm^{-1}/cm-atm). The coefficient of nonspecificity of intensity $\gamma = 0.37$. The polarization of the vibration also changes—the vector $\partial p/\partial Q_9$ will no longer be perpendicular to the C=C axis. The coefficients of nonspecificity of polarization, δ_t and δ_s, have the following values:

$$\beta_\tau=\left(\frac{\frac{\partial p_{z_1}}{\partial Q_9}}{\frac{\partial p}{\partial Q_9}}\right)=0.13;\qquad \delta_c=\left(\frac{\frac{\partial p_{z_2}}{\partial Q_9}}{\frac{\partial p}{\partial Q_9}}\right)=0.129.$$

The angle between the vector $\partial p/\partial Q_9$ and the perpendicular to the C=C axis equals 7°25'.

On going over to the group of coordinates consisting of changes in the lengths of two C—H bonds (q_3 and q_4), the specificity of frequency is not lost ($\nu_9 = 3095$ cm^{-1}, $\alpha = 0.01$), but the specificity of form is disrupted ($\beta_\gamma = 0.96$). Therefore, the first condition for specificity of the intensity (and of the polarization) is not fulfilled. In consequence of this, the intensity diminishes sharply ($I_9 = 58.7$ cm^{-1}/cm-atm). The coefficient of nonspecificity of intensity $\gamma = 0.91$. However, the polarization of the vibration does not change—the vector $\partial p/\partial Q_9$ will, for reasons of symmetry, be directed perpendicular to the C=C axis as before.

Thus the conditions formulated above for specificity of the polarization are sufficient but not necessary.

In Gribov's work,[6] the conclusion was reached that "a vibration can be specific with respect to polarization only when it is specific with respect to polarization only when it is specific with respect to form." In a later work,[7] Gribov asserts that "this conclusion has an approximate character." From the foregoing it follows that, in the general case, Gribov's quoted conclusion will not be valid.

REFERENCES

1. L. M. Sverdlov, Opt. i Spektr. 9, 40 (1960), Optics and Spectroscopy 9, 21 (1960).
2. L. S. Mayants, Trudy Fiz. Inst. Akad. Nauk SSSR 5, 63 (1950).
3. L. M. Sverdlov, Opt. i Spektr. 6, 729 (1959), Optics and Spectroscopy 6, 477 (1959).
4. L. M. Sverdlov, Opt. i Spektr. 8, 594 (1960), Optics and Spectroscopy 8, 316 (1960).
5. L. M. Sverdlov and N. L. Pakhomova, Zhur. Eksptl. i Teoret. Fiz. 26, 64 (1954).
6. L. A. Gribov, Doklady Akad. Nauk SSSR 127, 788 (1959).
7. L. A. Gribov, Opt. i Spektr. 8, 769 (1960), Optics and Spectroscopy 8, 404 (1960).

THE THEORY OF VIBRATION OF FINITE CRYSTAL LATTICES

O. P. Girin

Received 21 June 1960

The method of calculating vibration spectra which was worked out for molecules[1] can be applied to crystals if the latter are considered as gigantic molecules. Born's theory[2] can be used to calculate the spectra of large crystals, but it leads to erroneous results for structures containing a small number of unit cells. Nevertheless, the necessity of calculating the spectra of such structures often arises in the interpretation of the spectra of some compounds (e.g., hydrocarbons and glasses). The present paper presents a method for obtaining accurate values of the frequencies and amplitudes of vibration associated with structures possessing translational symmetry and any number of elementary cells (down to one).

Consider, for simplicity, the valence vibrations of a linear chain consisting of $N+1$ similar particles bound together by identical quasi-elastic forces. The bonds will be numbered symmetrically with respect to the central bond. Thus, for both even and odd values of N the number of end bonds will be $\pm(N-1)/2$; for even N, this number will be a fraction.

The system of equations of motion, constructed by the method of El'yashevich,[1] has the form

$$\left.\begin{aligned} -\frac{k}{m}q_{s-1}+\left(\frac{2k}{m}-\omega^2\right)q_s-\frac{k}{m}q_{s+1}=0,\\ -\left(\frac{N-1}{2}\right)\leqslant s\leqslant\left(\frac{N-1}{2}\right). \end{aligned}\right\} \tag{1}$$

where q_s is the vibrational amplitude of the s-th bond; k is the force constant and m is the mass of the particle. The substitution

$$q_s=\alpha\varepsilon^{i\frac{2\pi a}{\lambda}s}, \tag{2}$$

(where α is a constant, a is a dimension of the cell, in this case, the bond length, and λ is a parameter) leads to the disappearance of any dependence on the number of cells s. If the condition

$$q\left(\frac{s+1}{s}\right)=q-\left(\frac{s+1}{s}\right)=0 \tag{3}$$

holds, then instead of the system of equations (1), consisting of N different equations, one obtains N similar equations, any one of which leads to the allowed vibration frequencies

$$\omega=2\sqrt{\frac{k}{m}}\sin\frac{\pi a}{\lambda}. \tag{4}$$

The value of the undetermined parameter λ, which represents the wavelength of the vibration propagated through the lattice, is found from condition (3), whose physical meaning is that the end particles are not acted upon by any external forces. This is generally implied in calculating spectra of molecules without being specially stipulated. Conditions (3) are naturally referred to as the "free end" conditions.

From (2) and (3) we obtain

$$\frac{2\pi a}{\lambda}=\frac{j\pi}{N+1};\quad j=1,2,\ldots N. \tag{5}$$

In this simplest case, one can arrive at the exact solution of the secular equations corresponding to system (1) by direct evaluation of the determinant, without recourse to condition (3). The exact solution obtained in this way agrees with (4) when (5) is taken into account. Thus conditions (3), in contrast to the cyclic conditions of Born,[2] give an exact solution of the problem for any N down to $N=1$, i.e., for a diatomic molecule. This is natural, since conditions (3) separate out from the infinite system of equations for which substitution (2) is valid, a finite system of equations under a condition which is almost always satisfied; namely, that the interaction coefficients of the degrees of freedom be equal to zero, even if they are separated by only a single cell. Note that in the papers by Fermi,[3] Born,[4] and others it was erroneously asserted that a linear chain has a doubly degenerate vibration frequency (this came about because the cyclic conditions are incorrect).

The result which was obtained can easily be generalized to the more complicated case of n degrees of freedom in the unit cell. In this case, instead of (2) we have

$$q_s^t=\alpha_t\varepsilon^{i\frac{2\pi a}{\lambda}s};\quad t=1,2,\ldots n;\quad s=1,2,\ldots N. \tag{6}$$

Here the exponential factor takes into account the translational symmetry with respect to the cells (for it is only when such symmetry must be taken into account that one would consider introducing this factor) and α_t gives the phase of the vibration of the bonds inside the cell. The form of the "free end" condition remains as before, i.e., (3) and (5).

One can proceed in a similar fashion in the case of two- and three-dimensional lattices. Thus, for example, for a three-dimensional lattice, the vibration amplitude assumes the form

$$q_{s,p,r}^t=\alpha_t\varepsilon^{i\left(\frac{2\pi a}{\lambda_x}s+\frac{2\pi b}{\lambda_y}p+\frac{2\pi c}{\lambda_z}r\right)}.$$

where t takes values corresponding to the number of degrees of freedom in the cells, and s, p, and r are the running numbers of cells in the three directions which determine the translational symmetry of the lattice. The "free end" conditions lead to the relations

$$\frac{2\pi a}{\lambda_s} = \frac{\pi m_s}{N_s+1}; \quad \frac{2\pi b}{\lambda_p} = \frac{\pi m_p}{N_p+1}; \quad \frac{2\pi d}{\lambda_r} = \frac{\pi m_r}{N_r+1};$$

$$m_s = 1, 2, \ldots N_s; \quad m_p = 1, 2, \ldots N_p; \quad m_r = 1, 2, \ldots N_r,$$

where N_s, N_p, and N_r are the numbers of cells in the three directions.

When the frequencies of the normal vibrations have been evaluated, one can, by using the system of equations obtained for α_{ts}, determine the form of the normal vibrations. Consequently, the problem of calculating the frequencies and vibration patterns of a system which has a large number of degrees of freedom and possesses translational symmetry can be reduced to solving the problem of vibrations of the elementary cell. For the latter case all the methods worked out for molecules[1] can be used.

The frequency values found in this way will be functions of λ. It is readily seen that if one examines the functional relationship $\omega = f(\lambda)$, one can study the changes in frequency associated with changes in lattice dimensions. For $N_j = 1$, $m_j = 1$ (j = s, p, r), one obtains the frequencies of a single isolated cell. For $N_j = 2$, every frequency splits up (in particular cases, there can be degeneracy) into two values corresponding to $m_j = 1$ and 2, etc. This makes it possible to determine which frequencies are characteristic of the cell; i.e., which ones do not change much as λ changes (or when the dimensions of the lattice are changed, which is the same thing).

As is well known, in infrared and Raman spectra, the only lattice frequencies which are active are the limiting frequencies corresponding to the maximum wavelength λ of the vibrations propagated through the lattice.[2,3] It is easy to see that in the case of a lattice of small dimensions, when N_j is small, besides this limiting frequency, frequencies corresponding to other values of λ are also active. In spite of this, the most intense frequencies will be those which correspond to the largest value of λ in each branch.

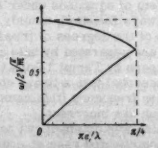

As an example, let us determine the intensity of bonds in the infrared spectra of linear chains, consisting of 6 and 18 oppositely charged particles. Although the frequencies of this chain are the same as the atomic frequencies, there are two bonds in a unit cell, and therefore two frequency branches, shown schematically in the Figure.

Knowing the total electric moment of the chain and the relationship between natural and normal coordinates, it is possible to calculate the squares of the derivatives of the moment with respect to the normal coordinates, which quantity determines the line intensities. The Table shows the relative values of the frequencies and intensities of the lines. It is easily seen that the intensities of the lines in the optical branch decrease with decreasing λ. For N = 17, the value of the limiting frequency is practically the same as the value for infinite lattice. Consequently, one can detect changes in dimensions of small structures from the frequency shift if the number of unit cells is less than twenty.

Number of particles in the chain		$N = 5$			$N = 17$				
Spectral characteristics	λ	12a	6a	4a	36a	18a	12a	9a	7.2a
Optical branch	$\omega / 2\sqrt{k/m}$	0.966	0.866	0.707	0.996	0.985	0.968	0.940	0.906
	I/I_{max}	1	0	0.134	1	0	0.113	0	0.043
Acoustic branch	$\omega / 2\sqrt{k/m}$	0.259	0.500	—	0.087	0.174	0.259	0.342	0.423
	I/I_{max}	0.072	0	—	0.008	0	0.008	0	0.009

The translational symmetry leads to the selection rule that of all the frequencies in each branch, only the limiting frequency is active if $N \geq 20$. The relative intensities of the limiting frequencies of the different branches are determined by the cell symmetry.

REFERENCES

1. M. V. Vol'kenshtein, M. E. El'yashevich, and B. I. Stepanov, "Molecular Vibrations," Vols. 1, 2. Gosudarst. Izd. Tekh.-Teoret. Lit., Moscow-Leningrad, 1949.
2. M. Born and Huan Kun', "Dynamic Theory of Crystal Lattices." Izd. Inostrannoi Lit., Moscow, 1958.
3. E. Fermi, "Molecules and Crystals." Izd. Inostrannoi Lit., Moscow, 1947.
4. M. Born and M. Goeppert-Mayer, "Theory of Solids." ONTI (United Scientific and Technical Press), Moscow, 1938.
5. E. F. Gross, P. P. Pavinskii, and A. I. Stekhanov, Uspekhi Fiz. Nauk **43**, 536 (1951).

THE LUMINESCENCE OF NONACTIVATED KI CRYSTALS

N. N Vasil'eva and Z. L. Morgenshtern

Received 24 June 1960

An emission band, located in the near ultraviolet region, is observed at liquid nitrogen temperature in the luminescence spectra of NaI[1] and CsI.[2] This band is easily excited by γ- and α-rays, but no reliable measurements of the photoexcitation spectrum have been made as yet. (This spectrum is probably located in the fundamental absorption band of the crystals). From all available data, it can be apparently concluded that this emission band must be attributed to the pure, undisturbed lattice.

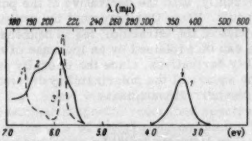

Emission (curve 1) and photoexcitation (curve 2) spectra of a KI crystal and the absorption spectrum (curve 3) of an evaporated KI layer at the boiling point of liquid nitrogen. The crystal had been grown from a solution; spectrum 3 is taken from ref. 5.

It is natural to expect that a similar emission band will also be present in the spectra of KI crystals. There are indications in the paper of Teegarden[3] that nonactivated KI crystals luminesce at low temperature, but traces of Tl present in the samples investigated prevented him from making a reliable identification of this emission band.

We have grown completely Tl-free KI crystals from solution. When these crystals were excited with γ-rays from Co^{60} at liquid nitrogen temperature, an emission band was observed in the near ultraviolet. Its maximum is at 370 mμ; its halfwidth is 0.48 ev (see Figure, curve 1); its decay is exponential, with $\tau = 0.9$ μsec. The photoexcitation region of this luminescence is in the intrinsic absorption band of this crystal and approximately corresponds to the first absorption band of KI at liquid nitrogen temperature (curves 2 and 3).[5] It is interesting to note that in the region where the second absorption band increases ($\lambda < 193$ mμ), the luminescence yield decreases.

This band also appears at low temperatures in spectra of KI crystals grown from the melt and containing traces of Tl, but the band overlaps the Tl emission band ($\lambda_{max} = 406$ mμ). The interaction effects of this band with activator bands can be apparently better studied on KI crystals activated with In, since the luminescence of the latter (in KI) is located in a longer wavelength region of the spectrum.[6]

Like the corresponding emission bands in NaI and CsI crystal spectra, the KI emission band investigated by us can be attributed to excitation radiation, although further investigation is required to definitely establish its nature.

The authors are grateful to M. D. Galanin for his interest in this work and for the measurements of τ, and to N. V. Kostina for her help with the work.

REFERENCES

1. W. Van Sciver, I.R.E. Trans. on Nuclear Sci. **NS-3**, No. 4, 39 (1957).
2. H. Enz and J. Rossel, Helv. Phys. Acta **31**, 25, 1958; Z. L. Morgenshtern, Opt. i Spektr. **8**, 672 (1960); Optics and Spectroscopy **8**, 355 (1960).
3. K. I. Teegarden, Phys. Rev. **105**, 1222, 1957.
4. Z. L. Morgenshtern, Opt. i Spektr. **7**, 231 (1959), Optics and Spectroscopy **7**, 146 (1959).
5. H. Fesefeldt, Z. Physik **64**, 623 (1930).
6. Yu. N. Zhvanko, Z. L. Morgenshtern, and L. M. Shamovskii, Opt. i Spektr. **2**, 821 (1957). A. A. Dunina, Z. L. Morgenshtern, and L. M. Shamovskii, Opt. i Spektr. **4**, 105 (1958).

THE INTENSITIES OF RAMAN LINES OF MIXTURES OF CCl_4, $SiCl_4$, AND $GeCl_4$ WITH BENZENE; PARAXYLENE; AND CYCLOHEXANE

Yu. G. Borok'ko and Ya. K. Syrkin

Received 5 July 1960

Different authors[1,2] have examined the intermolecular interactions in the CCl_4-benzene system. Ferguson[2] observed an intensity decrease for the infrared absorption bands of benzene in a mixture with CCl_4, which he ascribed to the formation of a benzene-CCl_4 complex. It will be of interest to investigate the Raman spectra of the CCl_4-benzene system, and also the analogous systems with $SiCl_4$ and $GeCl_4$.

We studied the concentration dependence of the frequencies and intensities of Raman lines in mixtures, containing as one component CCl_4, $SiCl_4$, or $GeCl_4$, and as the second component benzene, paraxylene, or cyclohexane. All of the measurements were made on an ISP-51 spectrograph with photoelectric recording. To exclude errors connected with the differences in refractive indexes and densities of the compounds investigated, an internal standard was introduced. For this we chose cyclohexane which, as experiments indicate, essentially does not interact either with the tetrahalides or with benzene and paraxylene.

The frequencies of all of the lines remained unchanged within experimental error (±2 cm^{-1}), indicating that the symmetry of the tetrachlorides (T_d) and of the benzene is maintained.

The results of the measurements of the integrated intensities $I = \int I_\nu d\nu$ are presented in Table 1. The intensities are expressed in an arbitrary scale, in which the intensity of the Raman line of the individual compound at t = 30°C, relative to one mole, is taken as 100.

As seen from the data presented, there is a significant increase in the intensities of the lines corresponding to the completely symmetrical stretching vibrations of the tetrachlorides in benzene and paraxylene. The intermolecular interactions affect the line intensities but not the vibrational frequencies. This raises the question of the character of the interaction of the nonpolar tetrahalide molecules with benzene and paraxylene. We can hardly attribute all of the effect to the common nonspecific dispersion interaction.[2,3] To the dispersion interaction in the given case can be added a chemical interaction of the donor-acceptor type. The benzene acts as a donor of its π-electrons, and the chlorine atom as an acceptor through its unfilled 3d orbitals. Such an interaction should lead to some shift in charge from the benzene to the tetrachloride, influencing the magnitude of the polarizability, and, consequently, also the derivative of the polarizability of the molecule. From this argument the growth of the line intensities of the tetrachlorides in benzene and paraxylene can be explained by an increase of the bond polarizability derivatives, since the intensity is proportional to the square of the polarizability derivative with respect to the normal coordinate

$$I \sim \left(\frac{\partial \gamma}{\partial Q}\right)^2.$$

Since the tetrahedral symmetry of the chlorides in the mixtures is maintained, we can, on the basis of the calculations of Long and Woodward,[4] find the relative values of the polarizability derivatives of the bonds C—Cl, Si—Cl, and Ge—Cl in the individual substances, and also in benzene from the formula

$$\frac{I_2}{I_1} = \frac{C_2}{C_1}\left(\frac{\nu_0 - \nu_2}{\nu_0 - \nu_1}\right)^4 \frac{\mu_1\nu_1}{\mu_2\nu_2} \frac{1 - e^{-\frac{h\nu_1}{kT}}}{1 - e^{-\frac{h\nu_2}{kT}}} \left(\frac{a_2'}{a_1'}\right)^2,$$

where I_1 and I_2 are the intensities of the lines corresponding to the completely symmetrical stretching vibrations, C_1 and C_2 are the molar concentrations, μ_1 and μ_2 are the reduced masses, a_1' and a_2' are the polarizabilities, ν_0 is the frequency of the exciting light, and ν_1 and ν_2 are the frequencies of the Raman lines.

In Table 2 are presented the results of the measurements of the line intensities, expressed on a cyclohexane scale, for the tetrahalides both pure and in benzene with extrapolation to infinite dilution. The relative values of the magnitude of the polarizabilities, computed from the intensities, are compared with the data of ref. 4 and with the refractions of the atomic groups.[5] Comparison of the values of the polarizabilities of the pure compounds with the data for their solutions in benzene shows that in benzene the polarizability derivatives of the tetrachlorides are increased approximately by 30%. Finally, it should be noted that the shift of the polarizability derivatives, calculated from the spectral data of the present work, agrees with the shift of the refraction of the atomic groups.

Table 1

CCl_4 + benzene				$SiCl_4$ + benzene				$SiCl_4$ + paraxylene		Benzene + cyclohexane	
C_1	I_{459}	C_2	I_{992}	C_1	I_{491}	C_2	I_{992}	C_1	I_{992}	C_1	I_{992}
10.3	100	11.2	100	8.7	100	11.2	100	8.7	100	11.2	100
7.5	120	7.8	91	6.5	120	7.8	92	5.2	130	6.1	98
6.2	134	6.1	86	4.7	143	6.3	86	3.0	144	4.5	95
4.4	144	4.5	83	3.9	150	4.8	83	1.8	156	2.7	86
3.2	146	2.7	78	2.5	160	2.8	74	0.7	174	1.5	82
2.6	153	0.8	73	1.7	170	0.7	65			0.8	75
1.5	161			0.7	185						
0.8	171										

$GeCl_4$ + benzene				$GeCl_4$ + paraxylene						
C_1	I_{459}	C_2	I_{992}	C_1	I_{459}	C_1	I_{992}	I_{1155}	I_{1385}	I_{1575}
8.75	100	11.2	100	8.75	100	8.1	100	100	100	100
7.5	105	8.1	90	7.0	116	6.8	106	96	91	100
6.5	117	5.3	81	6.1	124	5.3	114	93	85	102
5.8	118	3.2	73	5.2	130	3.6	124	91	77	103
4.5	130	2.05	70	4.05	138	2.4	132	88	70	98
3.2	139	1.2	64	3.1	150	1.8	134	84	67	105
2.7	142			2.2	155	0.6	142	83	64	101
1.8	152			1.4	164					
1.4	156			0.8	173					
0.6	160									

In the table are shown the concentrations C_1 and C_2 of the first and second components, respectively, of the system investigated (in moles/liter). The line intensities are given in an arbitrary scale (cf. text).

Table 2

Molecule	ν (cm^{-1})	$I_{individ.}$	$I_{individ.}^{rel}$	$I_{individ.}^{rel}$ (from ref. 4)	$I_{in\ benzene}$	$a_{individ.}^{2}$	$a_{individ.}^{2}$ (from ref. 4)	$a_{in\ benzene}^{2}$	Refraction of atom (from ref. 5)
CCl_4	459	1130	1	1	1900	1	1	1.3	1
$SiCl_4$	434	1700	1.5	1	3200	1.17	0.96	1.5	1.1
$GeCl_4$	397	2500	2.2	3.2	4100	1.34	1.8	1.7	1.22

*The value for pure CCl_4 is taken as 1.

The intensity of the benzene line with frequency $\Delta\nu$ = 992 cm^{-1}, corresponding to the symmetrical breathing vibration of the ring, decreases in the tetrachlorides almost the same amount as in cyclohexane. This testifies, first to the insensitivity of the intensity of this line to the interaction of benzene with a tetrachloride, and second to the fact that benzene associates with itself.[5,6] In the case of the system paraxylene-cyclohexane the intensities of the paraxylene lines do not depend on concentration. An analogous result is obtained for the systems CCl_4, $SiCl_4$, and $GeCl_4$ with cyclohexane.

Preliminary experiments on a study of the system $TiCl_4$-benzene have shown that the line intensities of $TiCl_4$ and benzene change, but the frequencies do not.

REFERENCES

1. J. R. Goates, R. J. Sullivan, and J. P. Ott, J. Phys. Chem. **63**, 589 (1959).
2. E. E. Ferguson, J. Chem. Phys. **26**, 1265 (1957).
3. C. A. Coulson and P. L. Davies, Trans. Faraday Soc. **48**, 777 (1952).
4. L. A. Woodward and D. A. Long, Trans. Faraday Soc. **45**, 1131 (1949).
5. C. P. Smyth, "Dielectric Behavior and Structure." New York, 1955.
6. K. E. Schuler, J. Chem. Phys. **21**, 765 (1953).

THEORY OF THE HYPERFINE STRUCTURE OF ELECTRON PARAMAGNETIC RESONANCE SPECTRA

I. V. Aleksandrov

Received 6 July 1960

In ref. 1 a method was proposed for determining the form of the nuclear magnetic resonance spectrum when the motion of the pair of nuclei responsible for the resonance is described by an effective potential well with two minima. It was assumed that the height of the barrier (and consequently, the magnitude of the splitting Γ of the energy levels in the well) is arbitrary. One can also apply the method of calculation used in ref. 1 for determination of the hyperfine structure (hfs) in EPR when the ground state of the unpaired electron is nearly degenerate because of the symmetry conditions (as, for example, in free radicals consisting of two benzene rings joined by several CH_2 groups).

The Hamiltonian describing the system has the form

$$\mathcal{H} = \mathcal{H}_m - g\beta H_0 S_z + W,$$

where $\mathcal{H}_m$ describes the motion of the unpaired electron in the field of the nuclei, the second term determines the interaction of the electron with the magnetic field H_0, and W represents the interaction of the electron with the magnetic moments of the nuclei.

Provided that the spectrum of $\mathcal{H}_m$ consists of two energy levels E_1 and E_2 ($E_1 - E_2 = 2\Gamma$) and all the remaining electron levels are sufficiently high, one can represent the operator W in the form $W = W_I + W_{II}$, where W_I and W_{II} are interaction operators appreciable only near nuclei (or group of nuclei) I and II, respectively; and the secular equation breaks down into second order equations (one assumes that $W \ll g\beta H_0 S_z$). Solution of the equation shows that in the general case for two equivalent nuclei with spin I (group of nuclei with total spin I) one observes lines in the EPR spectrum at frequencies

$$\omega = A(M_1 + M_2)$$

and

$$\omega = A(M_1 + M_2) \pm 2\sqrt{\Gamma^2 + \tfrac{1}{4}A^2(M_1 - M_2)^2}\,,$$

where $M_1 = -I, -(I-1), \cdots, +I$ (analogously for M_2), and 2A is the hyperfine splitting for $\Gamma \to 0$, i.e., for an infinite number of CH_2 links in the example cited above. Calculation of the intensities of the lines (performed by the same method as in ref. 1) shows that in the limiting case, $\Gamma \gg A$, one observes $4I + 1$ lines in the spectrum separated from one another by the amount A. In the opposite case ($\Gamma \ll A$) the spectrum consists of $2I + 1$ lines with a splitting equal 2A (the total splitting in both cases is the same).

Thus, at first sight the case $\Gamma \gg A$ corresponds to complete delocalization of the electron between positions I and II, and at the same time the second case ($\Gamma \ll A$) means a localization of the electron at one of these positions. However, such an interpretation of the results is wrong. Actually, by solution of the secular equation we obtained a series of degenerate states. It is easy to show that symmetrization relative to the (equivalent) nuclei of the wave functions corresponding to these states leads to a symmetrical distribution of the electron density between positions I and II. Hence, in all cases the electron is completely delocalized. This result follows simply from the fact that the total Hamiltonian is symmetrical relative to a transposition of the particles of groups I and II.

Finally, let us notice that the total second moment of the spectrum always remains constant (does not depend on Γ) in agreement with the general theory.[2]

REFERENCES

1. I. V. Aleksandrov, Doklady Akad. Nauk SSSR **133**, 1057 (1960).
2. G. Pake, "Solid State Physics," Vol. 2, p. 1. Academic Press, New York, 1956.

THE RELATIVE OSCILLATOR STRENGTHS OF CERTAIN LINES OF ZnI AND CdI

N. P. Penkin and T. P. Red'ko

Received 7 July 1960

The relative oscillator strengths of 30 ZnI and CdI lines having the levels $^3P_{0,1,2}$ as their lower levels were determined in this investigation. The f-values of these lines have been measured previously[1,2] by the line emission method. A carbon arc spectrum was used for excitation. Even though the intensities of the spectral lines are measured correctly (reabsorption taken into account or strongly reduced) a source of considerable error still remains in the emission method. This source of error is associated with the determination of the arc plasma temperature, which must be known in order to calculate the distribution of atoms with respect to energy levels. The necessity of determining the relative populations of the $^3P_{0,1,2}$ levels was eliminated in the present investigation by simultaneous application of A. S. Rozhdestvenskii's "hook" method and the line emission method.

The relative values of the f-numbers of lines having the same lower level were determined by the well-known "hook" method. A column of excited atoms was produced in a quartz discharge tube filled with zinc or cadmium vapor and an inert gas (argon or neon). The discharge tube had external electrodes; power was supplied by a high frequency generator (ν = 190 kc) produced in the experimental shop of the Scientific Research Institute of Leningrad University. The line emission method was used to relate the f-numbers of all the lines ending on the $^3P_{0,1,2}$ levels to one scale. The relative intensities of the components of the visible triplets of ZnI and CdI ($^3S_1 - {}^3P_{0,1,2}$) were measured by this method. The experimental apparatus used for this consisted of an ISP-51 spectrograph and an FEP-1 photoelectric attachment. The light source was a quartz bulb filled with zinc or cadmium vapor and argon. The discharge in the bulb was excited from a VG-3 high frequency generator. Apertures in the central part of the bulb defined a homogeneous radiating column 80 mm long. The measured intensities were corrected for reabsorption by a tube and mirror method. We used Ladenburg's[3] tables, since the work was conducted at a low vapor pressure of metal ($p < 10^{-3}$ mm Hg) and added gas, and with low-power discharges, so that the lines could be considered to have Doppler profiles. The spectral sensitivity of the photomultiplier tube and the transmission characteristics of the whole optical system were also taken into account in the treatment of the results.

The Tables show the results of our measurements (f_{data}), along with data obtained by Schuttevaer,[1] Larche,[4] and Hengstum[2] using the line emission method ($f_{em.}$), and also theoretical values of the quantity $gf_{theor.}$, calculated on the assumption that L-S coupling exists in atoms of zinc and cadmium. Our values for $gf_{exp.}$ are inserted in the next-to-last column of the table. Each value of f_{data} shown in the table was obtained by averaging measurements on 25-45 photographs. The standard deviation does not exceed 7%.

It was not possible to obtain easily measurable "hooks" from all of the lines of the diffuse series. Such lines are marked in the table by asterisks.

The data in the table indicate good agreement between the calculated and measured values of gf for the zinc lines. This implies the existence of L-S coupling in the zinc atom. The f-values of the lines designated by asterisks were determined on the basis of the theoretical ratios of oscillator strengths in multiplets. For this reason they cannot, of course, be considered as independently measured. L-S coupling works out less well for the cadmium atom than for the zinc atom. However, $gf_{exp.}$ agrees satisfactorily with $gf_{theor.}$ for multiplets of the diffuse series. This result is also confirmed by Hengstum's data. For this reason we assumed the ratio of f-values to be equal to the theoretical ratios for the four CdI lines marked with asterisks.

Tables of the Relative Oscillator Strengths of Certain ZnI and CdI Lines

Zn I

λ	Transition	j–j	f_{data}	$f_{em.}$[1]	$gf_{exp.}$	$gf_{theor.}$
4810.53	$4^3P - 5^3S$	2—1	1.08	1.07	540	543
4722.16		1—1	1.06	1.03	318	308
4680.14		0—1	1.00	1.00	100	100
3345.93 *	$4^3P - 4^3D$	2—1	0.03	0.04	1.2	1.2
3345.57 *		2—2	0.51	0.64	17.9	17.9
3345.02		2—3	2.85	3.00	100	100
3302.94		1—1	0.75	0.98	15.8	17.4
3302.59		1—2	2.49	3.16	52.4	52.2
3282.33		0—1	2.96	4.41	20.8	22.9
280 .17 *	$4^3P - 5^3D$	2—1	0.009	0.01	1.2	1.2
2801.06 *		2—2	0.13	0.16	17.6	17.9
2800.67		2—3	0.74	0.87	100	100
2770.98 *		1—1	0.22	0.27	17.8	17.5
2770.67		1—2	0.66	0.80	53.5	52.5
2756.45		0—1	0.83	0.99	25.1	23.0

Cd I

λ	Transition	j–j	f_{data}	$f_{em.}$[3]	$f_{em.}$[4]	$gf_{exp.}$	$gf_{theor.}$
5085.82	$5^3P - 6^3S$	2—1	1.03	1.00	0.86	515	500
4799.92		1—1	1.07	1.23	0.88	321	316
4678.16		0—1	1.00	1.00	1.00	100	100
3614.45 *	$5^3P - 5^3D$	2—1	0.03	0.04	—	1.2	1.2
3612.80		2—2	0.53	0.49	—	19.9	17.9
3610.51		2—3	2.86	3.04	—	100	100
3467.66		1—1	0.80	0.80	—	20.3	16.3
3466.20		1—2	2.66	2.41	—	60.0	49.7
3403.65		0—1	3.10	3.16	—	23.3	21.2
2981.99 *	$5^3P - 6^3D$	2—1	0.01	0.01	—	1.2	1.2
2981.34 *		2—2	0.15	0.13	—	17.4	17.9
2980.63		2—3	0.86	0.74	—	100	100
2881.23 *		1—1	0.23	0.19	—	16.0	16.6
2960.77		1—2	0.68	0.59	—	47.5	49.7
2836.91		0—1	0.80	0.71	—	18.6	21.6

The authors thank L. G. Rautian for her assistance with the measurements.

REFERENCES

1. J. Schuttevaer and J. Smit, Physica **10**, 502 (1943).
2. J. Hengstum and J. Smit, Physica, **22**, 81 (1956).
3. R. Ladenburg, Z. Physik **65**, 200 (1930).
4. K. Larche, Z. Physik **67**, 440 (1931).

EVENTS

XIII CONFERENCE ON SPECTROSCOPY

The XIII Conference on Spectroscopy was held in Leningrad from 4th through 12th July of this year. Some 1200 persons participated, of whom about 900 were nonresidents. At the first plenary session, after an introductory word by S. L. Mandel'shtam, President of the Commission on Spectroscopy of the Academy of Sciences of the USSR, two addresses were heard: O. A. Mel'nikov's "The Work of Kirchhoff and Bunsen and Contemporary Astrophysics," and A. N. Terenin's "Spectroscopy of the Adsorbed State of Molecules."

There were eight plenary sessions in all, at which twenty-six papers were given, on various general questions of atomic and molecular spectroscopy and the spectroscopy of condensed systems. The plenary sessions were held in the morning; the sectional sessions in the latter half of the day. Seven sections were held simultaneously. The papers at the sectional sessions were grouped around specific topics (theory of atomic spectra, plasma spectroscopy, various questions of molecular spectroscopy, optical properties of solids, microwave spectroscopy, etc.); in all, 270 papers were read at the sectional sessions.

During this Conference, only papers of a general theoretical and experimental nature were considered. The next Conference will be devoted to works on spectrochemical analysis.

Atomic spectroscopy occupied a significant place in the proceedings of the Conference. More than 15 papers were devoted to the theory of atomic spectra, and one may note with satisfaction the considerable broadening of the front of theoretical work on atomic spectroscopy and the creation of new scientific centers, as well as the expanding use of modern computer methods for performing complicated calculations.

The discussion of various problems of plasma spectroscopy generated considerable interest. A number of papers were concerned with the application of spectroscopic methods to the investigation of the properties of "hot" plasma. Such a complex subject of study requires the use of various methods, and various procedures for the interferometric study of a plasma, the application of electromagnetic light intensifiers, etc., were reported to the Conference. A powerful pulse discharge is now not the only device which draws the attention of spectroscopists; a number of reports were devoted to the study of the arc and other types of discharge under various conditions of spectrum excitation. These papers gave rise to a lively discussion.

Papers on the study of the luminescence arising during propagation of a shock wave in air or other gases were given, and these problems were discussed in detail.

The determination of atomic constants by spectroscopic methods was also discussed. The use of a combination of several methods (the hook method in conjunction with the absorption method) enables us to increase the precision with which transition probabilities may be determined, and the use of modern techniques of measurement leads to improvement in the reproducibility of the determination. Comparison of the theoretical and experimental investigations in this field becomes a very urgent problem.

The hyperfine structure and isotopic shift of spectral lines are under study in several laboratories of this country. A number of new investigations in this field were reported at the Conference, and the possibilities of using spectroscopic methods for the study of the properties of atomic nuclei were considered in detail.

N. I. Kaliteevskii

Five sections were devoted to the spectroscopy of free molecules and the spectroscopy of condensed phases.

Thirty-five papers were given on spectroscopy of the solid state in general. A number of theoretical and experimental works pertained specifically to questions of the exciton absorption of light in crystals.

Other papers concerned the spectral investigation of crystals at low temperatures and under the actions of (1) electric and magnetic fields, (2) free crystals and crystals subject to elastic deformation, (3) pure crystals and impure crystals, and (4) good dielectrics and semiconductors.

Consideration of the spectra of liquid and solid bodies when a hydrogen bond is formed between their molecules occupied a conspicuous place in the work of the molecular sections. In one of these papers, the long-wavelength spectra of pure and crystallized water (the region of intermolecular vibrations) were considered.

Several papers were devoted to the spectra of adsorbed molecules. The basic information in the molecular-spectroscopic papers was grouped according to spectral regions.

Thus, consideration of electronic spectra took up nine sectional sessions (about 60 papers) and several lectures at the plenary sessions. This group of papers treated a very broad range of problems, including both the theory of these spectra, their application to the study of absorption and radiation processes, molecular structure, energy transfer, influence of the environment of the molecule on its spectrum, etc.

Even greater attention was paid to the spectroscopy of the vibrational and rotational-vibrational motion of molecules (10 sectional sessions with 65 papers, and several lectures at the plenary sessions). In these papers, theoretical and experimental study of questions connected with band intensities during absorption in the infrared region and in Raman spectra occupied a large place. The remaining articles pertained, for the most part, to the study of the structure of complicated molecules, to the nature and structure of the complexes formed by them, to the influence of intermolecular forces and temperature changes on the vibrational spectrum, and so on.

The increased interest of Soviet investigators in the field of low-frequency spectra (microwave spectroscopy, electron paramagnetic resonance, and nuclear resonance spectra) should be especially noted. Four sectional sessions (32 papers) were devoted to these investigations.

A special sectional session was reserved for consideration of questions of the techniques of molecular spectroscopy, and, finally, a number of papers were given which were outside of the general scheme of classification mentioned above.

The Conference had a very heavy schedule of papers,

which nevertheless often aroused lively discussion. However, the number of papers was so great, and correspondingly the organization of the Conference was so complicated on account of the large number of sections, that its members could take part in only a small fraction of the sessions which interested them.

It seems to us that the time is already ripe for a search for new ways to carry on such conferences. Perhaps, for the purpose of carrying on conferences, other organizations should be drawn in to a greater extent with the Commission on Spectroscopy, which has taken on itself the fundamental organizational work and which should reserve for itself the planning and central management of the conferences. This would make it possible to devote the conferences to narrower fields and to hold them more often. On the other hand, if the attention of the participants in the conference were concentrated on a narrow field, it might be possible to conduct the meeting on a higher level. The number of participants in such conferences would be relatively small, which would facilitate their organization considerably.

Perhaps the program of papers of the large conferences, which certainly should be retained, should concern the problems of spectroscopy. These programs should be conducted not in the pattern of listening to a large number of individual papers which are only slightly related as to theme, but rather in the form of a discussion in terms of previously prepared general papers, the themes of which would have to be announced in advance.

It is clear that the hopes expressed here do not exhaust the question, and are directed rather toward attracting the attention of a wider circle of spectroscopists, and also toward arousing interested persons to serious reconsideration of the organizational forms of conferences on spectroscopy.

V. M. Chulanovskii

February 1961

Applied Optics

published by the Optical Society of America
1155 Sixteenth Street, N.W., Washington 6, D. C.
District 7-6177

Editor John N. Howard
Executive Editor Patricia R. Wakeling

APPLIED OPTICS will publish work in the areas of applied optics and closely related scientific and technical fields e.g. physical, electron, ion, ultraviolet and space optics, lens design and optical formulas, plasma, solid state and crystal physics. APPLIED OPTICS will be published bimonthly from January 1962, containing the following features:

.....A leader review paper on one of the major aspects of optics or its applications e.g. new infrared detectors, new optical materials, applications of physical optics in manufacturing process control. This review will be about 10,000 words long and will set the main subject of each issue.

.....Contributed technical papers - 3000/5000 words each - about ten per issue - in any area of applied optics.

Shop and technical notes Book reviews Letters to the Editor
Reports of Meetings Personalia Meetings Calendar
Optical Activities in
Government The Universities Industry

Each issue will concentrate primarily on one area of applied optics and be the responsibility of a Subject Editor; the first nine issues will be

1962	JANUARY	- OPTICAL PUMPING AND MASERS	BRUCE H. BILLINGS
	MARCH	- SPACE OPTICS	editor to be appointed
	MAY	- FOREIGN OPTICS	DAVID Z. ROBINSON
	JULY	- OPTICAL ENGINEERING	RODERIC M. SCOTT
	SEPTEMBER	- INFRARED	JOHN N. HOWARD
	NOVEMBER	- INFORMATION THEORY	editor to be appointed
1963	JANUARY	- ASTRONOMY	editor to be appointed
	MARCH	- INSTRUMENTATION	W. L. HYDE
	MAY	- INTERFEROMETRY	R. A. WOODSON

Reporters in various centers of optics across the country are:

L. H. Chasson	- SAN FRANCISCO	Mary E. Warga	- DC AND BALTIMORE
T. K. McCubbin	- PENNSYLVANIA	R. K. McDonald	- NORTH WEST
Stanley S. Ballard	- FLORIDA	M. Kent Wilson	- BOSTON
E. Scott Barr	- SOUTH EAST	David M. Gates	- DENVER
J. L. Rood	- ROCHESTER	K. M. Baird	- CANADA
E. M. Wormser	- CONNECTICUT	C. S. Williams	- TEXAS
R. A. Oetjen	- OHIO	A. J. Cussen	- LOS ANGELES

Reporters will be appointed for Chicago, New Jersey, New York City, Michigan and Hawaii

APPLIED OPTICS is the one publication devoted solely to applied optics in its broadest phases and designed to meet the interests of scientists, engineers, technologists, technicians ... in a word, opticists ... working in optics or its applications, in fields borderline to optics and employing optical techniques.

(FILLER MATERIAL - NOT IN RUSSIAN ORIGINAL)

OPTICAL SOCIETY *of* AMERICA

FUTURE MEETINGS

PITTSBURGH, March 2, 3, and 4, 1961

PICK-ROOSEVELT HOTEL

A symposium, New Frontiers in Optics and Spectroscopy, jointly sponsored by OSA and the Pittsburgh Conference on Analytical Chemistry and Applied Spectroscopy, will be held March 2 in the Penn-Sheraton Hotel.

LOS ANGELES, October 18, 19, 20, 1961

BILTMORE HOTEL
Details to be announced.

WASHINGTON, D. C., March 15, 16, 17, 1962

Jointly with Inter Society Color Council and National Academy of Sciences Vision Committee. Hotel to be announced.

ROCHESTER, N. Y., October 4, 5, 6, 1962

MANGER HOTEL

There will probably be exhibits at this meeting.

Papers are now being solicited for the Pittsburgh meeting. Duplicate copies of Abstract (no longer than 200 words) and Title should be submitted by December 29 to OSA Executive Office, attention Mary E. Warga. Copies of the Abstract forms may be obtained from Dr. Warga.

Information about later meetings will be announced as soon as possible.

Executive Office
1155 Sixteenth Street, N. W.
Washington 6, D. C.

FILLER MATERIAL - NOT IN RUSSIAN ORIGINAL

The Theory of Vibration of Finite Crystal Lattices . . . . . O. P. Girin 355 (673)
The Luminescence of Nonactivated KI Crystals . . . . . N. N. Vasil'eva and Z. L. Morgenshtern 357 (676)
The Intensities of Raman Lines of Mixtures of CCl_4, $SiCl_4$, and $GeCl_4$ with Benzene, Paraxylene, and Cyclohexane . . . . . Yu. G. Borod'ko and Ya. K. Syrkin 358 (677)
Theory of the Hyperfine Structure of Electron Paramagnetic Resonance Spectra . . . . . I. V. Aleksandrov 359 (679)
The Relative Oscillator Strengths of Certain Lines of ZnI and CdI . . . . . N. P. Penkin and T. P. Red'ko 360 (680)

EVENTS

XIII Conference on Spectroscopy 361 (683)

EDITOR'S NOTE

Comments on the scientific content of the translated Russian articles published in OPTICS AND SPECTROSCOPY are invited. They should be addressed as a Letter to the Editor of the Journal of the Optical Society of America and forwarded to the Editor of that journal, Dr. D. B. Judd, National Bureau of Standards, Washington 25, D. C.

VOL. IX, NO. 5 OPTICS AND SPECTROSCOPY NOVEMBER 1960

CONTENTS

(Numbers in parentheses are original Russian page numbers)

The Influence of Dipolar Molecules on the Absorption of the Mercury Resonance Line at 2537 A ..... V. N. Ivanov 293 (553)

Toward the Theory of Electronic-Vibrational Transitions in Systems with Many Vibrational Degrees of Freedom ..... K. K. Rebane 295 (557)

Effect of Vibrations on the Forbidden Transitions in a Molecule ..... A. M. Meleshina 299 (564)

The Form of the Raman Tensor ..... L. N. Ovander 302 (571)

Second-Order Lines in the Raman Spectra of Hydrocarbons ..... Yu. I. Naberukhin and M. M. Sushchinskii 304 (576)

The Temperature Dependence of the Intensity of Raman Lines in the Vapor and Liquid Phases ..... A. I. Sokolovskaya 307 (582)

Infrared Reflection Spectrum of Boric Anhydride and Fused Quartz at High Temperatures ..... E. P. Markin and N. N. Sobolev 309 (587)

The Luminescence of Chrysene Solutions and Powders at 77°K ..... P. N. Nurmukhametov, E. G. Popova, and N. S. Dokunikhin 313 (593)

The Concentration Quenching of Luminescence in Organoluminors ..... G. A. Mokeeva and B. Ya. Sveshnikov 317 (601)

The Theory of Photoionization of F-Centers ..... Yu. E. Perlin and M. E. Palistrant 320 (608)

The Interaction Between Activator and Non-Totally Symmetric Local Vibrations ..... N. N. Kristofel' 324 (615)

Effect of Deformations on the Absorption Spectrum of Cuprous Oxide Crystals at 20°K ..... V. V. Eremenko and L. I. Chuiko 327 (621)

Experimental Study of Light Amplification in a "Photoconductor-Ferroelectric-Electroluminor" Element ..... I. N. Orlov and N. I. Taborko 329 (626)

Measurement of Small Photocurrents in the Study of Photoelectric Emission ..... A. M. Tyutikov and Yu. A. Shuba 332 (631)

Reflection and Refraction of Light in Optically Isotropic Active Media ..... B. V. Bokut and F. I. Fedorov 334 (635)

The Magnitude and Sign of the Phase Difference $\Delta = \delta_p - \delta_s$ ..... I. N. Shklyarevskii, N. A. Vlasenko, V. K. Milosalvskii, and N. A. Nosulenko 337 (640)

Study of the Optical Properties and Structure of Titanium Dioxide Films ..... T. N. Krylova and G. O. Bagdyk'yants 339 (644)

Interference Filters with a Transmission Band of 1.5 A Half-Width ..... F. A. Korolev, A. Yu. Klement'eva and T. F. Meshcheryakova 341 (648)

Measurement of the Photoelectric Yield of the External Photoeffect under the action of X-Rays in the Wavelength Range 1.54-13.3 A ..... A. P. Lukirskii, M. A. Rumsh, and I. A. Karpovich 343 (653)

Intensities and Polarizations of Specific Vibrations in the Infrared Absorption Spectra of Polyatomic Molecules ..... L. A. Gribov 346 (658)

SHORT COMMUNICATIONS

A Method for Determination of the Radiation Probability of Gases and Vapors ..... Ya. I. Gerlovin 349 (664)

Infrared Absorption Band Intensities of the Hydroperoxide Group ..... L. A. Gribov and A. V. Karyakin 350 (666)

The Influence of the Refractive Index on the Temperature Shift of Raman Band Intensities ..... T. P. Tulub and Ya. S. Bobovich 352 (669)

Conditions for Specificity of the Polarization of the Infrared Bands of Polyatomic Molecules ..... L. M. Sverdlov 353 (671)

(Contents continued on inside back cover)